



WL-TR-91-3066
VOLUME 1



RISK ANALYSIS FOR AGING AIRCRAFT FLEETS

VOLUME 1 - ANALYSIS

ALAN P. BERENS
PETER W. HOVEY
DONALD A. SKINN



University of Dayton
Research Institute
Dayton, OH 45469-0120

October 1991

Final Report for Period
September 1987 - January 1991

Approved for public release; distribution is unlimited.

92-15741



Flight Dynamics Directorate
Wright Laboratory
Air Force Systems Command
Wright-Patterson Air Force Base, OH 45433-6553


92 6 1 106

NOTICE


When Government drawings, specifications, or other data are used for any purpose other than in connection with a definitely Government-related procurement, the United States Government incurs no responsibility or any obligation whatsoever. The fact that the government may have formulated or in any way supplied the said drawings, specifications or other data, is not to be regarded by implication, or otherwise in any manner construed, as licensing the holder, or any other person or corporation; or as conveying any rights or permission to manufacture, use, or sell any patented invention that may in any way be related thereto.

This report is releasable to the National Technical Information Service (NTIS). At NTIS, it will be available to the general public, including foreign nations.

This technical report has been reviewed and is approved for publication.


JOSEPH G. BURNS
Project Engineer


Capt JOHN K. RYDER, Tech Mgr
Fatigue, Fracture & Reliability Gp
Structural Integrity Branch


JAMES L. RUDD, Chief
Structural Integrity Branch
Structures Division

If your address has changed, if you wish to be removed from our mailing list, or if the addressee is no longer employed by your organization, please notify WL/FIBEC, WPAFB, OH 45433-6553 to help us maintain a current mailing list.

Copies of this report should not be returned unless return is required by security considerations, contractual obligations, or notice on a specific document.

REPORT DOCUMENTATION PAGE			Form Approved OMB No. 0704-0188	
<small>Public reporting burden for this collection of information is estimated to average 1 hour per response, including the time for reviewing instructions, searching existing data sources, gathering and maintaining the data needed, and completing and reviewing the collection of information. Send comments regarding this burden estimate or any other aspect of this collection of information, including suggestions for reducing this burden, to Washington Headquarters Services, Directorate for Information Operations and Reports, 1215 Jefferson Davis Highway, Suite 1204, Arlington, VA 22202-4302, and to the Office of Management and Budget, Paperwork Reduction Project (0704-0188), Washington, DC 20503.</small>				
1. AGENCY USE ONLY (leave blank)		2. REPORT DATE October 1991	3. REPORT TYPE AND DATES COVERED Final, September 1987 - January 1991	
4. TITLE AND SUBTITLE Risk Analysis for Aging Aircraft Fleets Volume 1: Analysis			5. FUNDING NUMBERS Contract No. F33615-87-C-3215 PE: 62201F PR: 2401 TA: 07 WU: 06	
6. AUTHOR(S) Alan P. Berens, Peter W. Hovey, and Donald A. Skinn				
7. PERFORMING ORGANIZATION NAME(S) AND ADDRESS(ES) The University of Dayton Research Institute 300 College Park Dayton, OH 45469-0120			8. PERFORMING ORGANIZATION REPORT NUMBER	
9. SPONSORING/MONITORING AGENCY NAME(S) AND ADDRESS(ES) Flight Dynamics Directorate (WL/FIBEC) Wright Laboratory Wright-Patterson AFB, OH 45433-6553 Joseph G. Burns (513) 255-6104			10. SPONSORING/MONITORING AGENCY REPORT NUMBER WL-TR-91-3066	
11. SUPPLEMENTARY NOTES				
12a. DISTRIBUTION/AVAILABILITY STATEMENT Approved for public release; distribution is unlimited.			12b. DISTRIBUTION CODE	
13. ABSTRACT (Maximum 200 words) <p>This report presents a detailed description of the computer program, <u>PRO</u>bability of <u>F</u>racture (<u>PROF</u>), which was written to quantify structural risks associated with the timing of inspection, replacement, and retirement decisions for aging fleets of aircraft. The programmed methodology calculates the history of a growing population of metallic fatigue cracks in zones of equivalent stress experience in the fleet. It accounts for inspection uncertainty and the repair of cracks that are detected. The risk assessment addresses both safety and durability. Safety is quantified in terms of the probability of a fracture resulting from the maximum load in a flight exceeding the critical stress intensity factor. Durability is quantified in terms of the expected number and sizes of the cracks to be detected and repaired at each inspection/maintenance cycle and the expected cost of these repairs. The input to the program is obtainable from existing damage tolerance analyses, individual aircraft tracking histories, loads/environment spectra surveys and maintenance data files.</p>				
14. SUBJECT TERMS Aging Aircraft Aircraft Structures Risk Analysis Reliability			15. NUMBER OF PAGES 214	
			16. PRICE CODE	
17. SECURITY CLASSIFICATION OF REPORT Unclassified	18. SECURITY CLASSIFICATION OF THIS PAGE Unclassified	19. SECURITY CLASSIFICATION OF ABSTRACT Unclassified	20. LIMITATION OF ABSTRACT Unlimited	

FOREWORD

This report summarizes the risk analyses for aging aircraft work performed by the Structural Integrity Division of the University of Dayton Research Institute for the Flight Dynamics Directorate of the Air Force Wright Laboratory under Contract F33615-87-C-3215. The period of performance for the effort was September 1987 through January 1991. Mr. Joseph G. Burns, WL/FIBEC, was the Air Force Project Monitor. Dr. Alan P. Berens of the University of Dayton Research Institute was the Principal Investigator.

The final report of this work comprises two volumes. Volume 1 contains a description of the model for implementing the risk analyses and example applications. The documentation of Probability of Fracture (PROF), the computer program written to perform the risk analyses, is presented in Volume 2.

Accession For	
NTIS CRA&I	<input checked="" type="checkbox"/>
DTIC TAB	<input type="checkbox"/>
Unannounced	<input type="checkbox"/>
Justification	
By _____	
Distribution /	
Availability Codes	
Dist	Avail and/or Special
A-1	

TABLE OF CONTENTS

SECTION		PAGE
1	INTRODUCTION	1
2	OVERVIEW	3
3	PROF METHODOLOGY	11
3.1	PROF INPUT DATA	11
3.1.1	Material/Geometry Data	13
3.1.1.1	K/ σ versus a	13
3.1.1.1.1	Format	14
3.1.1.1.2	Example	14
3.1.1.1.3	Comments	16
3.1.1.2	Distribution of Fracture Toughness	17
3.1.2	Aircraft/Usage Data	17
3.1.2.1	Aircraft Population Parameters	18
3.1.2.2	Crack Size versus Flight Time	19
3.1.2.2.1	Format	20
3.1.2.2.2	Example	21
3.1.2.2.3	Comments	21
3.1.2.3	Maximum Stress Distribution	23
3.1.2.3.1	Format	26
3.1.2.3.2	Example	26
3.1.2.3.3	Comments	29
3.1.2.4	Initial Crack Size Distribution	31
3.1.2.4.1	Format	31
3.1.2.4.2	Example	32
3.1.2.4.3	Comments	34
3.1.3	Inspection/Repair Data	35
3.1.3.1	Maintenance Times	35
3.1.3.2	Inspection Capability	36
3.1.3.3	Repair Crack Size Distribution	39
3.1.3.3.1	Format	40
3.1.3.3.2	Example	40
3.1.3.3.3	Comments	41
3.1.3.4	Maintenance Costs	41
3.1.4	Summary of Input for Example	42
3.2	COMPUTATIONS	42
3.2.1	Modeling the Crack Size Distribution	42
3.2.1.1	Growing Population of Crack Sizes	44
3.2.1.2	Maintenance Effect on Crack Size Distribution	44
3.2.2	Probability of Fracture	46
3.2.2.1	Single Flight Probability of Fracture	46
3.2.2.2	Interval Probability of Fracture	48
3.2.3	Expected Maintenance Costs	50
3.3	EXAMPLE OUTPUT	51

TABLE OF CONTENTS (continued)

SECTION		PAGE
4	SENSITIVITY ANALYSIS	59
4.1	BASELINE CONDITIONS	59
4.1.1	Material/Geometry Data	61
4.1.2	Aircraft/Usage Category Data	61
4.1.3	Inspection/Repair Category Data	67
4.1.4	Summary of Baseline Input	69
4.2	SENSITIVITY TO INPUT VARIATIONS	69
4.2.1	Variations in Material/Geometry Input	71
4.2.1.1	Fracture Toughness	71
4.2.1.2	K/ σ versus a	75
4.2.1.3	Discussion - Material/Geometry Input	78
4.2.2	Variations in Aircraft/Usage Input	82
4.2.2.1	Initiating Crack Size Distribution	82
4.2.2.2	a versus T	91
4.2.2.3	Maximum Stress per Flight Distribution	94
4.2.2.4	Discussion - Variation in Aircraft/Usage Input	96
4.2.3	Variations in Inspection/Repair Input	101
4.2.3.1	Inspection Schedule Effects	101
4.2.3.1.1	Scheduling Effect on Fracture Probability	101
4.2.3.1.2	Scheduling Effect on Expected Costs	108
4.2.3.2	Inspection Capability Effects	116
4.2.3.3	Repair Crack Size Effects	128
4.2.3.4	Discussion - Inspection/Repair Data	133
5	EXAMPLE APPLICATION	137
5.1	PROBLEM STATEMENT	137
5.2	INSPECTION INTERVAL ANALYSIS	143
5.3	INSPECTION CAPABILITY ANALYSIS	148
5.4	EXAMPLE SUMMARY	153
6	SUMMARY AND CONCLUSIONS	155
7	REFERENCES	159

APPENDIX		PAGE
A	CALCULATION DETAILS	A1
A.1	INTRODUCTION	A1
A.2	CRACK GROWTH CALCULATIONS	A1
A.2.1	Interpolation and Extrapolation Methods	A3
A.2.2	Crack Growth Calculations	A8
A.2.3	Inspection and Repair Calculations	A11
A.3	PROBABILITY OF FRACTURE CALCULATIONS	A13
A.3.1	Single Flight Probability of Fracture	A16
A.3.2	Usage Interval Probability of Fracture	A18
A.4	APPLICATION TO MULTIPLE DETAILS AND THE FLEET	A21
A.5	REFERENCES	A22

TABLE OF CONTENTS (concluded)

APPENDIX

PAGE

B	STOCHASTIC CRACK GROWTH	B1
C	CRACK SIZE DISTRIBUTIONS	C1
C.1	MODELS	C1
	C.1.1 Theoretical Models	C2
	C.1.2 Mixtures	C2
C.2	CRACK SIZE DATA AVAILABLE	C3
C.3	CRACK SIZE DATA NOT AVAILABLE	C6
	C.3.1 Equivalent Initial Flaw Size Distribution	C6
	C.3.2 Time to Crack Initiation	C8
C.4	CRACK SIZE DISTRIBUTION UPDATE	C10
C.5	REFERENCES	C12

LIST OF ILLUSTRATIONS

FIGURE		PAGE
1	Crack Size Distribution versus Spectrum Hours	5
2	Effect of Maintenance on Crack Size Distribution	6
3	Quantifying Safety in Terms of Probability of Fracture	7
4	Quantifying Maintenance Costs	8
5	Summary of PROF Input Data	12
6	Example K/σ versus Crack Size for an A/F/T Airframe	15
7	Crack Growth versus Flight Hours	22
8	Example Exceedance Curves for A/F/T Usage	27
9	Fit of Gumbel's Extreme Value Distribution to Severe A/F/T Spectrum	30
10	Example Initial Flaw Size Distribution	33
11	Example Probability of Detection Functions	38
12	Projection of Percentiles of Crack Size Distribution	45
13	Screen Plot of Example Analysis - Single Detail POF	52
14	Geometrical Description of WS27, the Lower Wing Skin Fastener Holes Located at the 44% Spar of the -29 Wing	60
15	Baseline Geometry Fastener for WS27	62
16	Baseline Distribution of Initial Crack Sizes - Mixture of Log Normal EIFS and Uniform (0,0.050)	64
17	Predicted Crack Growth for Baseline Conditions	65
18	Baseline Distribution of Max Stress per Flight - LIF Usage	66
19	POD(a) for Semiautomated Eddy Current Inspections	68
20	Normal Distributions for K_c	72
21	POF Varying K_c Mean with Fixed Standard Deviation	73
22	POF Varying K_c Standard Deviation with Fixed K_c Mean	74

LIST OF ILLUSTRATIONS (continued)

FIGURE		PAGE
23	POF at Limits of 90% Confidence Bounds on Mean and Variance of K_C	76
24	POF for Constant Fracture Toughness	77
25	K/σ versus a for Crack Geometries	79
26	Crack Size versus Spectrum Hours for Crack Geometries	80
27	POF for Different Crack Geometries	81
28	POF for Different Families of EIFS with Constant Median and 90th Percentile	85
29	POF with and without Mix of Large EIFS	86
30	POF for 10% Changes in Median and σ of EIFS	87
31	POF for Increased Proportions of Large EIFS	89
32	POF for Two Distributions of Cracks in Aging Aircraft	90
33	Crack Size versus Spectrum Hours - WS27, LIF Usage	92
34	POF for Different Stress Levels	93
35	Selected Fits to Distribution of Max Stress per Flight	95
36	POF for Selected Fits to Distribution of Max Stress per Flight	97
37	POF for Inspection Increments	102
38	POF Bounds at Defined Inspection Increments	104
39	POF Bounds for Initial Inspection Increments Shorter than Baseline	105
40	POF Bounds for Initial Inspection Intervals Larger than Baseline	106
41	POF Bounds for Combinations of Initial Interval and Increments	107
42	Expected Repair Costs as a Function of Repeat Inspection Increments	113
43	Expected Repair Costs for Selected Initial Inspection Intervals	115

LIST OF ILLUSTRATIONS (continued)

FIGURE		PAGE
44	POD(a) Functions for Potential Inspection Systems	118
45	POF Comparing Baseline to Visual NDE	119
46	POF Comparing Baseline to Potential Advanced NDE Systems	122
47	POD(a) for Parametric Variations from Baseline	123
48	POF Comparing Baseline to Parametric POD(a) Variations	124
49	POD(a) for Comparing a_{90} Values	126
50	POF Evaluates Effect of a_{90} Values from POD(a)	127
51	Cumulative Distribution Functions for Equivalent Repair Crack Size Distributions	130
52	POF for Equivalent Repair Crack Size Distributions	131
53	Stress Intensity Factor Coefficient for Analysis Region	138
54	Crack Growth for Projected Usage Spectrum	140
55	Gumbel Distribution Fit to Maximum Stress per Flight of Projected Spectrum	141
56	Crack Detection Probability for Competing Inspection	142
57	Probability of Panel Fracture in an Airframe for Baseline Conditions	144
58	Probability of Panel Fracture in an Airframe between Inspections for Selected Inspection Intervals	145
59	Normalized Expected Maintenance Costs as a Function of Inspection Interval	147
60	Probability of Panel Fracture in an Airframe between Inspections for Inspection Methods and Inspection Intervals	151
61	Normalized Total Expected Maintenance Cost for Two Inspection Methods as a Function of Inspection Interval	152
A1	Flow Chart of PROF Calculations	A2
A2	Illustration of the Three Interpolation Zones	A5
A3	Growth of a Distribution of Flaws	A9

LIST OF ILLUSTRATIONS (concluded)

FIGURE		PAGE
A4	Integration Surfaces for POF Calculations	A15
A5	Determination of a_F , the Crack Size That Will Grow to a_{last} in a Usage Interval	A19
B1	Schematic Illustrating Stochastic Crack Growth for a Population of Crack Sizes	B2
B2	Comparison of Projected Percentiles of Log Normal Crack Sizes to Log Normal Stochastic Growth	B5
B3	Comparison of Projected Percentiles of Weibull Crack Sizes to Weibull and Log Normal Stochastic Growth	B6
C1	Sizes of Cracks as a Function of Flight Hours	C5
C2	Weibull Plot of Crack Sizes Translated to a Common Number of Flight Hours	C7
C3	Schematic of Stochastic Structural Durability Analysis	C9
C4	Schematic of the Calculation of Crack Size Distribution from Time to Crack Initiation Distribution	C11

LIST OF TABLES

<u>TABLE</u>		<u>PAGE</u>
1	Example Calculations for Gumbel Fit to Max Stress per Flight Distribution A/F/T Severe Spectrum	28
2	Factors for Obtaining a_{90} from a_{50} for Selected Values of σ	39
3	PROF Input for Example Problem	43
4	Example PROF Report	54
5	Baseline PROF Input for Sensitivity Analyses	70
6	Percent Detections at Inspections for Initiating Crack Size Distributions	84
7	Total Percent of Sites at Which Cracks are Detected in 5000 Spectrum Hours	109
8	Expected Repair Costs	111
9	Expected Repair Costs - 700 and 1500 Hour Initial Intervals	114
10	Percent Detections at Inspections for Different Inspection Capabilities	121
11	Percent Detections at Inspections for Different Equivalent Repair Qualities	132
12	Expected Total Fracture and Maintenance Costs as a Percentage of Total Costs for 7200 Hour Inspection Intervals	149

SECTION 1

INTRODUCTION

The realized life of individual airframes is seldom equal to the design life planned for a fleet. The life of an aircraft fleet tends to be determined more by its inherent operational capability and maintenance costs than by the number of flight hours specified at the design stage. As a fleet ages, the Air Force must make many decisions concerning the timing and extent of inspections, repairs, modifications, and life extension options. Since the readiness and cost ramifications of these decisions are very large, the Air Force needs every possible tool that can assist in making cost effective decisions.

Of major concern are the real cracks in the individual airframes of the fleet at the time structural decisions must be made and the projected growth of these cracks. To obtain this specific information, extensive inspections of individual airframes would be necessary to obtain the required data on the number and size of the cracks; and even with such extensive inspections, not all of the cracks would be detected. Therefore, the status of the populations of fatigue cracks in an aging fleet must be inferred from inspections of a sample of the fleet or analytically estimated. In either case, decisions based on durability and damage tolerance analyses should reflect the uncertainty in the flaw size information.

Most durability and damage tolerance analyses have been based on deterministic methods making conservative assumptions when necessary to cover scatter. (It might be noted that the Air Force has used estimates of failure probability as aids in making structural integrity decisions regarding the F-111, C/KC-135, C-5A, and T-38 aircraft.) Due to the increased uncertainty regarding potential flaw sizes in an aging fleet of aircraft, a deterministic analysis does not necessarily provide the Air Force with the information needed to assess options. Rather, a risk analysis tool is needed whereby the risks and expected costs of

maintenance strategies and life extension options can be quickly assessed and compared. This risk analysis methodology should be as realistic as possible within the constraints of force management data available for different fleets of aircraft.

The objective of this program was to provide the Air Force with an additional tool for evaluating inspect, replace, repair or retire decisions in aging aircraft fleets. To achieve this objective, a risk analysis computer program, PRobability Of Fracture (PROF), was formulated and implemented. The programmed methodology is based on data available from the Air Force Aircraft Structural Integrity Program, ASIP. PROF calculates the history of a growing population of fatigue cracks in zones of equivalent stress experience. It accounts for inspection uncertainty and the repair of cracks which are detected. The risk assessment addresses both safety and durability. Safety is quantified in terms of the probability of a fracture resulting from the maximum load in a flight exceeding the critical load associated with the fracture toughness level. Durability is quantified in terms of the expected number and sizes of the cracks to be detected and repaired at each inspection and repair-if-necessary cycle and the expected costs of these repairs.

This report summarizes the complete development and application of the risk analysis program. Section 2 is a brief overview of PROF. Section 3 defines the detailed methodology that was implemented in the PROF computations, describes methods for obtaining the required input, and presents an example run of the program. Section 4 contains the results of PROF output sensitivity to variations in input and to the fleet management decisions. An example application of PROF is presented in Section 5. Conclusions and recommendations are contained in Section 6.

SECTION 2

OVERVIEW

The objectives of structural risk analyses are to provide quantitative information for the management and assessment of structural safety and useful life. This information is typically expressed in terms of the expected costs of competing maintenance scenarios and the probability of failure associated with the scenarios. There are many approaches that can be programmed to achieve these objectives. Differences in approach can be fundamental, for example, modeling the time to failure versus modeling the growth of a crack size distribution. Differences in approach can also be due to the selection of the many influencing factors and the methods for modeling these factors. However, implementing any structural risk analysis approach involves a compromise between the ability to model reality and the data that are available to feed the analytical model. In general, the more detail required by the model, the less reliable are the available data.

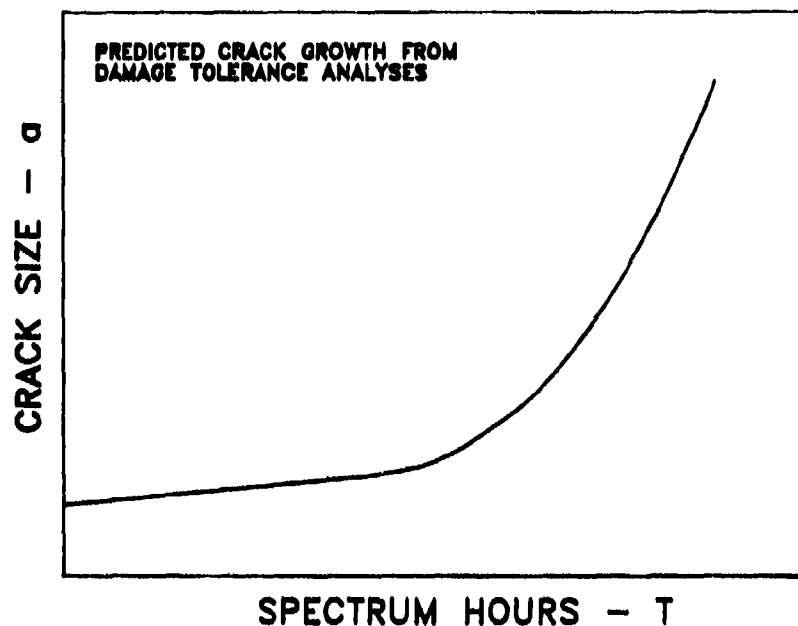
Because of the Aircraft Structural Integrity Program (ASIP) requirements of MIL-STD-1530A [1], the Air Force has an extensive data base on each system for the deterministic evaluation of structural integrity. The approaches usually taken in fulfilling these requirements, the availability of the resulting data, and the information content of the crack size distribution at critical locations were the primary reasons for the choice of the fracture mechanics based analysis that was implemented in PROF. Of particular importance to this risk analysis methodology are the ASIP data associated with the damage tolerance [2,3] and durability [2,4] analyses that are performed for all potential airframe cracking sites and the data associated with the force management tasks of ASIP [5]. Data requirements will be addressed in detail in Section 3.

The risk analysis model, PROF, addresses a single population of structural elements. The population is defined in

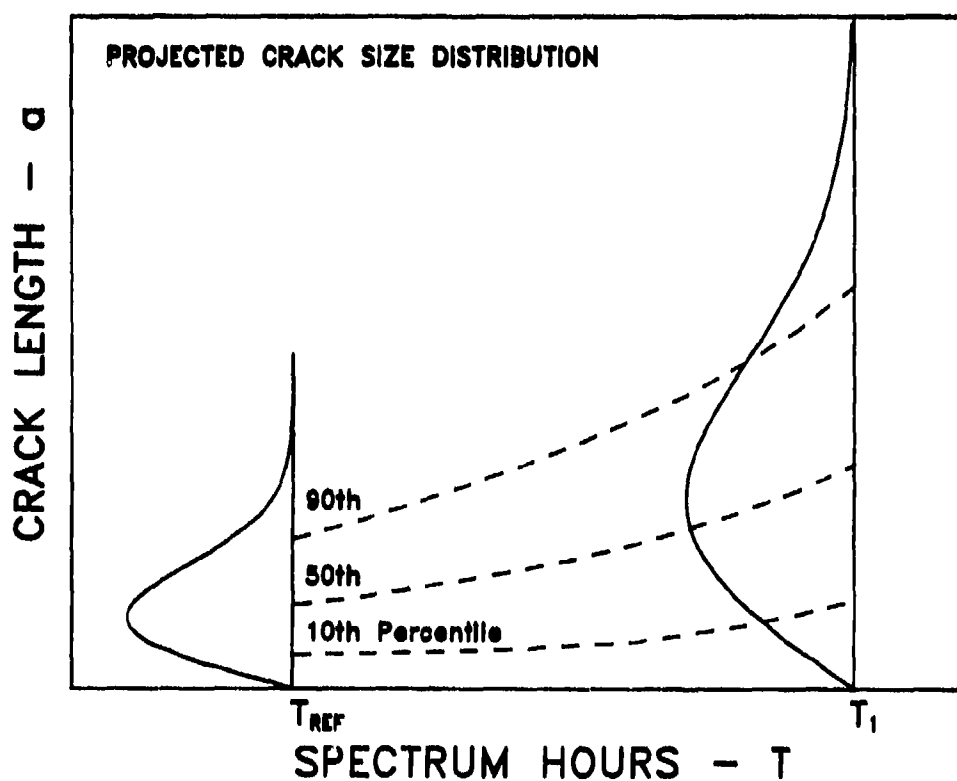
terms of all details which experience essentially equivalent stress histories and have equivalent stress intensity factor coefficients. Such populations of potential cracking sites are defined during the ASIP damage tolerance analyses. Each structural element in the population of details is assumed to contain a crack whose size at T spectrum hours is a random variable with probability density function, $f_T(a)$. There are three contexts for interpreting statements about this distribution of cracks: an individual structural element, a single airframe with many such "identical" elements, and the fleet of airframes. PROF addresses all three, but care should be taken to ensure that interpretations are being made in the correct context.

The crack size distribution forms the basis of PROF computations as illustrated in the schematics of Figures 1-4. An estimate of the distribution of crack sizes at a reference spectrum hour age is obtained from inspection feedback [6] or an initial quality analysis expressed in terms of flaw sizes [7,8,9]. The deterministic crack size versus spectrum hour ("a vs. T") relation from the damage tolerance analysis, Figure 1a, is used to project the percentiles of the crack size distribution, Figure 1b. (The sizes of individual cracks can be projected forward or backward to combine data from different airframes in obtaining the crack size distribution at the reference time.)

At a maintenance action, the crack sites are inspected. The capability of the inspection system is characterized by its probability of detection function, Figure 2a. If a crack is detected, it is repaired and the quality of the repaired cracks is quantified by an equivalent repair crack size distribution, Figure 2b. The equivalent repair crack size distribution is analogous to the equivalent initial crack size distribution used to characterize manufacturing quality [9]. (If desired, the repaired crack sites can be removed from further analyses by defining the equivalent repair crack sizes to be zero. The possibility of a rogue flaw being introduced at the maintenance

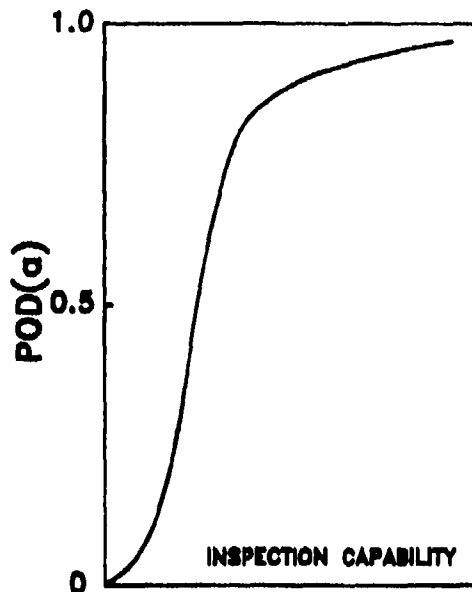


a) Deterministic a vs. T .

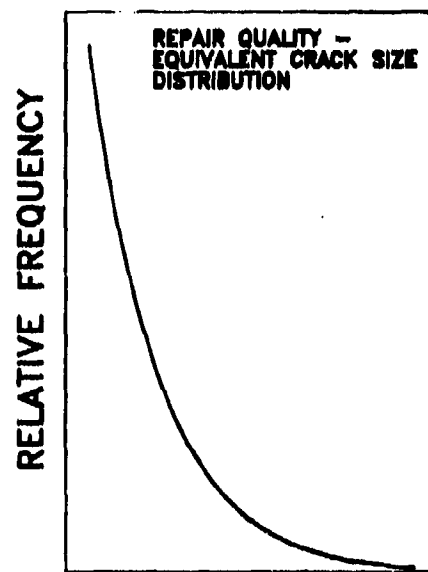


b) Projections of Crack Size Percentiles.

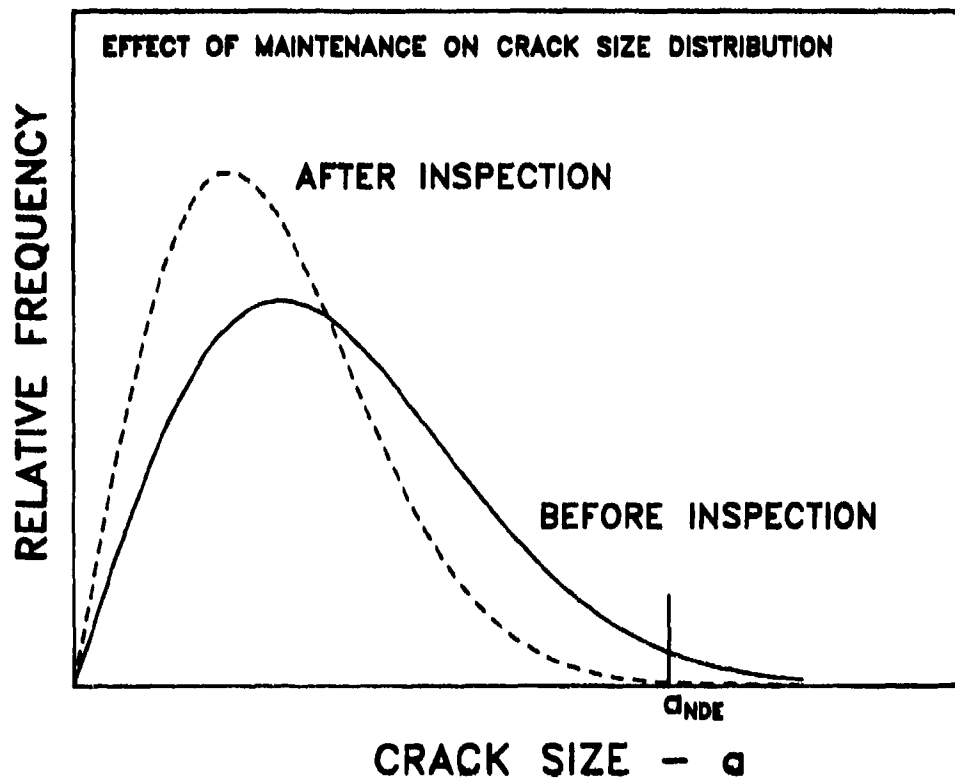
Figure 1. Crack Size Distribution versus Spectrum Hours.



2a) Probability of Detection.

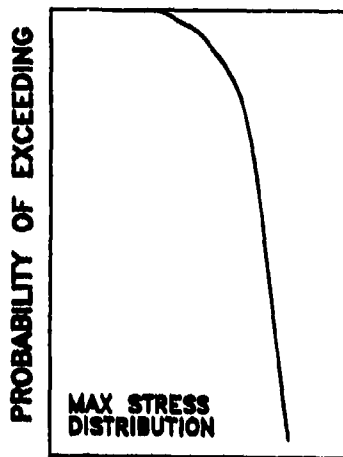


2b) Equivalent Repair Flaw Size Distribution.

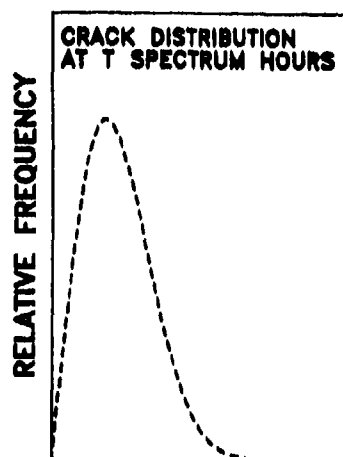


2c) Crack Size Probability Density Functions Before & After Inspection.

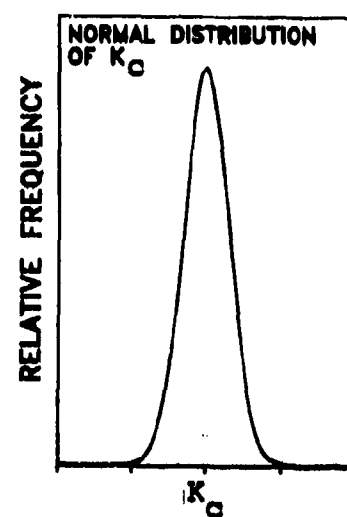
Figure 2. Effect of Maintenance on Crack Size Distribution.



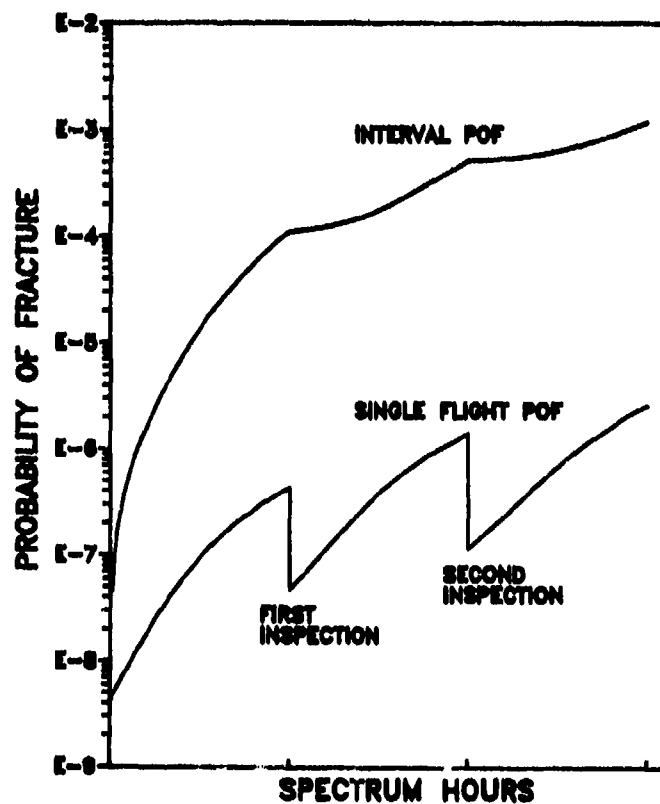
a) Distribution of Max Stress/Flight.



b) Crack Size Distribution.

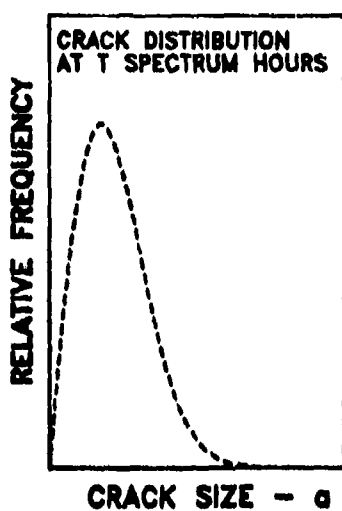


c) Distribution of Fracture Toughness

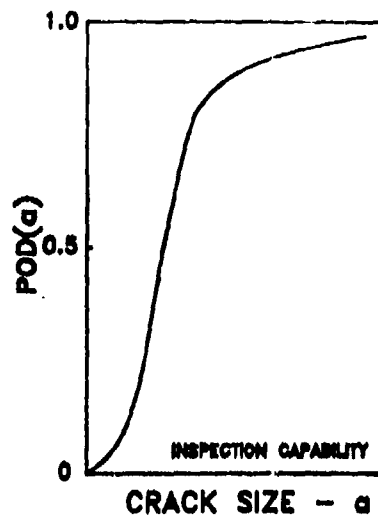


d) Probability of Fracture versus Spectrum Hours.

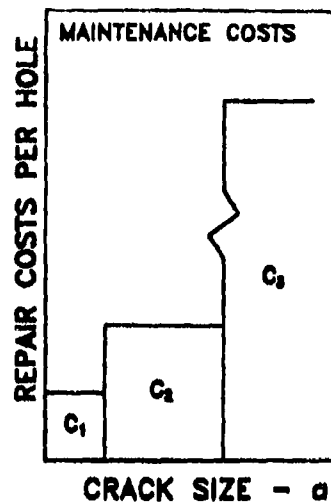
Figure 3. Quantifying Safety in Terms of Probability of Fracture.



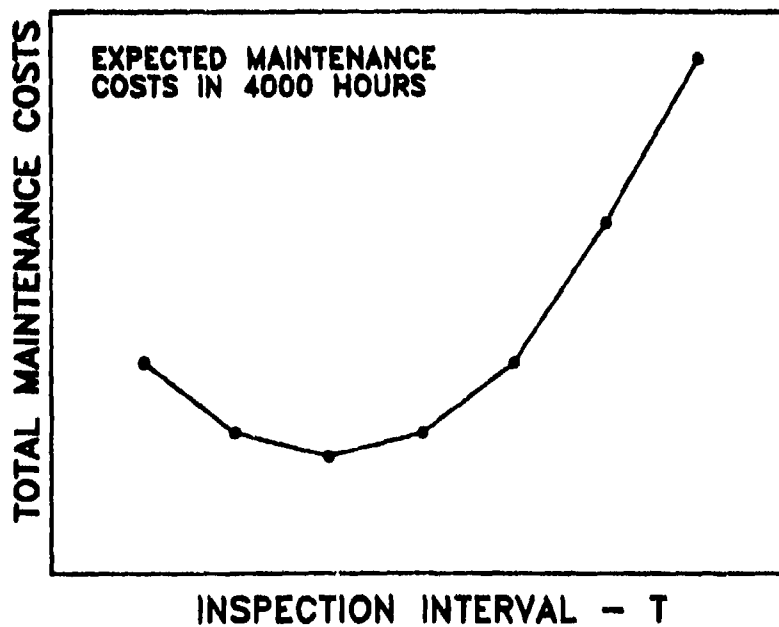
4a) Crack Size Distribution.



4b) Probability of Detection.



4c) Repair Costs as a Function of Crack Size.



4d) Expected Maintenance Cost versus Hours between Inspections.

Figure 4. Quantifying Maintenance Costs.

action can also be addressed by the method of modeling the equivalent repair crack size distribution.) The crack size distribution after the inspect and repair maintenance action is a mixture of the sizes from sites in which no cracks were detected and from the sites in which cracks were detected and repaired, Figure 2c. This after inspection crack size distribution is projected forward for the next period of uninspected usage. This process is continued for as many inspection intervals as desired.

The time history of the crack size distribution is used to evaluate both safety and maintenance costs. Safety is quantified in terms of the probability of fracture, Figure 3. Fracture occurs when an applied stress produces a stress intensity factor which exceeds the fracture toughness for the cracked detail, i.e., when

$$\sigma \geq \sigma_{cr} = K_C / [\sqrt{\pi a} \cdot \beta(a)] \quad (1)$$

where "a" is the crack depth, K_C is the fracture toughness of the material and $\beta(a)$ is a geometry dependent factor. The smallest time increment considered by PROF is a single flight, and it is assumed that potential fractures will occur at the random variable of maximum stress in a flight, Figure 3a. For an arbitrary element in the population of details, "a" and K_C are unknown and are modeled as random variables, Figures 3b and 3c. From the distributions of these three random variables, the probability of fracture (POF) is calculated as

$$\begin{aligned} \text{POF} &= P\{ \sigma_{\max} \geq \sigma_{cr} \} \\ &= P\{ \sigma_{\max} \geq K_C / [\sqrt{\pi a} \cdot \beta(a)] \} \end{aligned} \quad (2)$$

POF is calculated for a single flight and for any flight in the interval between the start of analysis and each inspection, Figure 3d. POF is also calculated for any flight within each inspection interval.

Maintenance costs are quantified in terms of the expected number of cracks that will be detected and repaired at each inspection and the total expected costs of the planned maintenance scenario, Figure 4. The expected number and sizes of cracks to be repaired are obtained from the distribution of crack sizes at the time of the inspection, Figure 4a, and the capability of the inspection system, Figure 4b. The expected costs are obtained from the costs of inspection, the expected number and sizes of cracks to be repaired, Figure 4c, and the expected costs due to element fracture. Figure 4d is a schematic illustration of the expected costs of maintenance for different intervals between maintenance actions.

SECTION 3

PROF METHODOLOGY

This section presents the risk analysis methodology that has been implemented in PROF. The input and methods for obtaining this input in the required formats are presented first. These input requirements are followed by a general mathematical description of the programmed computations. (Details of these computations are contained in Appendix A and Volume 2 of this report.) An example of PROF output is then displayed by presenting the results of a PROF run using a set of example input for an Attack/Fighter/Trainer (A/F/T) class aircraft.

3.1 PROF INPUT DATA

The risk analysis methodology implemented in PROF requires input on nine distinct data items. Since PROF is an interactive program, it obtains this input by querying the user in a series of screens. The answers to the queries depend on the data item and comprise a) names of files which contain input tables, b) parameters of programmed functions, and, c) stand alone constants.

Figure 5 presents a list of the nine PROF input data items and indicates the required formats. This subsection presents the specific requirements for each item and describes methods for obtaining the input in the required format. An example is presented for each data item which is representative of an inner lower wing location for an Attack/Fighter/Trainer application. The example input will be used to generate the example output of Subsection 3.3. Expected maintenance costs are currently calculated using PROF output, so inspection and repair costs are not required to run PROF. Inspection and repair costs, however, would be required for a complete analysis.

Although not addressed in detail in this report, some of the input data can be modeled at different levels of stratifications. For example, the distribution of max stress per

DATA TYPE	FORMAT	SOURCE/COMMENT
MATERIAL/GEOMETRY		
K/σ vs a	File	DTA analysis - stress intensity factor coefficient
$g(K_c)$	Parameter values	Normal distribution of fracture toughness, [10]
AIRCRAFT/USAGE		
Locations	Constants	Number of analysis locations per airframe and number of airframes in the fleet
$f_0(a)$	File	Crack size distribution at start of analysis
a vs T	File	DTA analysis - crack growth life curve
$h(\sigma)$	Parameter values	Gumbel distribution of max stress per flight - from L/ESS data or sequences of DTA analysis
INSPECTION/REPAIR		
T_1, T_2, \dots	Constants	Inspection times - user defined
POD(a)	Parameter values	Cumulative lognormal POD function for NDE system [11]
$f_r(a)$	File	Crack size distribution of repaired crack sites

Figure 5. Summary of PROF Input Data.

flight can be modeled for different mission types or for a composite of all mission types. For these types of input, both the effect on the interpretation of probability of fracture and the method for combining probabilities of fracture across the stratifications are also discussed in this section.

3.1.1 Material/Geometry Data

Under current Air Force regulations, damage tolerance analyses are performed for every critical location on an airframe. As part of these analyses, the stress intensity factor geometry correction, $\beta(a)$, for correlating stress, loading condition, global geometry, and crack size will have been determined. Further, fracture toughness data, K_C , for the material will have been collected. The following subsections describe the format required by PROF for these geometry and material dependent properties.

3.1.1.1 K/σ versus a

The defining relation between stress intensity factor, stress, and crack size is expressed as

$$K = \sigma \cdot \sqrt{\pi a} \cdot \beta(a) \quad (3)$$

To isolate the crack size random variable, a , PROF requires the geometry factor input to be expressed in terms of " K/σ versus a ," i.e.,

$$K/\sigma = \sqrt{\pi a} \cdot \beta(a) \quad (4)$$

For every critical location in an airframe, $\beta(a)$ will be known. Closed form solutions for $\beta(a)$ have been obtained for many typical detail geometries [12,13]. However, finite element analyses may be required to obtain $\beta(a)$ due to such factors as complex geometry, boundary conditions, or load transfer

[14,15,16]. In these cases, $\beta(a)$ is typically expressed in tabular or graphical form.

The "K/ σ versus a" relation must extend to a sufficiently large crack size, a_{last} , such that for cracks larger than a_{last} , the structural element can be considered to be in a failed state. PROF uses a_{last} to define limits of integration for the calculation of fracture probabilities.

As currently written, the fracture probability calculations of PROF do not properly account for large discontinuities in the "K/ σ versus a" relation introduced by edges, holes, etc. In this situation, a crack may temporarily experience rapid growth and still be stopped before the structure fractures. Modifications to account for such discontinuities and to extend the analysis to cover continuing damage are planned for a future version of the program.

3.1.1.1.1 Format

Since the geometry factor, $\beta(a)$, is not always stated in explicit terms, PROF was designed to expect a tabular input for the "K/ σ versus a" relation. In particular, PROF requests the name of the file which contains (a,K/ σ) data pairs. This data file can be generated from a closed form solution, from a table, or from a digitization of an analog definition of $\beta(a)$. Since interpolation is used to obtain intermediate values, the (a,K/ σ) pairs must define a single valued function.

The format of the "K/ σ versus a" data file is as follows. The first row of the file identifies the source of the data and will appear in the PROF output. The second row of the file must contain the number of (a,K/ σ) pairs in the table. The first pair must be (0,0) and the last pair defines the maximum crack size, a_{last} , that is considered in the analysis. The filename must contain a ".DAT" extension.

3.1.1.1.2 Example

Figure 6 presents an example "K/ σ versus a" curve for an A/F/T aircraft. The data were obtained from a manufacturer's

GEOMETRY FACTOR — FASTENER HOLE

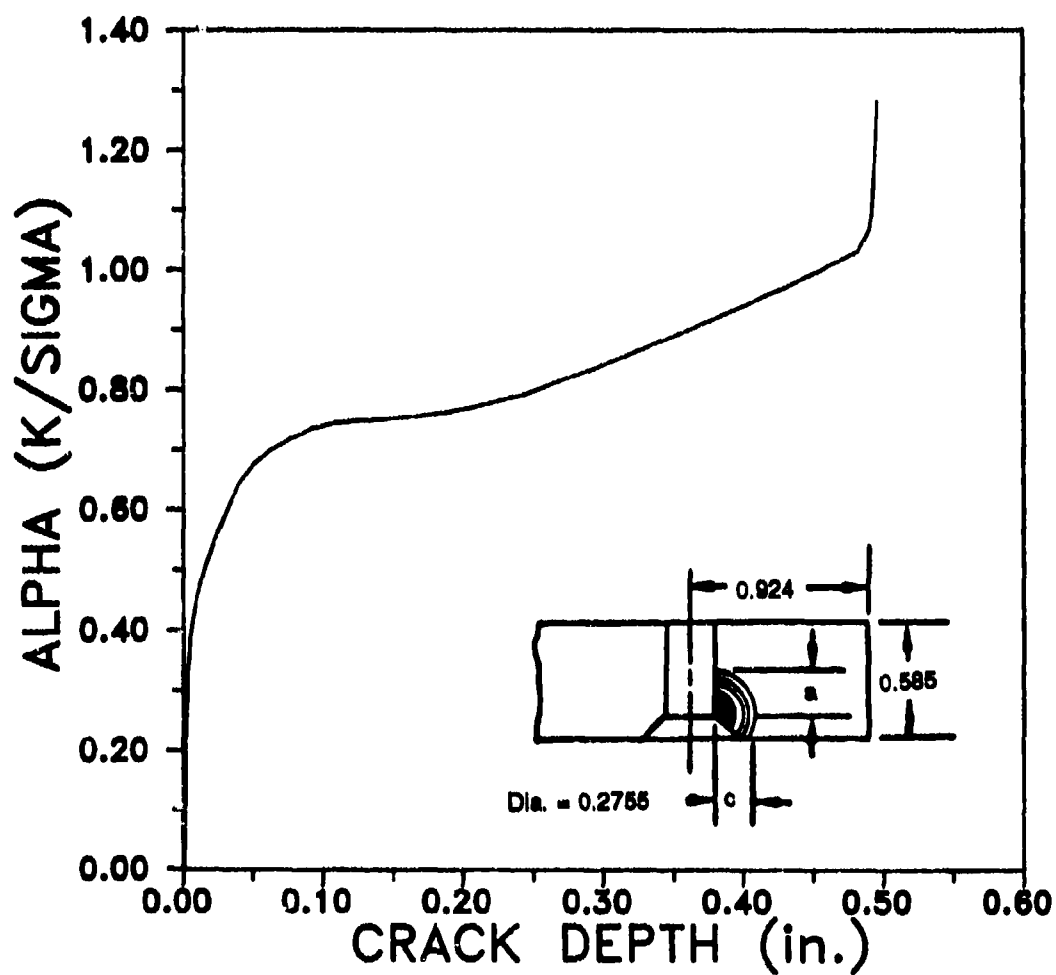


Figure 6. Example K/σ versus Crack Size for an A/F/T Airframe.

Damage Tolerance Analysis (DTA) report. It was assumed (presumably conservatively) that cracks would originate at the intersection of the countersink and the bore of the rivet hole. Unstable crack growth occurs in both the depth and surface directions when the crack depth (a) reaches 0.5 in. For $a = 0.5$ in. and average $K_{\sigma} = 30 \text{ KSI} \sqrt{\text{in.}}$, the residual strength is 24 KSI, a stress level exceeded in about 80 percent of all flights. Thus, for this example $a_{\text{last}} = 0.5 \text{ in.}$

3.1.1.1.3 Comments

PROF treats $\beta(a)$ as a deterministic relationship for the structural detail. Given an initiated crack, the deterministic model is reasonable in the sense that deviations from the model for a particular crack would have a second order effect on the calculations as compared to uncertainty in other inputs. However, cracks do not necessarily initiate at the "correct" location, and there are significant differences in the geometry factors for different locations. The conservative approach to the problem of multiple crack initiation sites is to assume all cracks initiate at the location with the most severe geometry correction. Probability of fracture (POF) as calculated by PROF would then be conservative with respect to geometry factor.

Multiple crack initiation sites in a given detail can be directly modeled by using multiple runs of PROF and interpreting the results as follows. If the proportion of the total number of cracks governed by each initiation site is known, then the best estimate of POF is obtained from a weighted average of the fracture probabilities for each crack geometry (each " K/σ versus a " description). For example, if p_1 represents the proportion of cracks that initiate at the intersection of the countersink and the rivet bore, p_2 represents the proportion of cracks that initiate in the bore, and p_3 represents the proportion of cracks that initiate at a bore corner, then the probability of fracture for the detail is given by

$$POF = p_1(POF_1) + p_2(POF_2) + p_3(POF_3) \quad (5)$$

where POF_i is the fracture probability for the i th crack initiation geometry. The calculation of Equation 5 would have to be made using output results from three individual runs of PROF as there is no provision in PROF for combining results from different analyses.

3.1.1.2 Distribution of Fracture Toughness

Fracture toughness is best modeled in terms of a distribution of values for the particular material application [17]. PROF assumes that fracture toughness values have a normal distribution and requests the mean and standard deviation of K_{IC} for the particular material of the application. In general, these values can be obtained from the Damage Tolerant Design Handbook [10]. Coefficients of variation (σ/μ) for K_{IC} values range from about 0.03 to 0.10 for aluminum and titanium alloys and most steels.

For the example application, assume the material of the structural detail, Figure 6, is 7075-T7351 aluminum alloy plate. The mean and standard deviation of fracture toughness for this material are listed at 29.4 and 2.2 KSI $\sqrt{\text{in.}}$, respectively, in the Damage Tolerant Design Handbook [10], Table 8.9.1.1. These values were based on a sample of 47 specimens and the mean closely agrees with the fracture toughness used by the manufacturer in the DTA of this detail.

3.1.2 Aircraft/Usage Data

The input data in this category are specific to the past and expected usage of the fleet of aircraft being analyzed. The initial structural design, manufacturing quality, and past usage determine the distribution of crack sizes that are in the analysis locations at the start of the analysis. The expected usage determines the projected growth of the cracks and the operational stress peaks that may be encountered. This section

addresses the methods used to model these elements as well as their PROF input requirements.

3.1.2.1 Aircraft Population Parameters

An individual execution of PROF is based on the analysis of a single distribution of crack sizes emanating from stress raisers in metallic structure. The population modeled by this distribution can represent a single location in each airframe of the fleet. If there are multiple locations in each airframe that will experience essentially equivalent stress histories and have equivalent stress intensity factors, the crack size distribution would also apply to each of the stress raisers in the zone of equivalence. There are three fracture probabilities of interest to cover these populations: a) the POF at a single stress raiser, b) the POF at any stress raiser in a single airframe of the fleet, c) the POF for any stress raiser in any airframe of the fleet.

PROF first calculates the POF at a single stress raiser and, assuming independence, calculates the POF for the other two cases based on the number of stress raisers, k , in the zone of equivalence on a single airframe and the number of airframes, N , in the fleet being analyzed. To perform the last two computations, PROF asks for the number of analysis locations per aircraft and the number of aircraft in the fleet. The number of analysis locations per aircraft is determined from the number of stress raisers in the zone of equivalence. The number of aircraft in the fleet is the number of aircraft that will experience the equivalent expected usage.

The probability of fracture is calculated on the basis of the maximum stress that might be encountered in a flight, i.e., on a flight-by-flight basis. Aircraft usage, however, is typically expressed in terms of flight hours or equivalent flight (spectrum) hours. PROF expects time data in terms of hours and converts to number of flights when necessary. This conversion is

done in terms of average hours per flight. Therefore, average hours per flight is a required input to the program.

For the example, it is assumed that there are three of the countersunk rivet holes (Figure 6) on each side of the wing that will experience the same stress history. Thus, there are six analysis locations per aircraft. It is assumed that there are 125 aircraft experiencing the common operational usage and that the average flight is one hour.

3.1.2.2 Crack Size versus Flight Time

Crack growth is inherently a stochastic phenomena. If specimens containing cracks of "constant" size are subjected to a common stress history in the laboratory, a distribution of sizes will result. Further, if different airframes contain cracks of a "constant" size and are subjected to a "common" usage, the resulting distribution of crack sizes will contain significantly more scatter. The increase in scatter is due to the additional variability introduced by the differences in operational loadings actually encountered. To implement a complete stochastic model of the growth of a distribution of cracks in a fleet of aircraft would require a stochastic model for the effect of usage variation as well as a stochastic model for the crack growth process for a fixed stress sequence. The data for such models are currently not available for aircraft applications.

PROF uses a deterministic correlation between spectrum flight hours and crack size as the basis for projecting the growth of the distribution of cracks assumed to be in the population of structural detail. This is accomplished by projecting percentiles of the crack size distribution based on the deterministic "a versus T" relationship for the expected stress sequence. There were three major reasons for implementing this method of modeling crack growth:

- a) The damage tolerance requirements assure that this deterministic crack growth prediction will always be available for known critical locations.

- b) The POF calculated from average usage is the POF for a detail in a randomly selected aircraft of the fleet. The specific usage of any single aircraft is unknown at the time of analysis. If the potential usages for the airframes of the analysis are ranked in severity, a distribution of the severities can be postulated. The expected usage of the DTA analysis represents the average of the distribution of severities. Different percentiles of the severity distribution would produce different "a versus T" curves and different distributions of maximum stress per flight (to be discussed in Subsection 3.2.3). If POF were calculated for these different severity percentiles, a distribution of POF values would be generated. The POF for a randomly selected aircraft would be the mean of this POF distribution, i.e., the POF obtained from the mean usage. Note that POF values can be generated for stress sequences that are representative of the percentiles of the severity distribution, and these could be interpreted in terms of the population of individual aircraft usage.
- c) There are no generally accepted methods for modeling stochastic crack growth and the methods that have been proposed require data that have not been obtained for existing aircraft. There are indications that the added stochastic effect of the growth of cracks of the same size may be of second order when compared to the uncertainty in the crack size distribution in the population. A heuristic analysis of the effects of stochastic crack growth on the crack size distribution is presented in Appendix B.

3.1.2.2.1 Format

Since PROF uses table lookup with interpolation to project the growth of the crack size distribution, the "a versus T" relation is input to PROF in the form of a table of (a,T) data

pairs. PROF requests the name of a file which contains the table. The first row of the file must contain an identification which will appear in the summary output file. The second row of the file must contain the number of (a,T) data pairs which are in the table. The table of (a,T) data pairs must define a single valued function. The first pair in the table must be (0,0) and the last crack size must be greater than or equal to the maximum in the "K/ σ versus a" data file. The "a versus T" filename must end with a ".DAT" extension.

3.1.2.2.2 Example

Example "a versus T" curves for an inner lower wing location on an A/F/T aircraft flying severe and moderate load spectra are presented in Figure 7. For crack sizes larger than 0.005 in., the curves were obtained by digitizing a figure from the aircraft manufacturer's DTA report. For the crack sizes less than 0.005 in., the curves were obtained by back extrapolation using an exponential fit as the shape of the curve for the sizes less than 0.005 in. The fit was obtained as follows.

For $a \leq 0.005$, it was assumed that the "a versus T" curve has an equation given by

$$a = a_0 \exp(bT) \quad (6)$$

The parameter b was estimated from a least squares fit over a range of linear "ln a versus T" (0.005 to 0.028 in. for the severe spectrum and 0.005 to 0.024 in. for the moderate spectrum). It was arbitrarily assumed that $a_0 = 0.0005$. For $a \geq 0.005$, the original T values were increased by the time required for a 0.0005 in. "crack" to grow to 0.005 in. using Equation 6. The adjustment added 2045 and 2330 hours, respectively, for the severe and moderate spectra.

3.1.2.2.3 Comments

In general, the population of cracks being modeled will have a significant proportion with sizes smaller than the minimum

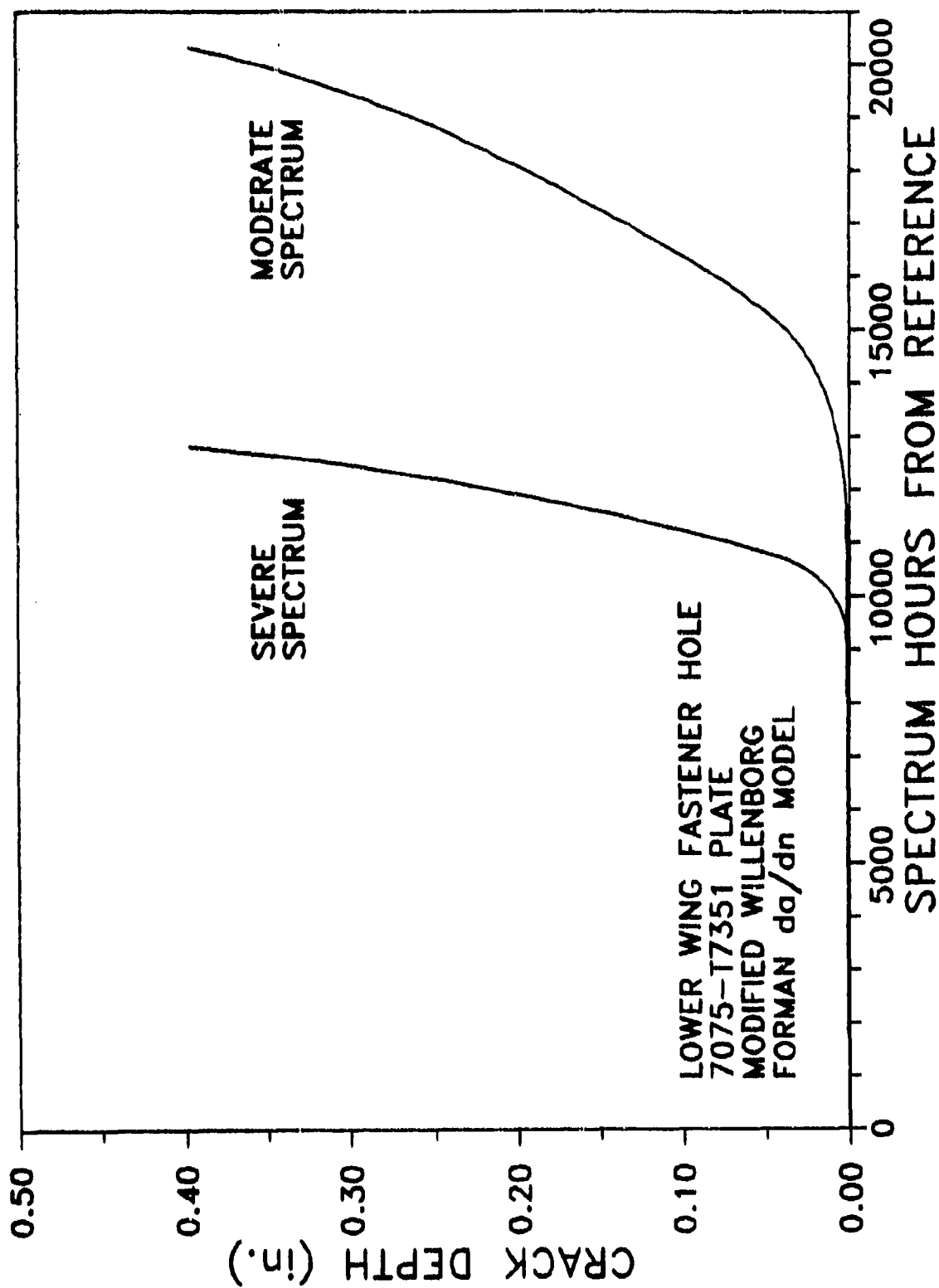


Figure 7. Crack Growth versus Flight Hours.

size considered in damage tolerance analyses. The importance of these small cracks in risk analysis depends on the primary concern. To date, sensitivity studies have shown that these very small cracks have an insignificant effect on POF. However, for long analysis periods, the rapidity of growth of the small cracks does affect the expected number of cracks detected and repaired at a maintenance action. Reasonable care should be taken in accounting for the growth of the small cracks.

Current methods for obtaining crack growth at very small sizes center on the empirical methods associated with durability analyses [7]. These methods are based on an exponential fit to the "a versus T" curve for very small cracks in the expected stress environment. If the crack size distribution (see Subsection 3.2.4 and Appendix C) was obtained as an equivalent flaw size distribution for durability analyses, then crack growth curves that extend to time zero will be available. In the absence of such data for back extrapolation, it is reasonable to assume that the shape of the crack growth curve is exponential [9]. The parameters can be estimated from the smallest cracks for which data are available and a size at time zero. See Subsection 3.2.2.2 for an example of this calculation.

Evidence is accumulating that, at least for aluminum alloys and steels, cracks grow from the first application of a significant stress cycle. Considerable research effort is being expended on modeling the growth of such small cracks (0.0002 to 0.010 in.) [8,18]. It is expected that analytical methods for extending crack growth curves to very short cracks will be available within a reasonable time period.

3.1.2.3 Maximum Stress Distribution

POF is calculated as the probability that an applied stress will exceed the residual strength of the cracked structural detail. For practical purposes, it can be assumed that the stress peak that will cause fracture is the largest peak to be encountered in a flight. Since available data might not extend

to the largest stresses that might be encountered, a consistent basis for extrapolation was required. In PROF, the distribution of this maximum stress peak in a flight is modeled in terms of a Gumbel distribution of extreme values. The following discussion presents the rationale for this choice and a method for estimating the parameters of the model.

In an operational flight, the number and magnitude of the experienced stress peaks are random variables both of which are influenced by the mission being performed. Let $F_{all}(\sigma)$ represent the cumulative distribution function of the magnitude of all stress peaks greater than a threshold for the stratification of the operation being modeled. Let $H(\sigma)$ represent the cumulative distribution function of the maximum stress encountered in a flight. If a flight consists of n stress cycles selected at random from the population described by $F_{all}(\sigma)$ and if σ_{max} represents the largest peak in a flight, then

$$\begin{aligned} H(\sigma) &= P(\sigma_{max} < \sigma) \\ &= P(\text{all } n \text{ peaks} < \sigma) \\ &= [F_{all}(\sigma)]^n \end{aligned} \tag{7}$$

Gumbel [19] showed that for exponential type distributions and large n , Equation 7 can be approximated by

$$H(\sigma) = \exp\{-\exp[-(\sigma-B)/A]\} \tag{8}$$

Flights which contain large stress peaks are usually very active and also contain a large number of peaks. Therefore, this asymptotic relation was incorporated as the model for extrapolating and describing the distribution of the maximum stress per flight.

The parameters of this Gumbel distribution can be estimated as follows. (Numerical examples of this process are presented in Subsection 3.2.2.2.) First, the cumulative distribution of the

maximum stress per flight is estimated from data. Peak stress data will be available as flight-by-flight stress sequences or exceedance curves for the expected usage at the analysis location. If a flight-by-flight stress history is available, the maximum stress in each flight can be extracted and the cumulative distribution function of these maximum stresses per flight is calculated directly as:

$$H(\sigma_i) = n_i / N \quad (9)$$

where n_i is the number of stress maximums less than σ_i and N is the total number of flights. If only an exceedance curve is available for describing the magnitude of the expected stresses for the POF calculation, the exceedance curve must first be converted to the distribution function, $F_{all}(\sigma)$.

$$F_{all}(\sigma_i) = 1 - \lambda(\sigma_i) / \lambda(\sigma_{thr}) \quad (10)$$

where $\lambda(\sigma_i)$ is the number of peak stresses per unit time exceeding σ_i and $\lambda(\sigma_{thr})$ is the number of exceedances per unit time of the stress threshold. Let \bar{n} represent the average number of stress peaks per flight greater than threshold. Then the cumulative distribution of the maximum stress per flight is estimated by

$$F_{max}(\sigma_i) = [1 - \lambda(\sigma_i) / \lambda(\sigma_{thr})]^{\bar{n}} \quad (11)$$

Next note that Equation (8) can be transformed to

$$\ln\{-\ln[-H(\sigma_i)]\} = -\sigma_i/A + B/A \quad (12)$$

A least squares fit of the $(\sigma_i, \ln\{\ln[-H(\sigma_i)]\})$ data pairs will yield estimates of $-1/A$ and B/A . To ensure that the fit is acceptable at the high stress levels of most influence in the POF

computation, only the four or five highest stress ranges in the data should be used in determining the least squares fits. It might be noted that B is the stress that is exceeded in 63 percent of the flights and A is proportional to the steepness of the exceedance probability versus stress curve. The larger the value of A, the less steep the exceedance probability curve (resulting in a larger probability of large maximum stress peaks in a flight). A practical approach to estimating A and B is to vary these parameters until an acceptable fit is obtained for the probability of exceeding the high stress levels which drive the probability of fracture calculation.

3.1.2.3.1 Format

The PROF maximum stress per flight input are the two parameters A and B of the Gumbel asymptotic distribution for maxima of exponential type distributions. Substitution of a different two parameter family of distributions of maximum stress per flight could be readily accomplished.

3.1.2.3.2 Example

Stress data for the example calculation in the A/F/T application were available in the form of flight-by-flight stress sequences. These data were analyzed using both the flight-by-flight and exceedance curve methods to estimate A and B.

Figure 8 presents exceedance curves for moderate and severe usage spectra. The spectra have approximately equivalent exceedance rates at the highest stress peaks but the severe spectra has significantly greater exceedance rates at the lower stress peaks. Table 1 presents the data and analysis for the severe spectra. Both exceedance data and maximum peak per flight data are included in Table 1. In the exceedance rate analysis, the third, fourth and fifth columns are obtained using Equations (10) and (11) and the $\ln\text{-}\ln$ transformation in Equation (12). The calculations for the "observed" maximum stress per flight are more direct, but notice that in Table 1 the data are expressed in terms of the total number of maximum stress peaks per flight

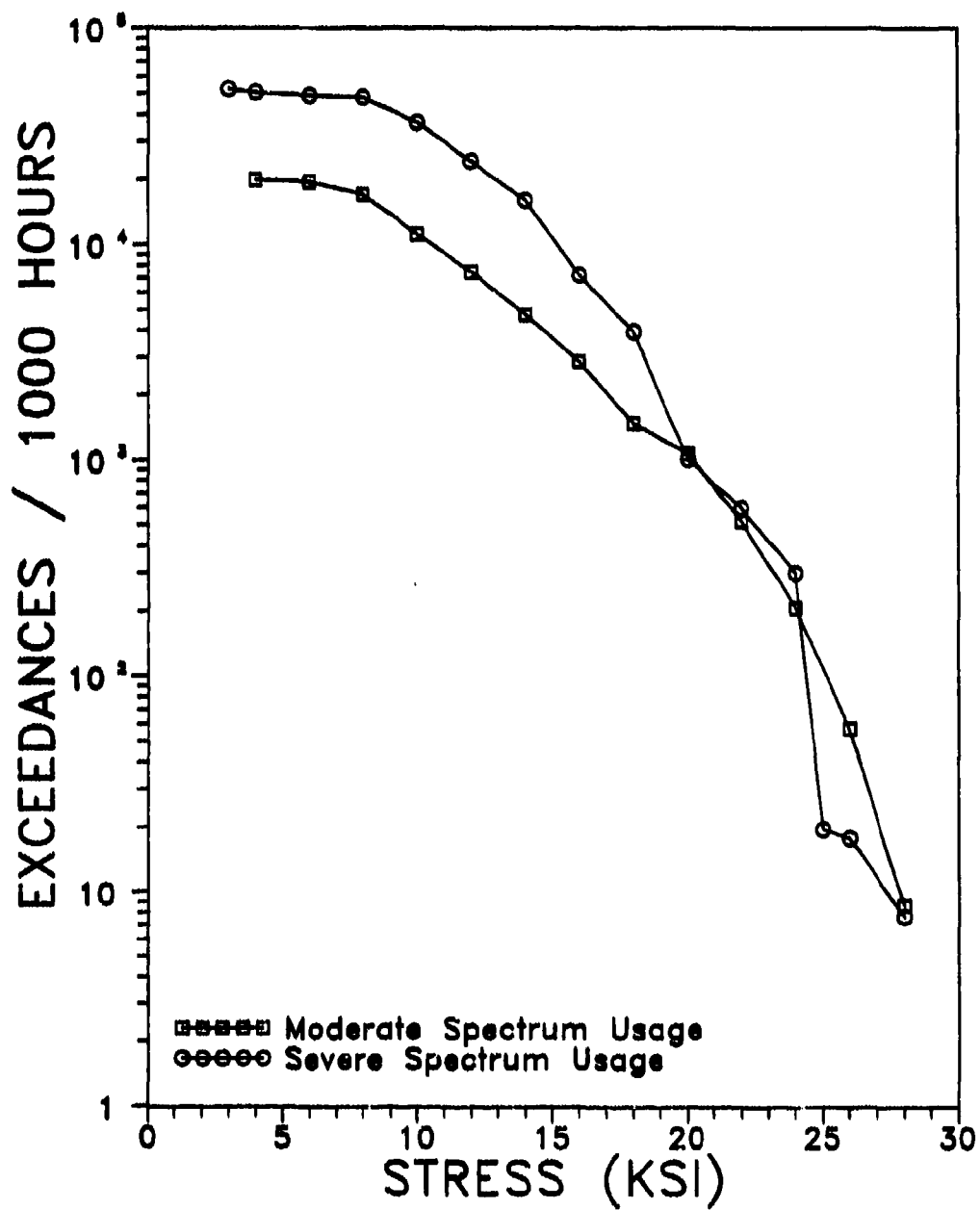


Figure 8. Example Exceedance Curves for A/F/T Usage.

TABLE 1

EXAMPLE CALCULATIONS FOR GUMBEL FIT
TO MAX STRESS PER FLIGHT DISTRIBUTION
A/F/T SEVERE SPECTRUM

Exceedance Data					Maximum Peak/Flight Data		
A	B	C	D	E	F	G	H
Peak Stress KSI	Exceed per Flts	Peak CDF	Estimate CDF max peak per flt	Gumbel Transform of CDF	Observed exceed max peak per flt	Observed CDF max peak per flt	Gumbel Transform CDF
3	61738	0	0		1179	0	
4	59513	0.0360	3E-76	5.157907	1179	0	
6	57566	0.0675	6E-62	4.948210	1179	0	
8	56538	0.0842	6E-57	4.862930	1179	0	
10	43174	0.3006	5E-28	4.140713	1179	0	
12	28547	0.5376	8E-15	3.479961	1179	0	
14	18832	0.6949	0.00000	2.946087	1177	0.00169	1.853054
16	8474	0.8627	0.00044	2.044010	1127	0.04410	1.138210
18	4621	0.9251	0.01709	1.403354	952	0.19253	0.499241
20	1182	0.9808	0.36384	0.010954	628	0.46734	-0.27353
22	701	0.9886	0.55033	-0.51544	450	0.61832	-0.73241
24	352	0.9942	0.74152	-1.20716	244	0.79304	-1.46155
26	21	0.9996	0.98236	-4.02896	21	0.98218	-4.01892
28	9	0.9998	0.99240	-4.87636	9	0.99236	-4.87136

Least squares fits:

	Highest 5	Highest 4	Highest 5	Highest 4
-1/A =	-0.8644	-0.7952	-0.6241	-0.7487
B/A =	13.82	17.22	12.71	15.95
A =	1.51	1.26	1.6	1.34
B =	20.6	21.7	20.36	21.3

COLUMN B FROM SPECTRUM

COLUMN C = $1 - (\text{COLUMN B} / 61738)$ COLUMN D = $\text{COLUMN C}^{52.3}$ (52.3 = AVERAGE PEAKS PER FLIGHT)COLUMN E = $\text{LN}(-\text{LN}(\text{COLUMN D}))$

COLUMN F FROM STRESS SPECTRUM

COLUMN G = $1 - (\text{COLUMN F} / 1179)$ COLUMN H = $\text{LN}(-\text{LN}(\text{COLUMN G}))$

CDF = CUMULATIVE DISTRIBUTION FUNCTION

exceeding the stress level, rather than the number below the stress level. A and B for the two sets of data were obtained from least squares fits of both the highest four and highest five stress levels. The four sets of A and B values are also listed in Table 1.

The fit of the Gumbel distribution using the top four and top five stress values for the severe spectrum are presented in Figure 9. (Using lower stress values may provide a better fit at the lower levels at the expense of a poorer fit at the largest levels. The highest stress levels are the only ones of importance in the fracture probability calculations.) The fits as shown in this figure were calculated from the exceedance data and not the observed distribution of maximum stress per flight. In the numerical example of Section 5, the subjective decision was made to use the fit through the top four stress values of the probabilities obtained from the exceedance count data, i.e., $A = 1.26$ and $B = 21.7$. The notation in PROF for these parameters is ASIG and BSIG.

3.1.2.3.3 Comments

This method of modeling the distribution of maximum stress peaks per flight was checked against several sets of data from A/F/T aircraft usages. The calculation always provided an acceptable fit at the highest stress levels. These are the stress levels which dominate the POF calculation, and it is important that the model fits the data at these levels. The model tends to predict higher probability of occurrences for the smaller stress peaks. Since the observed data actually represent a mixture of mission types, they are not a random sample from a single population. The maximum stresses from flights of less severe mission types are not as large, and they bias the observed distribution of maximum stresses per flight. By restricting the Gumbel fit to the high stress ranges, this bias is avoided at the expense of more conservative POF estimates.

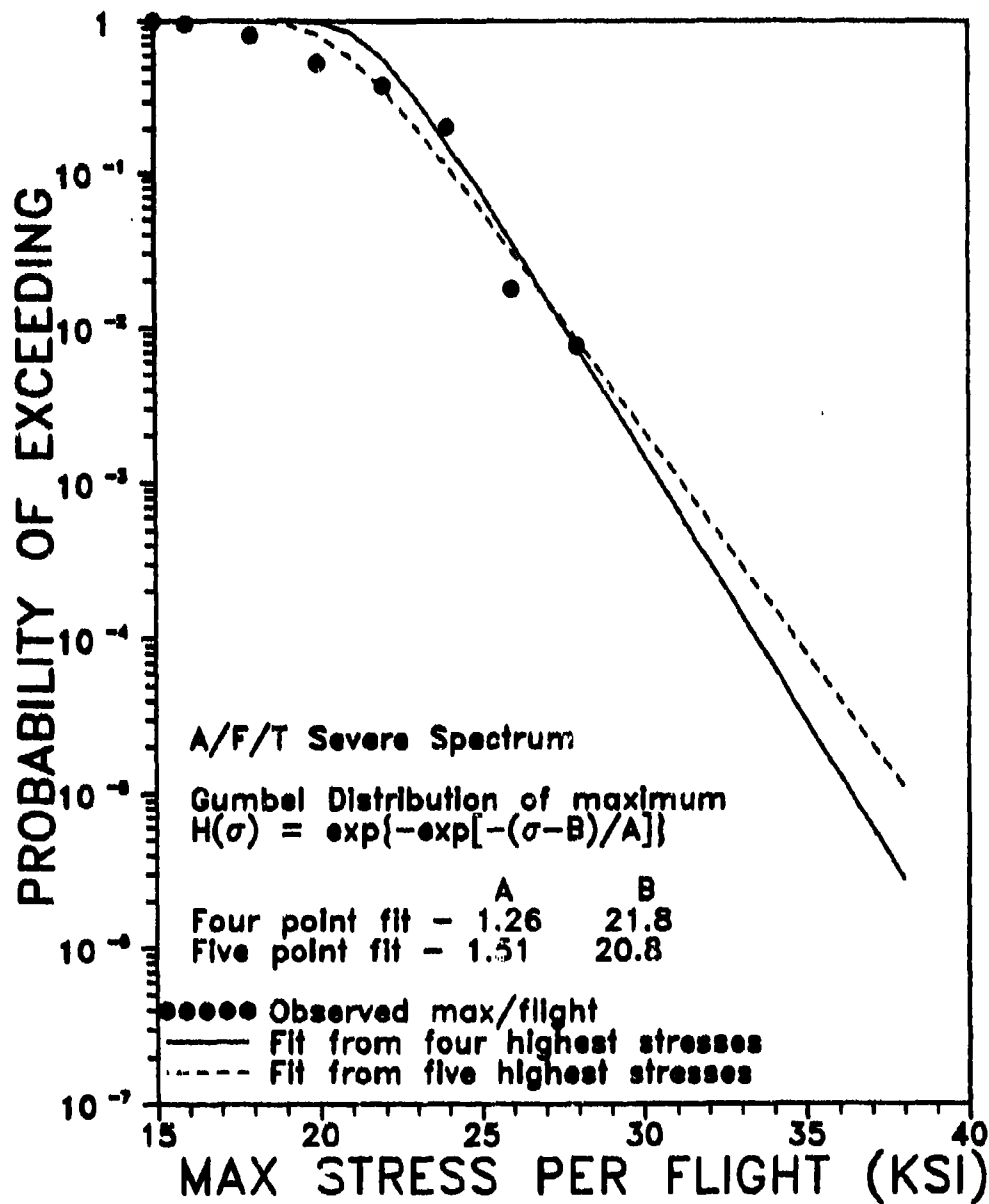


Figure 9. Fit of Gumbel's Extreme Value Distribution to Severe A/F/T Spectrum.

The best estimate of POF can be obtained from stress spectra for each of the mission types. If such data are available, POF can be calculated for each mission type using the distribution of peak stresses for only that mission type. These POFs can then be interpreted for the individual mission types or a weighted average can be calculated using the mission mix percentages. The weighted average would be calculated using a formula analogous to Equation 5 where the p_i are now the percentages of flights for each of the mission types.

3.1.2.4 Initial Crack Size Distribution

The risk analysis calculations of PROF are based on the distribution of the sizes of the cracks that are in the population of structural details at the start of the analysis. There are several approaches to obtain this distribution. The choice of method for a specific application would be primarily determined by the available data. These approaches are discussed in Appendix C. The calculations of PROF are independent of the methods of modeling the initial crack size distribution. PROF requires only that the initial crack size distribution file contains a valid cumulative distribution function.

3.1.2.4.1 Format

The initial crack size data is input to PROF in the form of a table of the cumulative distribution function of the crack sizes at the start of the analysis. There were three reasons for this choice of format:

- a) There are no commonly accepted distributions for modeling crack sizes in a population of structural details. Families with two, three, or four parameters have been used; e.g., the lognormal, Weibull, Johnson S_u , and Weibull Compatible Time-to-Crack-Initiation families [7]. There are also data [6] which suggest that in some applications a mixture of such distributions would be more appropriate than any single family.

- b) After an inspection/repair cycle is completed in the analysis, the crack size distribution is a mixture of unrepaired and repaired crack sizes. This mixture has no general form as it depends on the distribution of the crack sizes at the inspection time, the $POD(a)$ function, and the method for modeling the crack sizes at the sites which were repaired.
- c) Since the "a versus T" relation used to transform the crack size distribution will not preserve the particular model of a family, PROF had to be designed to handle an arbitrary distribution, i.e., one specified by a table of values.

PROF requests the name of a file which contains $(a, F_0(a))$ data pairs, where $F_0(a)$ is the proportion of crack sizes less than or equal to "a" at the start of the analysis. The first line of the file must contain an identification which will appear in the PROF output. The second line must contain the number of $(a, F_0(a))$ data pairs that will follow. Since this distribution will have to be extrapolated, PROF requires the user to provide at least two pairs for which $F_0(a) \geq 0.99$. The filename must contain a ".DAT" extension.

3.1.2.4.2 Example

Figure 10 presents an exceedance distribution (i.e., complement of the cumulative distribution) of equivalent initial crack sizes that are assumed to be representative of the initial quality of the wing location of the example. This crack size distribution is a mixture of the equivalent crack sizes found to be representative of the A-7D aircraft [20] and a uniform distribution of "rogue" flaws. The example distribution assumes that 99.9 percent of the locations have a crack size from a log normal distribution with median crack size of 0.0008 in. and standard deviation (of log crack sizes) of 0.63, and 0.1 percent are from a uniform distribution on the interval of 0 to 0.050 in.

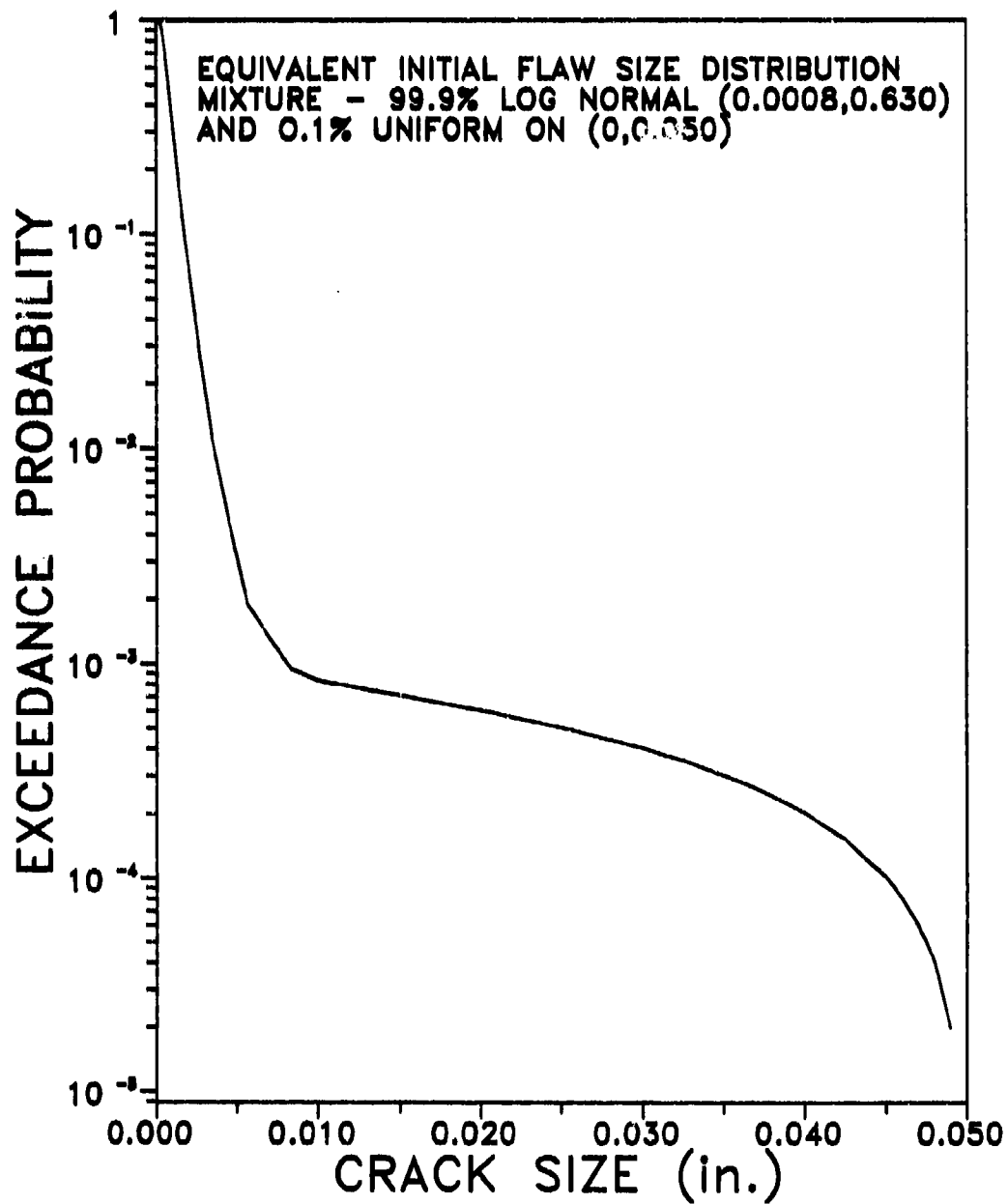


Figure 10. Example Initial Flaw Size Distribution.

3.1.2.4.3 Comments

The initial crack size distribution affects the probability of fracture and the expected cost of maintenance calculations in different ways. Since fracture probabilities will be small in any realistic application, the upper tail of the crack size distribution will dominate the POF calculation. Expected repair costs, on the other hand, will be dominated by the detected cracks. These will come from the crack size ranges that have a higher probability of occurrence, i.e., the mid ranges of the crack size distribution. The distinction is important since it affects the type of data needed to meet different objectives. If the objective of the analysis is limited to evaluations or comparisons of fracture probabilities, then only the upper tail of the crack size distribution will influence the analysis. If repair costs are also being analyzed, the mid ranges of the crack size distribution must also be reasonably modeled.

The crack size distributions are the most difficult PROF input to obtain. The best source of crack size data from a mature fleet is obtained from teardown inspections in which rather complete inspection results are obtained from laboratory inspections of a sample of structural details. These inspections can detect all cracks greater than a known minimum size. Although the crack sizes observed in teardown inspections of elements from different airframes must be adjusted to account for differences in age, this extrapolation would be over reasonably short intervals. Since all of the largest cracks will be detected and the total number of inspected sites is known, the teardown inspection results will provide a valid set of data for estimating at least the upper tail of the crack size distribution.

In the absence of teardown inspections, the crack size distribution will have to be estimated from a) routine inspection results, b) a flaw size based initial quality characterization, c) time to crack initiation distributions, or, d) combinations of all three (Appendix C). Characterizing initial quality in terms

initial crack size distribution. This implies that the analysis would be applicable to operational usage after an inspection at the reference age. The length of usage intervals has typically been set at half the number of flight hours required to grow a crack from the reliably detected crack size to critical size. Other scenarios can be easily evaluated since any interval can be analyzed.

For the example, the inspection times have been determined by the MIL-STD-1530 requirements. Since the initial crack size distribution is an equivalent initial flaw size distribution, the first interval will be at 1100 hours, one-half the time required for a 0.050 in. crack to grow to critical (Figure 7) under the severe spectrum. Subsequent intervals will be set at 900 hours, one-half the time required for a 0.100 in. crack to grow to critical. For the assumed inspection capability, $POD(0.100) = 0.90$ (Subsection 3.3.2).

3.1.3.2 Inspection Capability

Inspection capability is quantified in terms of the probability of detection as a function of the crack size, $POD(a)$. In PROF, $POD(a)$ is modeled by the log-logistic function, which has been found to provide an acceptable fit to both manual and automated inspection reliability data [21,11]. In particular, let a_{min} be the size of the smallest crack that can be detected by the system. Then, $POD(a) = 0$, if $a < a_{min}$ and

$$POD(a) = \left\{ 1 + \exp - \left[\frac{\pi}{\sqrt{3}} \left(\frac{\ln(a - a_{min}) - \mu}{\sigma} \right) \right] \right\}^{-1} \quad (13)$$

where a = size of crack being inspected, $a > a_{min}$,
 μ = natural logarithm of the median detectable crack size - crack size which is detected 50 percent of the time,

σ = scale parameter - larger σ implies flatter POD(a) function and lower detectability at bigger crack sizes.

Equation (13) is essentially equivalent to a cumulative log normal distribution with the same parameters.

Inspection capability is input to PROF by specifying the minimum and median detectable crack sizes and the parameter σ . (PROF refers to σ as the steepness parameter.) The minimum detectable crack size may be a function of the location of the crack or the inspection system. For example, if the crack initiates in the bore of a rivet hole, the inspection system may be physically prevented from detecting the crack until it clears the head of the rivet. Ideally, the inspection system that will be used to inspect the population of details will have been evaluated through an experiment designed to estimate the POD(a) function. More often, the POD(a) function parameters will be based on engineering judgement or by analogy with other inspection situations. The median detectable crack size can often be estimated at the time the inspection method for the detail is determined. The parameter σ can include uncertainty resulting from the inspection process itself and also uncertainty due to the human factors associated with the difficulties of the inspections.

The best estimate of fracture probability will be obtained from using the best estimate of the POD(a) function, the so-called mean POD(a) function. However, any valid POD(a) function can be input to PROF. For example, if the POD(a) function was obtained from an NDE reliability experiment, a lower confidence bound on the POD(a) function would be available. This lower bound could be used as PROF input to provide protection against the potential sampling errors in the POD(a) parameter estimates. Such POF values would be expected to be conservative.

To provide an indication of the relative importance of the parameters of the log-logistic POD(a) function, Figure 11 displays POD(a) for a median detectability of 0.030 in. and σ =

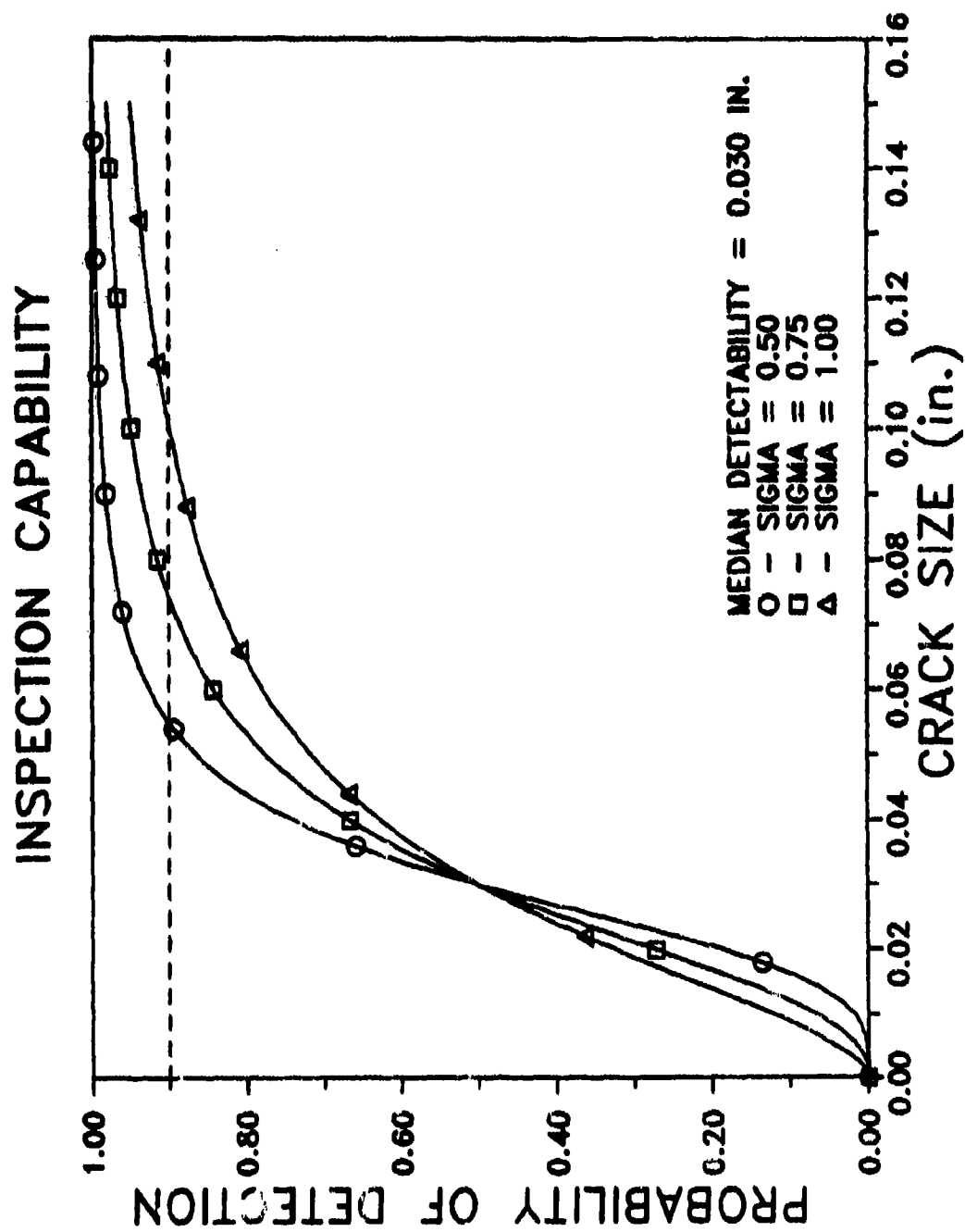


Figure 11. Example Probability of Detection Functions.

0.5, 0.75, and 1.0. In this figure, $a_{\min} = 0$. Introducing a non-zero a_{\min} value merely shifts the zero value of "a" in Figure 11 to a_{\min} . It has become the custom to quantify the capability of an inspection system by the crack length for which the probability of detection is 0.9. Let a_{90} be defined by $\text{POD}(a_{90}) = 0.90$. For selected values of σ , Table 2 presents approximate multipliers of the median detectable crack size a_{50} to obtain a_{90} .

TABLE 2
FACTORS FOR OBTAINING a_{90} FROM a_{50} FOR SELECTED VALUES OF σ

σ	0.25	0.50	0.75	1.00	1.25	1.50
C	1.38	1.90	2.62	3.60	4.97	6.84

$$a_{90} = C \cdot a_{50} \text{ and } C = \exp(1.282 \cdot \sigma)$$

Fully automated eddy current inspection systems with the part removed from the aircraft can have σ values in the range of 0.2 to 0.7, depending on the material and geometry of the parts [22]. Depot inspections using manual and semiautomated eddy current inspections have values of σ greater than 1.0 [20,23].

In the example calculation, it will be assumed that the inspection process will be a semiautomated eddy current inspection without removing the rivet. For the example, $a_{\min} = 0$, the median detectable crack size is 0.050 in. and $\sigma = 0.5$. For this inspection capability, $\text{POD}(0.100) = 0.925$. The inspection schedule as determined from the damage tolerance analysis was based on a reliably detected crack size, a_{NDE} , of 0.100 in.

3.1.3.3 Repair Crack Size Distribution

To account for the cracks in the population which are detected and repaired at an inspection, PROF uses an equivalent repair crack size distribution. The equivalent repair crack size

distribution is analogous to the equivalent initial quality distribution in concept. The repaired flaws can essentially be removed from further analysis by restricting the repair crack size distribution to extremely small sizes. If repair quality is considered to be equivalent to initial quality, the equivalent initial quality distribution can be defined as the repair crack size distribution. Other subjective choices based on engineering judgement can be made. For example, it can be assumed that each repair will leave a flaw equivalent to a crack and that the size of the equivalent cracks will be uniformly distributed between 0 and 0.050 in., i.e., the probability of a large equivalent flaw is equal to the probability of a small equivalent flaw. The uniform distribution is considered to be conservative. The repair crack size distribution has a relatively small effect on the fracture probabilities but can have a major effect on the expected number of cracks detected at repeat inspections.

3.1.3.3.1 Format

The equivalent repair quality distribution is input to PROF as a table of the cumulative distribution of the equivalent crack sizes that are present in those structural details which are repaired at a maintenance cycle. PROF requests the name of a file which contains $(a, F_r(a))$ data pairs, where $F_r(a)$ is the proportion of equivalent crack sizes less than or equal to the crack size, "a". The first line of the file must contain an identification which will appear in the PROF output. The second line must contain the number of $(a, F_r(a))$ data pairs that are in the file. Since this distribution is extrapolated, at least two data pairs for which $F_r(a) \geq 0.99$ must be contained in the file. The filename must contain a ".DAT" extension.

3.1.3.3.2 Example

In the example, it will be assumed that any crack that is detected will lead to a replacement of the wing. Thus, it will be assumed that a repaired wing is as good as new and the repair crack size distribution is the same as the initial crack size

distribution. The equivalent repair crack size distribution to be used in the example, a mixture of a log normal and an exponential, is shown in Figure 10.

3.1.3.3.3 Comments

The equivalent repair crack size distribution is analogous to the equivalent initial crack size distribution for characterizing initial quality. Strictly speaking, the equivalent repair crack size distribution would need to be characterized in the manner described in [7]. This characterization of repair quality has not been researched in any detail. Since the choice of an equivalent repair crack size distribution is arbitrary, only three approaches to selecting this distribution have been used. These are a) repeating the initial quality distribution (repaired is as good as new), b) assuming a uniform distribution of equivalent repair cracks (conservative), and c) removing the repaired structural details from the analysis. The third approach is implemented by defining $F_r(a)$ so that essentially all equivalent repair cracks are too small to grow during the analysis, e.g., $F_r(0.00001) = 0.99999$. Under this third approach, the analysis could be restarted after a maintenance cycle with a reduced number of aircraft in the fleet. (PROF output includes the crack size distribution immediately before and after an inspection. The after inspection crack size distribution can be input as the initial crack size distribution for a new run of the analysis.)

Since the equivalent repair crack sizes will be, in general, relatively small, they tend to have no immediate effect on the fracture probability. However, they can have a significant effect on the expected number of cracks to be detected in future inspections.

3.1.3.4 Maintenance Costs

Expected maintenance costs are not computed in PROF. Rather, PROF provides an output from which expected maintenance costs can be calculated. In particular, structural maintenance

costs comprise the costs of inspecting the population of interest and repairing or replacing cracked details. In addition, the costs of an in-service fracture must also be included. PROF crack size output is expressed in terms of proportions of the total population. It is compatible with the use of unit costs of inspection, repair as a function of crack size, and in-service fracture.

3.1.4 Summary of Input for Example

The order and form in which PROF requests input are illustrated by data for the example problem whose output is presented in Section 6. The example parameter values and filenames in the PROF requested format are presented in Table 3.

3.2 COMPUTATIONS

The computations performed within PROF are centered on the distribution of the crack sizes in the population being modeled as a function of flight hours. The crack size distribution is the basis for the calculation of the three primary outputs: a) the single flight probability of fracture at ten intermediate times between inspections, b) the probability of fracture at any time within each inspection interval, and, c) the distribution of the sizes and the number of cracks expected to be detected at an inspection. This section addresses in a general way, the methods used by PROF in performing the required calculations. Details of the numerical methods actually programmed in PROF are contained in Appendix A.

3.2.1 Modeling the Crack Size Distribution

There are two basic crack population calculations: growing the distribution of cracks from a beginning reference time to an arbitrary time within a period of uninterrupted usage, and quantifying the effect of the inspect and repair-if-necessary actions at the maintenance times. These calculations are addressed in the following subsections.

TABLE 3
PROF INPUT FOR EXAMPLE PROBLEM

DATA TYPE	EXAMPLE INPUT	REFERENCE
1. PEAK STRESS/FLIGHT	ASIG = 1.26 BSIG = 21.7	Section 3.2.3 Figure 9
2. POD FUNCTION	MEDIAN DET. = 0.050 STEEPNESS = 0.5 MINIMUM = 0.0	Section 3.3.2 Figure 11
3. K_c DISTRIBUTION	MEAN = 29.4 STD. DEV. = 2.2	Section 3.1.2
4. AIRCRAFT PARAMETERS	LOCATIONS/AC = 6 # OF AC = 125 AVG FLT LENGTH = 1.0	Section 3.2.1
5. a VS K /SIGMA	GEOMETRY1.DAT (Figure 6)	Section 3.1.1
6. a VS TIME	A-TSEVERE.DAT (Figure 7)	Section 3.2.2
7. INITIAL CRACK SIZES	INITCRAKS.DAT (Figure 10)	Section 3.2.4
8. REPAIR CRACK SIZES	INITCRAKS.DAT (Figure 10)	Section 3.3.3
9. USAGE INTERVALS	T_1 = 1100 hours T_2 = 900 hours T_3 = 900 hours T_4 = 900 hours	Section 3.3.1

3.2.1.1 Growing Population of Crack Sizes

Given an initial distribution of crack sizes at a reference time, T_R , (Subsection 3.1.2.4), the program estimates the distribution of crack sizes at $T_R + \Delta T$ flight hours by projecting the percentiles of the initial crack size distribution using the deterministic crack growth versus flight hours relation (Subsection 3.1.2.2). This calculation is performed in PROF by table look-up. Figure 12 is a schematic of the process. The analytical formulation of the process is as follows.

Let $a_p(T_R)$ represent the p th percentile of the crack size distribution at T_R flight hours, i.e., $P[a < a_p(T_R)] = p$. Let the $a = \phi(T)$ represent the "a versus T" relation (defined for PROF by a table of (a_i, T_i) data pairs). Then the p th percentile of crack size distribution at $T_R + \Delta T$ is given by

$$a_p(T_R + \Delta T) = \phi(\phi^{-1}[a_p(T_R)] + \Delta T) \quad (14)$$

This calculation is repeated for all percentiles in the table which defines the crack size distribution.

3.2.1.2 Maintenance Effect on Crack Size Distribution

At a maintenance action, the population of details are inspected and all detected cracks are repaired. The maintenance action will change the crack size distribution and the change is a function of the inspection capability and the quality of repair. Inspection capability is modeled in terms of the probability of detection as a function of crack size, $POD(a)$. Repair quality is expressed in terms of the equivalent repair crack size distribution, $f_r(a)$. If $f_{\text{before}}(a)$ and $f_{\text{after}}(a)$ represent the density function of crack sizes in the population of structural details before and after a maintenance action, then

$$f_{\text{after}}(a) = P \cdot f_r(a) + [1-POD(a)] \cdot f_{\text{before}}(a) \quad (15)$$

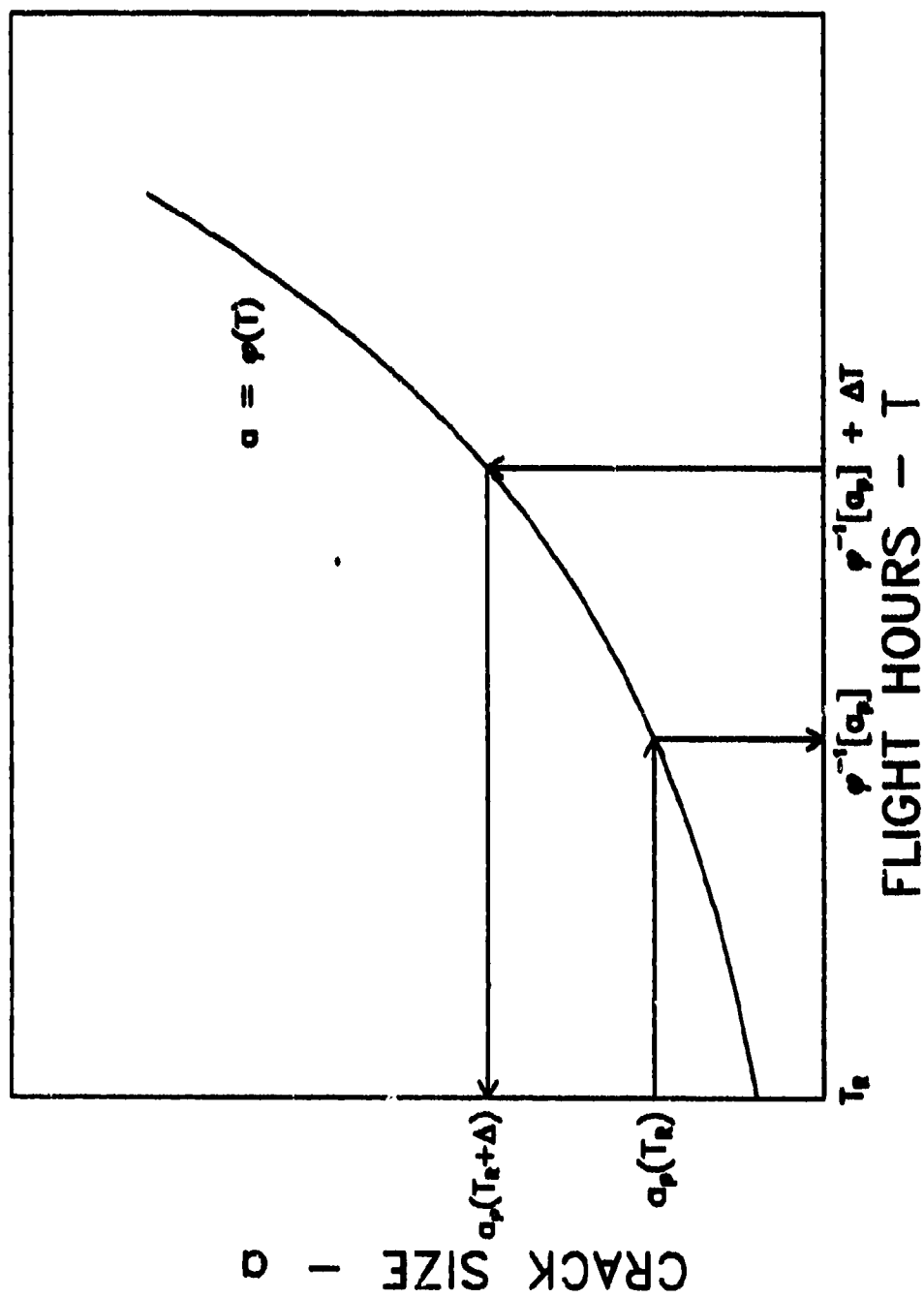


Figure 12. Projection of Percentiles of Crack Size Distribution.

where P is the percentage of cracks that will be detected during the inspection.

$$P = \int_0^{\infty} \text{POD}(a) \cdot f_{\text{before}}(a) \cdot da \quad (16)$$

The post maintenance crack size distribution, $f_{\text{after}}(a)$, is then projected forward for the next interval of uninspected usage. The process is continued for as many inspection intervals as desired.

3.2.2 Probability of Fracture

Safety is quantified in terms of the probability of fracture (POF) due to the maximum stress encountered in a flight. POF is calculated as the probability that the maximum stress encountered in a flight will produce a stress intensity factor that exceeds the critical stress intensity factor for a structural detail. This calculation is performed in two contexts. The single flight POF is the probability of fracture in the flight given that the detail has not fractured previously. This number can be compared to other single event types of risks, such as the risk of death in an automobile accident in an hour of driving. The interval probability is the probability of fracture at any flight between the start of an analysis (reference time of zero or after a maintenance action) and the number of spectrum hours, T. This POF is useful in predicting the expected fractures in a fleet of aircraft in an interval and is required for the expected costs associated with a maintenance schedule. Because significantly more computer time is required to calculate interval POF than single flight POF, interval POF is calculated only for the entire interval between inspections.

3.2.2.1 Single Flight Probability of Fracture

The equation for calculating the probability of fracture at a single stress raiser in a single flight at T hours is given by

$$\begin{aligned}
\text{POF}_E(T) &= \text{Single element POF during flight at } T \text{ hours} \\
&= P[\sigma_{\max} > \sigma_{\text{cr}}(a, K_C)] \\
&= \int_0^{\infty} \int_0^{\infty} f_T(a) \cdot g(K_C) \cdot \bar{H}(\sigma_{\text{cr}}(a, K_C)) \, dK_C da \quad (17)
\end{aligned}$$

where

$f_T(a)$ = probability density function of crack sizes at T flight hours;

$g(K_C)$ = probability density function of the fracture toughness of the material;

$\bar{H}(\sigma_{\text{cr}}(a, K_C)) = P[\sigma_{\max} > K_C / \sqrt{\pi a} \cdot \beta(a)]$, i.e., the probability that the maximum stress in the flight exceeds the critical stress given " a " and K_C .

The single element POF, $\text{POF}_E(T)$, is interpreted as the probability that one of the elements in an airframe with T equivalent flight hours will experience a fracture due to a combination of crack size, fracture toughness, and stress. This calculation is based on the assumption that the size of the crack in the stress raiser of the element and the fracture toughness are independent.

To calculate the single flight probability of a fracture from any one of the k equivalent elements (stress raisers) in a single airframe at T flight hours, $\text{POF}_A(T)$, it is assumed that the fracture probabilities between elements are independent.

Then

$$\text{POF}_A(T) = 1 - [1 - \text{POF}_E(T)]^k \quad (18)$$

$$\approx k \cdot \text{POF}_E(T)$$

Similarly, $POF_F(T)$, the probability of a fracture in any of the N airframes in the fleet as they age through T flight hours, is calculated as

$$POF_F(T) = 1 - [1 - POF_A(T)]^N \quad (19)$$

$$\approx N \cdot POF_A(T)$$

All three of these single flight POFs are calculated at ten equally spaced increments in each usage interval. The results are printed in the summary output report.

3.2.2.2 Interval Probability of Fracture

Fracture can result during any flight in a usage period, and the probability of a fracture during an entire period is required to estimate the expected costs of a fracture. Since the fracture toughness of an element does not change from flight to flight, single flight POFs as obtained above cannot be combined to obtain interval POF. The assumption of independence needed to make this calculation possible is not valid.

An approach to estimating interval POF which accounts for the constancy of fracture toughness over the interval was formulated as follows:

- a) determine the contribution to the total POF from each possible pairing of fracture toughness and crack size at the beginning of the usage interval, say $PF(a, K_C)$;
- b) weight each contribution by the probability of the crack size-fracture toughness combination, say $f(a)da \cdot g(K_C)dK_C$;
- c) sum the weighted contributions over all possible combinations of crack size and fracture toughness.

To calculate the contribution to the total POF from a crack size-fracture toughness pair, the total usage interval is divided into m subintervals. It is assumed that the crack size is essentially constant in a subinterval, and the critical stress is calculated for the crack size of the subinterval and the fracture toughness.

The distribution of maximum stresses in a subinterval is calculated from the distribution of maximum stresses in a flight. The probability of fracture in a subinterval is the probability that the maximum stress exceeds the critical stress for the subinterval. The POFs from the subintervals are combined to obtain the POF of the total usage interval for the initial crack-fracture toughness pair.

The interval POF process is implemented mathematically by the equation:

$$POF_E(I_j) = \int_0^\infty f_j(a) \int_0^\infty g(K_C) \cdot PF(a, K_C) \cdot dK_C da \quad (20)$$

where

$POF_E(I_j)$ = probability of fracture at a single stress raiser in the j th usage interval;

$f_j(a)$ = probability density function of crack sizes at the start of the j th analysis interval;

$g(K_C)$ = probability density function of fracture toughness for the structural detail;

$$PF(a, K_C) = 1 - \prod_{i=1}^m H_{\Delta T}[\sigma_{cr}(a(T_i), K_C)]$$

$H_{\Delta T}[\sigma_{cr}(a(T_i), K_C)]$ = probability that the maximum stress in ΔT flights is less than the critical stress

$$= \{H[\sigma_{cr}(a(T_i), K_C)]\}^{\Delta T}$$

$H(\sigma)$ = Gumbel distribution of max stress per flight;

$$\sigma_{cr}(a(T_i), K_C) = K_C / \sqrt{\pi \cdot a(T_i) \cdot \beta(a(T_i))}$$

ΔT = number of flights in a subinterval;

$$T_i = i \cdot \Delta T, \quad i = 1, \dots, m.$$

Since the computation time to implement equation (20) is both significant and depends on the number of subintervals, the number of flights in a subinterval is a trade-off between accuracy (change of crack size in the subinterval) and computer time. Crack growth per flight is relatively slow over most of the crack sizes in the crack size distribution and long usage intervals imply slow crack growth per flight. Therefore, the number of flights in a subinterval was determined based on the total time in a usage interval as follows:

$$\begin{aligned} 0 < m \cdot \Delta T &\leq 1000, \Delta T = 10 \\ 1000 < m \cdot \Delta T &\leq 2000, \Delta T = 20 \\ 2000 < m \cdot \Delta T &\leq 3000, \Delta T = 30 \\ &\text{etc.} \end{aligned}$$

The sensitivity of the interval POF to this method for determining the number of flights in a subinterval was evaluated. It was concluded that changes in the interval POF from using smaller subintervals would be practically negligible.

Interval fracture probabilities for the aircraft and for the fleet are calculated using equations analogous to equations (18) and (19), respectively.

3.2.3 Expected Maintenance Costs

Given the predicted crack size distribution at the time, T_j , of an inspect/repair maintenance action and the $POD(a)$ function, the expected number and sizes of the cracks that will be detected can be calculated. In particular, PROF calculates the cumulative proportion of cracks that will be detected as a function of crack size as

$$P(a_i) = \int_0^{a_i} POD(a) \cdot f_{\text{before}}(a) \cdot da \quad (21)$$

The proportion of detected cracks in the arbitrary range defined by $\Delta a_i = a_{i+1} - a_i$ is given by

$$P(\Delta a_i) = P(a_{i+1}) - P(a_i) \quad (22)$$

Expected costs of maintenance are not calculated in PROF. However, PROF output can be used to estimate the expected costs of a maintenance scenario (as defined by flight hours between inspections, inspection capability, and repair quality). If the total population being modeled comprises k details in each of N airframes, then the expected number of cracks to be repaired at T_j between sizes a_i and a_{i+1} is $k \cdot N \cdot P(\Delta a_i)$. If C_i represents the cost of repairing a crack in size range i , C_F represents the cost of a fracture, and I represents the cost of inspecting each detail, then the expected costs of fracture and repairs in the usage interval are given by

$$E_j(C) = \text{POF}(T_j) \cdot N \cdot C_F + k \cdot N \cdot [I + \sum_i P(\Delta a_i) \cdot C_i] \quad (23)$$

Summing over usage intervals (maintenance periods) yields the total expected maintenance costs.

3.3 EXAMPLE OUTPUT

PROF output comprises three types of information: a screen plot, a tabular summary file, and data files. At the end of the calculations, PROF executes a plotting routine called PROFPLOT. If the system computer graphics library contains PLOT-10 (w/AGII), PROFPLOT produces a screen plot of the single stress raiser, single flight POF versus flight hour data. Note also that PROFPLOT does not support all terminals. Figure 13 is the screen plot of the example analysis whose input was defined in Section 3.1.

The report file summarizes the results of the PROF run and contains the following information:

- a) a summary of the input data either in the form of file names and the file description or the parameter values;

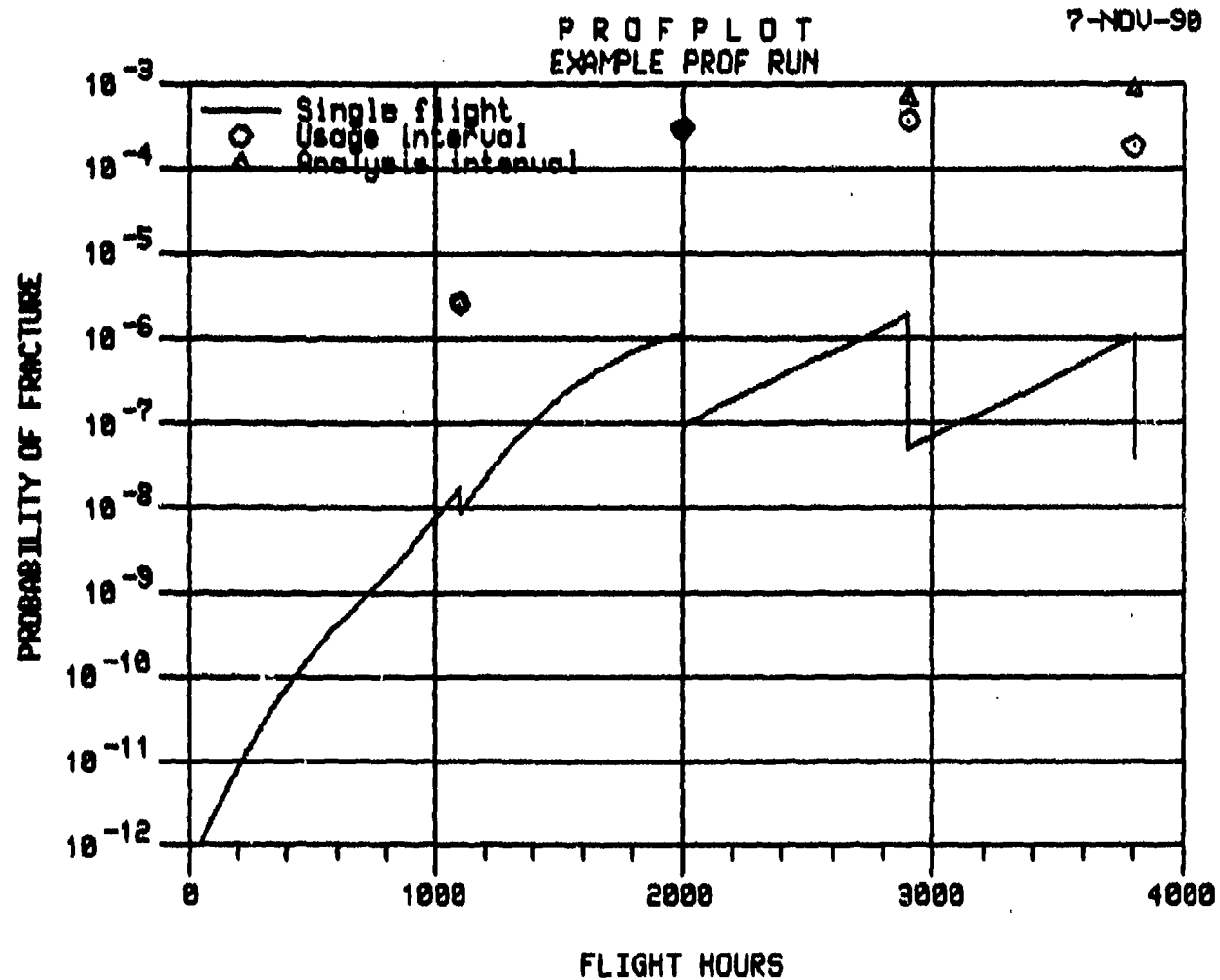


Figure 13. Screen Plot of Example Analysis - Single Detail POF.

- b) single flight POF values for single details, single airframes and total fleet at ten time intervals between each inspection;
- c) percent of inspection sites at which cracks are expected to be detected at each inspection;
- d) POF values for each usage interval for single details, single airframes and total fleet;
- e) POF values for the total analysis interval (0 to T) for single details, single airframes, and total fleet;
- f) crack size data at each inspection/repair - the crack size distribution before the inspection and after the cracks are repaired, the cumulative proportion of detected cracks, and the cumulative distribution of the sizes of the detected cracks.

Table 4 presents the summary report for the example analysis. To conserve space, only the crack size data for the third inspection are included in the table.

PROF also writes data files which contain the single flight and interval POF values and the crack size distribution data. These files can be used as plot files on the user's system. The after inspection crack size distribution files can also be used to reinitiate PROF if an analysis is desired for a set of conditions that are not constant throughout the total analysis interval.

TABLE 4
EXAMPLE PROF REPORT

7-NOV-90
EXAMPLE_REPORT.DAT

PROBABILITY OF FRACTURE REPORT

EXAMPLE PROF RUN

SUMMARY OF TABLES USED IN ANALYSIS

A-VS-K/SIGMA

Filename: GEOMETRY1

a VS K/SIGMA - A/T/C AIRCRAFT, INNER LOWER WING LOCATION

A-VS-TIME

Filename: A-TSEVERE

a VS T - A/T/C AIRCRAFT, LOWER INNER WING, SEVERE SPECTRUM

Initial Crack Size Distribution

Filename: INITCRACKS

Mix of $\ln(.0008, .63)$ and Uniform (0-.050), $P=0.001$

Repair Crack Distribution

Filename: INITCRACKS

Mix of $\ln(.0008, .63)$ and Uniform (0-.050), $P=0.001$

PEAK STRESS PER FLIGHT DISTRIBUTION PARAMETERS

ASIG: 1.26

BSIG: 21.70

PROBABILITY OF DETECTION PARAMETERS

Median Detectability: 0.050

Steepness: 0.57

Smallest Detectable Crack: 0.000

KIC DISTRIBUTION PARAMETERS

Mean: 29.400

Standard Deviation: 2.200

AIRCRAFT PARAMETERS

Analysis Locations Per Aircraft: 6

Number of Aircraft: 125

Avg flight duration (hrs): 1.0000

TABLE 4 (continued)
PROBABILITY OF FRACTURE REPORT

EXAMPLE PROF RUN

SINGLE FLIGHT PROBABILITIES

FLIGHT HOURS	MEDIAN CRACK SIZE	SINGLE DETAIL POF	SINGLE AIRCRAFT POF	FLEET WIDE POF	% OF CRACKS FOUND DURING INSPECTION
0.0	0.0008	0.1000E-11	0.2754E-11	0.3442E-09	
120.0	0.0010	0.3003E-11	0.1802E-10	0.2252E-08	
240.0	0.0010	0.1383E-10	0.8300E-10	0.1038E-07	
360.0	0.0010	0.4937E-10	0.2962E-09	0.3703E-07	
480.0	0.0010	0.1488E-09	0.8928E-09	0.1116E-06	
600.0	0.0010	0.3931E-09	0.2359E-08	0.2948E-06	
720.0	0.0010	0.8807E-09	0.5284E-08	0.6605E-06	
840.0	0.0010	0.2102E-08	0.1261E-07	0.1576E-05	
960.0	0.0010	0.5465E-08	0.3279E-07	0.4099E-05	
1080.0	0.0010	0.1422E-07	0.8531E-07	0.1066E-04	
1100.0	0.0010	0.1683E-07	0.1010E-06	0.1263E-04	1.79
1100.0	0.0010	0.8529E-08	0.5118E-07	0.6397E-05	
1190.0	0.0010	0.2063E-07	0.1238E-06	0.1547E-04	
1280.0	0.0010	0.4424E-07	0.2654E-06	0.3318E-04	
1370.0	0.0010	0.8640E-07	0.5184E-06	0.6480E-04	
1460.0	0.0010	0.1850E-06	0.9298E-06	0.1162E-03	
1550.0	0.0010	0.2612E-06	0.1567E-05	0.1959E-03	
1640.0	0.0010	0.3881E-06	0.2328E-05	0.2910E-03	
1730.0	0.0010	0.5499E-06	0.3300E-05	0.4124E-03	
1820.0	0.0010	0.7359E-06	0.4415E-05	0.5518E-03	
1910.0	0.0010	0.9289E-06	0.5573E-05	0.6964E-03	
2000.0	0.0011	0.1740E-05	0.6838E-05	0.8544E-03	11.00
2000.0	0.0011	0.9104E-07	0.5462E-06	0.6828E-04	
2090.0	0.0011	0.1262E-06	0.7573E-06	0.9466E-04	
2180.0	0.0011	0.1746E-06	0.1048E-05	0.1309E-03	
2270.0	0.0011	0.2409E-06	0.1445E-05	0.1807E-03	
2360.0	0.0011	0.3215E-06	0.1929E-05	0.2411E-03	
2450.0	0.0011	0.4329E-06	0.2597E-05	0.3246E-03	
2540.0	0.0011	0.5705E-06	0.3423E-05	0.4276E-03	
2630.0	0.0011	0.7526E-06	0.4516E-05	0.5643E-03	
2720.0	0.0011	0.9996E-06	0.5998E-05	0.7494E-03	
2810.0	0.0011	0.1355E-05	0.8132E-05	0.1016E-02	
2900.0	0.0011	0.1889E-05	0.1133E-04	0.1416E-02	7.44
2900.0	0.0011	0.4961E-07	0.2977E-06	0.3721E-04	
2990.0	0.0011	0.6980E-07	0.4188E-06	0.5235E-04	
3080.0	0.0011	0.9444E-07	0.5667E-06	0.7083E-04	
3170.0	0.0011	0.1241E-06	0.7444E-06	0.9305E-04	
3260.0	0.0011	0.1644E-06	0.9862E-06	0.1233E-03	
3350.0	0.0011	0.2148E-06	0.1289E-05	0.1611E-03	
3440.0	0.0011	0.2870E-06	0.1722E-05	0.2152E-03	
3530.0	0.0011	0.3849E-06	0.2310E-05	0.2887E-03	
3620.0	0.0011	0.5276E-06	0.3166E-05	0.3956E-03	
3710.0	0.0011	0.7355E-06	0.4413E-05	0.5515E-03	
3800.0	0.0011	0.1063E-05	0.6376E-05	0.7967E-03	5.74
3800.0	0.0011	0.3940E-07	0.2364E-06	0.2955E-04	

TABLE 4 (continued)

7-NOV-90
EXAMPLE_REPORT.DAT

PROBABILITY OF FRACTURE REPORT

EXAMPLE PROF RUN

USAGE INTERVAL PROBABILITIES

FLIGHT HOURS AT INSPECTION	SINGLE DETAIL POF	SINGLE AIRCRAFT POF	FLEET WIDE POF	% OF CRACKS FOUND DURING INSPECTION
1100.0	0.2633E-05	0.1580E-04	0.1973E-02	1.79
2000.0	0.2927E-03	0.1755E-02	0.1971E+00	11.00
2900.0	0.3691E-03	0.2213E-02	0.2419E+00	7.44
3800.0	0.1853E-03	0.1111E-02	0.1298E+00	5.74

ANALYSIS INTERVAL PROBABILITIES

FLIGHT HOURS AT INSPECTION	SINGLE DETAIL POF	SINGLE AIRCRAFT POF	FLEET WIDE POF
1100.0	0.2633E-05	0.1580E-04	0.1973E-02
2000.0	0.2953E-03	0.1771E-02	0.1987E+00
2900.0	0.6643E-03	0.3979E-02	0.3925E+00
3800.0	0.8495E-03	0.5086E-02	0.4713E+00

TABLE 4 (concluded)

7-NOV-90
EXAMPLE_REPORT.DAT

PROBABILITY OF FRACTURE REPORT

EXAMPLE PROF RUN

CRACK SIZE DATA
3rd Inspection

CRACK SIZE	PRE-INSPECTION CUMULATIVE DISTRIBUTION	CUMULATIVE PROPORTION DETECTED	CUMULATIVE DISTRIBUTION OF DETECTED CRACKS	POST-INSPECTION CUMULATIVE DISTRIBUTION
0.0010222	0.0001010	0.0000	0.0000	0.0479
0.0010222	0.0010010	0.0000	0.0000	0.0488
0.0010222	0.0099930	0.0000	0.0000	0.0578
0.0010222	0.0249790	0.0000	0.0000	0.0727
0.0010222	0.0499550	0.0000	0.0000	0.0977
0.0010764	0.0999070	0.0000	0.0000	0.1502
0.0010764	0.1498580	0.0000	0.0000	0.2002
0.0010764	0.1998090	0.0000	0.0000	0.2501
0.0010764	0.2997110	0.0000	0.0000	0.3500
0.0010764	0.4995160	0.0000	0.0000	0.5498
0.0011120	0.5555467	0.0000	0.0000	0.6076
0.0012033	0.6993220	0.0000	0.0001	0.7541
0.0013590	0.7683842	0.0000	0.0001	0.8278
0.0014285	0.7992270	0.0000	0.0001	0.8601
0.0015360	0.8026419	0.0000	0.0001	0.8658
0.0017930	0.8108093	0.0000	0.0001	0.8777
0.0022550	0.8254918	0.0000	0.0001	0.8961
0.0027500	0.8412229	0.0000	0.0001	0.9137
0.0030004	0.8491800	0.0000	0.0001	0.9220
0.0034650	0.8514730	0.0000	0.0001	0.9250
0.0056060	0.8620390	0.0000	0.0002	0.9363
0.0083300	0.8754822	0.0000	0.0005	0.9498
0.0100000	0.8837238	0.0001	0.0011	0.9580
0.0131228	0.8991350	0.0002	0.0031	0.9732
0.0200000	0.9033026	0.0004	0.0048	0.9773
0.0300000	0.9093625	0.0010	0.0132	0.9827
0.0400000	0.9154225	0.0025	0.0331	0.9873
0.0450000	0.9184525	0.0036	0.0484	0.9892
0.0955656	0.9490950	0.0255	0.3425	0.9980
0.1481335	0.9740800	0.0489	0.6578	0.9995
0.1867196	0.9890790	0.0636	0.8550	0.9999
0.2616883	0.9981130	0.0726	0.9753	0.9999
0.2817686	0.9990660	0.0735	0.9881	1.0000
0.2857318	0.9992000	0.0736	0.9899	1.0000
0.2931395	0.9994000	0.0738	0.9925	1.0000
0.3001033	0.9996000	0.0740	0.9952	1.0000
0.3249653	0.9998000	0.0742	0.9979	1.0000
0.3439904	0.9999000	0.0743	0.9992	1.0000

This page is left blank.

SECTION 4

SENSITIVITY ANALYSIS

Eight of the nine PROF input items can significantly effect the output of PROF. This subsection presents the results of an analytical study designed to evaluate the sensitivity of the PROF output to variations in the input. Since some of the input is defined by actions that are taken in the management of the fleet, trade-off studies reflecting the results of specific actions are also evaluated.

The analyses were performed using representative input from a wing location (WS27) of a replacement wing on the T-38 aircraft. The baseline conditions for the analysis are defined in Subsection 4.1. Although there is overlap, the input were categorized as being determined by design (material/geometry), usage, or force management decisions. Subsection 4.2 presents the results of the sensitivity analysis for each of these three categories of input.

4.1 BASELINE CONDITIONS

Figure 5 presented a list of the various categories and data input elements required by PROF. To test the sensitivity to these elements, representative data from a critical location on the lower wing skin of the T-38 aircraft was selected to represent the baseline condition.

WS27 is the designation for the population of lower wing skin fastener holes at the 44% spar. There are three such holes on each side of the airframe, Figure 14, [24]. All six holes are assumed to be exposed to the same stress sequences during usage. Because of a mission change which increased stress levels at WS27, the fleet was retrofit with new wings. The analyses of this report are performed using the specifications and damage tolerance results from the new (-29) wing. The T-38 experiences two distinct usages, Air Training Command (ATC) and Lead-In-Fighter (LIF). For WS27, the LIF usage is more severe.

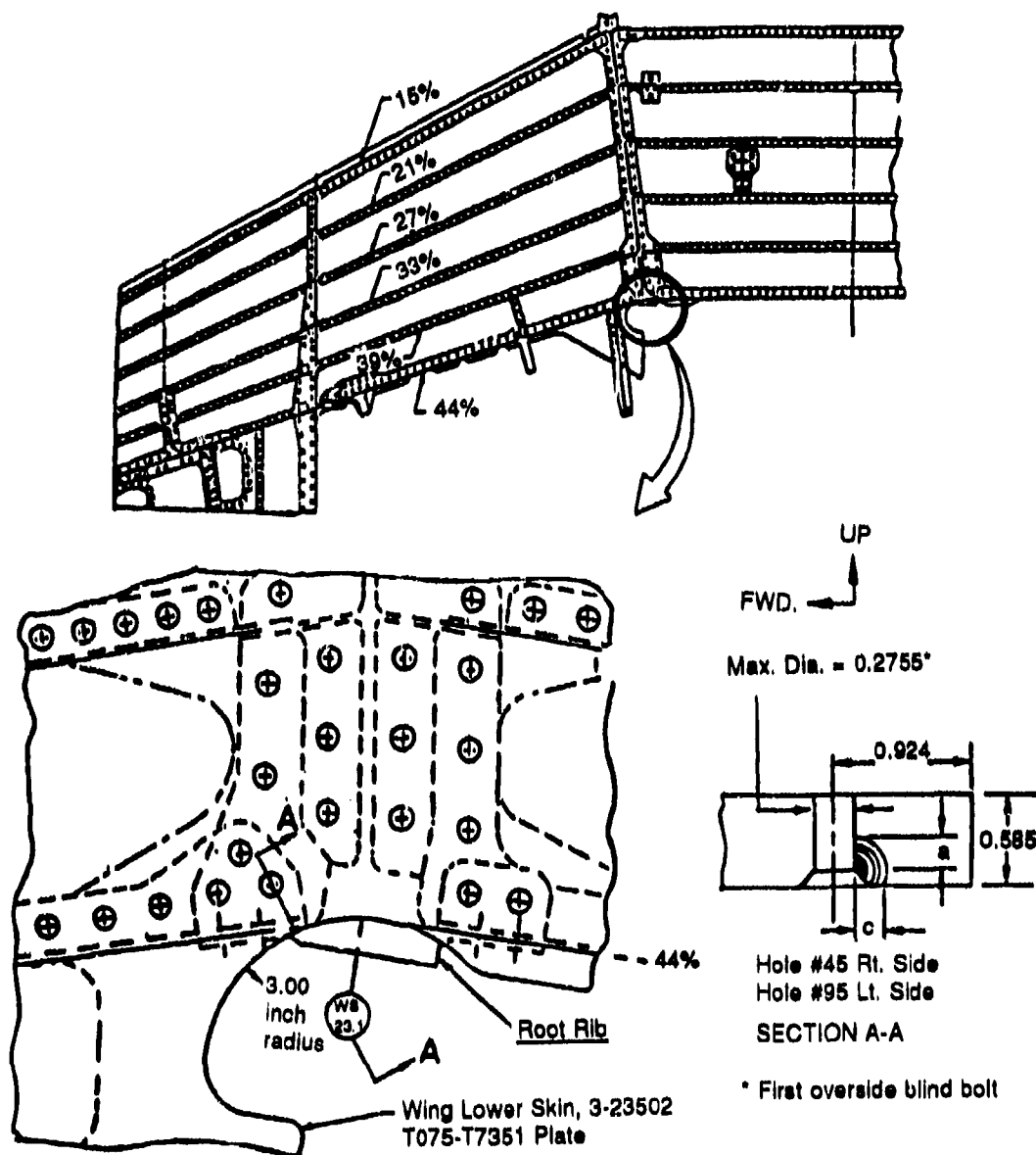


Figure 14. Geometrical Description of WS27, the Lower Wing Skin Fastener Holes Located at the 44% Spar of the -29 Wing.

Representative conditions for the approximately 125 aircraft that experience the LIF usage will be used as the baseline.

4.1.1 Material/Geometry Data

There are two types of data covered in this category - the stress intensity factor and the fracture toughness. The stress intensity factor solution for cracks initiating at the corner of the countersink is given in Figure 15. For this configuration and the maximum stresses per flight of baseline expected usage (subsection 4.1.2), fracture would occur at crack sizes less than 0.5 in. Cracks initiating at other sites down the bore of the hole are considered in the sensitivity analyses.

The -29 wing is made of 7075-T7351 aluminum alloy plate and is 0.585 in. thick at WS27. For this thickness, the fracture toughness can be characterized by the plane strain fracture toughness, K_{IC} . The mean and standard deviation of K_{IC} for 7075-T7351 are listed at 29.4 and 2.2 KSI $\sqrt{\text{in.}}$, respectively, in the Damage Tolerant Design Handbook, Table 8.9.2.1 [10]. The sensitivity to fracture toughness will be tested by arbitrary changes to these values to reflect sampling variation in their estimation.

4.1.2 Aircraft/Usage Category Data

There are four types of data in the aircraft/usage category. The first of these define the number of analysis locations in each aircraft and the number of aircraft in the fleet. For WS27, there are six locations in each of the 125 aircraft. These numbers will not be varied in the sensitivity analysis as they are known exactly and are not variable in any trade-off studies.

The second data type defines the crack size distribution at the start of the analysis. The sensitivity studies for WS27 will begin at zero spectrum hours since new wings were installed on the airplanes. Accordingly, the initial crack size distribution will be assumed to be an equivalent initial flaw size

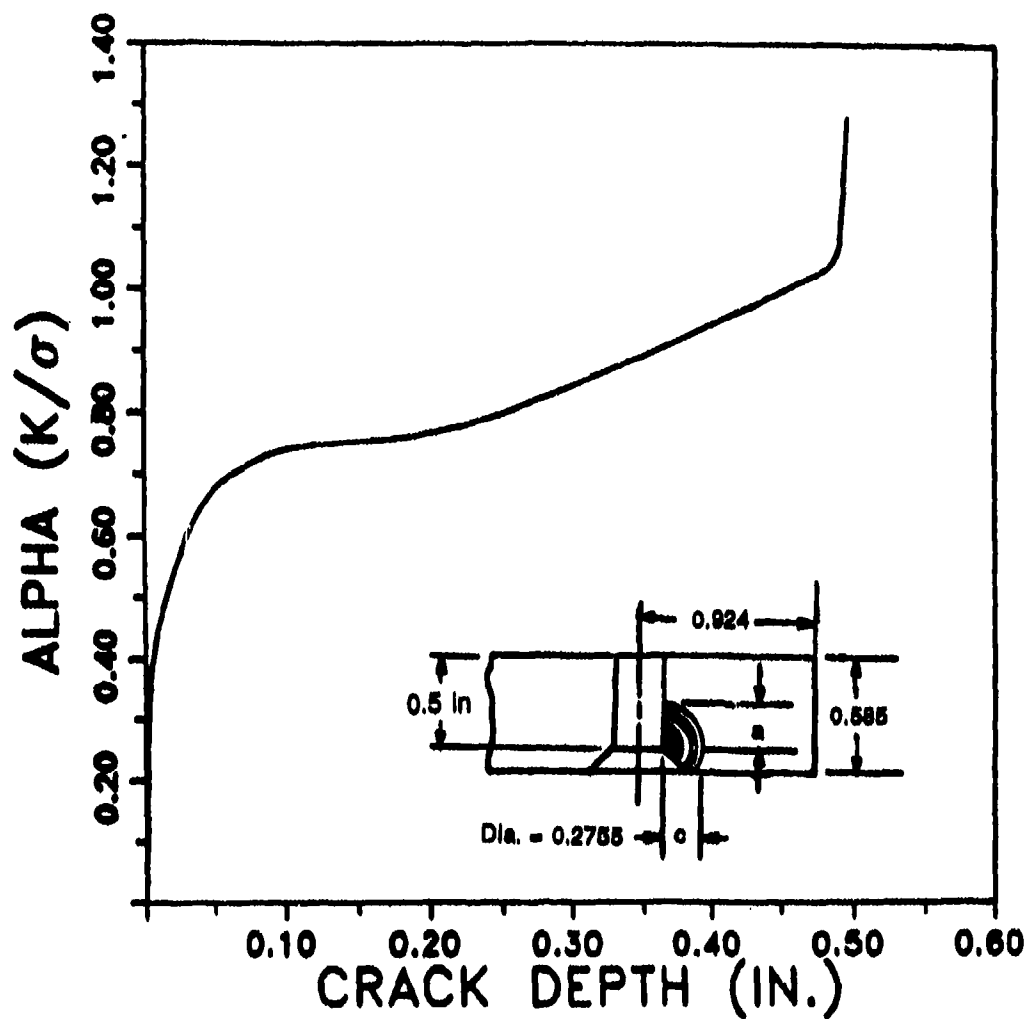


Figure 15. Baseline Geometry Fastener for WS27.

distribution even though this method of characterizing durability was not used in the damage tolerance of the wing. The baseline equivalent initial flaw size distribution will be a mixture with 99.9% of the equivalent initial cracks from a log normal distribution with median of 0.0008 in. and standard deviation of 0.63. The remaining 0.001% of the cracks will be uniformly distributed on the interval 0 to 0.050 in. This distribution is shown in Figure 16. The lognormal (0.0008,0.63) was determined to be a reasonable model for equivalent initial flaw sizes in the A-7 aircraft. The one in a thousand cracks between 0 and 0.050 in. was introduced to allow for the rare possibility of a much larger initial flaw. (It should be noted that these fastener holes in the -29 wing were cold worked. The effect of this cold working was not accounted for in the crack growth analyses or in this characterization of initial quality.)

The third data type of this category defines the fatigue crack growth as a function of usage time. The baseline crack growth ("a versus T") curve for WS27 is presented in Figure 17 for the LIF spectrum. This curve was obtained from a modified Willenborg model with parameters as given in [24]. Sensitivity of PROF to the "a versus T" relation can only be investigated in conjunction with changes related to the stress intensities or the stress sequences which drive the crack. For example, changes in the scaling of the maximum stress in the spectrum causes changes in both the "a versus T" relation and the distribution of the maximum stress per flight. Similarly, changes in the crack initiation site cause changes in the stress intensity factor and the "a versus T" relations. The changes resulting from the scaling of the maximum stress will be considered sensitivity to "a versus T." The joint effect with stress intensity will be considered in the crack geometry sensitivity analysis.

The fourth data type is the stochastic model of the maximum stress per flight of the expected usage. Figure 18 presents the Gumbel fit to the distribution of the maximum stress per flight for the stress sequence at WS27 of the LIF spectrum. The

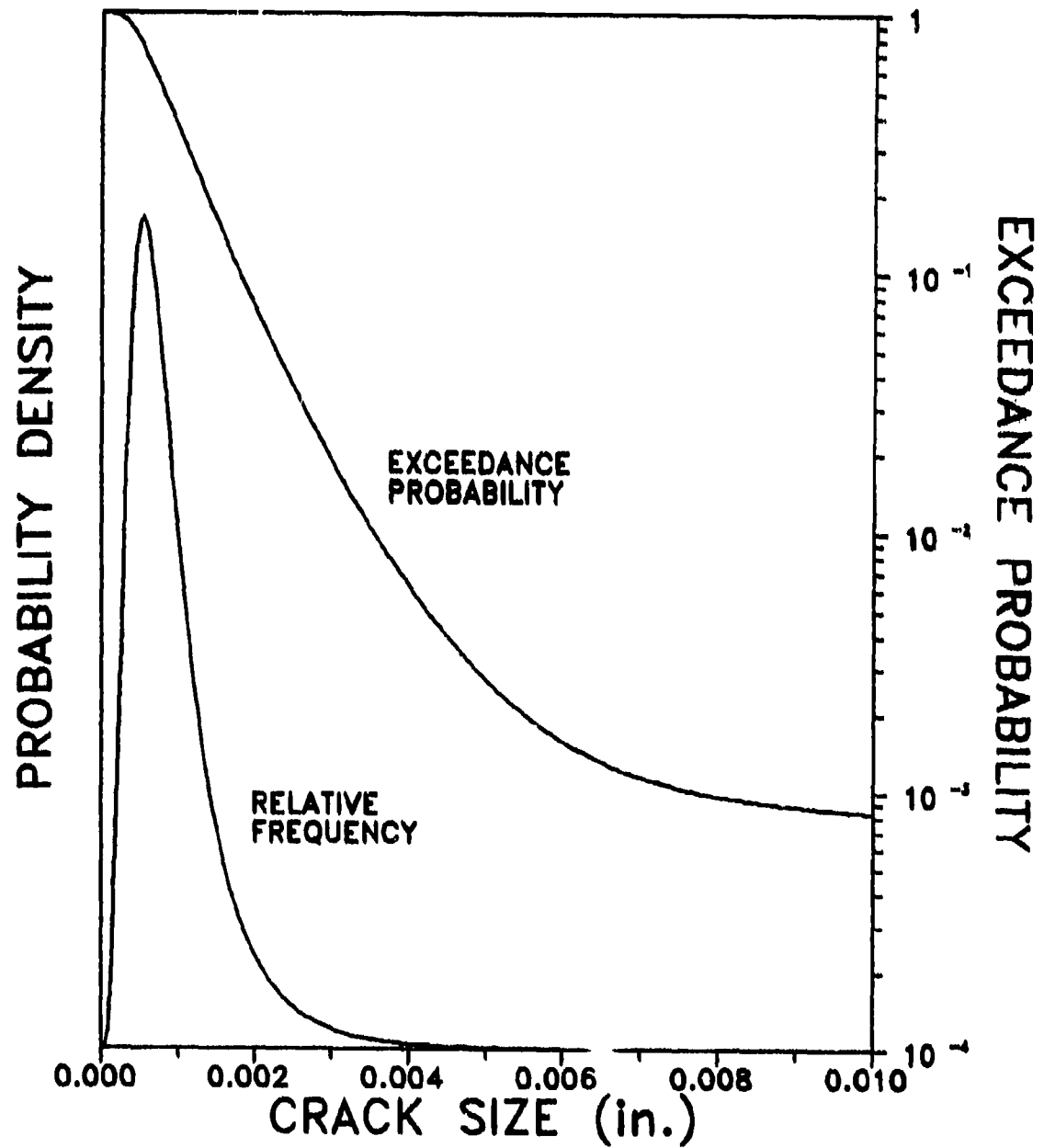


Figure 16. Baseline Distribution of Initial Crack Sizes - Mixture of Log Normal EIFS and Uniform (0,0.050).

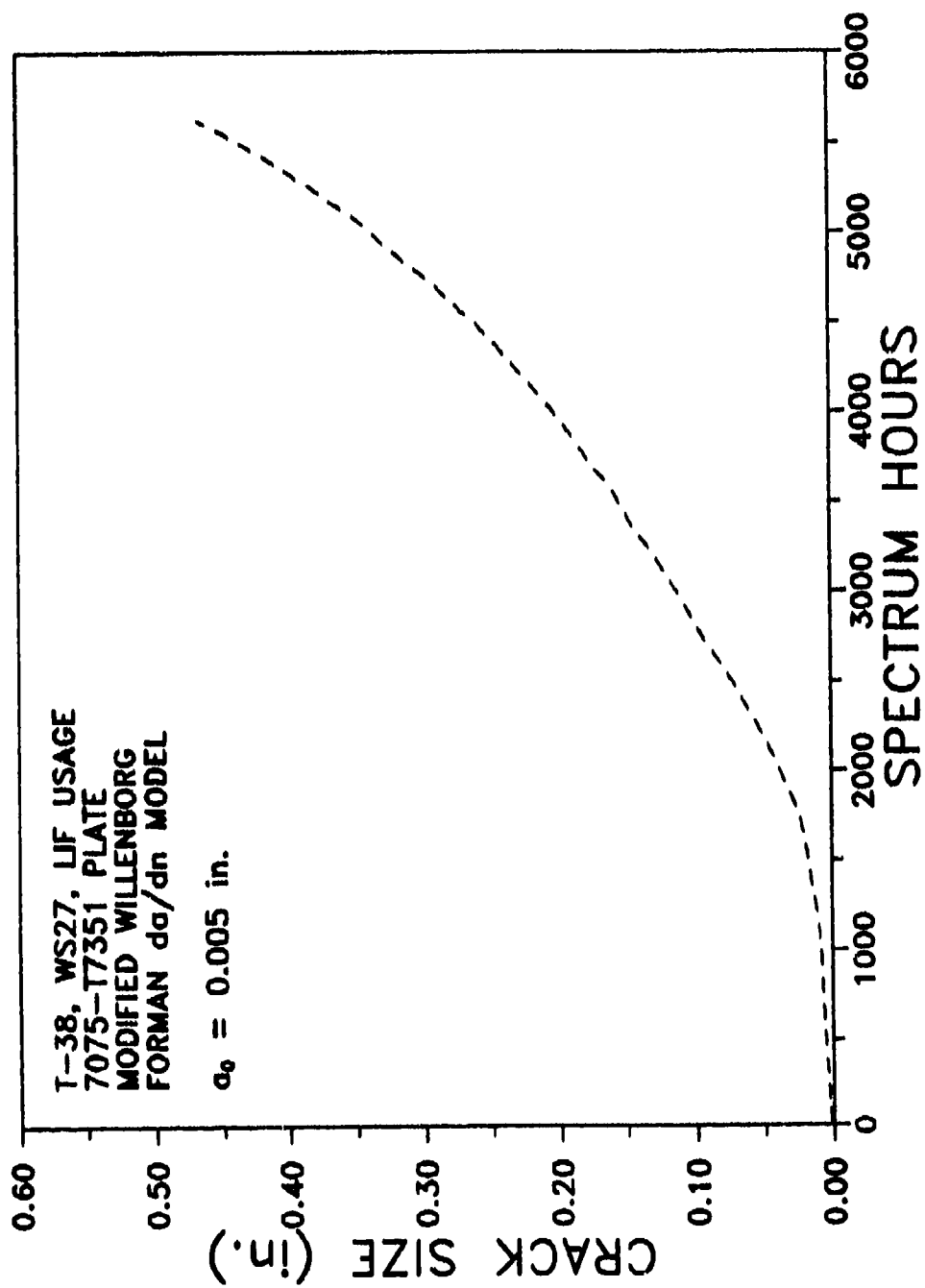


Figure 17. Predicted Crack Growth for Baseline Conditions.

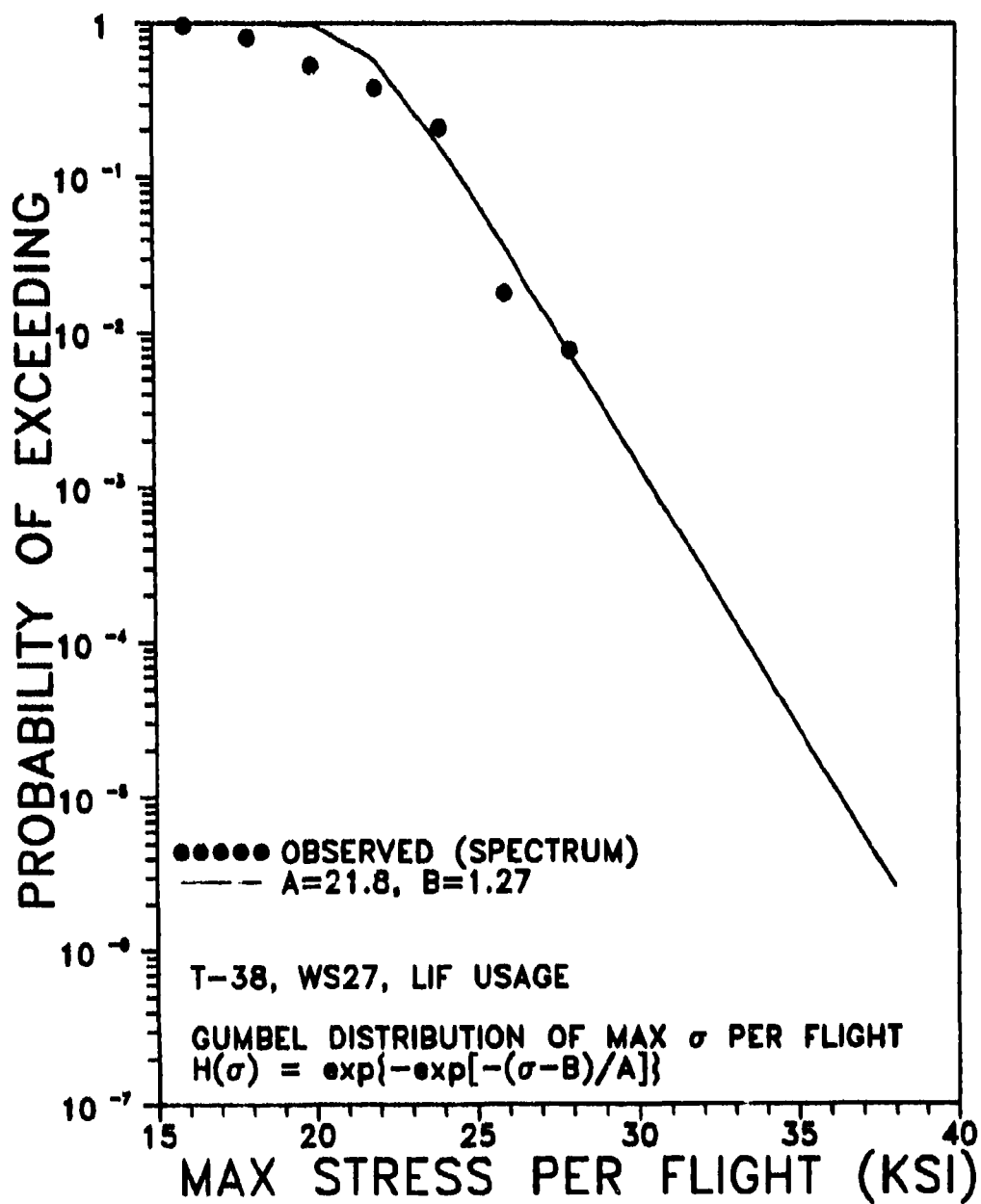


Figure 18. Baseline Distribution of Max Stress per Flight - LIF Usage.

fracture probabilities are dependent on the fit of this distribution at the high stress levels. The sensitivity of POF to this fit was tested by arbitrary shifts in the population parameters that still produced acceptable fits to the data.

4.1.3 Inspection/Repair Category Data

The inspection and repair data reflect force management decisions that are made in defining maintenance scenarios. The baseline inspection intervals were defined as those that would be specified by the requirements of MIL-STD-1530A. The first inspection would be scheduled at 1100 spectrum hours and all subsequent inspections at 900 spectrum hours thereafter. These inspection intervals will be varied as prime controllable factors in risk analysis trade-offs.

The inspections for this critical location are performed using a semiautomated eddy current probe with the fastener in the hole. The reset crack size after an inspection (a_{NDE}) is 0.100 in. Experiments to quantify the inspection reliability for this specific inspection have not been performed. The baseline POD(a) function will be assumed to have a minimum detectable crack size of zero and a median detection capability of 0.050 in. with $\sigma = 0.54$, Figure 19. This combination of parameters yields $POD(0.100) = 0.90$ and is in reasonable agreement with experiments for eddy current systems.

Repair of cracks found at this location are considered to be a major repair. The equivalent repair flaw size distribution will be assumed to be the same as the initial quality distribution, i.e., repaired is as good as new. Sensitivity to this assumption will be made by introducing equivalent repair flaw size distributions that are not as "small" as those of the baseline.

Inspection and repair costs are exceedingly difficult to estimate. Overhead costs associated with inspecting a particular location are shared with the scheduled maintenance of many other individual details that are not necessarily structure related.

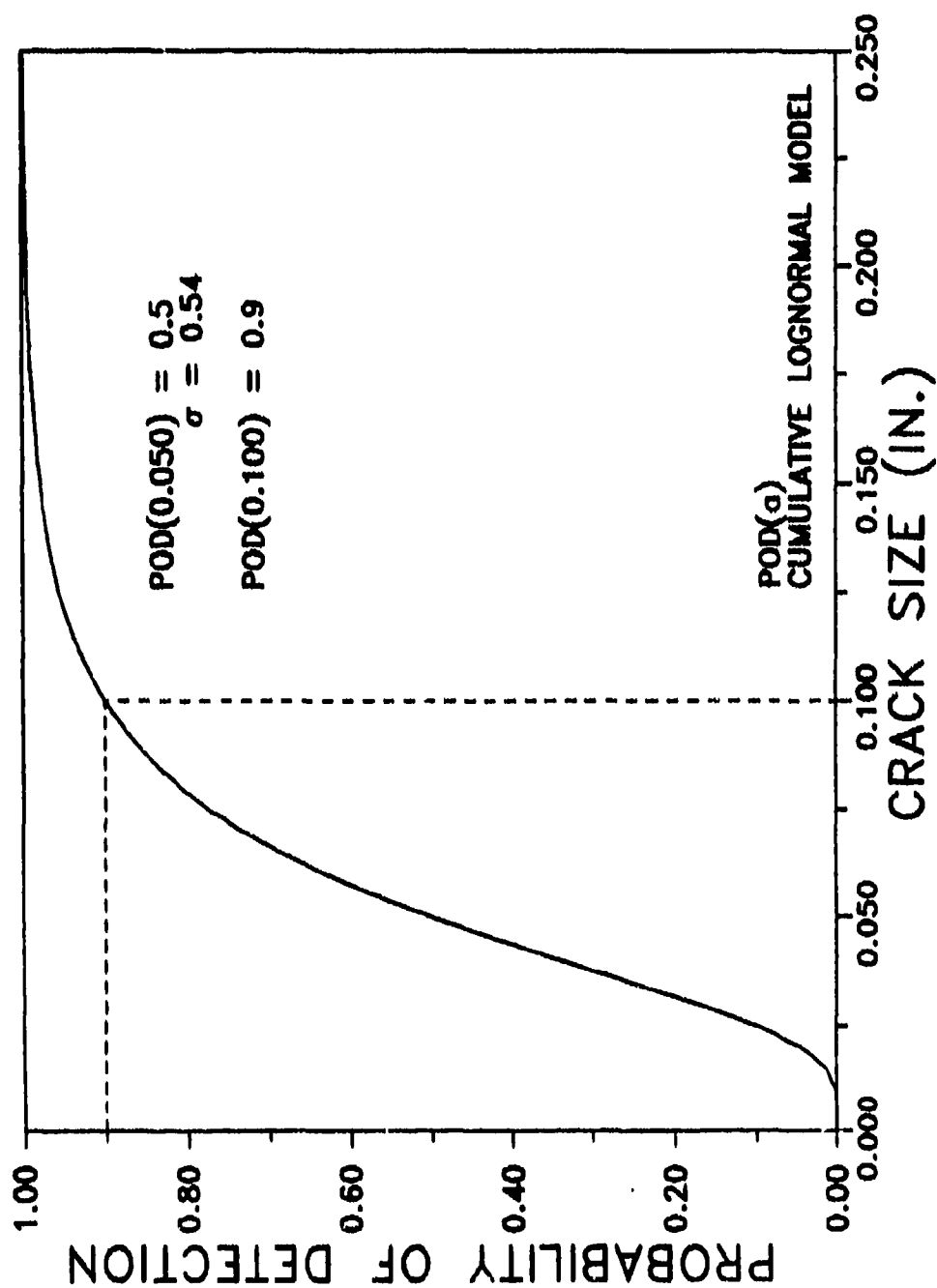


Figure 19. POD(a) for Semiautomated Eddy Current Inspections.

As a basis of cost comparison, it is assumed that the relative cost of inspection is \$100 per hole, the cost of repairing a crack less than 0.100 in. is \$100, the cost of repairing a crack greater than 0.100 in. is \$100,000 (wing replacement), and the cost of a fracture is \$10,000,000 (loss of aircraft). Note that these costs are fictitious; they are not based on actual experience, and do not represent T-38 experience.

4.1.4 Summary of Baseline Input

Table 5 presents a summary of the input data which provided the baseline for sensitivity analyses.

4.2 SENSITIVITY TO INPUT VARIATIONS

The objectives of the sensitivity analyses were to provide a basis for judging the validity of the PROF output and to perform trade-off studies on those inputs which are associated with fleet management decisions. Trade-off studies were only considered for the maintenance scheduling, repair quality, and inspection capability options. The material/geometry data and the aircraft/usage data are considered to be inputs which are not associated with fleet management. Strictly speaking, aircraft could be rotated among different usages as a planned part of fleet management. Such rotation could be modeled using PROF but in PROF's current configuration, multiple runs would be required to accommodate the changes in the crack growth ("a vs. T") curve and the peak stress per flight distribution.

The sensitivity analyses are presented for the three categories of input data. Discussion of the results are presented for each of the three categories even though there is a correlation between some of the input data. Single flight POF values were selected as the basic parameter for evaluating the sensitivity of PROF to input variables. Multiple sites on a single airframe and multiple airframes in a fleet are approximately accounted for by multiplying the single flight POF by a constant factor. Conclusions drawn from the single flight

TABLE 5
BASELINE PROF INPUT FOR SENSITIVITY ANALYSES

CATEGORY AND DATA TYPE	DESCRIPTION
MATERIAL/GEOMETRY	
K/σ vs a	Geometry correction for crack initiating at a lower wing skin fastener hole at the corner of the countersink. Figure 15, [24].
$g(K_C)$	Normal distribution of K_C with $\mu = 29.4$ and $\sigma = 2.2 \text{ KSI}\sqrt{\text{in.}}$.
AIRCRAFT/USAGE	
Locations	6 holes per aircraft, 125 aircraft in the fleet, average flight length of 1 hour.
$f_0(a)$	Equivalent initial flaw size distribution - Mixture of 99.9% Lognormal (0.0008 in., 0.63) and 0.001% Uniform (0,0.050 in.). Figure 16.
a vs T	Severe (LIF) usage. Figure 17, [24].
$h(\sigma)$	Gumbel distribution of max stress peak per flight, $A = 21.8 \text{ KSI}$, $B = 1.27$. Figure 18.
INSPECTION/REPAIR	
T_1, T_2, \dots	DTA defined inspection schedule. First inspection at 1100 spectrum hours. Subsequent inspections at 900 spectrum hours.
POD(a)	Semi-automated eddy current. $\mu = \ln(0.050)$, $\sigma = 0.54$. Reliably detected crack size, $a_{90} = 0.100 \text{ in.}$ Figure 19.
$f_r(a)$	Same as initial crack size distribution, i.e., repaired is as good as new. Figure 16.

POF would be unchanged by comparisons of the airframe or fleet POF. POF in the inspection and total analysis interval were also considered and none of the conclusions were altered. Expected maintenance costs were also considered in the evaluation of fleet management decisions and will be discussed in subsection 4.2.3.

4.2.1 Variations in Material/Geometry Input

Sensitivity to the K_{IC} distribution and variations in the "K/v versus a" relation are defined by the material and specific design of the structural detail under consideration. In essence, these factors are determined when the detail is designed.

4.2.1.1 Fracture Toughness

The fracture toughness is input to PROF by specifying the mean, μ , and standard deviation, σ , of the assumed normal distribution of K_{IC} for the material of the detail. Sensitivity to variations in fracture toughness were performed by varying μ and σ to reflect potential uncertainty in these parameters because they are estimated from samples of different fabrication lots of the material. For the 0.585 in. plate of WS27, the baseline values of $\mu = 29.4$ and $\sigma = 2.2$ were based on 47 samples of plane strain fracture toughness, K_{IC} [10], Table 8.9.2.1]. Ninety percent confidence intervals for μ and σ from a sample of size 47 are (28.9,29.9) and (1.8,2.5), respectively. Figures 20a and 20b display the differences in the distribution of fracture toughness when μ and σ are at the extremes of these confidence intervals.

To reflect the influence of uncertainty in K_{IC} on the calculation of the probability of fracture (POF), PROF sensitivity runs were made at the limits of the 90 percent confidence bounds. Figure 21 compares the single flight POF for $\mu = 28.9, 29.4$, and 29.9 for the baseline $\sigma = 2.2$. Figure 22 compares the single flight POF for $\sigma = 1.8, 2.2$, and 2.5 for the baseline $\mu = 29.4$. Combining the upper limit on μ and the lower limit on σ yields an upper bound on the distribution of K_{IC} . Similarly, the lower limit on μ and the upper limit on σ yields a

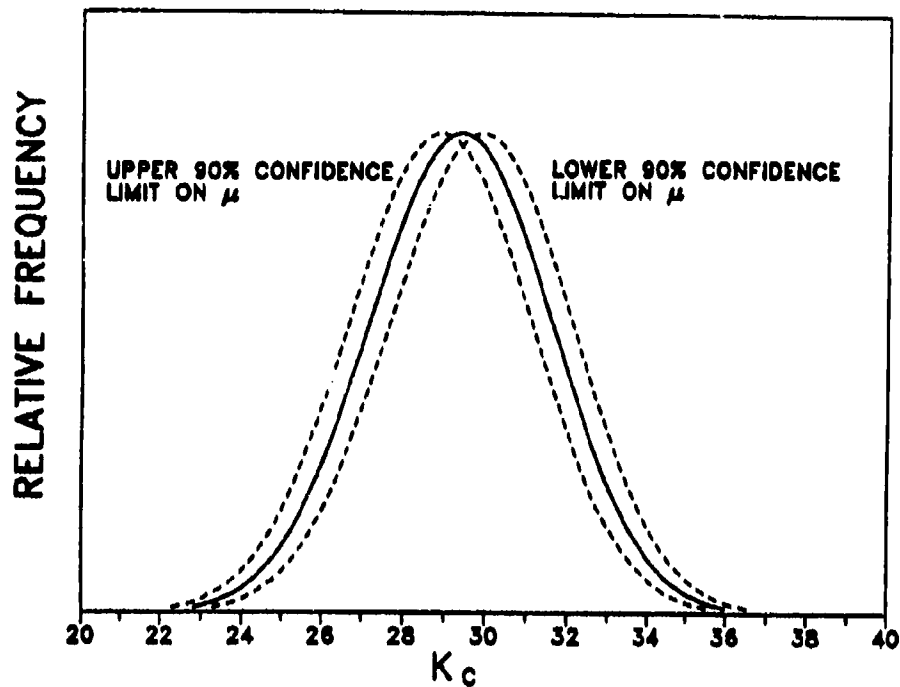


Figure 20a. Distribution of K_c for Bounds on μ .

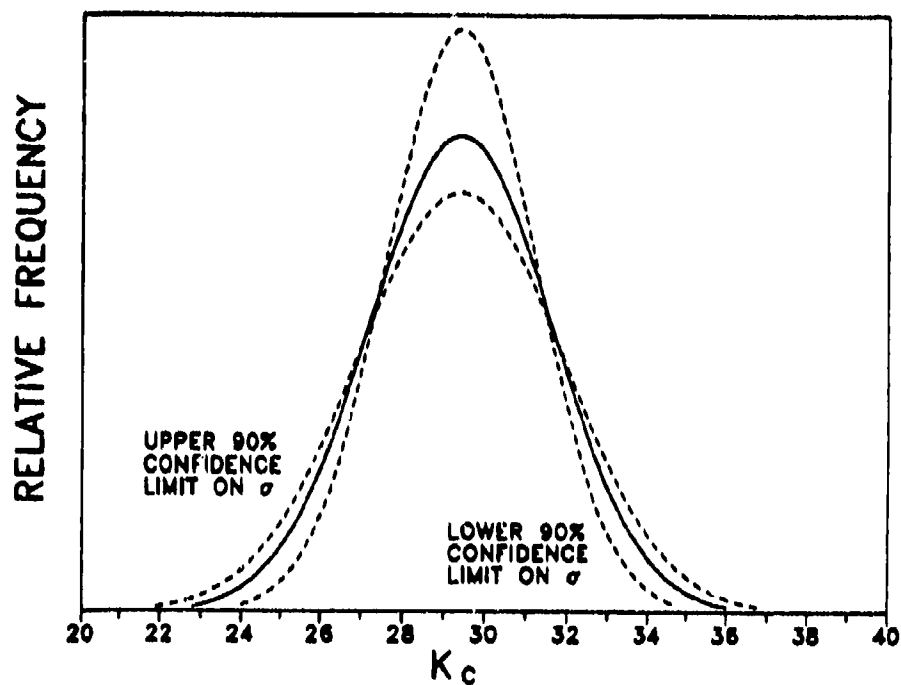


Figure 20b. Distribution of K_c for Bounds on σ .

Figure 20. Normal Distributions for K_c .

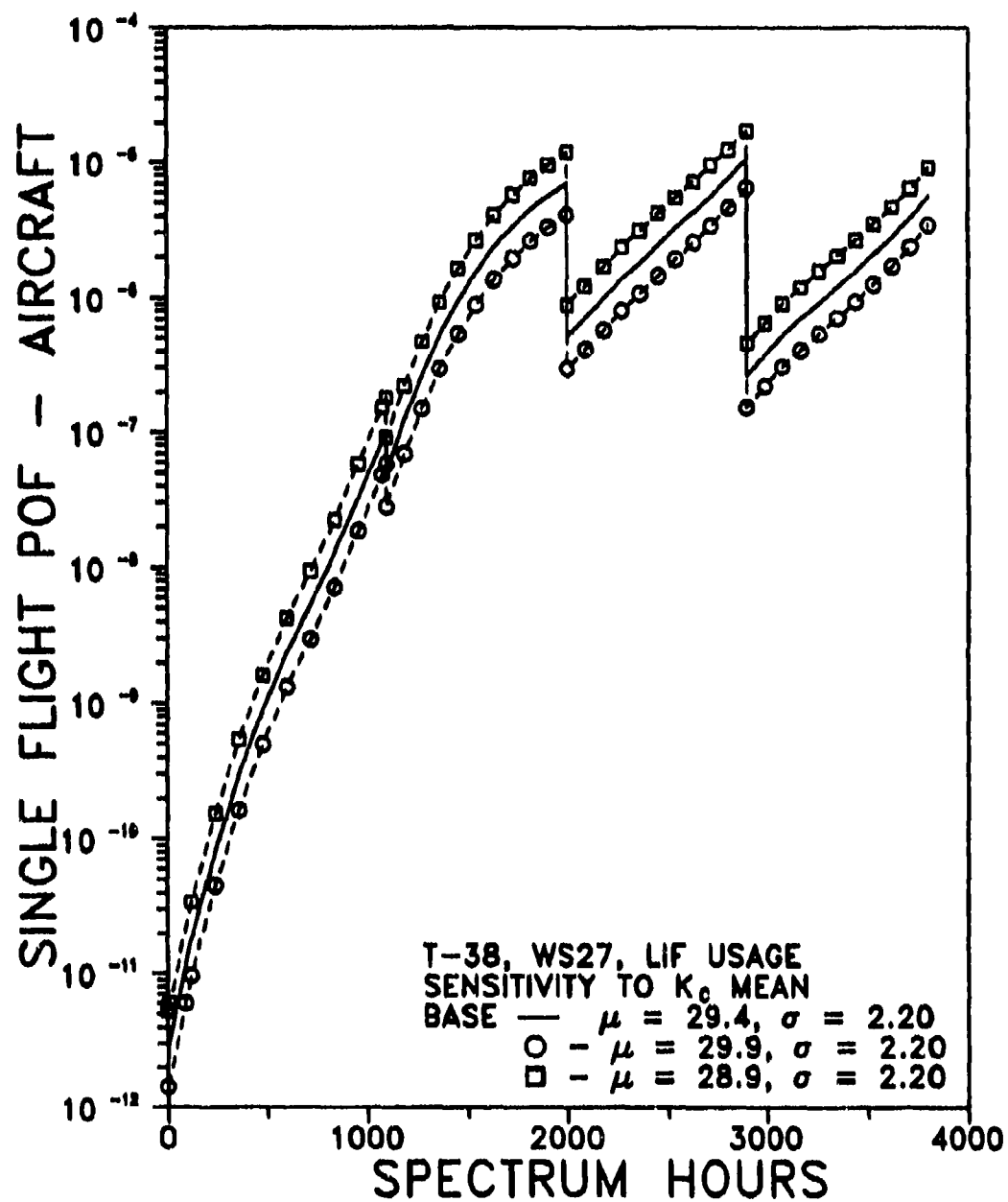


Figure 21. POF Varying K_0 Mean with Fixed Standard Deviation.

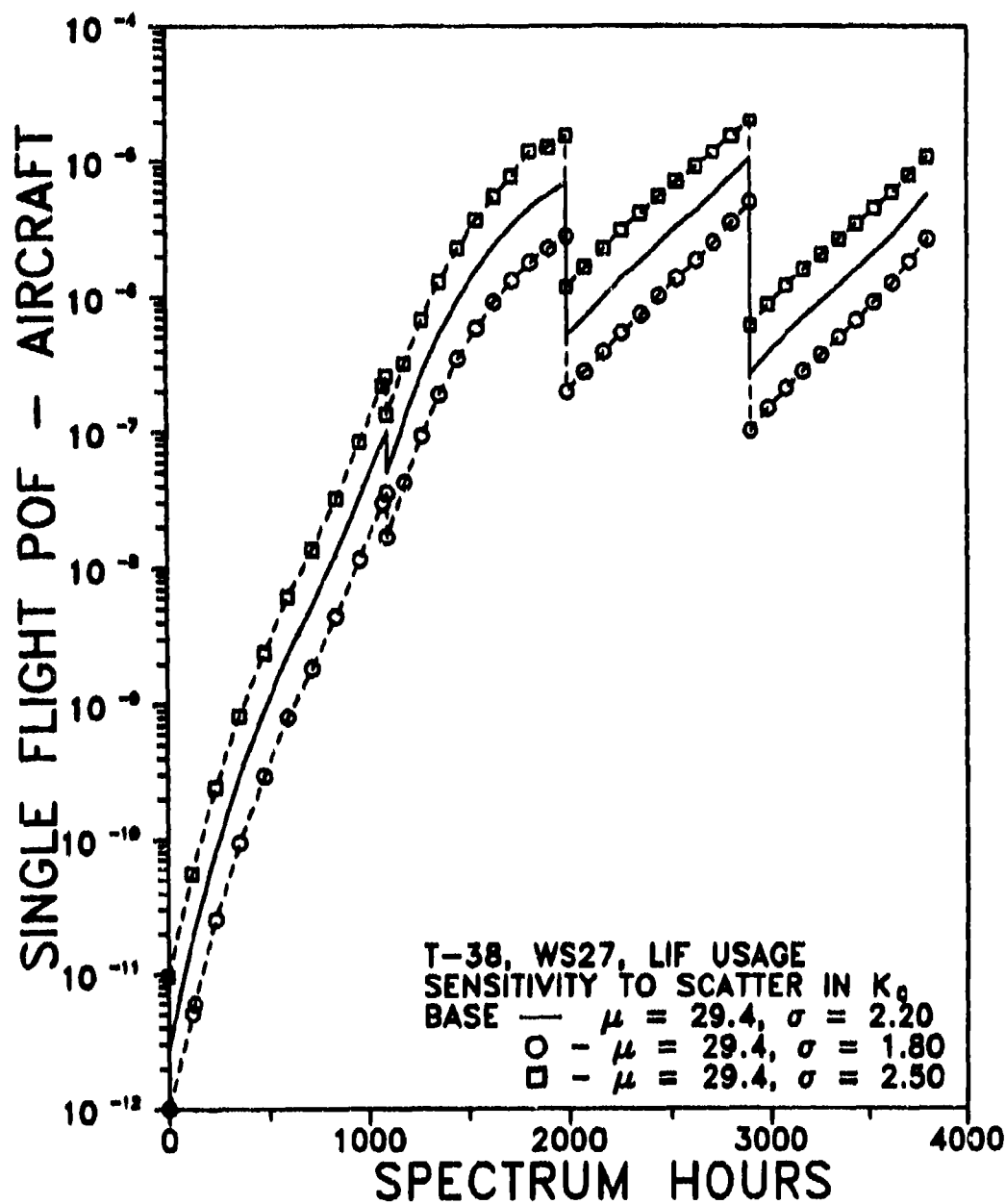


Figure 22. POF Varying K_0 Standard Deviation with Fixed K_0 Mean.

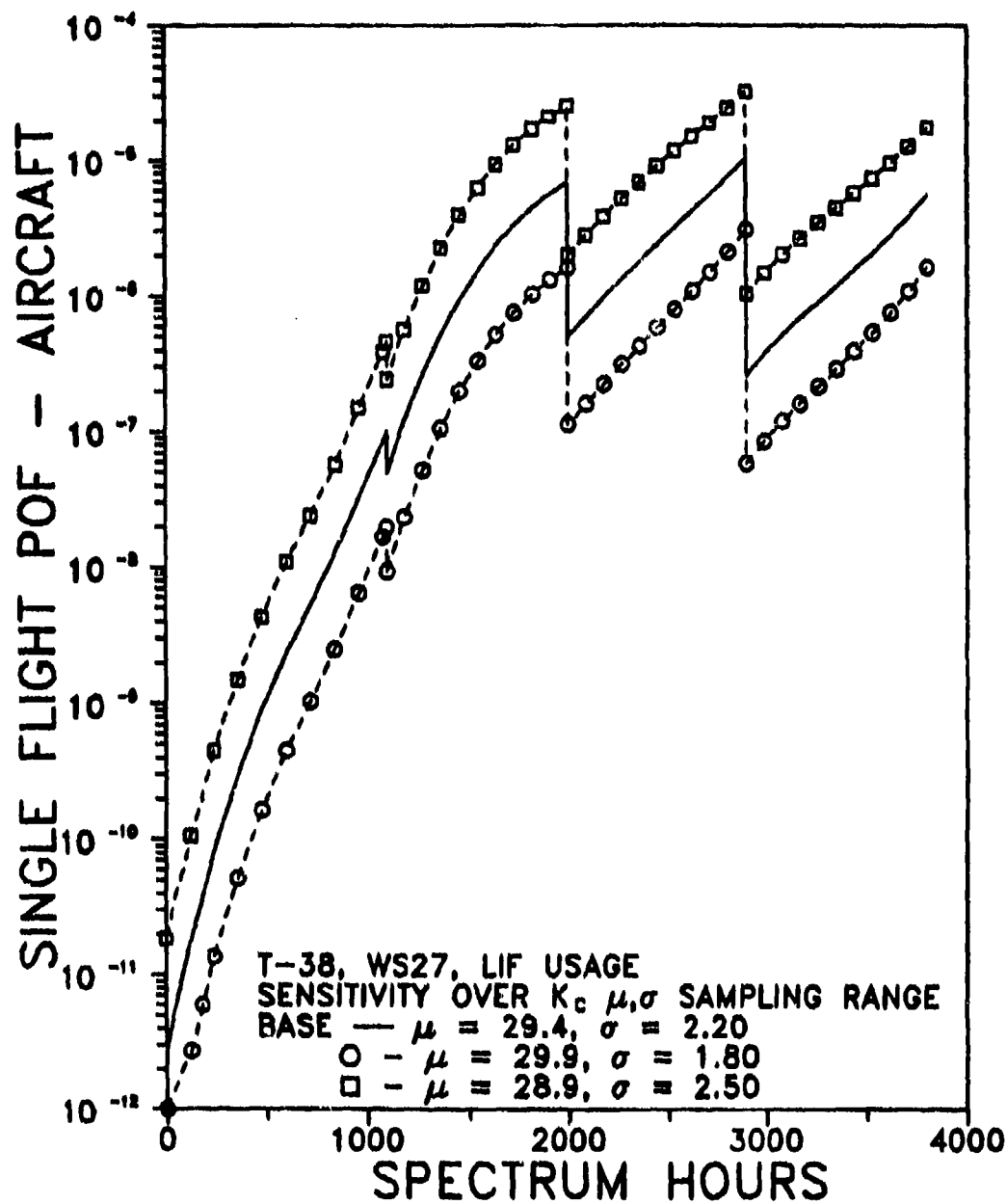


Figure 23. POF at Limits of 90% Confidence Bounds on Mean and Variance of K_c .

lower bound on the distribution of K_{IC} . Figure 23 compares the POF values from these combinations of the parameters with the baseline. Finally, since K_{IC} is often considered to be a constant, POF values were calculated for $\mu = 29.4$ and $\sigma = 0.01$ and compared with the baseline POF, Figure 24.

The sampling variation in the estimates of the parameters of the K_{IC} distribution produced possible differences in POF over a range of about a factor of 4 from uncertainty in the mean alone and over a range of about a factor of 6 from uncertainty in the standard deviation alone. These potential differences are based on the sample size of 47. (Note that many materials do not have this large of a sample of K_{IC} values on which to estimate the mean and variance. Smaller sample sizes would produce wider confidence intervals and a larger range of POF values.) Combining the reinforcing extremes of the confidence bounds produced possible differences in POF of more than order in magnitude over the total possible range of values, Figure 23.

Assuming that K_{IC} is a known constant produced POF values that were more than an order of magnitude less than the baseline values. The baseline assumed that the fracture toughness for a structural detail chosen at random from the population is a random sample from a normal distribution of K_{IC} values with $\sigma = 2.2$. This result is not surprising since the baseline conditions provide a much greater chance of combining a small fracture toughness with a large stress. Regardless, it should be noted that assuming K_{IC} is constant produces significantly smaller (non-conservative) POF values.

4.2.1.2 K/σ versus a

The stress intensity factor correlation with crack size is modeled as a deterministic input and is essentially defined by the design detail geometry and the crack initiation site. To test the sensitivity of PROF to the " K/σ versus a " relation, stress intensity solutions were obtained for cracks initiating in the bore of the hole and also in the corner away from the

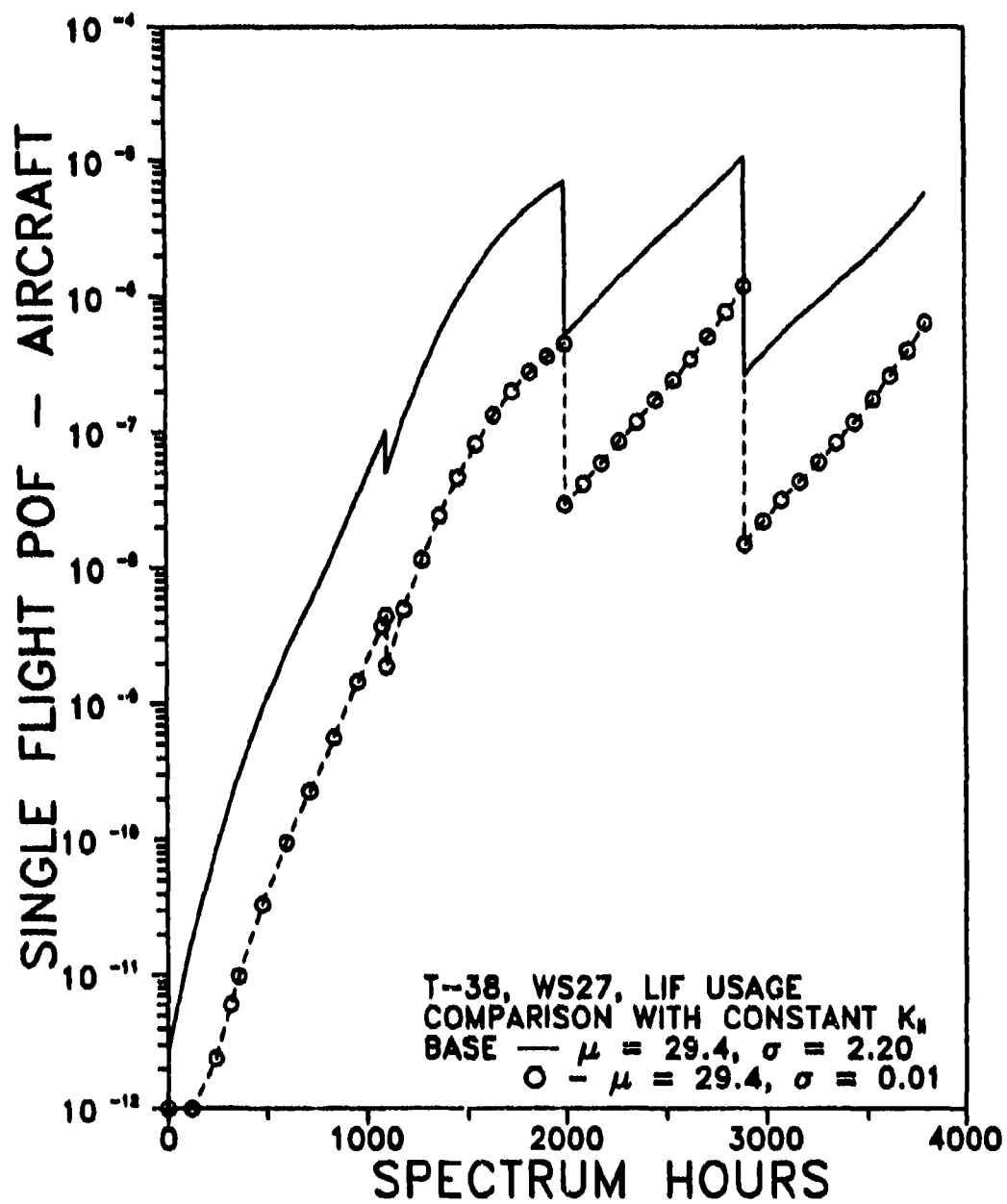


Figure 24. POF for Constant Fracture Toughness.

countersink, Figure 25. Strictly speaking, these crack geometries are not directly comparable as the holes in these solutions did not include a countersink. Changing the stress intensity geometry factor changes both the "a versus T" relation, Figure 26, and the critical stress for a given K_{IC} .

Figure 27 presents single flight POF as a function of flight hours for the three crack geometries. In general, the POFs are significantly lower for the corner and bore cracks as compared to the cracks initiating at the countersink corner. (The corner crack POF after 3800 hours is greatly reduced for the next few maintenance cycles.) The significantly larger POF values for the countersink corner geometry is apparently due to the larger K/σ values for the small crack sizes.

If all three geometries are potential crack initiating sites in the field, POF for the mixture would be a weighted average of the three POF's from the three geometries with weights given by the percentage of cracks initiating at each site. Because of the dominance of the countersink POF values, the weighted average would be closely approximated by the percentage of cracks initiating in the countersink corner multiplied by the baseline POF. The baseline POF is an upper bound on the mixture when all single crack initiation sites are considered.

4.2.1.3 Discussion - Material/Geometry Input

The estimates of the parameters of the K_{IC} distribution can significantly influence the calculation of POF. The smaller the sample size, the greater the potential effect. However, the differences tend to yield "parallel" POF curves. Although the estimated value might be in "error" by as much as a factor of five (assuming all other input is exactly correct), relative POF values would be unchanged from the "true" value.

The different geometries from the different crack initiation sites produced significantly different POF curves, both in magnitude and shape. In application, the percentage of cracks initiating at the different locations should be estimated

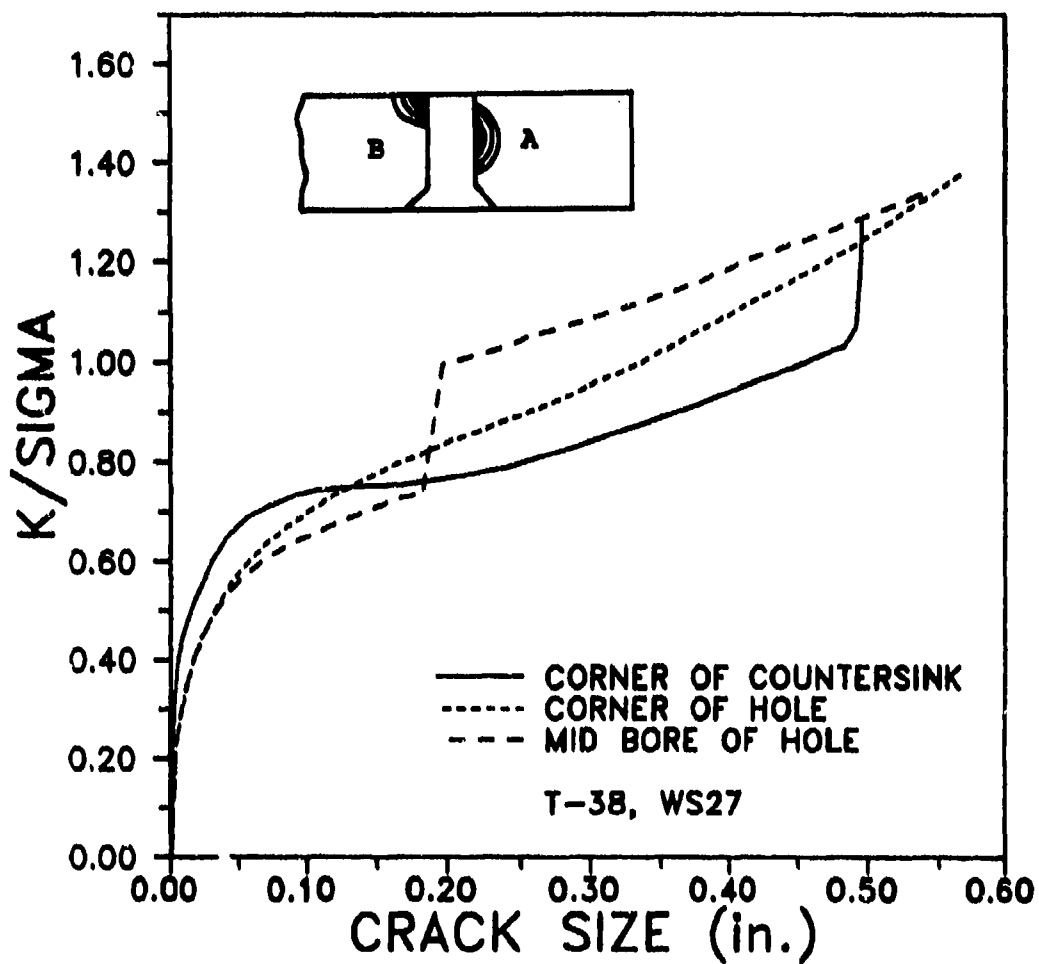


Figure 25. K/σ versus a for Crack Geometries.

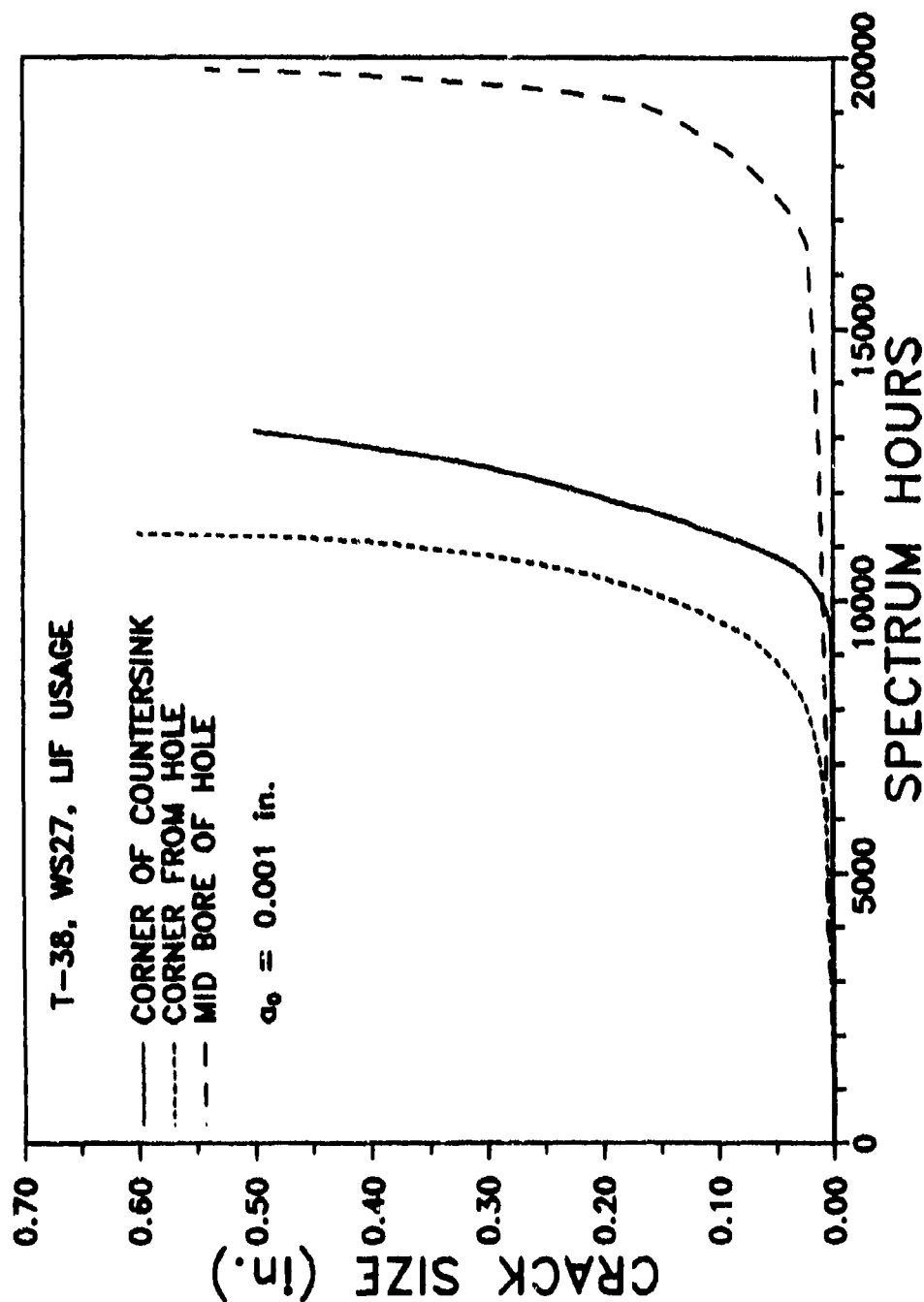


Figure 26. Crack Size versus Spectrum Hours for Crack Geometries.

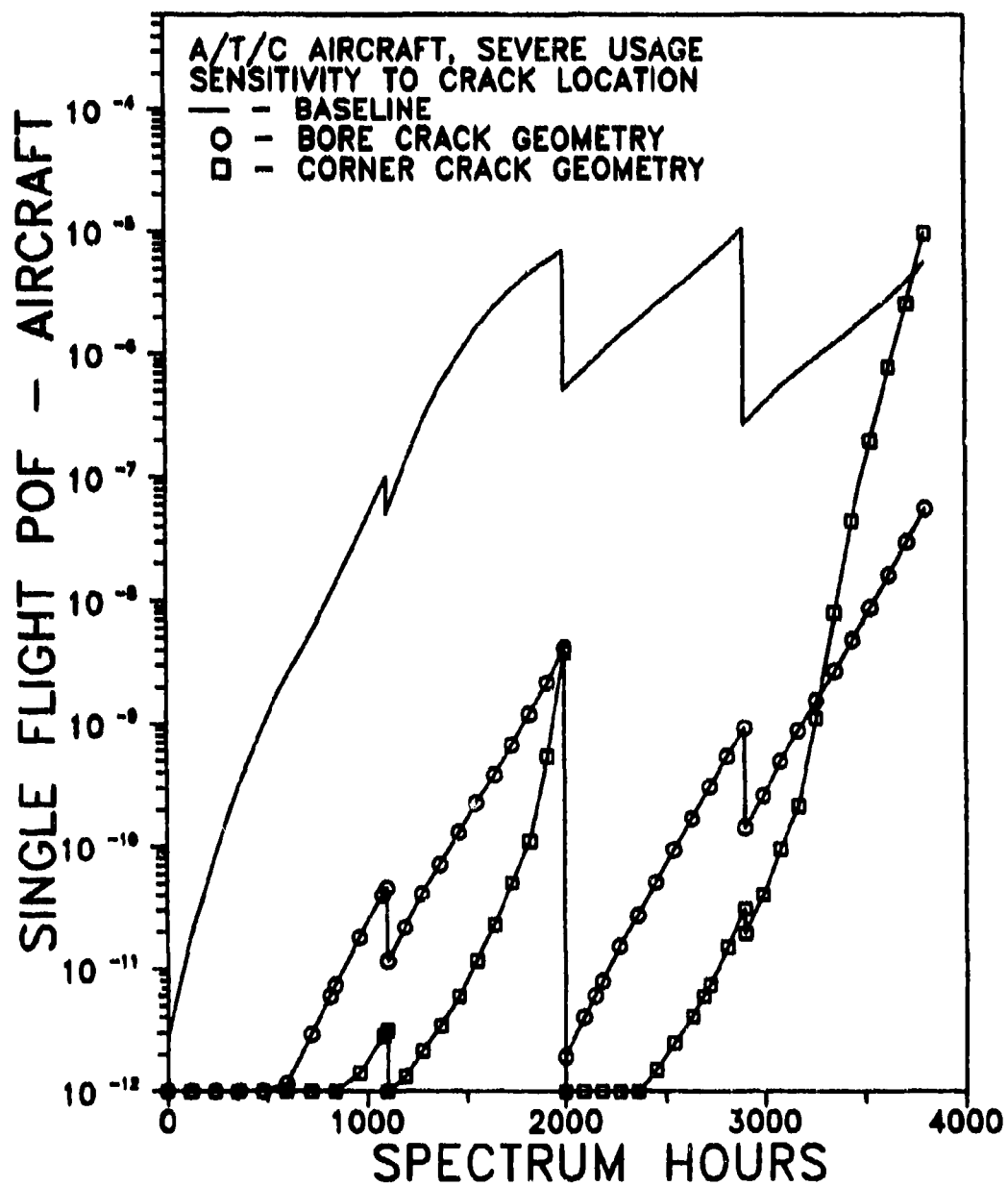


Figure 27. POF for Different Crack Geometries.

either from tests or feedback from field inspections. Given stress intensity factor solutions for each geometry, POF values can easily be generated and combined into a composite estimate of the POF for the population of details.

4.2.2 Variations in Aircraft/Usage Input

The PROF input associated with the prediction of crack size versus time and the distribution of maximum stress per flight are dominated by the anticipated usage of the aircraft. The initial crack size distribution is dominated by the initial quality of the structure if the analysis is to start with virgin structure. In the case of application to aging aircraft, the initial crack size distribution is influenced by both the initial quality and also by the past usage experienced by the airframe.

4.2.2.1 Initiating Crack Size Distribution

The sensitivity of POF to the initial crack size distribution was investigated by altering the baseline in four different ways.

- a) A Weibull distribution, rather than a log normal distribution, was mixed with the uniform (0,0.050) for the basic equivalent initial flaw size distribution (EIFS). The median and 90th percentile of the EIFS were kept the same.
- b) A log normal (0.0008,0.63) without the uniform distribution of big cracks was used as the EIFS.
- c) The median of the baseline log normal was arbitrarily increased 10 percent with σ at baseline.
- d) The standard deviation of the baseline log normal was arbitrarily increased 10 percent with μ at baseline.
- e) The mixing percentage of big cracks was increased.

In each of these cases, the equivalent repair crack size distribution was the same as the EIFS.

The evaluations of PROF sensitivity to variations in the initial crack size distributions were primarily made on the basis of the calculated POF values. However, the initiating crack size

distribution also influences the number of cracks detected at an inspection. This output of PROF is summarized in Table 6 for the various EIFS distributions. As will be noted, the differences in percent detections are as would be expected and they correlated with differences in the POF values.

Figure 28 compares the POF as a function of spectrum hours using the log normal and Weibull distributions to mix with the larger cracks of the uniform (0,0.050) as the models for the EIFS. The log normal POF values are slightly larger at the start of the analysis reflecting the higher tail probabilities of the log normal distribution. In general, the differences between the two curves are relatively minor (at least when compared to differences from other sources).

The comparison using the log normal mixture versus only the log normal distribution for the EIFS is shown in Figure 29. There is a significant difference in the interval before the first inspection but the differences thereafter are minor. The early differences are due to the relatively few large cracks (1 in 1000) introduced in the mixture. Apparently, these cracks were detected at the inspection as the baseline mixture containing the larger cracks had about 50 percent more detections at the first inspection. Note that differences at the very small POF values are determined by the extreme tails of the input random variables.

Increasing the median of the EIFS by 10 percent increased the POF by an order of magnitude during the first usage interval, but the differences were negligible thereafter, Figure 30. Forty percent more detections were predicted for the larger EIFS median. Increasing the standard deviation by 10 percent, produced a minor change in POF even though a higher percentage of detections were made at the first inspection.

Changing the percentage of big cracks by increasing the mixing proportion of the baseline log normal and uniform (0,0.050) cracks produced significant changes in POF during the

TABLE 6
Percent Detections at Inspections for Initiating Crack
Size Distributions

	INSPECTION TIMES IN SPECTRUM HOURS			
	1100	2000	2900	3800
Baseline (Log Normal Mix)	1.70	11.12	7.44	5.73
Weibull Mix	1.70	11.00	7.41	5.93
Log Normal Only	1.16	11.06	8.01	9.03
Log Normal Mix - Larger Median	2.40	11.17	7.91	5.14
Log Normal Mix - Larger Scatter	2.41	12.69	8.51	9.52
Log Normal Mix - 1% Mix Percentage	2.47	11.16	7.92	5.10
Log Normal Mix - 10% Mix Percentage	10.10	11.44	9.22	5.93

Baseline mix - 99.9% log normal (median = 0.0008 in., σ = 0.63)
and 0.1% uniform on 0 to 0.050 in.

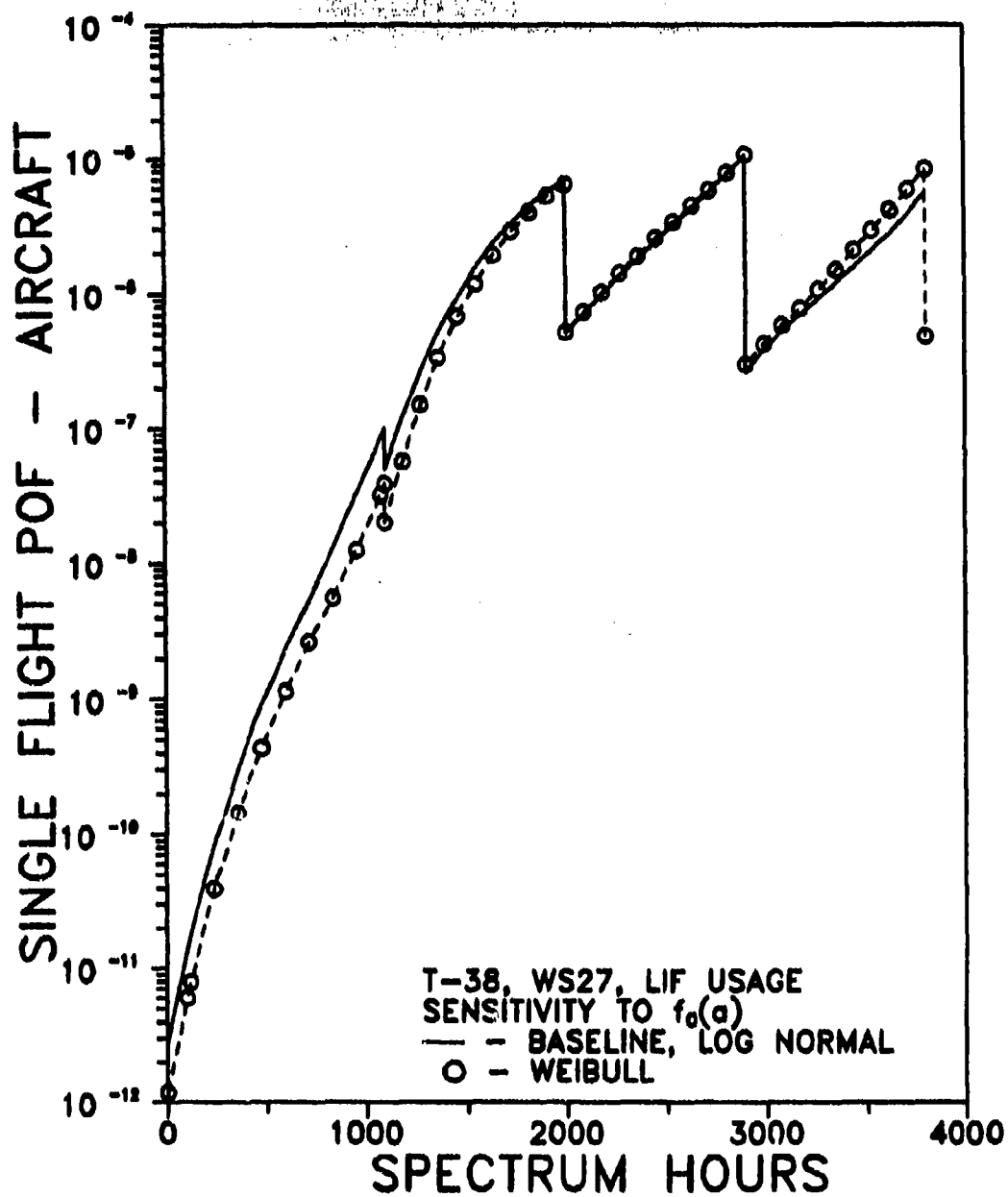


Figure 28. POF for Different Families of EIFS with Constant Median and 90th Percentile.

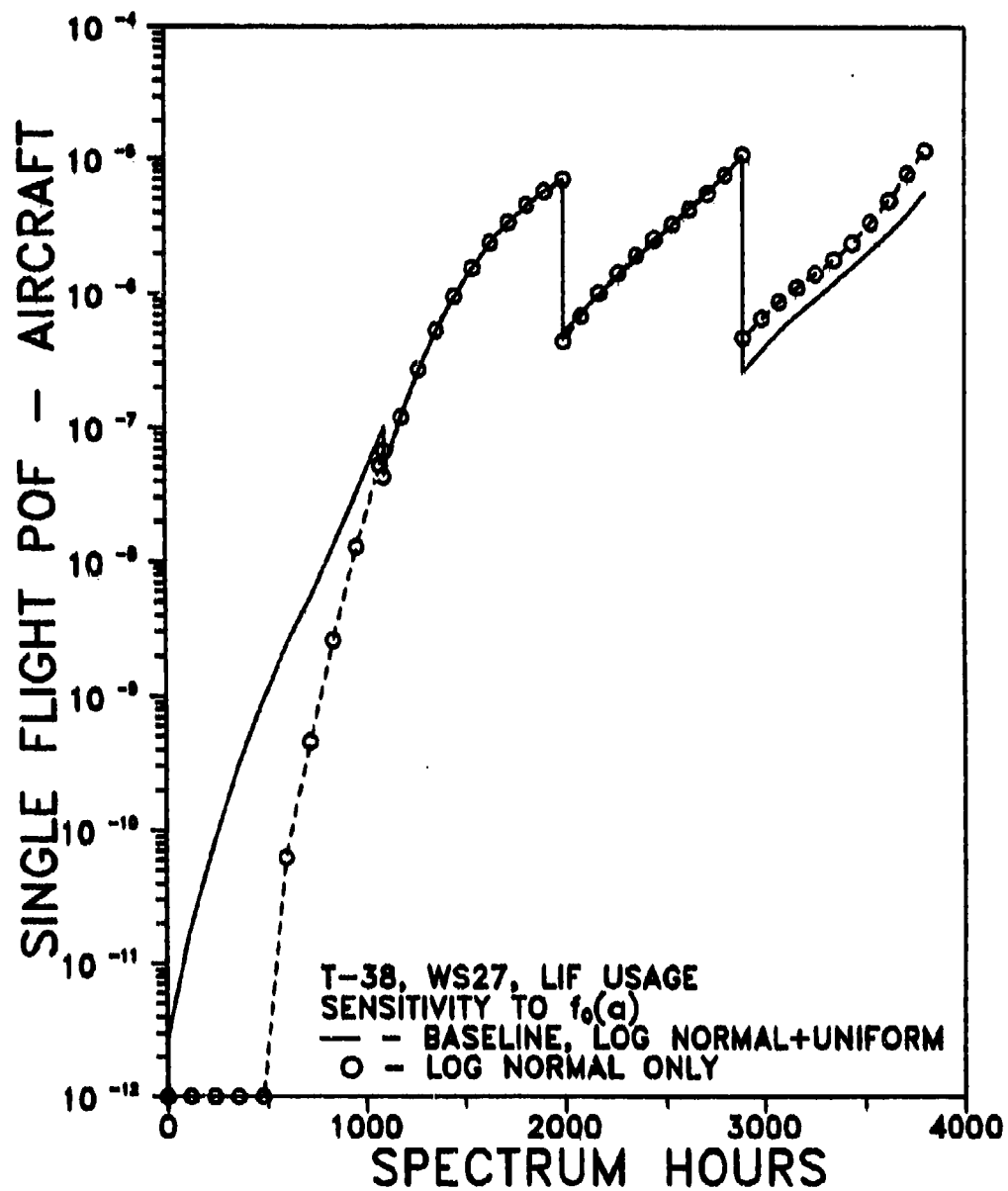


Figure 29. POF with and without Mix of Large HIFs.

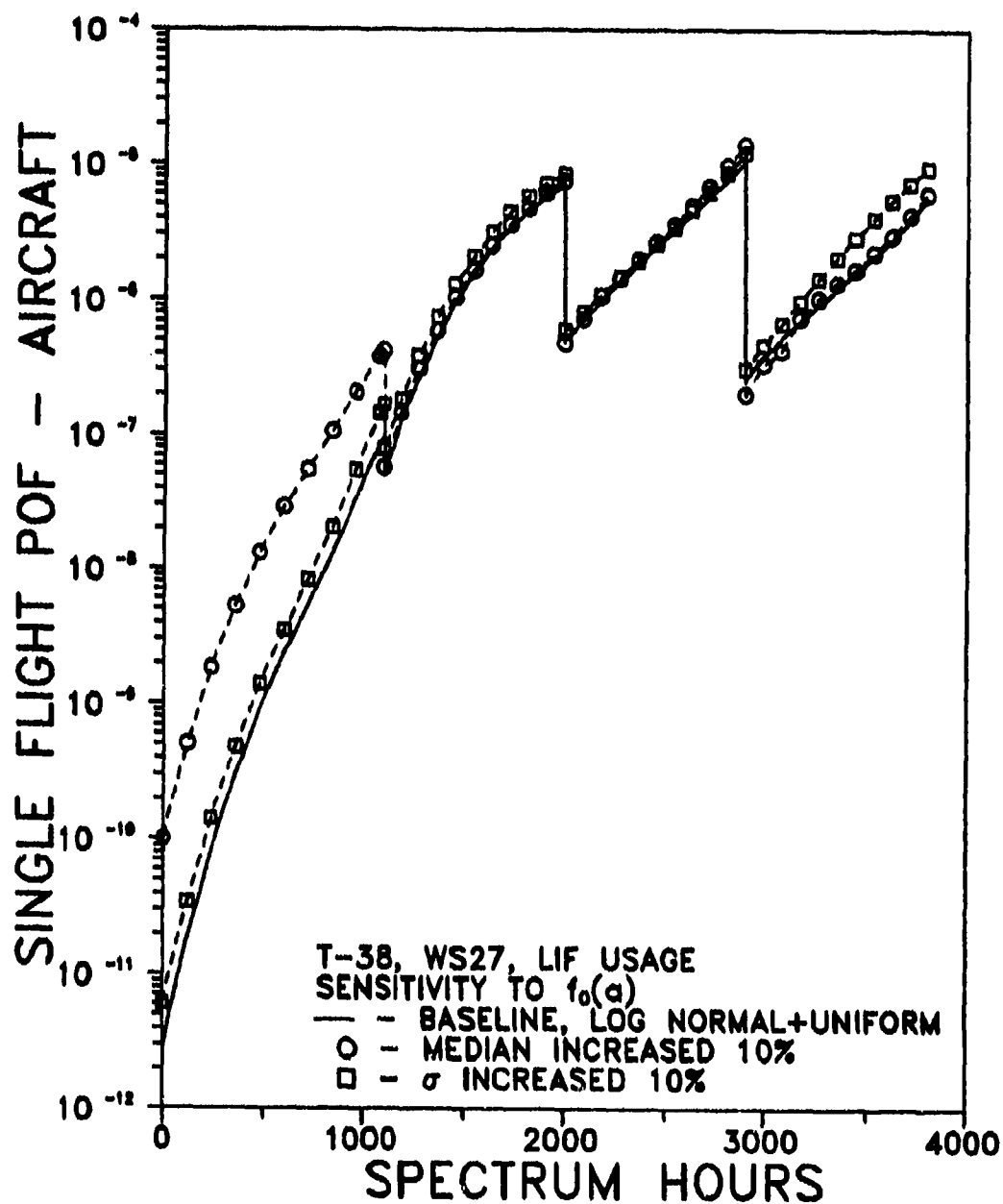


Figure 30. POF for 10% Changes in Median and σ of EIFS.

first usage period only. Figure 31 displays POF as a function of spectrum hours for mixing percentages of 0.1% (baseline), 1%, and 10%. Again, a significantly larger number of crack detections were made at the first inspection. At subsequent inspections, the percentage of detections varied, but the resulting mixtures of crack size density functions did not produce significant effects on POF.

The effect of the model chosen to describe the crack size distribution if larger cracks were used to initiate the analysis was also investigated. A crack size distribution was assumed for the cracks that might be present in the population of details in an aging fleet. This distribution, although arbitrary for the -29 wing, was representative of the cracks found in the original T-38 wing [6]. Weibull (scale of 0.010 in. and shape of 0.9) and log normal (median = 0.00665 in. and $\sigma = 1.041$) distributions were used to fit this distribution of larger initial cracks. The Weibull model was fit to the data and log normal parameters were determined to make the two distributions agree at the median and 90th percentiles. Because these distributions of larger cracks are representative of aging aircraft, the reference time to initiate the analysis is not zero flight hours. The analyses were started with the first inspection at the reference time ($T = 0$), i.e., immediately after an inspection for the larger cracks which may be in the structure. When using these distributions of larger initial cracks, the baseline equivalent initial crack size distribution was used to model the equivalent repair crack size distribution. (These distributions will be used again in the analysis of PROF sensitivity to the equivalent repair quality distributions.)

The model selected to represent the distribution of cracks in the "aging" aircraft produced differences in POF values that were relatively small when compared to differences from variation in other inputs, Figure 32. The thicker tail of the log normal apparently led to higher POF values after four inspections (the first being at $T = 0$), but the effect of mixing in the equivalent

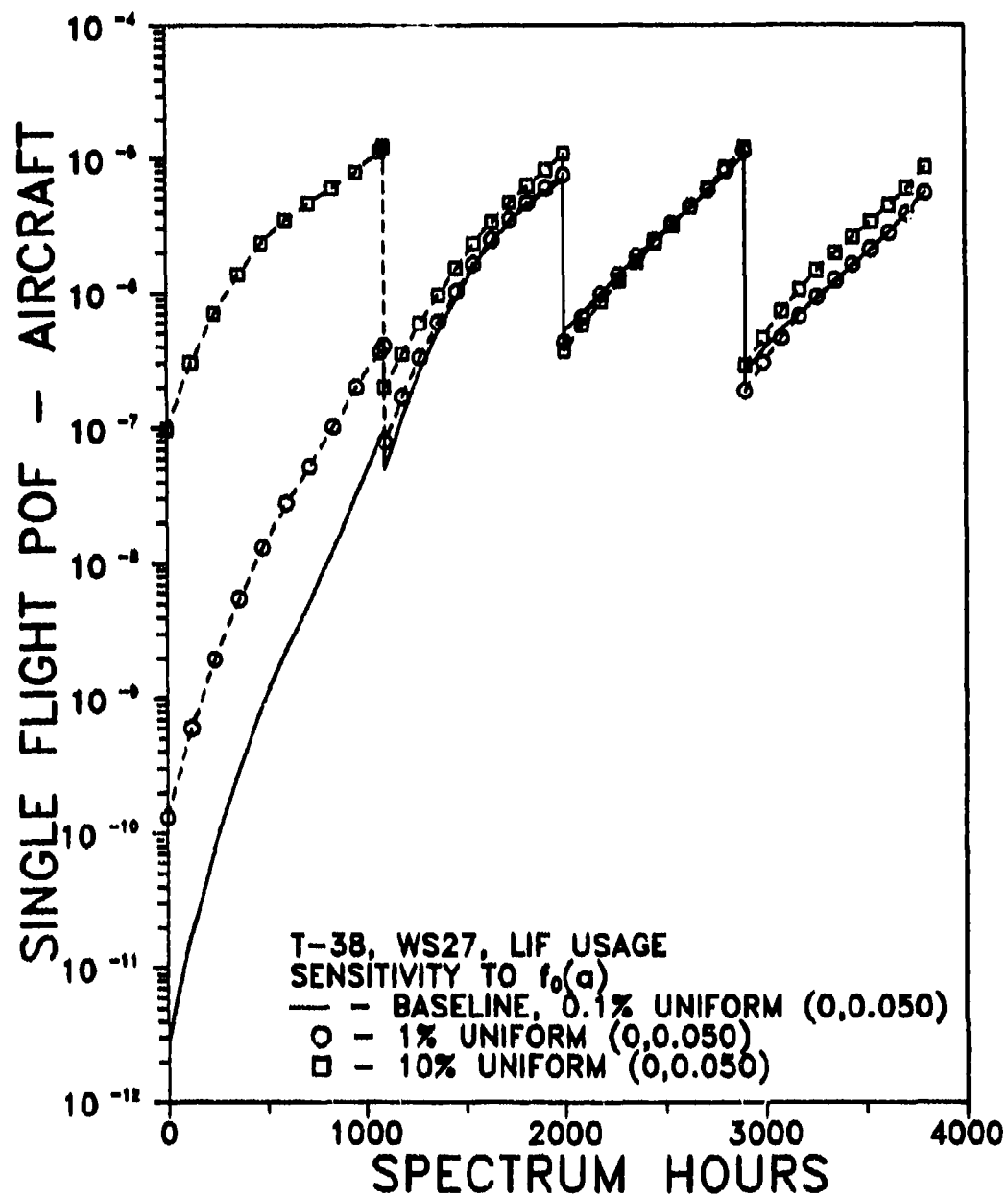


Figure 31. POF for Increased Proportions of Large EIFS.

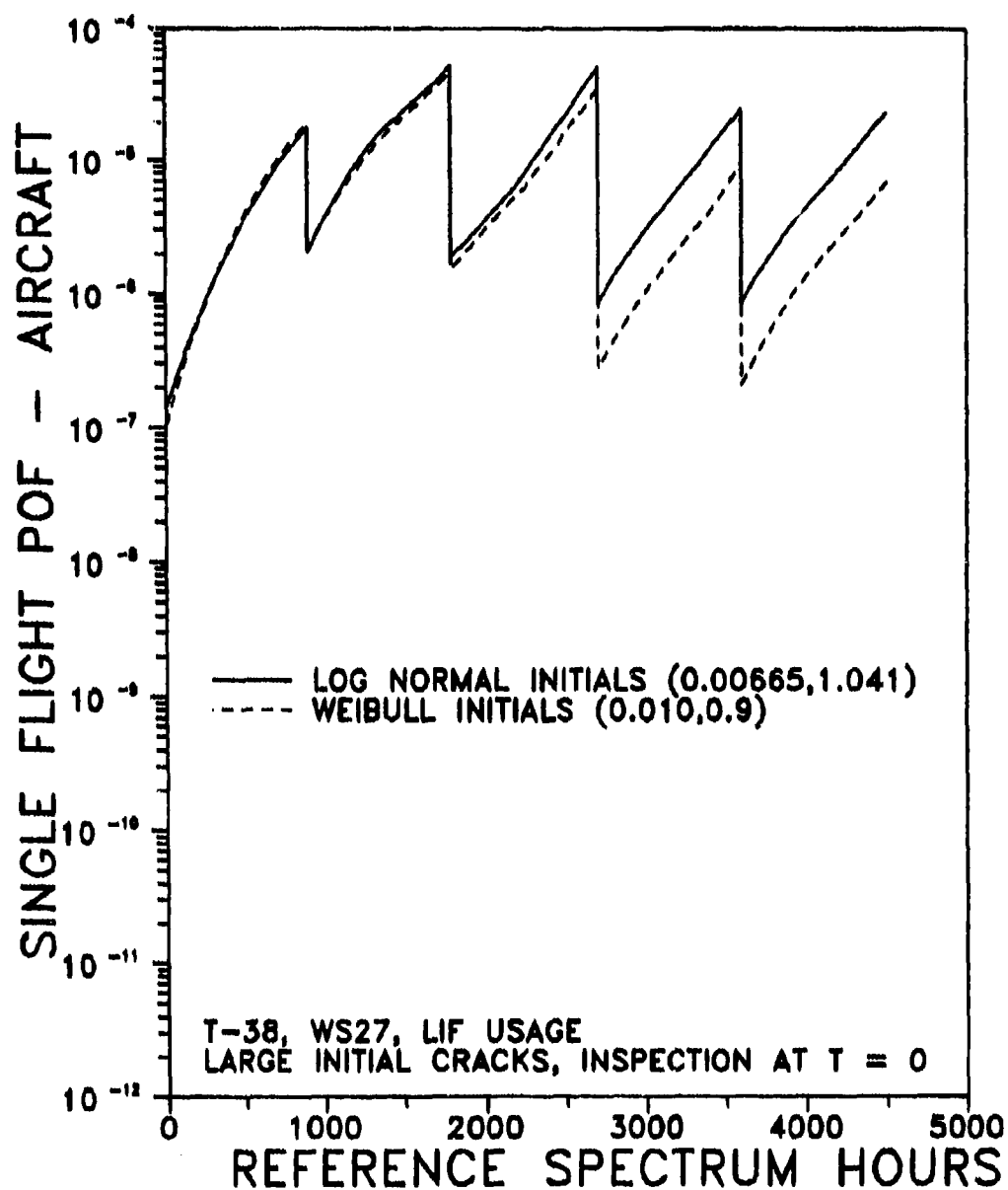


Figure 32. POF for Two Distributions of Cracks in Aging Aircraft.

repair size distributions is the probable cause of this difference.

For the log normal model, PROF predicts that cracks will be detected in 42% of the details at the 900 hour and 1800 hour inspections and in about 20% thereafter. After the first four inspections, a significant proportion of the larger initial cracks have been "repaired" and the crack distribution in the POF calculations is dominated by the equivalent repair crack size distribution. For the Weibull model, a somewhat similar pattern of percent detections was predicted, 5 percent at 900 hour, 39 percent at 1800 hours, 11 percent at 2700 hours, and about 7 percent thereafter. Since the percentages were smaller for the Weibull model, the equivalent repair crack sizes were apparently introduced more slowly. This may be the cause of the lower POF values for the Weibull model at high spectrum hours.

4.2.2.2 a versus T

The deterministic crack growth ("a versus T") relationship is driven by the sequence of stress peaks expected in usage, the stress intensity factor solution for the geometry of the detail, and the analytical models used to predict crack growth. The effect of detail geometry on the "a versus T" relation was considered previously. The stress sequence and model were determined by the manufacturer to be representative of the LIF usage and were not varied in this study. To consider the sensitivity to stress levels, the stress peaks in the spectrum were scaled by factors of 90 and 110 percent. The resulting "a versus T" curves are presented in Figure 33. The distribution of maximum stress per flight was also altered in the PROF runs to reflect the changes in the distribution of maximum stress per flight. To account for the change in stress levels, the location parameter of the Gumbel distribution of maximum stress per flight was scaled by 90 and 110 percent from the baseline.

Figure 34 presents POF as a function of spectrum hours for the three stress magnitudes. The 10 percent changes in stress

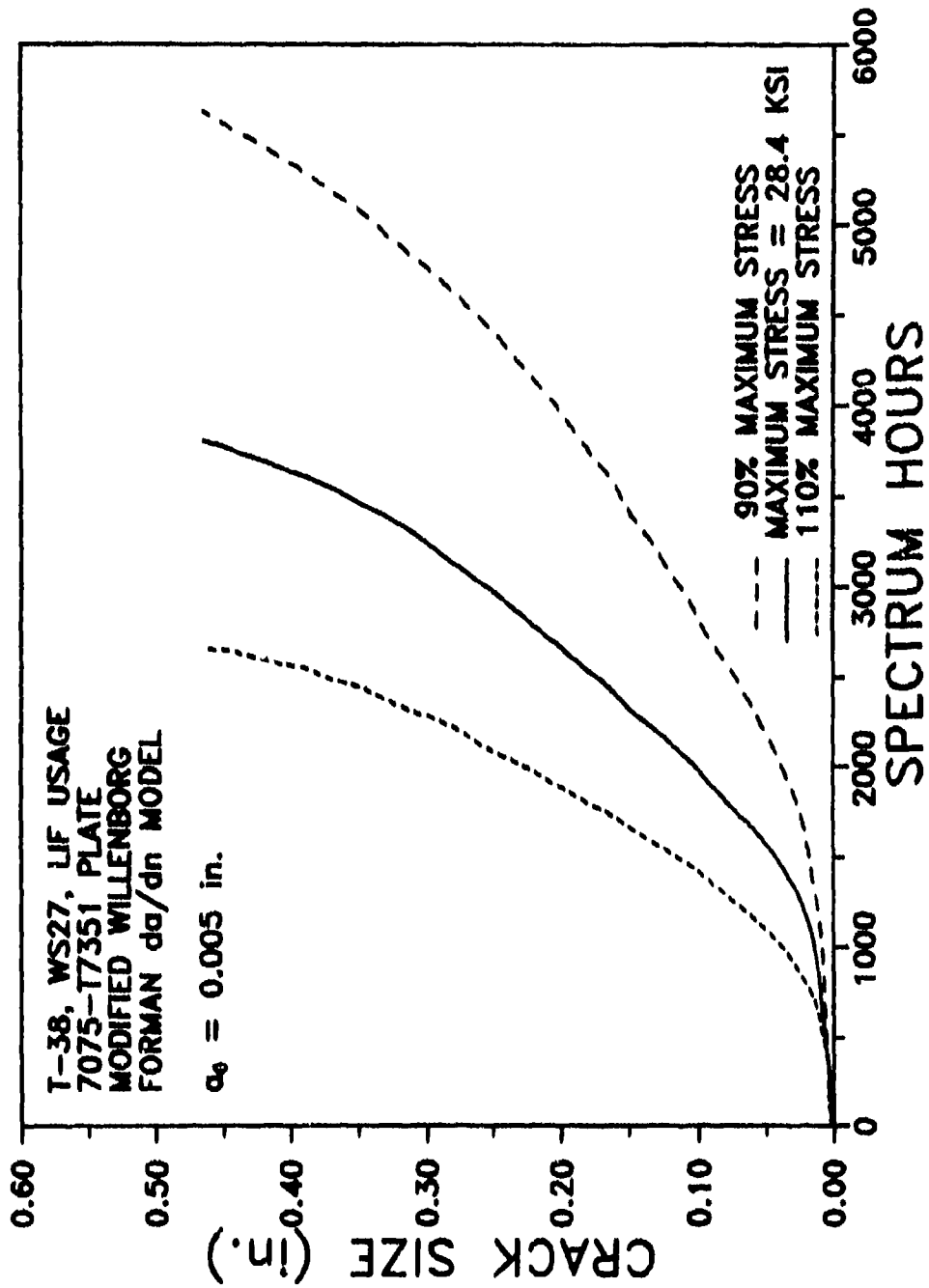


Figure 33. Crack Size versus Spectrum Hours - WS27, LIF Usage.

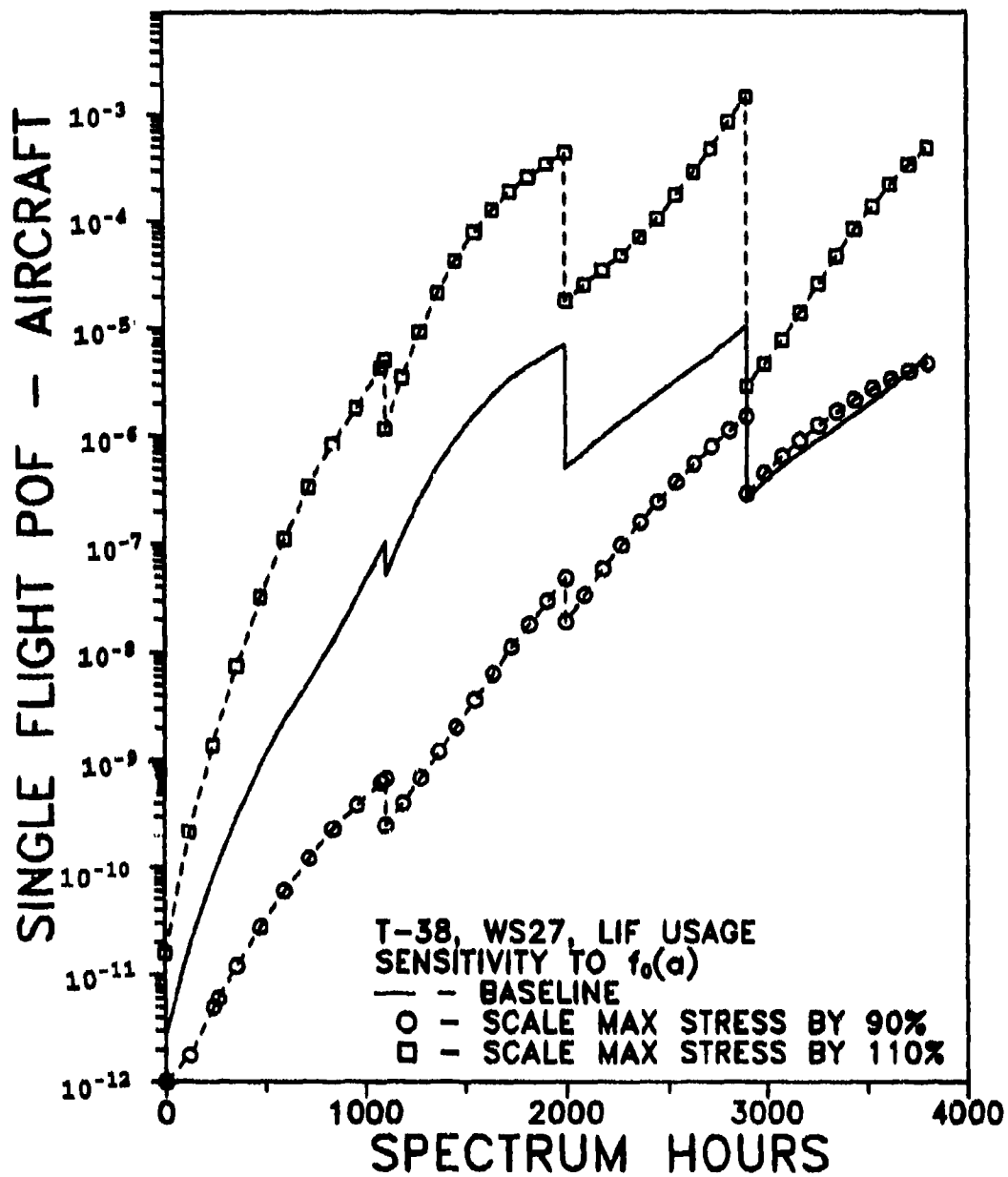


Figure 34. POF for Different Stress Levels.

levels produce more than an order of magnitude difference in POF over much of the analysis interval. It is interesting to note that after the third inspection, the baseline and 90 percent stress level POF values are approximately equal. This would imply that the earlier differences were more due to the rate of growth of the cracks rather than the change in the maximum stress per flight distribution.

One other type of "a versus T" change was introduced into the analyses. The baseline "a versus T" curve starts at $a_0 = 0.001$ in. This was the smallest value for which cracks would grow for the geometry and stress sequences of the baseline. Since most of the cracks in the baseline initial crack size distribution are less than 0.001 in., PROF immediately grows these cracks to 0.001 in. To test if this fast extrapolation had any effect on the analysis, it was assumed that crack growth below 0.001 in. was exponential. The parameters of the exponential fit were estimated over the range of small calculated "a versus T" values, which were well approximated by an exponential fit. It was $a_0 = 0.0001$ at $T = 0$. This extrapolation added about 70,000 hours to the "a versus T" curve. However, when this extended curve was run under the remaining baseline conditions, the differences in POF values were not visible on the POF plots, and the percentage of crack detections at the inspections were approximately equal. It was concluded that the very small cracks do not significantly influence the POF analysis over a practical number of spectrum hours.

4.2.2.3 Maximum Stress per Flight Distribution

The Gumbel extreme value distribution is used as the basis for extrapolating the maximum stress per flight distribution to larger values than are present in the spectrum. The parameters of this distribution are easily estimated from maximum stress per flight data but the estimates are somewhat subjective. The sensitivity of PROF to two approaches for fitting the data were tested by arbitrarily assigning different values to the parameters of the distribution, Figure 35. The baseline

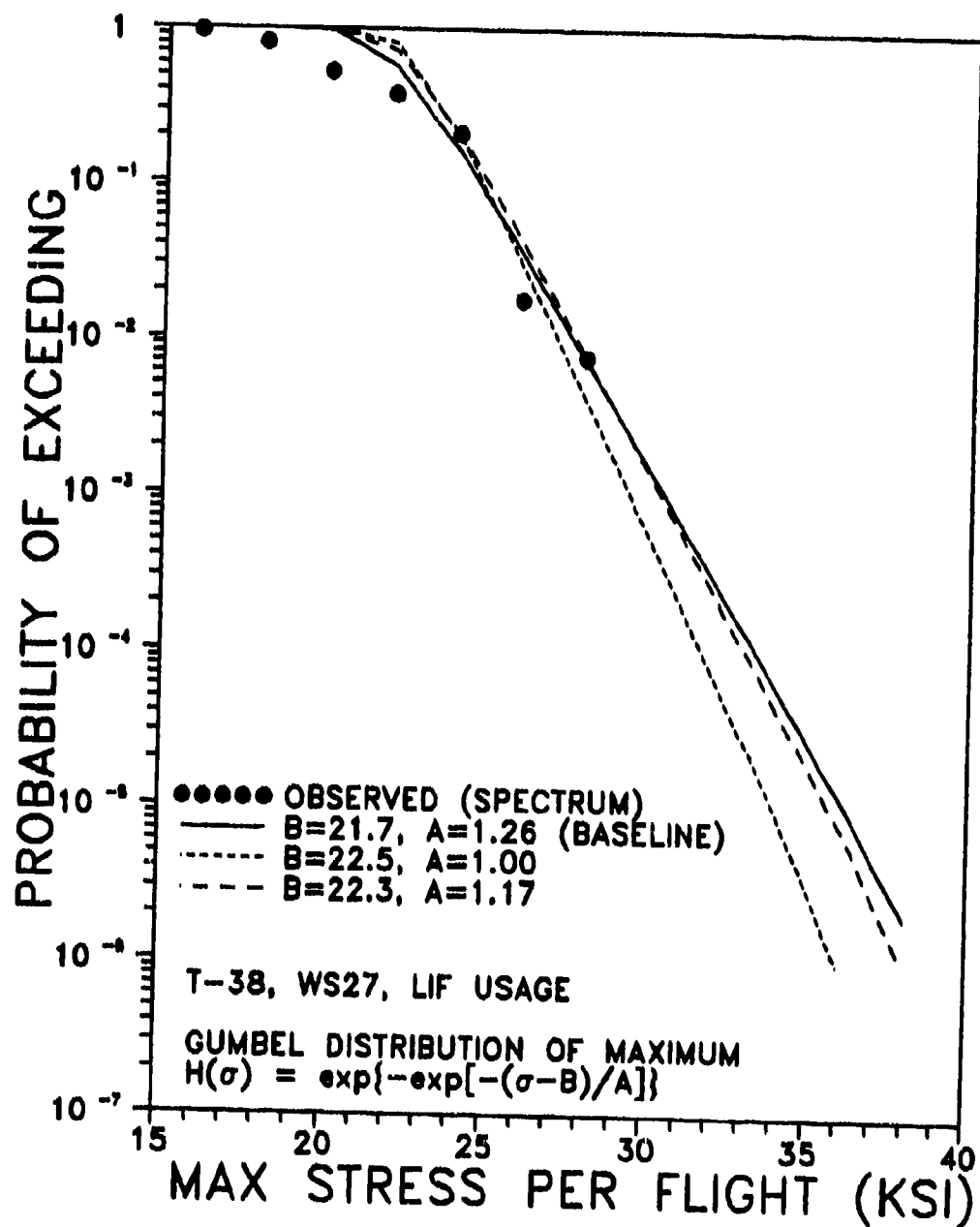


Figure 35. Selected Fits to Distribution of Max Stress per Flight.

parameters were estimated by a least squares fit to the highest four stress levels of the distribution of maximum stresses in each flight of the cycle-by-cycle spectrum (Subsection 3.1.2.3). In the first change, a steeper exceedance curve was generated which provided an acceptable fit at the largest stress levels but overpredicted the probability of exceeding smaller stress levels. The POF is dominated by the higher stress levels so the lack of fit at the lower levels does not significantly affect POF. In the second change, the slope and location parameters were modified to produce an exceedance probability curve which was a conservative bound on all data points.

Figure 36 presents the POF values for the baseline max stress per flight distribution and the two perturbations of the parameters of the Gumbel fit. The steeper slope reduced the POF values by a factor of four to five. The conservative bound produced essentially equivalent POF values, but the exceedance probability fit for this condition was also essentially equivalent to that of the baseline. Differences in the fit can significantly influence the POF values, but since the POF curves are somewhat parallel, the fit should not have significant effects on results based on variation of other inputs to the model.

4.2.2.4 Discussion - Variation in Aircraft/Usage Input

Initiating Crack Size Distribution: The crack size distribution at the start of the analysis is a driver of PROF output but is currently difficult to determine. These sensitivity analyses are primarily based on the equivalent initial flaw size concept using a distribution found to be representative of quality in an attack/fighter/trainer airframe. Although the POF levels appear reasonable, the number of crack detections is far higher than could be tolerated. When the aging aircraft crack size distribution was introduced, the number of crack detections at the inspections would certainly be indicative of noneconomical repair. Relatively large percentages of crack

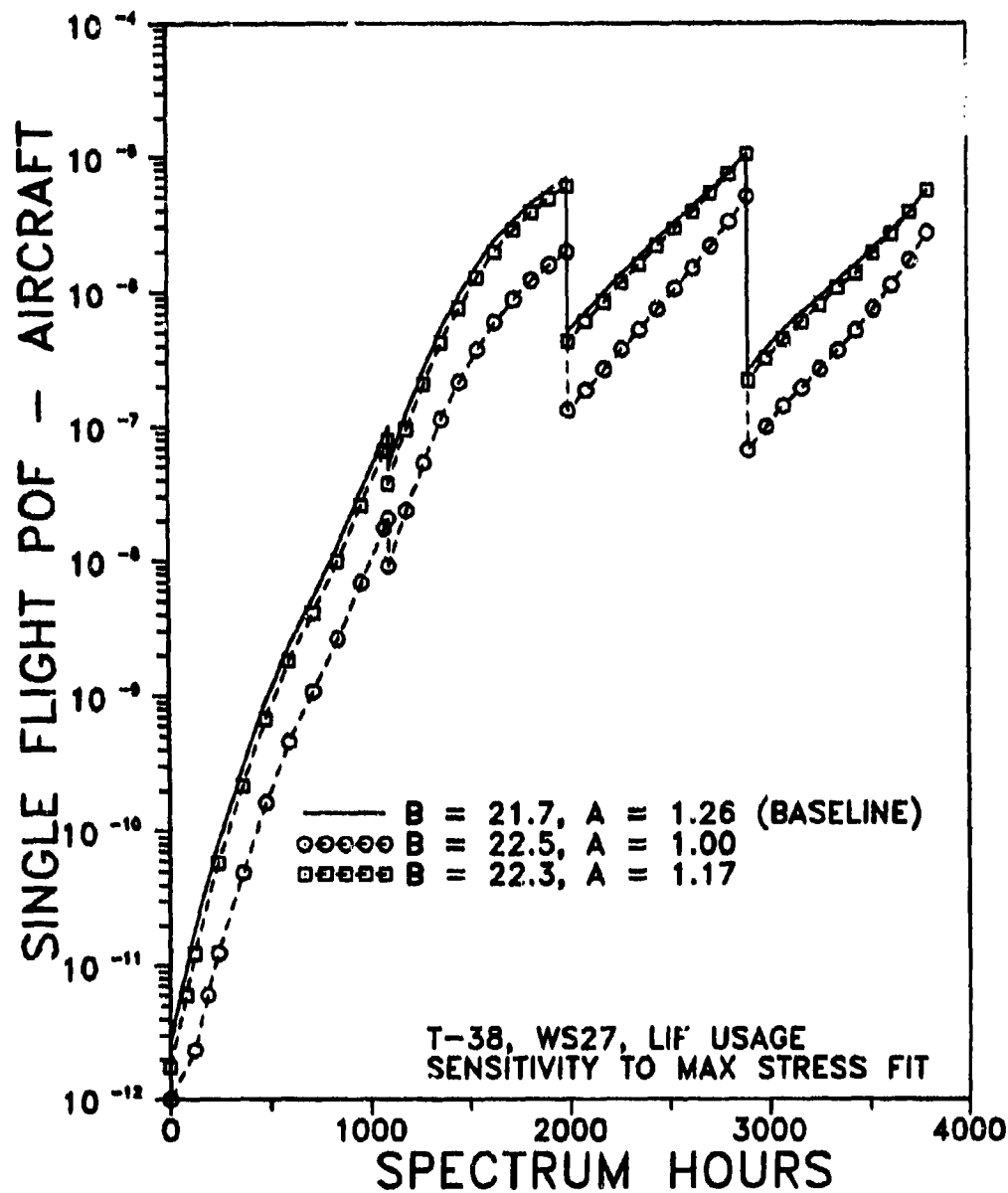


Figure 36. POF for Selected Fits to Distribution of Max Stress per Flight.

indications have been observed on most runs of PROF. It is postulated that the large detection percentages are the result of assuming that all sites have a "crack" and that PROF cannot discriminate between a real crack and an "equivalent" crack.

The examples of this report are based on two types of initial crack size distributions: equivalent initial flaw sizes and observed crack sizes in an aging aircraft. The EIFS distribution is a concept being developed for characterizing initial quality, but the proposed method is based on data that were not available for the T-38 aircraft of this study. The proposed method may not have projected the relatively large proportion of large crack sizes to the inspection interval. Since the proposed method is based on the distribution of time to initiate cracks of a known size, the proper data may have produced crack size distributions with fewer detectable real cracks at the end of the usage periods.

The crack size distribution obtained from inspections in aging aircraft are based on crack sizes observed in some of the details from airframes that have experienced different numbers of spectrum hours. To fit a distribution to these data, all crack sizes are first translated to a common number of spectrum hours using the appropriate "a versus T" relation. A distribution is then fit to the translated crack sizes by assuming that the cracks at all sites in which no cracks were found were smaller than the minimum translated crack size. This process may produce a model of the crack size distribution that is reasonable for the larger cracks which dominate the calculation of POF. However, the distribution at the more central region of the distribution is subject to potentially significant errors from the method of accounting for the sites at which no cracks were found, i.e., in accounting for the equivalent cracks.

In a teardown inspection, all cracks greater than a defined minimum will be found. For example, in the T-38 teardown inspection which led to the aging aircraft crack size distribution of the above analysis, actual cracks as small as

0.001 in. were reported. All cracks were then translated to the average number of spectrum hours experienced by the torn down wings. Translating a 0.001 in. crack to a larger number of spectrum hours increases the minimum cutoff of the data and translating it to a smaller number of hours decreases the minimum cutoff. At the common number of spectrum hours, the effect of the inspection sites at which no cracks were found has a mixed effect on the lower percentiles of the crack size distribution. Again, the method may produce an acceptable fit to the upper tail of the distribution which governs POF calculations for the early usage periods of the analysis.

A better model is needed for separating the real cracks from the equivalent cracks. Such a model could be expressed in terms of the proportion of crack sites which contain a real crack of a predefined size. PROF can handle an arbitrary initial crack size distribution since this input is in a tabular format. At a fixed number of hours if the proportion of uncracked sites is known, the PROF output can be reduced accordingly. (POF and the percent crack detections would be multiplied by the proportion of sites that contain real cracks.) However, PROF cannot currently handle a changing proportion of cracked sites that would be involved in a model of crack sizes that incorporates time to crack initiation and growth of initiated cracks.

The methods of defining the initiating crack size distribution in this study cause a discrepancy between the predicted number of crack detections at inspections and the anticipated actual. Until a better method can be implemented for modeling the initiating crack size distribution, evaluations of maintenance scenarios based on cost estimates do not have reasonable validity. However, evaluations based on relative changes in POF for different maintenance scenarios still have meaning for at least the first couple of usage intervals.

a versus T: The "a versus T" relation used in the analysis is driven by the geometry at the crack site and the stress

sequences derived from the anticipated stress spectrum. No single aircraft will actually experience the sequences which drive the crack growth. It is assumed that the sequences of the analysis will produce an "a versus T" relation that is representative of the average aircraft in the fleet being analyzed. Under this assumption, the calculated POF values are representative of a randomly selected airframe in the fleet.

If a subset of the fleet is known to be consistently flown to a more severe stress spectrum, a separate analysis could be run for this subset. The analysis would require the generation of a new stress sequence from the spectrum, new "a versus T" curve, and new distribution of maximum stress per flight. (This procedure was done for the LIF usage of the T-38.) The limits of the analyses and their interpretation will be dictated by the degree of detail that is reasonable to pursue. PROF will be applicable to the same degree of detail that deterministic damage tolerance analyses are currently performed.

Distribution of Maximum Stress per Flight: In these sensitivity studies, the distribution of the maximum stress per flight was determined from the stress sequences of the crack growth analysis. Strictly speaking, more or less severe maximum stress per flight distributions could be used for special purpose analyses, but the maximum stress should be consistent with the crack growth drivers over entire usage intervals. Since this distribution is derived from the sequences which drive crack growth, the previous discussion also applies here.

Different estimates of the parameters of the distribution of the maximum stress per flight can produce acceptable fits to the data. Relatively small changes in these parameters can produce differences of a factor five or more in the calculation of POF. However, the relationship between the POF curves for the different sets of apparently equivalent parameters remains approximately constant. Absolute interpretation of the POF values is clouded by this effect. However, relative comparisons

under the same maximum stress per flight distribution should be valid.

4.2.3 Variations in Inspection/Repair Input

The PROF inspection and repair input are associated with the scheduling of inspections, the capability of the inspection system, and the quality of necessary repairs. While the inspection schedule is the easiest to modify, alternative inspections with varying inspection costs are sometimes available. Similarly, more expensive repairs could be performed which presumably produce a better quality repair as quantified by the equivalent repair flaw size distribution. This subsection addresses the trade-offs that result from changes in the maintenance scenario as defined by the inspection schedule, the inspection capability, and the repair quality.

4.2.3.1 Inspection Schedule Effects

The effect of the inspection schedule on PROF output was analyzed by running the program at an array of inspection times about the baseline DTA schedule. Both the initial inspection, T_1 , and the subsequent inspection increments were varied. The sensitivity to the inspection schedule was addressed from the viewpoints of both fracture probability and cost of maintenance over a 5000 spectrum hour usage period. Fracture probabilities will be considered first.

4.2.3.1.1 Scheduling Effect on Fracture Probability

PROF outputs fracture probabilities at increments of spectrum hours as determined by the inspection schedule. The output from different inspection schedules are difficult to compare in the form of overlaying plots of POF versus spectrum hours as previously used. For example, Figure 37 presents a plot of fracture probability for four inspection increments with the initial inspection being performed at 1100 hours. To simplify comparisons for different inspection times, the fracture probability immediately prior to an inspection will be plotted at

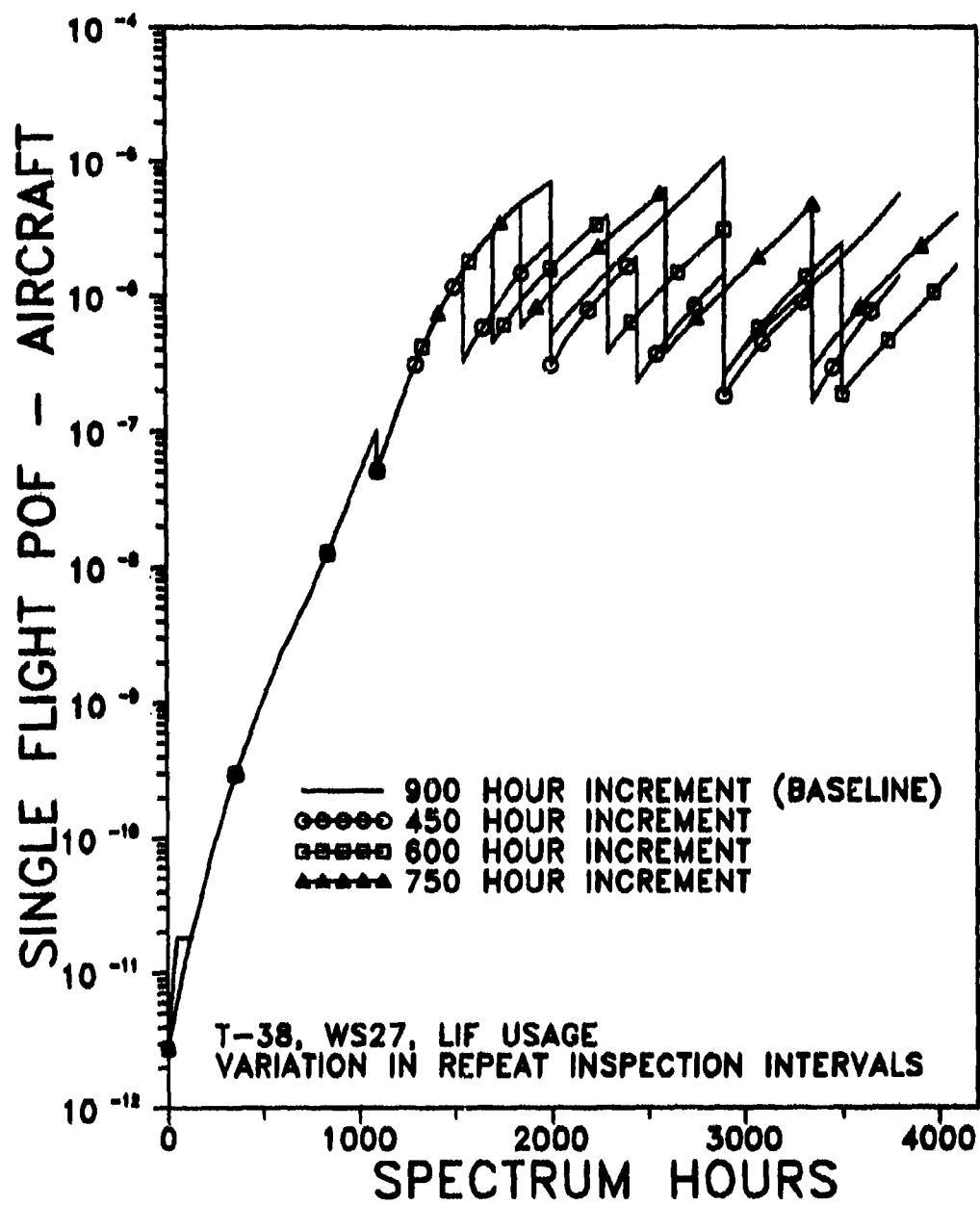


Figure 37. POF for Inspection Increments.

the inspection times. This simpler plot is an upper bound on the fracture probability over the entire analysis period since maximum fracture probability in any usage interval occurs immediately prior to an inspection. The maximum fracture probability would most likely also be used to characterize the risk in a usage interval between inspections or over an entire analysis period.

Figure 38 presents single flight POF bounds for inspection schedules defined by an initial inspection at 1100 spectrum hours and increments of 450, 600, 750, 900, and 1050 hours thereafter. Shortening the inspection increment produces a distinct and somewhat consistent reduction in fracture probabilities. They also tend to converge to an equilibrium value for each inspection increment.

Figure 39 presents single flight POF bounds for inspection schedules defined by initial inspections at 500, 700, 900, and 1100 hours with the repeat inspections at 750 hours thereafter. Over this range of initial inspection intervals, the fracture probabilities are approximately equivalent except, perhaps, at about 2000 spectrum hours. After 2500 hours, all of the POF bounds tended to converge to a common equilibrium value as determined by the subsequent inspection intervals (and other conditions).

Figure 40 presents a similar set of POF bounds for longer initial inspection intervals. The effect of postponing the first inspection begins to be significant for initial inspection intervals greater than 1900 spectrum hours. The fracture probabilities for these longer initial inspection intervals are also tending to converge to the same equilibrium level.

To test for a joint effect of initial and subsequent inspection intervals, POF as a function of spectrum hours was calculated for all four combinations of 750 and 1500 hour initial inspection intervals and 450 and 1050 hour subsequent inspection intervals. Figure 41 presents the bounds on single flight POF

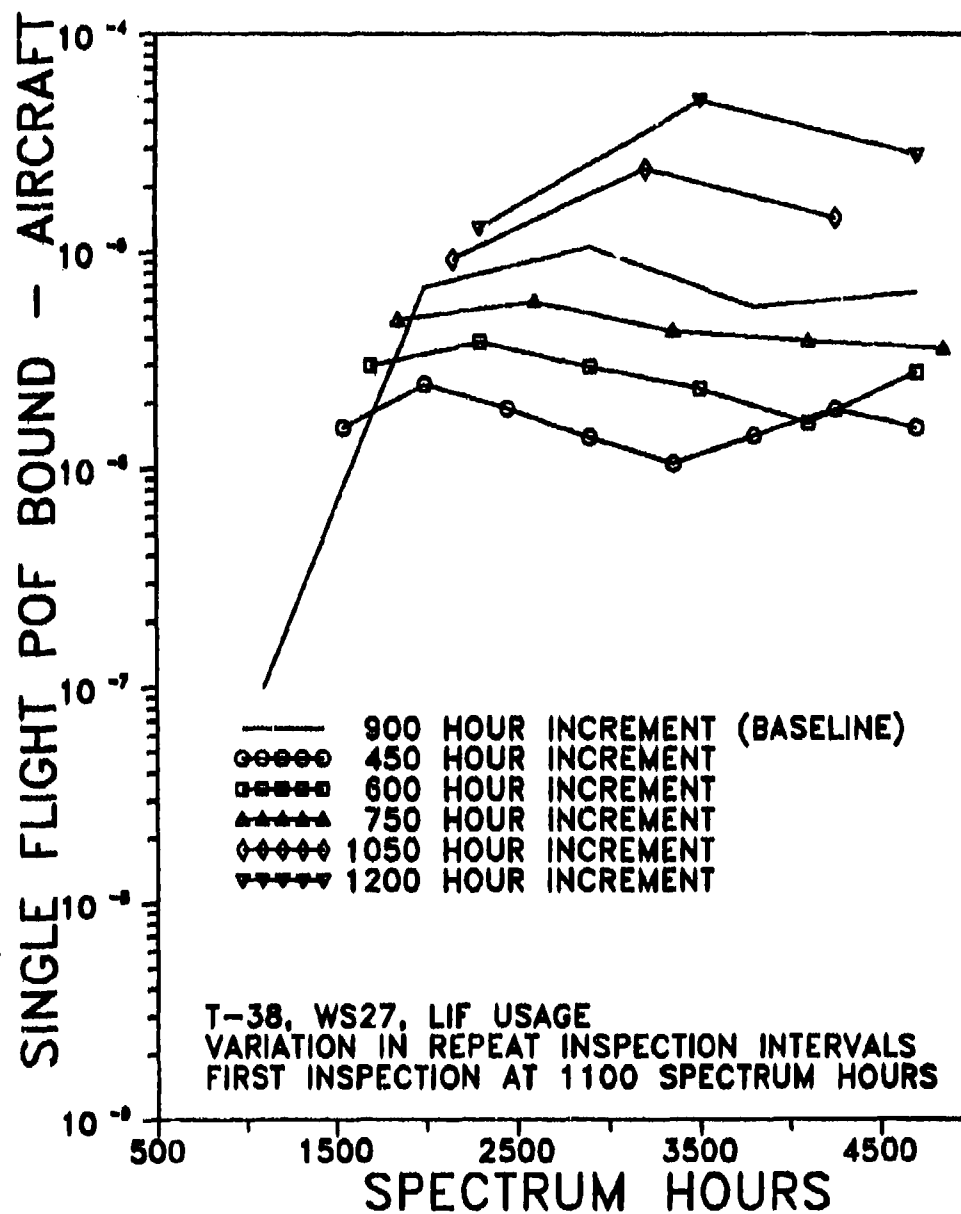


Figure 38. POF Bounds at Defined Inspection Increments.

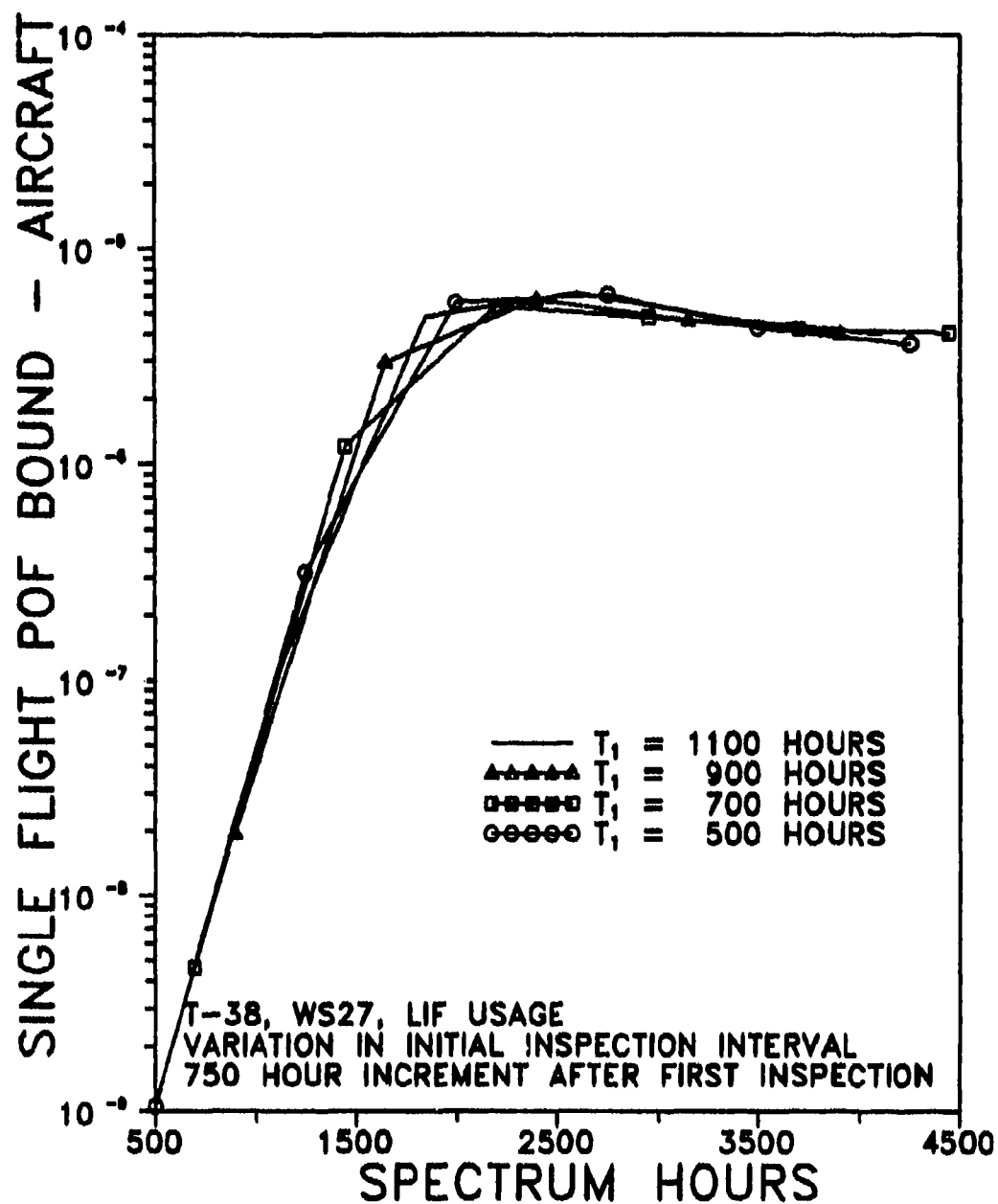


Figure 39. POF Bounds for Initial Inspection Increments Shorter than Baseline.

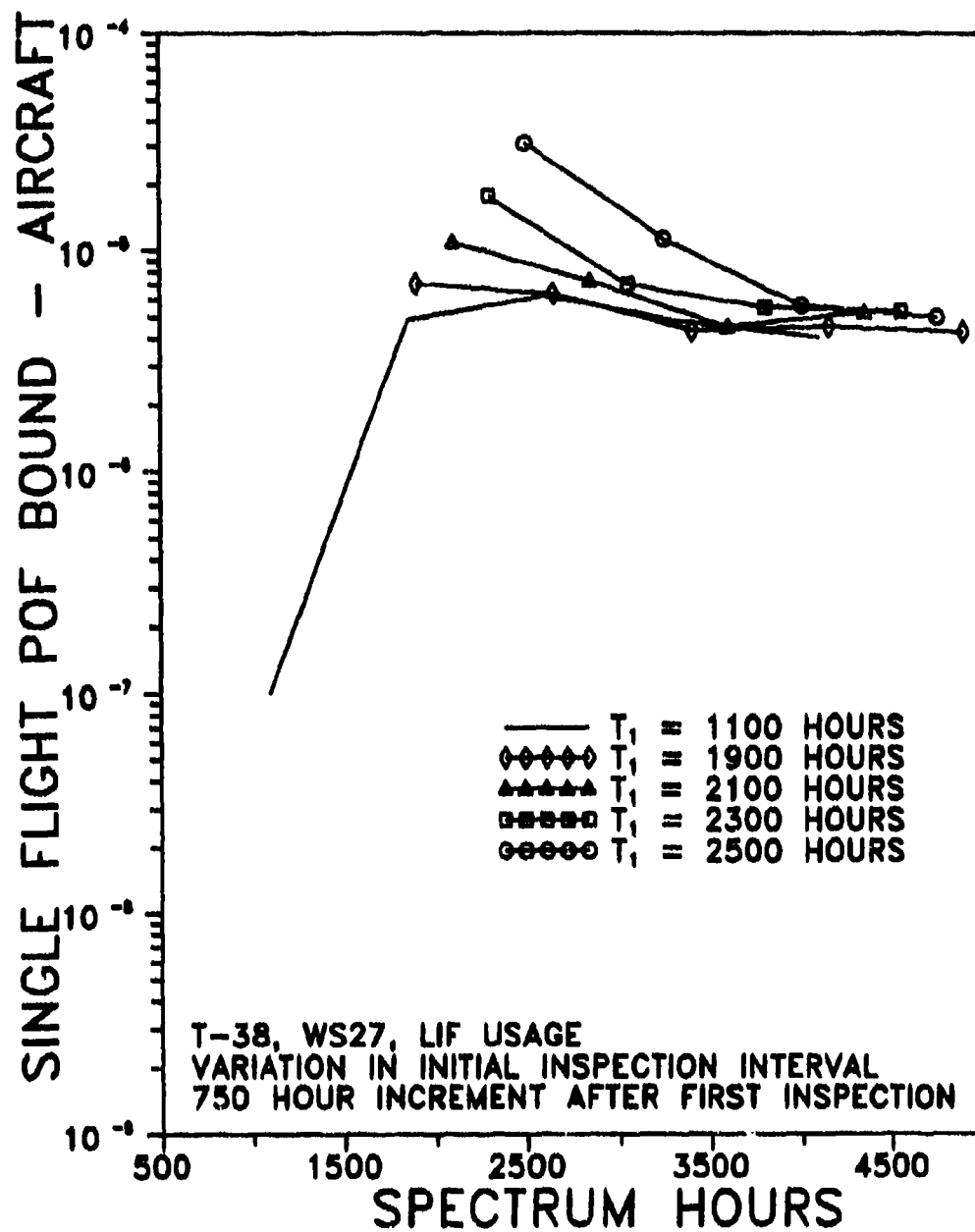


Figure 40. POF Bounds for Initial Inspection Intervals Larger than Baseline.

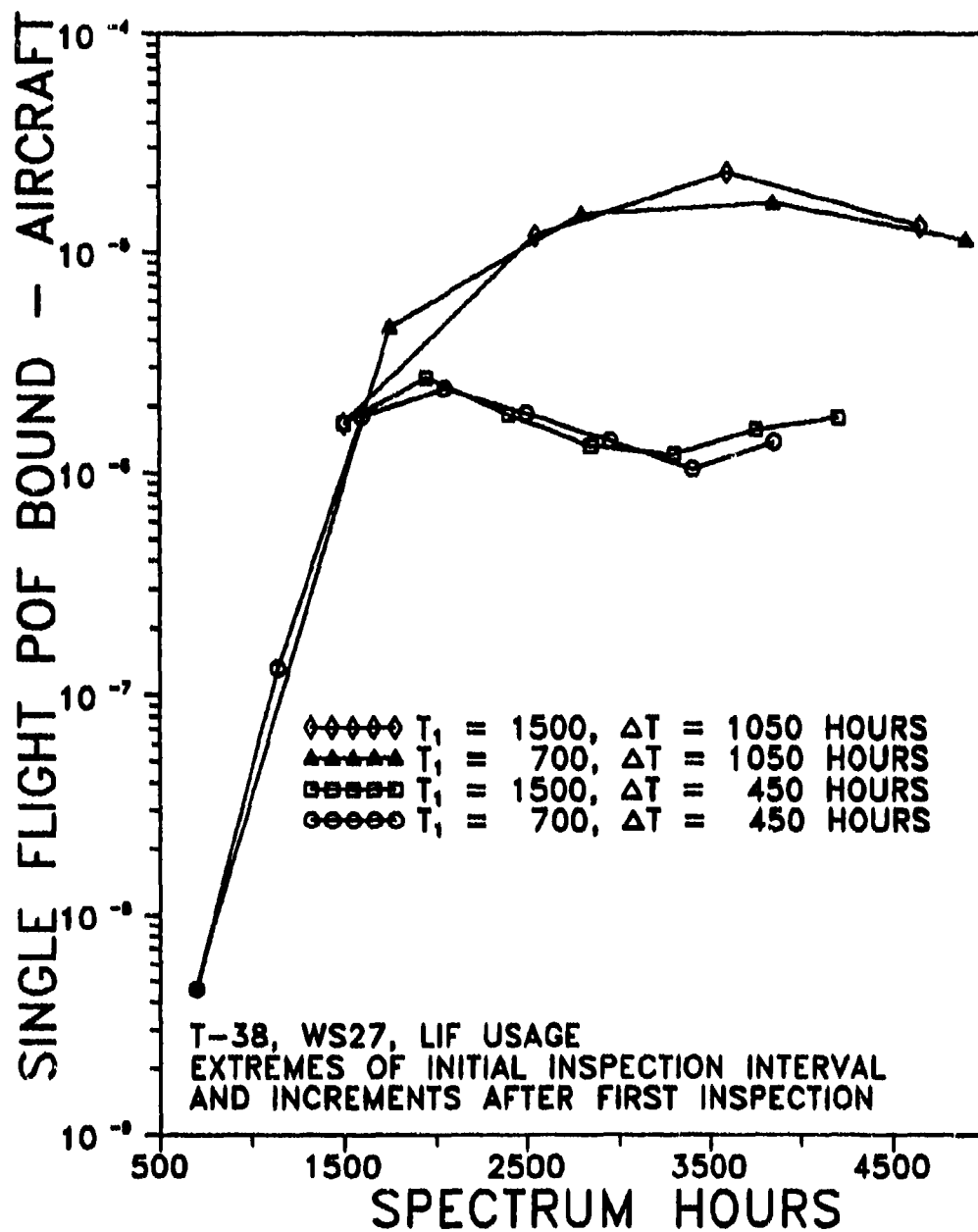


Figure 41. POF Bounds for Combinations of Initial Interval and Increments.

for the four combinations. These initial inspection intervals did not produce significant differences in the POF bounds but the effect of the 600 hour difference in subsequent inspections was larger than an order of magnitude after 2500 spectrum hours.

4.2.3.1.2 Scheduling Effect on Expected Costs

To consider the costs of the maintenance schedules, first recall that there are a total of 750 analysis sites in the fleet. PROF will provide estimates of the number of these analysis sites for which cracks will be detected in a 5000 spectrum hour period. Table 7 presents the sum of the percentages of crack detections for all inspections that occur before 5000 hours for the different schedules of the previous POF bound plots. For example, under the baseline conditions of initial inspection at 1100 hours and subsequent inspections at 900 hours, 33.1 percent of the total number of sites (750) will have undergone repair prior to 5000 spectrum hours. As noted earlier, the initial crack size distribution and crack growth model of the baseline conditions result in an unrealistic distribution of crack sizes. However, for these comparative studies it is assumed that the relative effect would be the same for a more realistic model of crack sizes at the inspection intervals.

The total number of detected cracks over the 5000 hour period is approximately the same for all of the maintenance schedules considered. The mechanisms for modeling crack growth remain unchanged, and the inspection process tends to find the larger cracks. The differences arise from the timing of the crack detections and the subsequent opportunities for the equivalent repair cracks to grow. Table 7 indicates that the inspection schedule does not significantly affect the total number of detections under the baseline conditions.

To determine if smaller cracks were being detected at the more frequent inspections of the shorter intervals, cumulative repair costs were calculated using the assumptions of Subsection 4.1.3. Incremental inspection costs are assumed to be \$100 per

TABLE 7
Total Percent of Sites at Which Cracks Are Detected in
5000 Spectrum Hours

FIRST INSPECTION (HOURS)	INSPECTION INTERVAL AFTER FIRST INSPECTION (HOURS)				
	450	600	750	900	1050
500			34.7		
700	36.3		31.3*		34.2
900			32.2		
1100	37.3	33.6	34.6	33.1	29.0*
1300			35.1		
1500	36.8		31.4*		32.4
1900			34.3		
2100			32.9*		
2300			35.6		
2500			35.1		

* - Last inspection at 4500 hours or less.

site per inspection. The cost model assumes that cracks less than 0.100 in., i.e., not visible to the eye since they are hidden by the fastener head, can be repaired at a nominal additional cost of \$1,000. It is assumed that cracks larger than 0.100 in. require major repair at a cost of \$100,000. If fracture occurs, the loss is assumed to be \$10,000,000.

For the first inspection at 1100 hours and subsequent inspections at 450, 600, 750, and 900 hours, the proportion of sites at which cracks greater and less than 0.100 in. was obtained at each inspection. These percentages and the resulting incremental and total cost for the four inspection schedules are presented in Table 8. Figure 42 presents the cumulative total costs as a function of spectrum hours. For the assumptions of this analysis, although the total number of sites to be repaired is approximately the same for the different repeat inspection intervals, the shorter inspections are finding the cracks when they are smaller and cheaper to repair. The expected costs due to fracture also increases as a function of the time between inspections.

A similar cost analysis was performed varying the initial inspection interval while holding the subsequent inspection intervals constant. Table 9 presents the detection percentages, incremental costs, and total costs for initial inspection times of 700 and 1500 hours with subsequent inspections at intervals of 750 hours. Table 8b contains data for an 1100 hour initial interval with 750 hour increments thereafter. The expected total repair costs for these data are plotted in Figure 43. Under the conditions of this analysis, starting the inspections sooner resulted in the smallest expected repair costs. The savings resulted from both the expected repair cost and the expected costs of failures.

The absolute magnitudes of the above expected costs are not realistic due to the arbitrary cost assumptions and inadequate initial crack size model. However, regardless of the relative repair costs for cracks of different sizes, the conclusion that

TABLE 8
Expected Repair Costs

EXPECTED REPAIR COSTS - VARIATIONS FROM BASELINE

NUMBER OF A/C	125	C1 =	1000	(FOR a < 0.100 in.)
COST PER A/C	10000000	C2 =	100000	(FOR a > 0.100 in.)
HOLES PER A/C	6			
INS COST/AC	100			

BASELINE INSPECTION SCHEDULE - DTA DEFINED
T1 = 1100 HOURS WITH 900 HOUR INTERVALS

T	INT POF	EXP COST DUE TO FRACTURE	PROP. DETECTED BY SIZE RANGE		EXP COST OF MAINT.	INCR TOTAL COSTS	CUM TOTAL COSTS
			C1	C2			
1100	1.58E-05	19750	0.0164	0.0006	69800	89550	89550
2000	1.77E-03	2213750	0.0494	0.0618	4684550	6898300	6987850
2900	2.11E-03	2632500	0.0280	0.0483	3506000	6138500	13126350
3800	1.05E-03	1307500	0.0358	0.0215	1651850	2959350	16085700
4700	1.71E-03	2142500	0.0481	0.023	1773575	3916075	20001775

T1 = 1100 HOURS WITH 450 HOUR INTERVAL

T	INT POF	EXP COST DUE TO FRACTURE	PROP. DETECTED BY SIZE RANGE		EXP COST OF MAINT.	INCR TOTAL COSTS	CUM TOTAL COSTS
			C1	C2			
1100	1.58E-05	19750	0.0171	0.0008	85325	105075	105075
1550	2.22E-04	277375	0.0547	0.0043	376025	653400	758475
1900	4.73E-04	591000	0.0396	0.0187	1444700	2035700	2794175
2450	3.73E-04	466750	0.0308	0.0133	1033100	1499850	4294025
2900	2.89E-04	336750	0.0237	0.0099	772775	1109525	5403550
3350	2.10E-04	262750	0.0225	0.0082	644375	907125	6310675
3800	2.53E-04	316250	0.0364	0.0083	662300	978550	7289225
4250	3.56E-04	445000	0.0341	0.0125	975575	1420575	8709800
4700	2.98E-04	372125	0.0281	0.0101	791075	1163200	9873000

(a) 900 and 450 Hour Inspection Increments

TABLE 8
Expected Repair Costs (concluded)

EXPECTED REPAIR COSTS - VARIATIONS FROM BASELINE

NUMBER OF A/C 125 C1 = 1000 (FOR a < 0.100 in.)
 COST PER A/C 10000000 C2 = 100000 (FOR a > 0.100 in.)
 HOLES PER A/C 6
 INS COST/AC 100

T1 = 1100 HOURS WITH 600 HOUR INTERVAL

T	INT POF	EXP COST DUE TO FRACTURE	PROP. DETECTED BY SIZE RANGE		EXP COST OF MAINT.	INCR TOTAL COSTS	CUM TOTAL COSTS
			C1	C2			
1100	1.58E-05	19750	0.0173	0.0006	70475	90225	90225
1700	5.27E-04	658625	0.0603	0.0168	1317725	1976350	2066575
2300	8.99E-04	1123375	0.0417	0.0282	2158775	3262150	5348725
2900	6.88E-04	835250	0.0309	0.0212	1625675	2460925	7809650
3500	5.27E-04	658750	0.0164	0.0227	1727300	2386050	10195700
4100	3.42E-04	427250	0.0306	0.0102	800450	1227700	11423400
4700	5.83E-04	729125	0.0415	0.0176	1363625	2092750	13516150

T1 = 1100 HOURS WITH 750 HOUR INTERVAL

T	INT POF	EXP COST DUE TO FRACTURE	PROP. DETECTED BY SIZE RANGE		EXP COST OF MAINT.	INCR TOTAL COSTS	CUM TOTAL COSTS
			C1	C2			
1100	1.58E-05	19750	0.0172	0.0007	77900	97650	97650
1850	1.04E-03	1301250	0.0540	0.0412	3143000	4444250	4541900
2600	1.45E-03	1610000	0.0342	0.0383	2910650	4720650	9262550
3350	9.32E-04	1164875	0.0336	0.0239	1830200	2995075	12257625
4100	9.24E-04	1155375	0.0246	0.028	2130950	3266325	15543950
4850	7.93E-04	991625	0.0145	0.024	1823375	2815000	18358950

(b) 600 and 750 Hour Inspection Increments

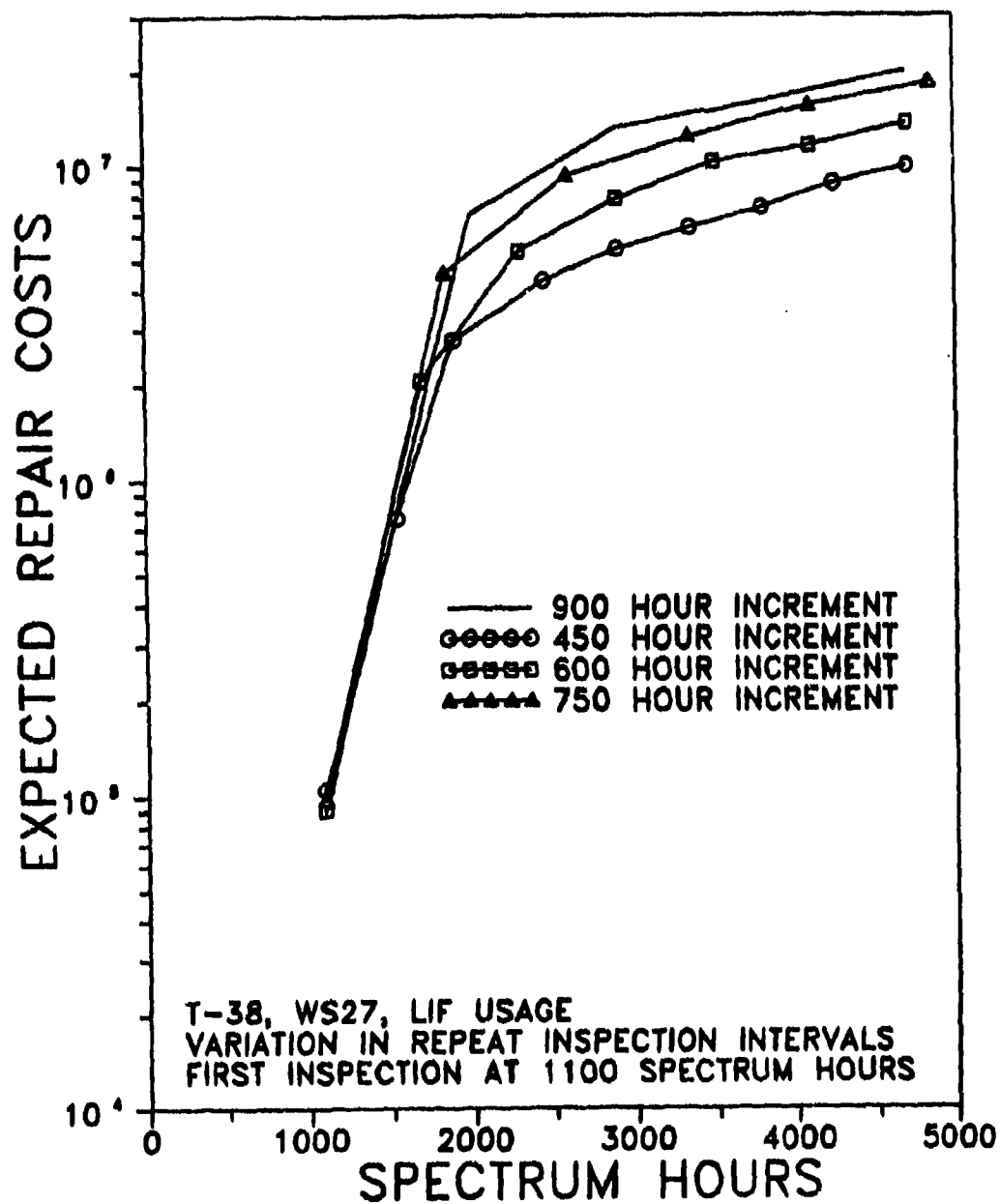


Figure 42. Expected Repair Costs as a Function of Repeat Inspection Increments.

TABLE 9
Expected Repair Costs - 700 and 1500 Hour
Initial Intervals

EXPECTED REPAIR COSTS - VARIATIONS FROM BASELINE

NUMBER OF A/C	125	C1 =	1000	(FOR a < 0.100 in.)
COST PER A/C	10000000	C2 =	100000	(FOR a > 0.100 in.)
HOLES PER A/C	6			
INS COST/AC	100			

BASELINE INSPECTION SCHEDULE - DTA DEFINED
T1 = 1500 HOURS WITH 750 HOUR INTERVALS

T	INT POF	EXP COST DUE TO FRACTURE	PROP. DETECTED BY SIZE RANGE		EXP COST OF MAINT.	INCR TOTAL COSTS	CUM TOTAL COSTS
			C1	C2			
1500	2.75E-04	344000	0.0641	0.0641	4868075	5212075	5212075
2250	1.53E-03	1918250	0.0359	0.0359	2731925	4648175	9860250
3000	1.05E-03	1313750	0.0319	0.0319	2428925	3742675	13602925
3750	9.88E-04	1209500	0.0285	0.0285	2171375	3380875	16983800
4500	8.81E-04	1100750	0.0198	0.0198	1512350	2813100	19596900

T1 = 700 HOURS WITH 750 HOUR INTERVAL

T	INT POF	EXP COST DUE TO FRACTURE	PROP. DETECTED BY SIZE RANGE		EXP COST OF MAINT.	INCR TOTAL COSTS	CUM TOTAL COSTS
			C1	C2			
700	1.58E-05	19750	0.0019	0.0003	36425	56175	56175
1450	2.22E-04	277375	0.0555	0.0016	174125	451500	507675
2200	4.73E-04	591000	0.0369	0.0470	3565175	4158175	4663850
2950	3.73E-04	466750	0.0333	0.0273	2084975	2551725	7215575
3700	2.69E-04	336750	0.0294	0.0289	2202050	2538800	9754375
4450	2.10E-04	262750	0.0241	0.0271	2063075	2325825	12080200

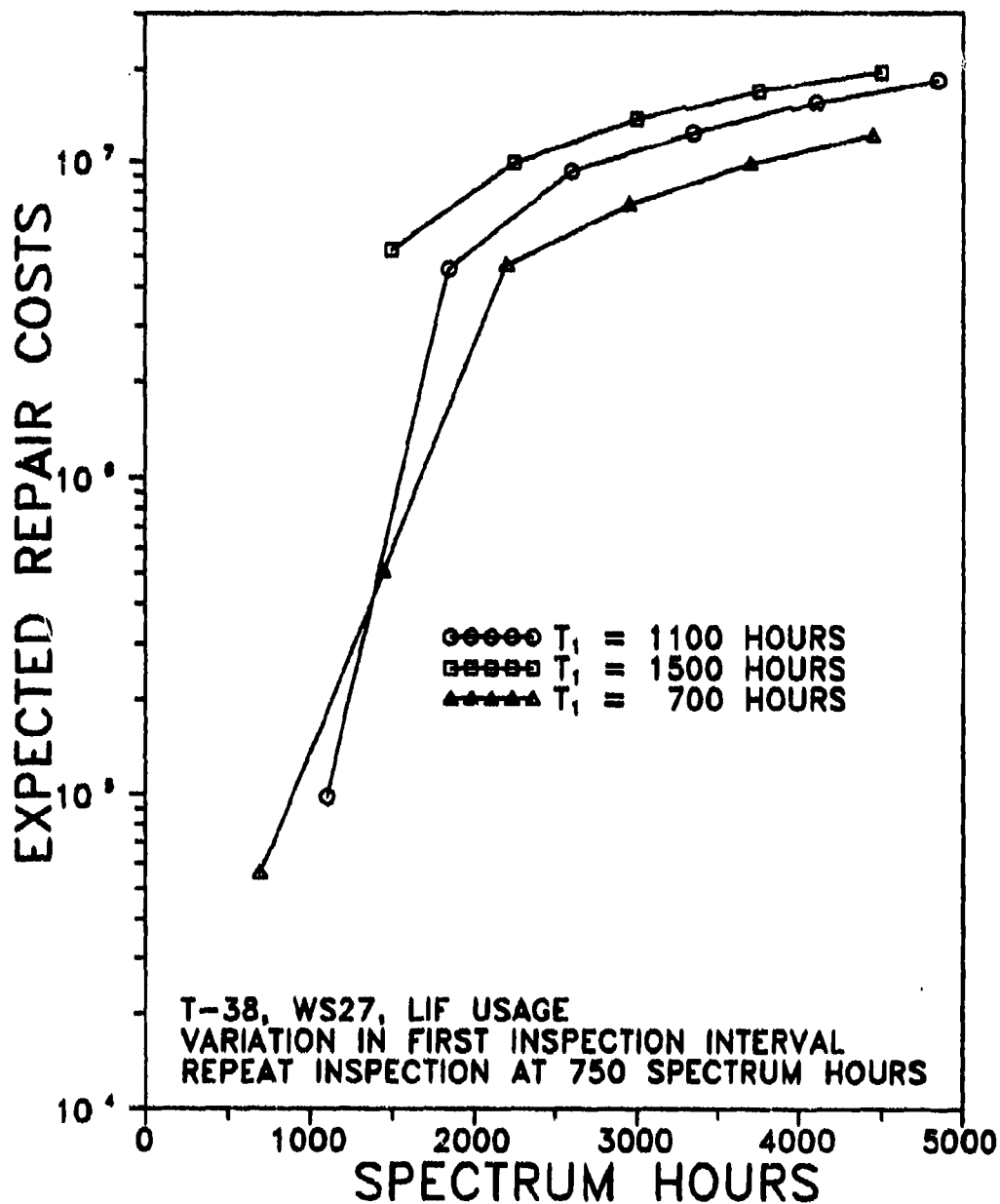


Figure 43. Expected Repair Costs for Selected Initial Inspection Intervals.

expected repair costs would be less at the shorter initial and subsequent inspection intervals would be valid. This is due to the reduced expected costs associated with fracture at the shorter initial and subsequent inspection intervals.

4.2.3.2 Inspection Capability Effects

As noted in the previous subsection, the inspections play a critical role in controlling the POF. The capability of the inspection systems are quantified in terms of the probability of crack detection as a function of crack size, $POD(a)$. Different inspection systems (particular applications of a defined inspection method) have different capabilities, and the choice for a given detail is a force management decision. In general, less automated systems have poorer $POD(a)$ functions than more automated systems. Further, less automated systems are not necessarily less expensive in a specific application. Given the inspection system to be used in an application, its capability must be characterized. This can be done through NDE reliability experiments but more typically is inferred from past experience with the system.

The trade-offs to be evaluated in terms of their effect on the POF will be defined in two contexts. First, two different $POD(a)$ capabilities will be introduced to quantify the effect of different, but potentially available, inspection systems. Second, the parameters of the $POD(a)$ function will be varied over a range of values that would represent sampling variation from an experiment to evaluate the inspection capability of the baseline semiautomated eddy current system.

The capabilities of the two different inspection systems are rationalized as follows. For the first system, assume the inspections of the baseline structure were to be made by a visual inspection of the six holes in each aircraft without removing the fastener. Visual inspections are not reliable for detecting small cracks, and they are incapable of detecting a crack less than 0.100 in. because such cracks are under the fastener head

(i.e. $a_{\min} = 0.100$). However, because of the focus of the inspections at only six locations on an airframe, it will be assumed that a 0.150 in. crack will be detected 50 percent of the time ($a_{50}=0.150$) and a 0.200 in. crack will be detected 90 percent of the time ($a_{90}=0.200$). These three conditions are sufficient to calculate the parameters of the POD(a) function as shown in Figure 44. Because of the reduced capability, the inspection interval for this capability will be set at 450 spectrum hours.

For the second, assume that an advanced system is under development which will be capable of obtaining two different objectives: a) it can be set to detect a 0.030 in. crack (under the fastener head) 50 percent of the time and a 0.075 in. crack 90 percent of the time ($a_{50}= 0.030$ and $a_{90}= 0.075$); or, b) it can be set to detect a 0.050 in. crack 50 percent of the time and a 0.075 in. crack 90 percent of the time ($a_{50}= 0.050$ and $a_{90}= 0.075$). That is, the system can be configured to detect either a higher percentage of small cracks or a higher percentage of large cracks, but not both. Figure 44 displays the POD(a) functions for the two configurations as well as that of the baseline system. Both configurations have the same a_{90} value. The first configuration, when compared to the second, has higher detection probabilities for cracks less than 0.75 in. and lower detection probabilities for cracks greater than 0.75 in. Both configurations are better than the baseline for cracks larger than 0.050 in.

Figure 45 compares POF as a function of spectrum hours for the visual and baseline inspection systems. The baseline is presented for inspection intervals of 450 and 900 spectrum hours. After the cracks have grown to detectable sizes, about 1500 - 2000 hours for the baseline eddy current system, there is more than an order of magnitude difference in the bounds on POF over the inspection intervals when the same schedule is used for both inspection systems. If the baseline (eddy current) system is used at the 900 hour schedule, the POF bound for the visual

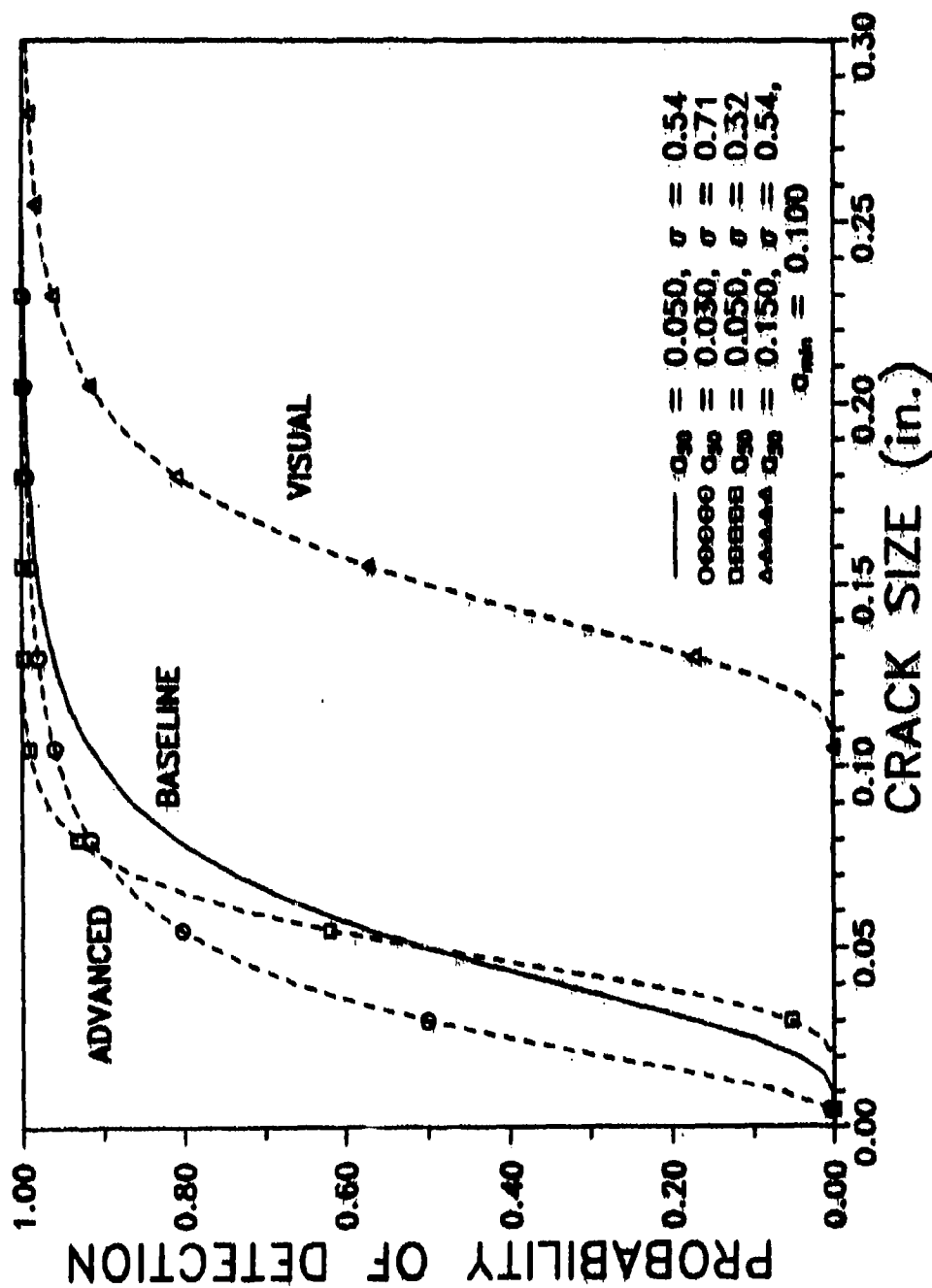


Figure 44. POD(a) Functions for Potential Inspection Systems.

system is about 2.5 to 3 times higher than that of the eddy current system. Table 10 presents the percent of detections that were made during 900 hour increments. Over the entire 4700 hour period, approximately the same number of cracks were detected by the two inspection procedures, but the eddy current system was detecting much smaller cracks.

Figure 46 compares the fracture probabilities for the "advanced" and baseline NDE systems. The configuration of the advanced system which has a larger POD(a) at the larger crack sizes did not provide the expected lower POF values. The configuration with the higher POD(a) values for cracks less than 0.075 in. had lower POF values throughout the 4700 hour period. As expected, both configurations of the advanced system had lower POF values after the cracks reached detectable sizes. The differences range up to a factor of about 2.5 for the configuration with the steeper POD(a) function (smaller σ) and about 3 for the configuration with the lower median detection capability. The configuration with the lower median detection capability also had six percent more cracks detected over the 4700 hour period, as seen in Table 10.

Baseline variations to reflect potential errors in the characterization of inspection capability were introduced arbitrarily. The POD(a) function of the baseline analyses had $a_{50}=0.050$ in. and $\sigma = 0.54$. For these parameter values, $a_{90}=0.100$ in. Three variations which lowered the capability were considered: a) the median detectability size was held at 0.050 in. and σ was increased to 1.0 ($a_{90}=0.180$ in.); b) the median detectability was increased to 0.070 in. for the baseline σ ($a_{90}=0.140$ in.); and, c) both the median detectability and σ were increased to 0.60 in. and 0.70, respectively ($a_{90}=0.147$ in.). Figure 47 presents the POD(a) function for the baseline and these variations.

The different POF values resulting from the defined variations in capability are presented in Figure 48. The three variations had quite similar effects on POF, increasing the POF

TABLE 10
Percent Detections at Inspections for Different
Inspection Capabilities

	a_{50}	σ	a_{90}	INSPECTION TIMES (HOURS)					
				1100	2000	2900	3800	4700	TOTAL

BASELINE	0.050	0.54	0.100	1.7	11.1	7.4	5.7	7.1	33.0

VISUAL	0.150	0.54	0.200	0.0	2.1	11.5	7.2	12.6	33.4

CONFIG. 1	0.030	0.71	0.075	4.7	10.2	8.2	6.9	5.0	35.0

CONFIG. 2	0.050	0.32	0.075	1.0	11.9	7.4	6.2	7.2	33.7

VAR. 1	0.050	1.00	0.180	3.0	9.8	8.2	6.8	6.4	34.2

VAR. 2	0.070	0.54	0.140	0.8	9.5	7.7	7.1	6.9	32.0

VAR. 3	0.060	0.70	0.147	1.5	9.9	7.7	6.6	6.6	32.3

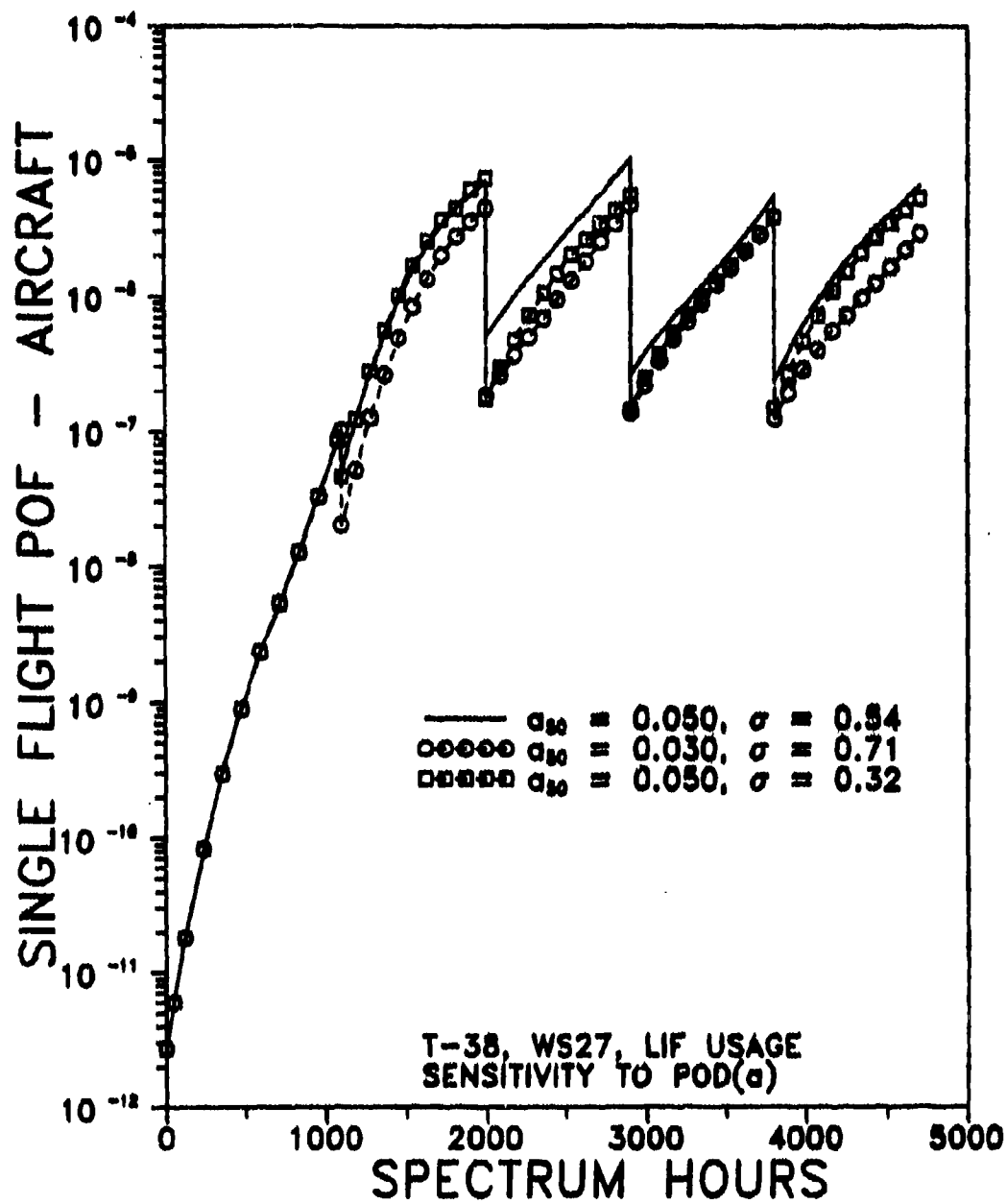


Figure 46. POF Comparing Baseline to Potential Advanced NDE Systems.

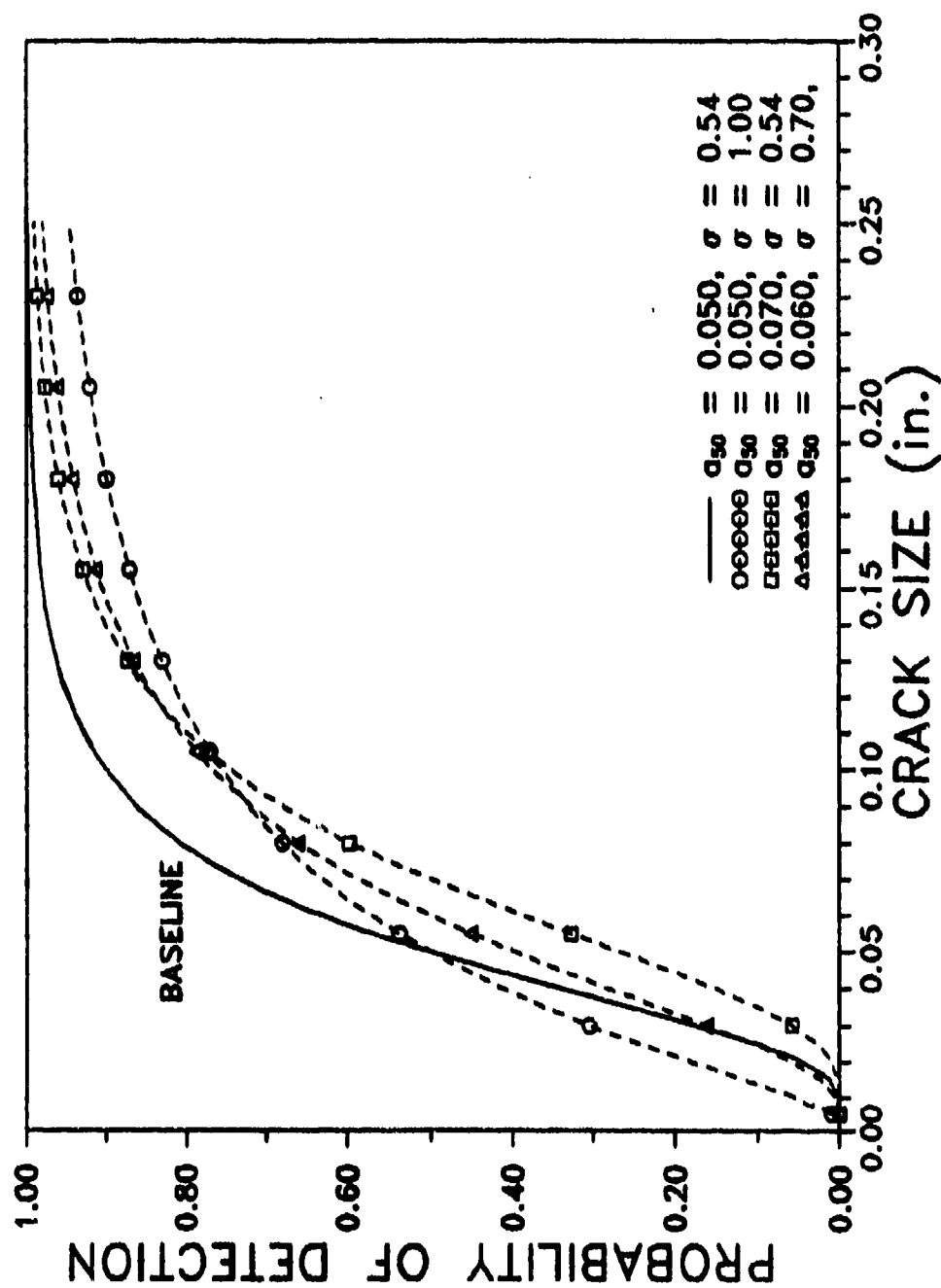


Figure 47. POD(a) for Parametric Variations from Baseline.

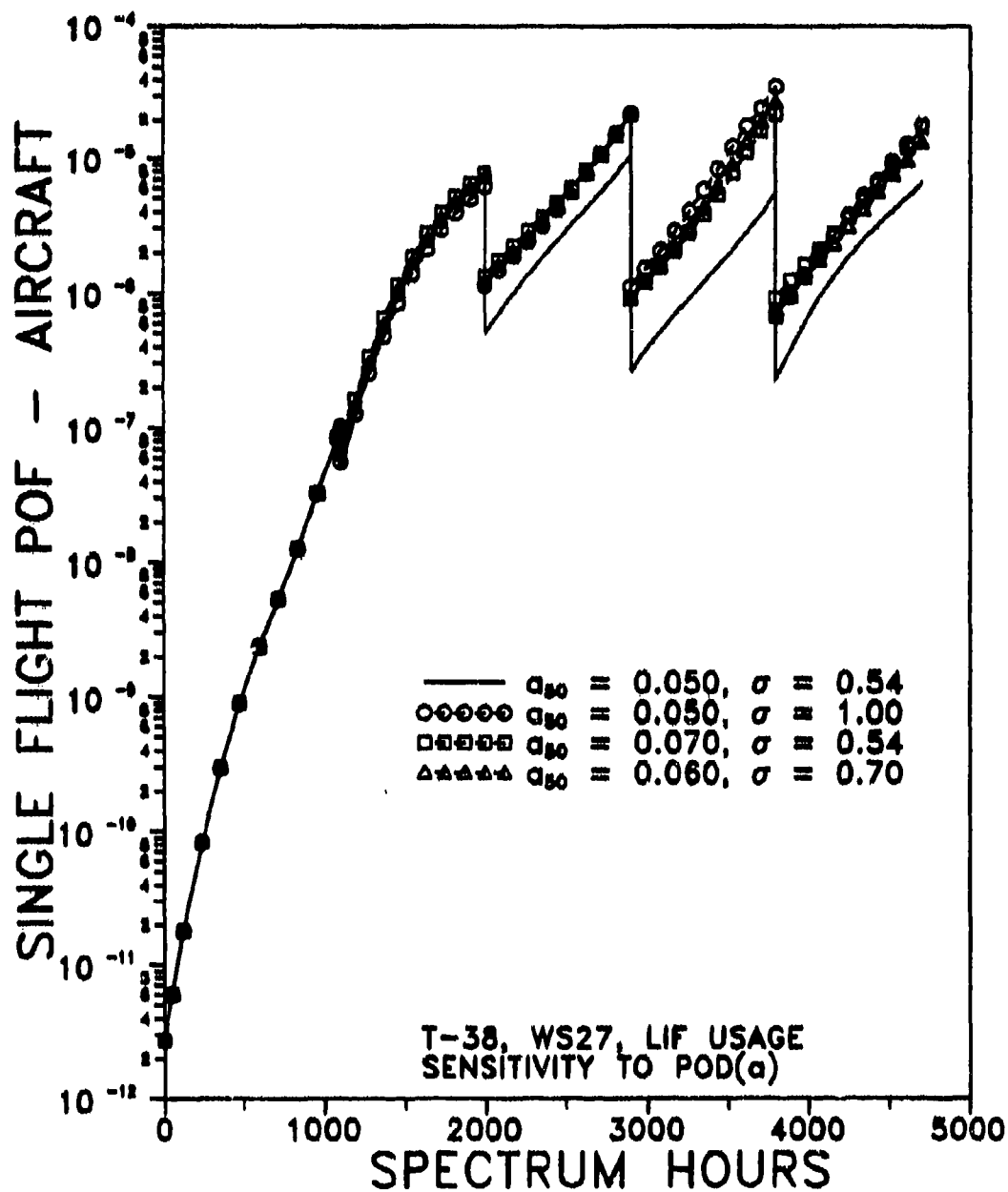


Figure 48. POF Comparing Baseline to Parametric POD(a) Variations.

values by factors of 3 to 6 over those of the baseline. Although the differences are small, the variation which had the lower detection probabilities over the range of larger cracks (greater than 0.100 in.) had higher POF values. Approximately the same number of cracks were detected by all four inspection capabilities in the 4700 hour period.

All of the variations in the characterization of the inspection capability produced POF functions which tended to be parallel. Although the inspection capability might not be precisely characterized for a particular application, relative comparisons due to variations in other PROF inputs would still be valid.

It is interesting to note in the above analyses that the inspection capabilities with the lower a_{90} values had the lower POF values. To further investigate this observation, PROF runs were made at four sets of combinations of a_{50} and σ with a_{90} equal to either 0.075 or 0.125 in. Figure 49 presents the four POD(a) functions. Two of the POD(a) functions intersect at 0.075 in. and two intersect at 0.125 in. The POD(a) functions with the higher a_{50} values also had higher detection probabilities for crack sizes larger than the a_{90} values. Figure 50 presents POF as a function of spectrum hours for the four inspection capabilities. The capabilities with the lower a_{90} values had lower fracture probabilities. The capabilities with the lower a_{50} value for fixed a_{90} value had the lower POF over the period. The larger detection probabilities for cracks greater than a_{90} did not offset the greater chances of detecting the smaller cracks. However, It was not necessarily true that the inspection capabilities with the lower a_{50} values had lower POF values as can be seen by comparing the POF values for squares and diamonds of Figure 50. Since two parameters determine the POD(a) function, combinations of a_{50} and a_{90} can be found for which POF is not less for the smaller a_{90} value. However, the a_{90} value, which tends to occur at about the "knee" of the POD(a)

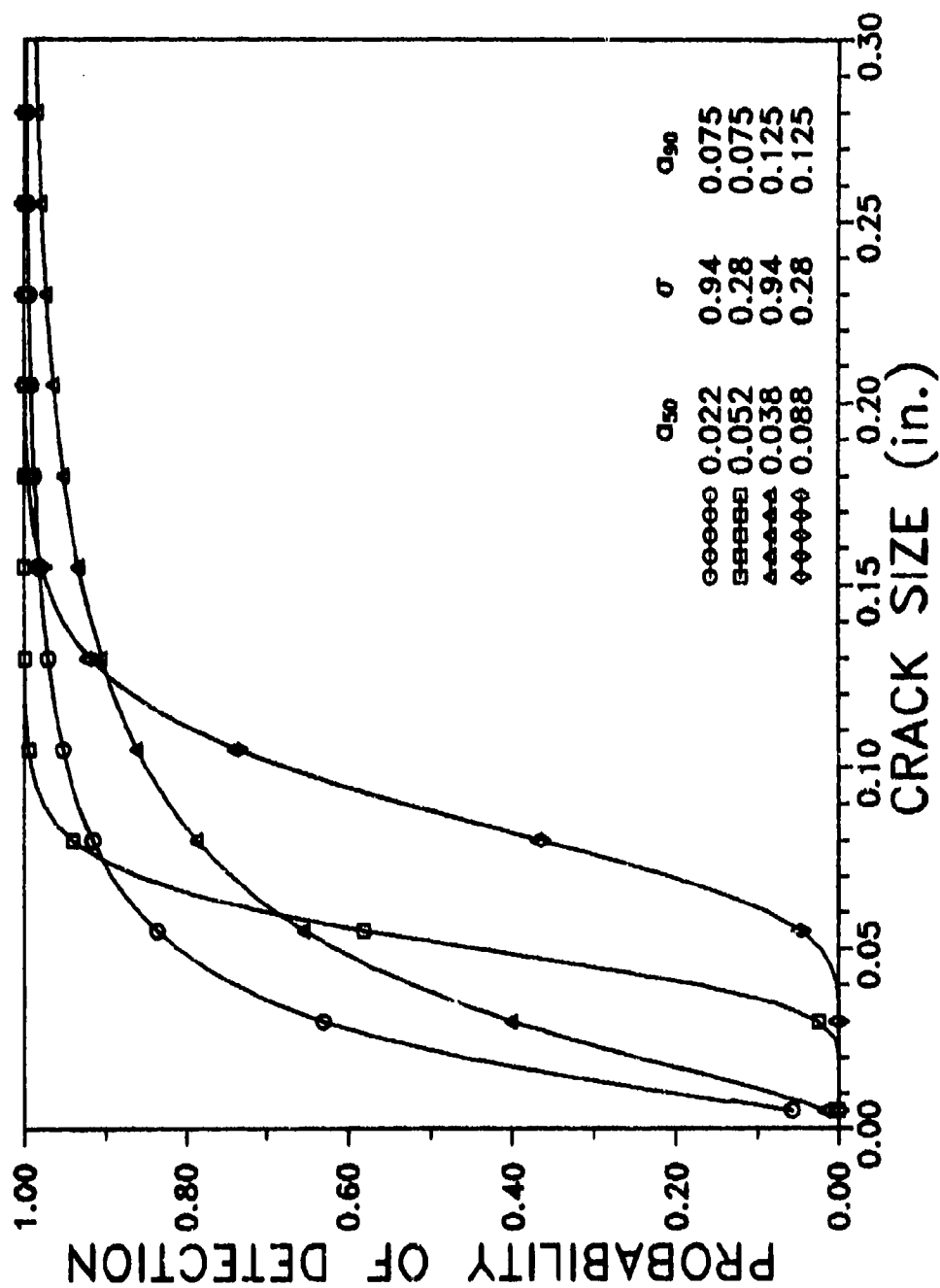


Figure 49. POD(a) for Comparing a_{90} Values.

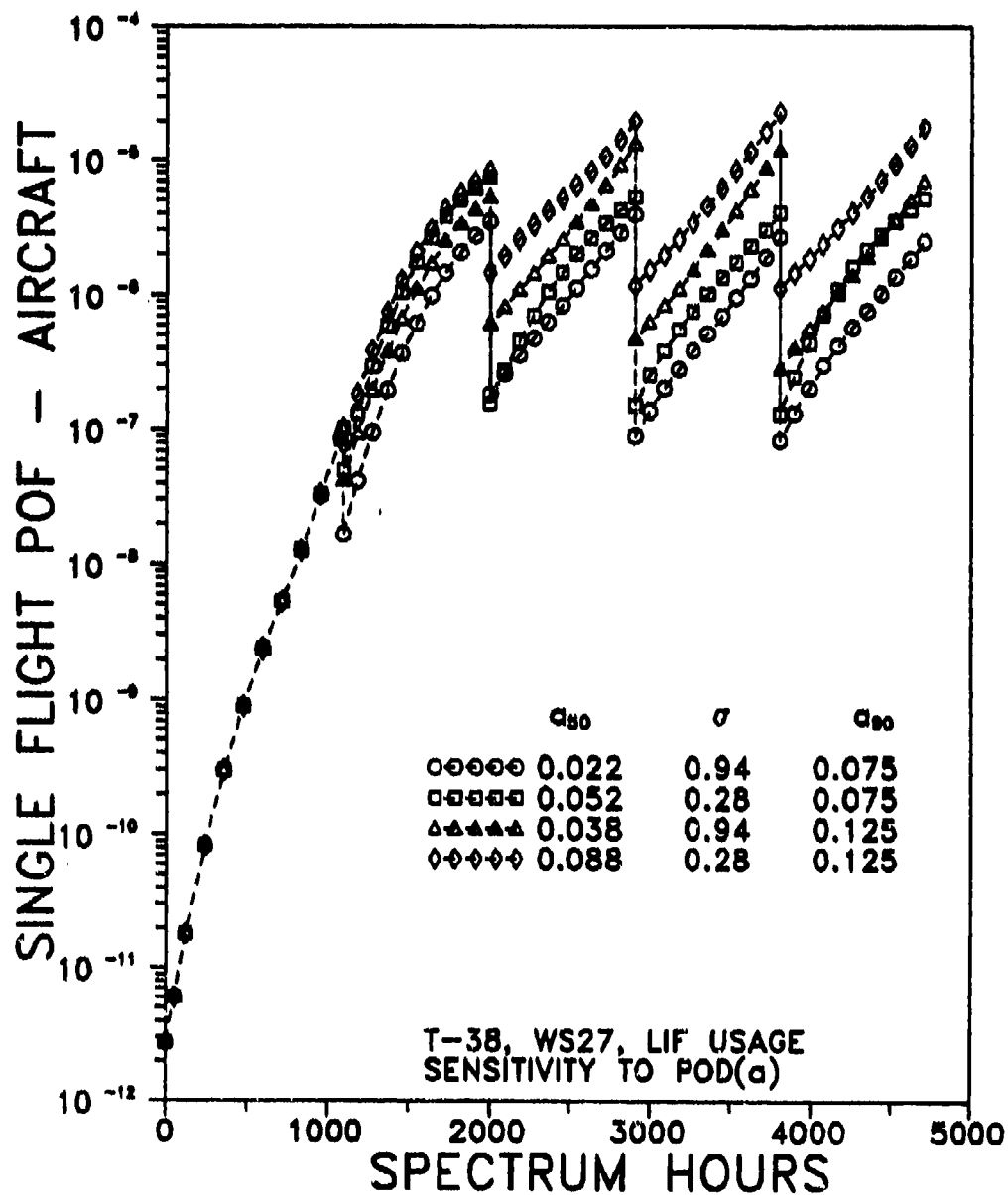


Figure 50. POF Evaluates Effect of a_{90} Values from POD(a).

functions, may well be a reasonable single value characterization of POD capability.

4.2.3.3 Repair Crack Size Effects

When a crack is detected at a site, it is assumed to be immediately repaired and the quality of the repair is characterized in terms of an equivalent repair crack size distribution. The baseline analysis assumed that a repaired crack was as good as new, and the equivalent initial flaw size distribution was used to characterize repair quality. That is, it was assumed that the equivalent repair flaw size distribution was a mixture with 99.9 percent of the repaired sites having a log normal distribution with a median of 0.008 in. and a standard deviation of 0.63 and 0.1 percent of the repaired sites having a uniform distribution between 0 and 0.050 in. (Subsection 4.1.2).

There are no published studies on methods of characterizing repair quality in terms of an equivalent crack size distribution other than those for durability analysis of new structure. Rational choices of alternatives can be made based on engineering judgement.

Three alternatives to the baseline equivalent initial flaw size distribution were evaluated. It is assumed that every repair produces a flaw with a corresponding equivalent crack size. The alternatives were then formulated as follows:

- a) The equivalent repair cracks are equally likely to be any size between 0 and 0.050 in. That is, the equivalent flaws are characterized by a uniform distribution of cracks on the interval of 0 to 0.050 in.
- b) Smaller equivalent repair cracks are more likely than larger. They are assumed to be exponentially distributed with a 0.001 chance of being greater than 0.050 in.
- c) The repair changes the structural detail to the extent that it cannot be considered to be from the original population of details. A distribution of extremely small cracks is used for the equivalent repair crack size

distribution, viz., lognormal with median crack size of 0.0001 in. and $\sigma = 0.05$.

Figure 51 displays the cumulative distribution for the baseline, the uniform (0,0.050), and the exponential equivalent flaw size distribution. The distribution of the third alternative could not be seen on this plot.

Figure 52 compares the fracture probabilities for the four equivalent repair qualities. After the cracks have grown to detectable size, POF for the repair quality as characterized by the relatively large cracks of the uniform distribution is always greater than the others. Considering the difference in the uniform, exponential, and initial quality distribution functions, larger differences were anticipated after three inspections. Table 11 presents the percentage of sites at which cracks would be detected at each inspection and the total over the 4700 hour period. Under the poorer repair quality represented by the uniform distribution, a significantly larger number of cracks were detected in the 4700 hour period. This larger percentage of detections implies that cracks were being detected at sites that were previously repaired.

The POF values for which the repaired detail is removed from analysis are very close to those of the baseline. These POF values represent the growth of only the original distribution with the large cracks being eliminated at the inspections. From Table 11, about 29.5 percent of the sites had cracks which were detected in the 4700 hour period. This implies that 4 percent of the total 33.1 percent of the detected cracks under the baseline conditions were from details that had previously been repaired. For the uniform and exponential repair quality, the percentages of multiple repairs at a site are much larger.

Although the equivalent repair quality distribution does affect the absolute magnitude of POF, the relative magnitudes remain consistent. Again, relative comparisons for other PROF

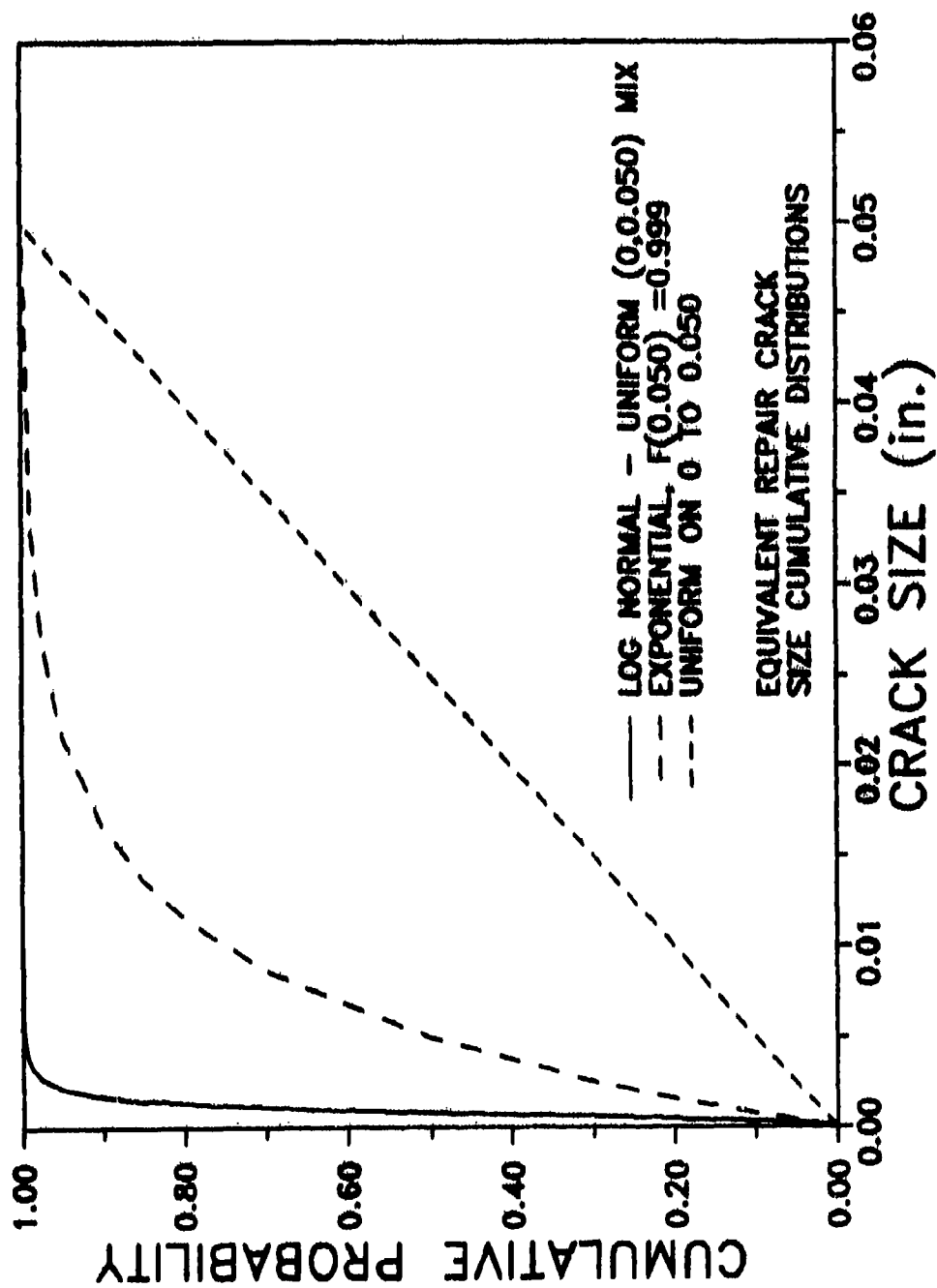


Figure 51. Cumulative Distribution Functions for Equivalent Repair Crack Size Distributions.

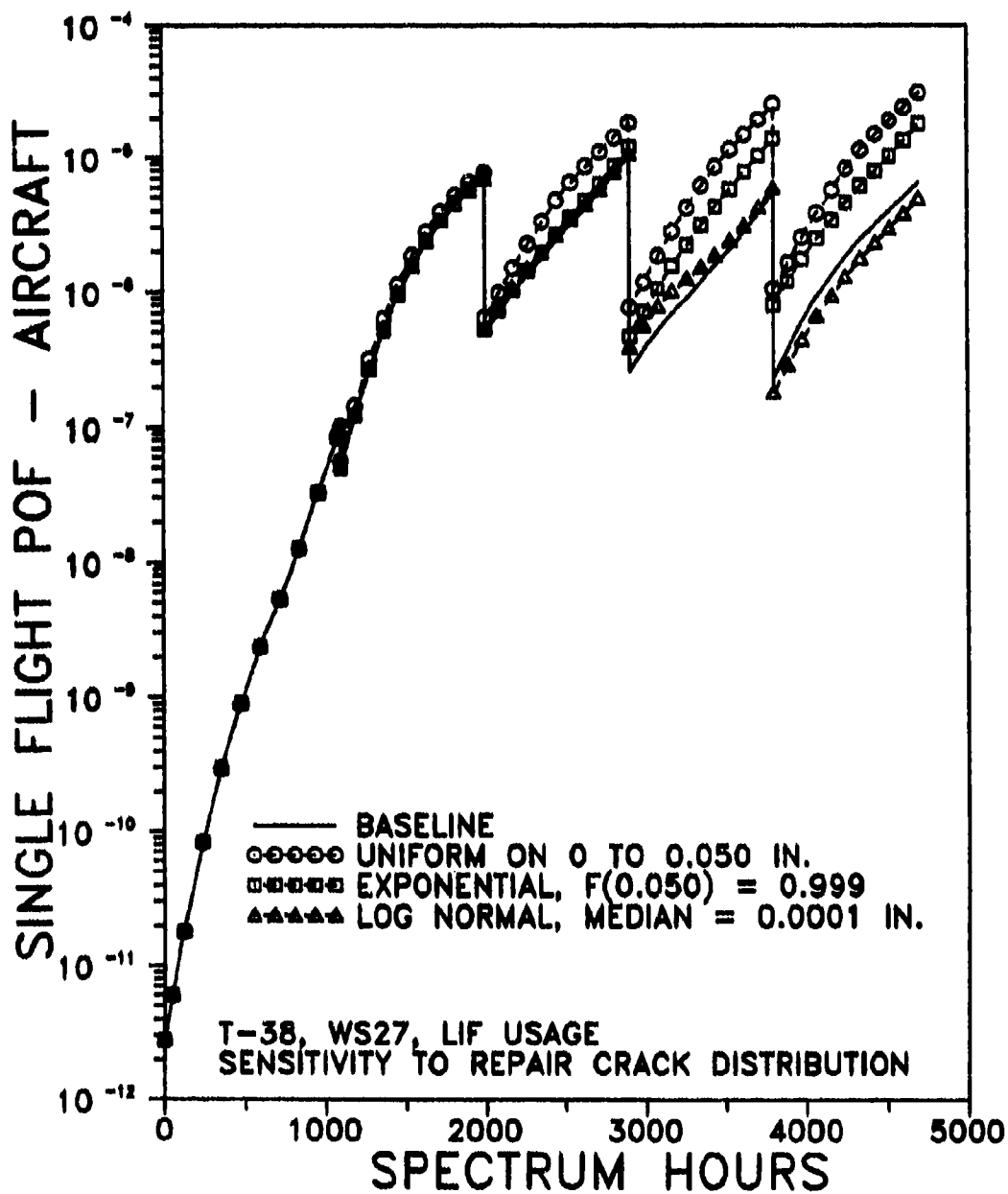


Figure 52. POF for Equivalent Repair Crack Size Distributions.

TABLE 11
Percent Detections at Inspections for Different
Equivalent Repair Qualities

	INSPECTION TIMES (HOURS)					
	1100	2000	2900	3800	4700	TOTAL
-----	-----	-----	-----	-----	-----	-----
BASLINE - SMALL CRACK MIXTURE	1.7	11.1	7.4	5.7	7.1	33.0
-----	-----	-----	-----	-----	-----	-----
UNIFORM ON 0 TO 0.050 IN	1.7	11.9	16.4	22.0	23.8	75.8
EXPONENTIAL - F(0.050) = 0.999	1.7	11.4	11.5	17.3	17.1	59.0
REMOVED FROM ANALYSIS						
LOG NORMAL (0.0001, 0.05)	1.7	11.1	7.3	4.6	4.8	29.5
-----	-----	-----	-----	-----	-----	-----

inputs would not be changed by selecting a different model for the equivalent repair quality distribution.

4.2.3.4 Discussion - Inspection/Repair Data

Since the input which defines the inspection schedule, NDE capability, and repair quality can be defined as part of the Force Management Plan, variations in these data can be viewed in terms of both trade-offs in planning decisions and sensitivity of PROF to input.

Inspection Schedule: The timing of the maintenance schedule (inspections, repairs, replacements, and retirement) is strictly a force management decision. The guidelines from deterministic damage tolerance analyses are based on a conservative approach, but in the general application, the degree of conservativeness has not been quantified. PROF provides a tool for comparing the relative degrees of risk for any proposed inspection schedule. If representative crack size and cost of maintenance data become available, the impact of scheduling alternatives can also be quantified.

From a safety of flight perspective, delaying the first inspection on a new structure had a deleterious effect on the chances of a fracture. The increase in fracture probability was relatively minor until the upper tail of the initial crack size distribution grew to a critical size (as determined by the fracture toughness and maximum stress per flight distributions). Delaying the first inspection beyond this time (about 2000 hours for the baseline conditions of this analysis) caused a significant increase in fracture probability. However, from the expected repair cost perspective, there was significant advantage to earlier first inspections. Although all inspection schedules produced about the same number of total crack detections in a 5000 hour period, performing the first inspection earlier reduced the expected costs from potential fractures and apparently led to the repair of smaller cracks.

A similar set of conclusions can be drawn concerning the repeated inspection increments after the initial inspection. The fracture probabilities tend to converge to a level determined by the repeat increment. For the baseline conditions, shorter inspection increments imply lower fracture probability and lower expected maintenance costs. The POF values should only be interpreted in a comparative sense. The choice between two repeat inspection increments would have to be made in terms of whether one is two, three, or whatever times safer than the other. The expected cost data of this analysis were tainted by the inadequate initial crack size information and the inspection and repair cost data. Therefore, no clear criterion for selecting a sufficiently short inspection increment was discerned.

Inspection Capability: Inspection capability as quantified by the probability of detection as a function of crack size was evaluated from two viewpoints: different inspection systems and perturbations of the parameters of a single system. The different inspection capabilities usually produced POF differences in the anticipated direction but not necessarily in the anticipated magnitudes. Relatively large apparent differences in the $POD(a)$ function did not result in large differences in the fracture probabilities if the inspection increment is changed to reflect the a_{90} capability of the inspection systems.

The $POD(a)$ model is characterized by two parameters, a_{50} and σ . a_{50} locates the 50 percent detectable crack size and σ determines the "flatness" of the $POD(a)$ function. Smaller σ for the same a_{50} produce a higher detection probability for larger cracks. It was somewhat expected that steep $POD(a)$ functions (small σ) would produce lower fracture probabilities over a period of several inspections since there would be a higher probability of detecting the larger cracks. This did not prove to be the case. In general, lower POF values resulted from $POD(a)$ functions which tended to detect smaller cracks. Although

not perfect, the 90 percent detectable crack size provided a reasonable discriminator between the effects of POD(a) functions on fracture probability.

Over the usage period considered, all of the POD(a) characterizations resulted in about the same number of cracks being detected. The basic crack population continues to grow regardless of the inspection system, and all of the systems considered had a reasonable chance of detecting the cracks. Although no expected costs studies were performed, the better inspection systems were finding smaller cracks which are presumably less costly to repair. Further, the factor of two to three reduction in POF can produce significant reductions in expected costs due to fracture.

In all of the cases considered, the relative differences in fracture probabilities were somewhat consistent over the total usage period. Thus, assuming a representative, but not necessarily exact, POD(a) function would lead to consistent results when comparing relative magnitudes of fracture probabilities obtained by varying other input factors.

Repair Quality: The effects of repair on the population of details being analyzed must be accounted for in a risk model that encompasses inspections and repair. In PROF, repaired details are assumed to have an equivalent repair flaw size distribution. This distribution is analogous to the equivalent initial flaw size distribution of durability analyses but, to date, has not been applied. Three rationalizations were considered for this input parameter in the trade-off studies: a) repaired is as good as new, b) repairs leave an equivalent flaw whose size is distributed over the interval 0 to 0.050 in., and, c) the repaired detail is removed from further analysis. Two distributions were assumed for the equivalent repair cracks on the 0 to 0.050 in. interval.

Although the above alternatives were quite distinct, the resulting fracture probabilities were consistent between inspections. The differences in magnitude were less than those observed from some of the better characterized inputs, e.g., the fracture toughness. Therefore, as long as the equivalent repair crack size distribution is held constant throughout an analysis, relative comparisons on other input factors will be valid.

SECTION 5

EXAMPLE APPLICATION

To demonstrate the application of the risk analysis computer code, representative data for an aging military transport/bomber were used to evaluate the timing of inspections and the capability of the inspection method. In particular, it was assumed that the objectives of the analyses were a) to seek the most cost effective inspection intervals for the population of structural details, and b) to determine the cost effectiveness of a better but more expensive inspection method. It was assumed that there were 75 aircraft in the fleet which experience the same expected operational usage and that all of the aircraft will have undergone maintenance at a fixed reference number of flight hours. The risk analyses will pertain to periods of operational usage (or inspection or maintenance intervals) after this reference age, whatever it might be.

5.1 PROBLEM STATEMENT

The assumed population of structural details comprises rows of fastener holes in a fail-safe zone of equivalent stress experience on the upper rear fuselage. Figure 53 presents a schematic of the holes in the region and the stress intensity factor coefficient used for crack growth calculations. The critical crack size is approximately 0.986 in. Cracks that are detected before fracture can be repaired by a patch. Assume that each airframe contains 50 separate regions such that the repair patch for any single crack in a region repairs all of the cracks in the region. However, if fracture (uncontrolled rapid crack growth) occurs, the entire panel must be replaced. The fracture toughness of the 7079-T6 aluminum alloy has an average value of 88.4 KSI $\sqrt{\text{in.}}$ with a standard deviation of 4.4 KSI $\sqrt{\text{in.}}$

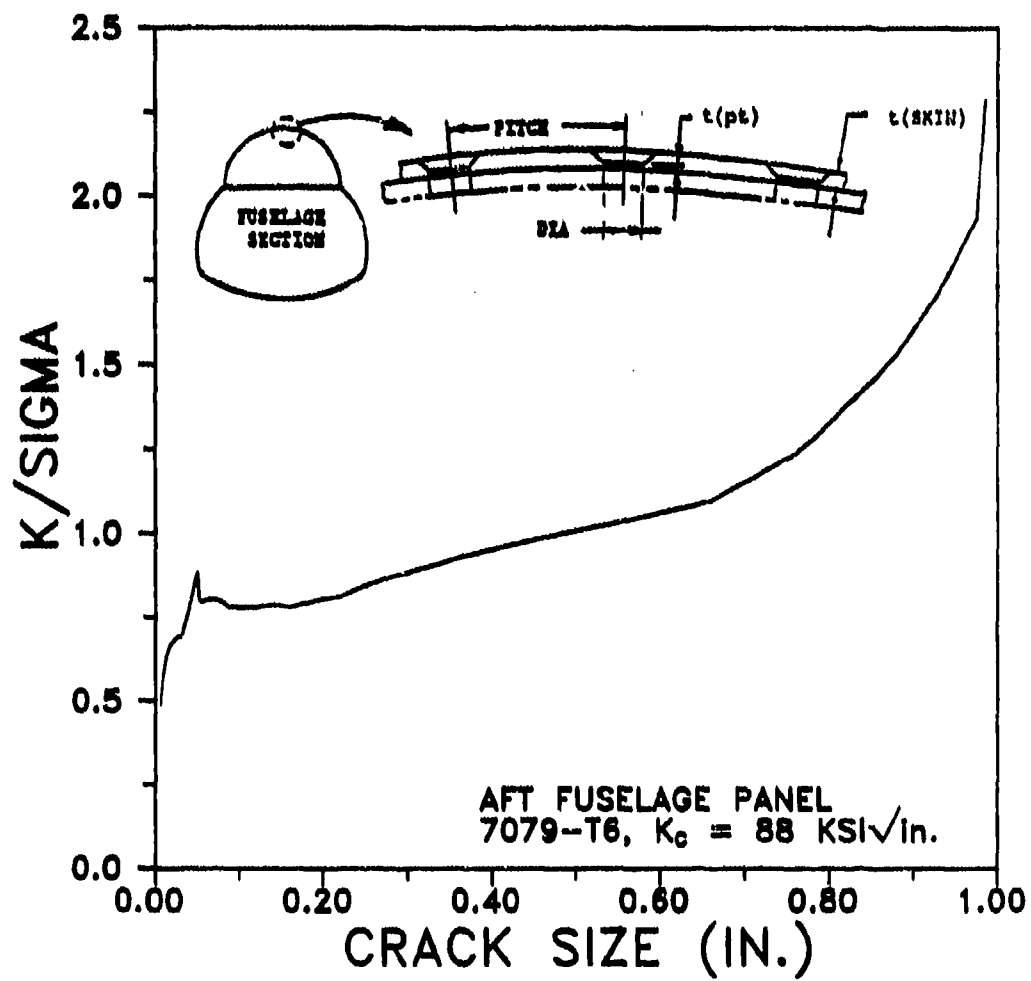


Figure 53. Stress Intensity Factor Coefficient for Analysis Region.

Figure 54 presents the projection of crack growth from a flight-by-flight spectrum of planned mission usage for the fleet. For the visual inspections of the region of interest, the reliably detected crack size was assumed to be 0.220 in. The reliably detected crack size is usually interpreted to be the smallest crack size for which there is a 90 percent probability of detection. Under Air Force guidelines for establishing inspection intervals, subsequent inspections would be set at one-half the time required for a crack of the reliably detectable size to grow to critical. For the example application, the baseline damage tolerance reinspection interval was set at 7200 flight hours. The Gumbel fit to the maximum stress per flight of the flight-by-flight stress spectrum is presented in Figure 55.

At the start of the analysis (reference time of zero), it was assumed that the distribution of the largest cracks in each region was described by a Weibull distribution with a scale parameter of 0.006 in. and a shape parameter of 0.768. For this distribution, 1 in 1000 of the holes can be expected to have cracks larger than 0.075 in. and 3 in 10,000 can be expected to have cracks larger than 0.100 in. Cracks are repaired by patches and it is assumed that the repair quality of a patch is described by a uniform distribution of equivalent crack sizes on the interval 0.050 in. That is, a patch replaces the largest crack in the patched region with an equivalent flaw that is equally likely to be any size between 0 and 0.050 in.

For the baseline analysis, the reliably detected crack size of 0.220 in. is assumed to be the result of a close visual inspection. This capability is interpreted as a 90 percent detection capability at 0.220 in. Because of the fastener heads, no crack smaller than 0.100 in. could be detected, i.e., $POD(a)=0$ for $a \leq 0.100$ in. To complete the definition of the $POD(a)$ function, it was also assumed that a 0.150 in. crack would be detected half of the time. The cumulative log normal $POD(a)$ function that meets these specifications is shown in Figure 56. Also shown in Figure 56 is the $POD(a)$ function for a potential

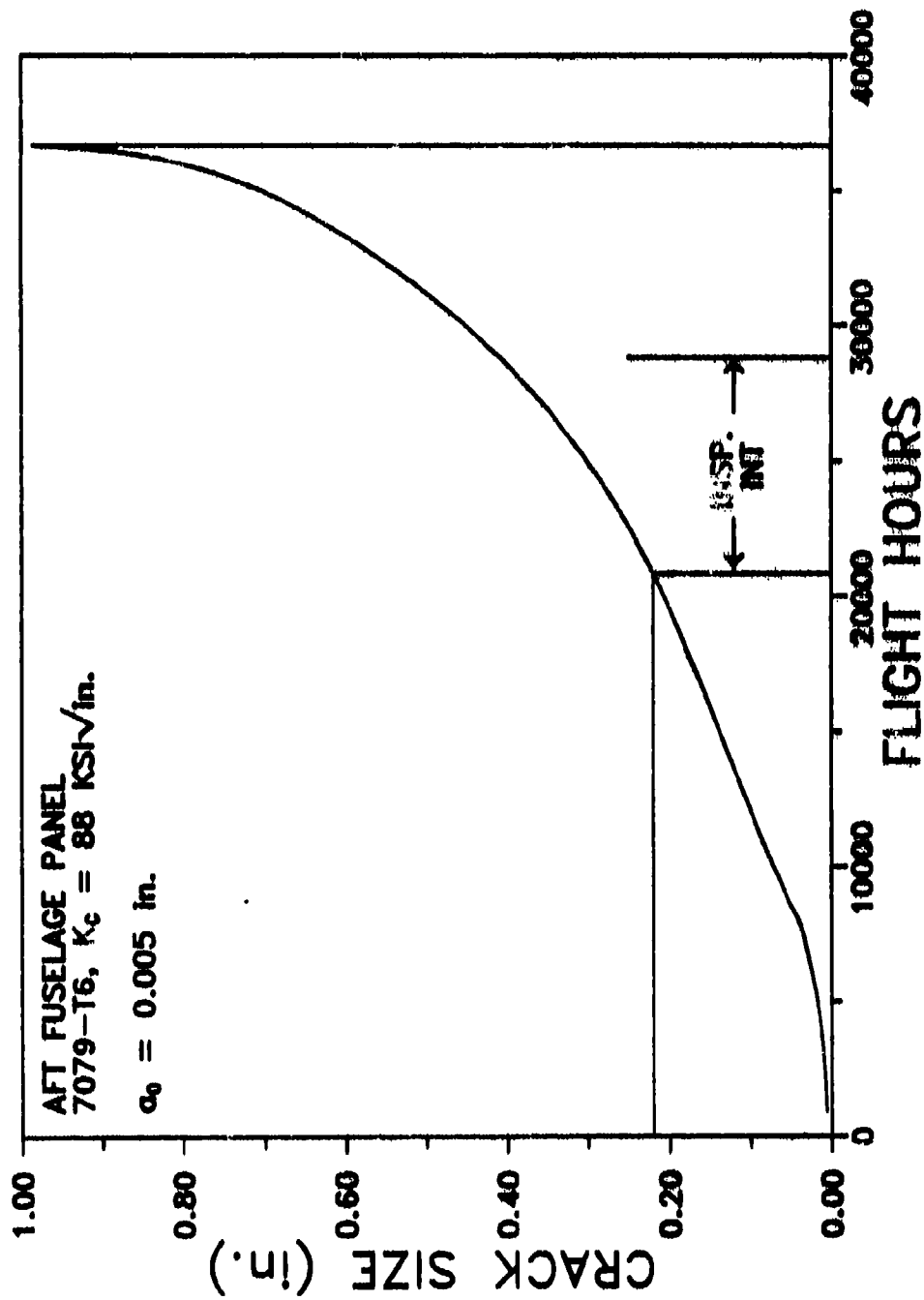


Figure 54. Crack Growth for Projected Usage Spectrum.

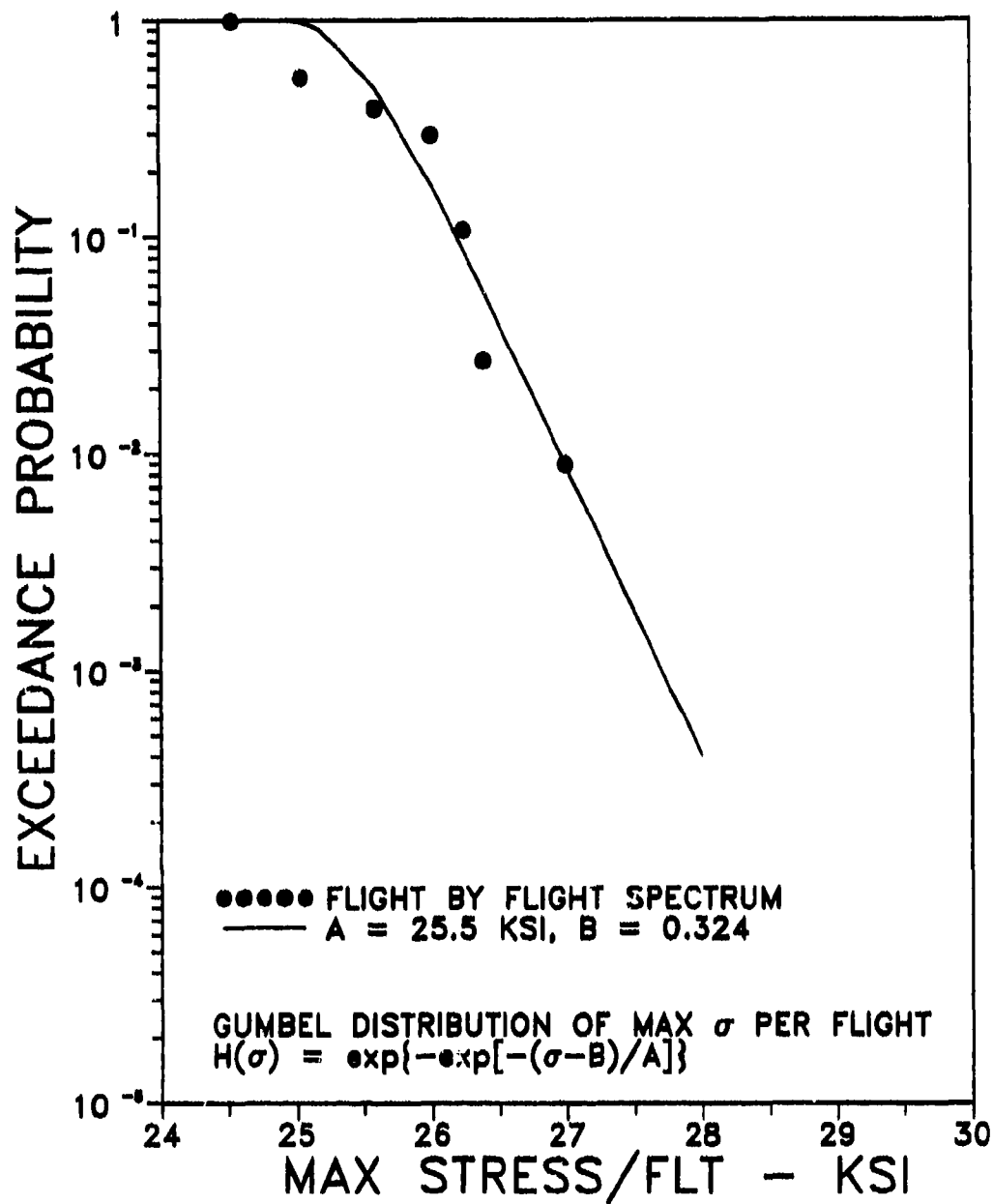


Figure 55. Gumbel Distribution Fit to Maximum Stress per Flight of Projected Spectrum.

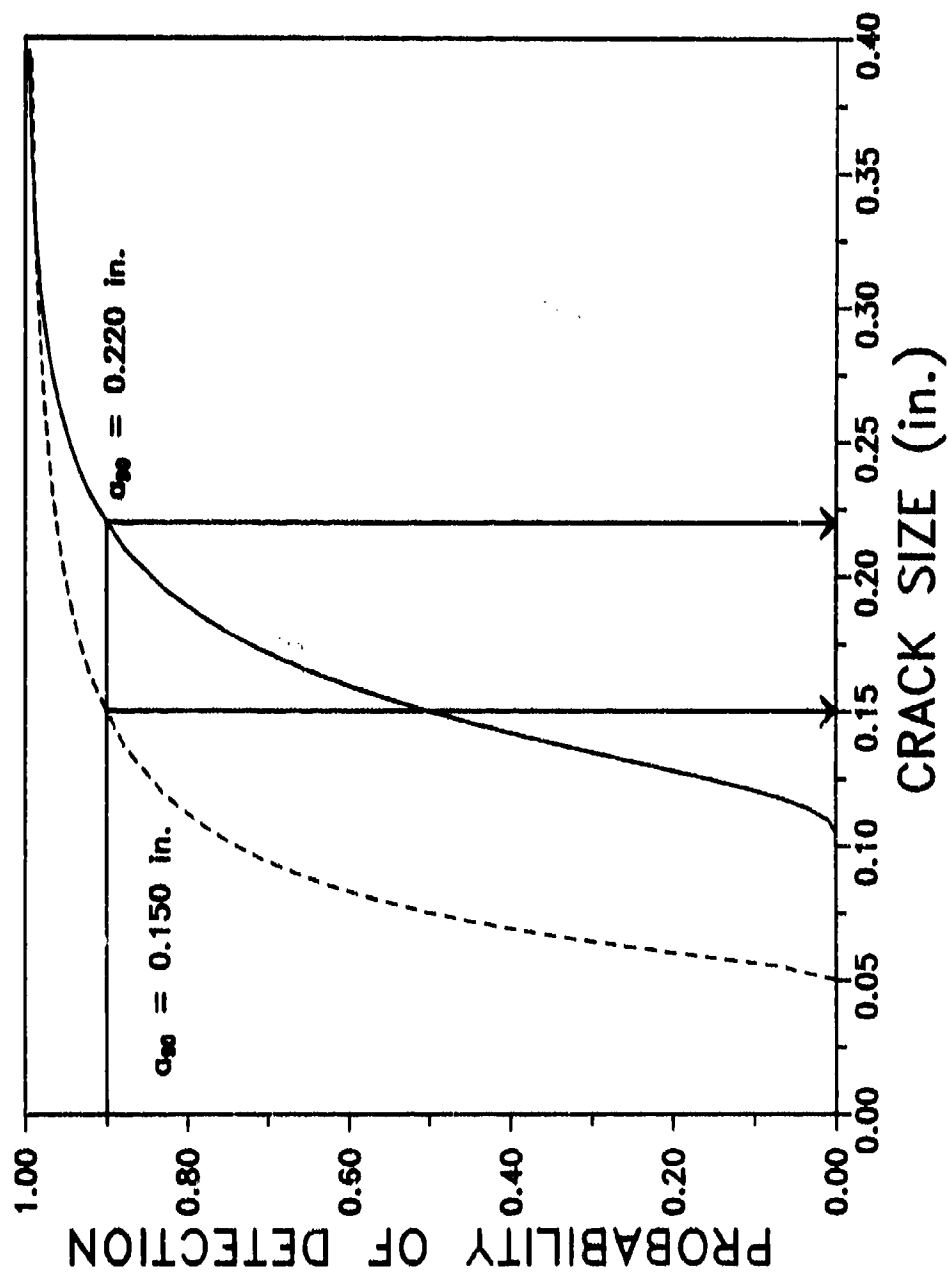


Figure 56. Crack Detection Probability for Competing Inspection.

eddy current inspection system with a smaller reliably detected crack size. This will be discussed further in Subsection 5.3.

Because of the comparative nature of the analysis objectives, inspection and repair costs need only be specified on a relative basis. For baseline analyses, it was assumed that the cost of the visual inspection of each region is one, the cost of patching the region is 100 and the cost of replacing a fractured panel is 100,000. Expected costs for different maintenance scenarios are normalized in terms of the total expected costs for the baseline inspection interval (7200 hours) and inspection capability.

5.2 INSPECTION INTERVAL ANALYSIS

The probability of fracture (POF) for any one of the 50 panels on a fuselage under the baseline conditions is presented as a function of spectrum hours in Figure 57. The solid line represents the fracture probability during a single flight, and the dashed line (circles) represents the probability of a fracture in any panel of an airframe at any time during the previous usage period. The large changes in single flight probability result from the removal of large cracks at the inspection/repair maintenance cycles and the growth of the population of cracks during the usage periods. PROF does not output fracture probabilities below 10^{-12} , so smaller POF values are plotted at this value. Since the structure under analysis is fail-safe and the costs are driven by the fracture probability in the entire usage period and the costs of maintenance, the single flight fracture probabilities will not be considered further.

To investigate the effect of a constant usage interval between inspections, a total analysis period of 36,000 hours was assumed. Equally spaced inspection intervals were then defined to provide between 3 and 12 inspections in the 36,000 hour period. Figure 58 presents the probability of fracture in each interval between maintenance (inspection and repair-if-necessary) actions for seven of the inspection intervals. The fracture

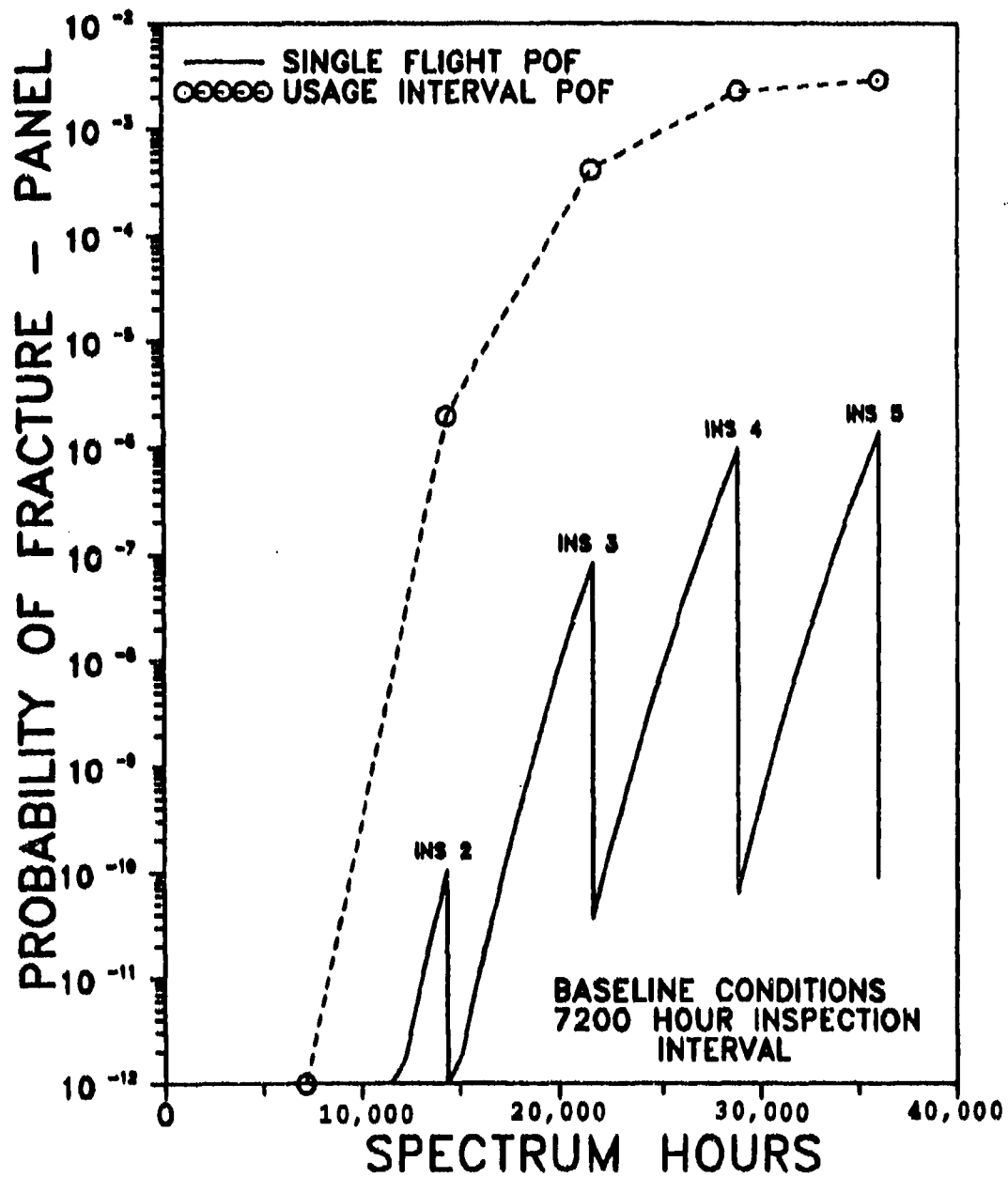


Figure 57. Probability of Panel Fracture in an Airframe for Baseline Conditions.

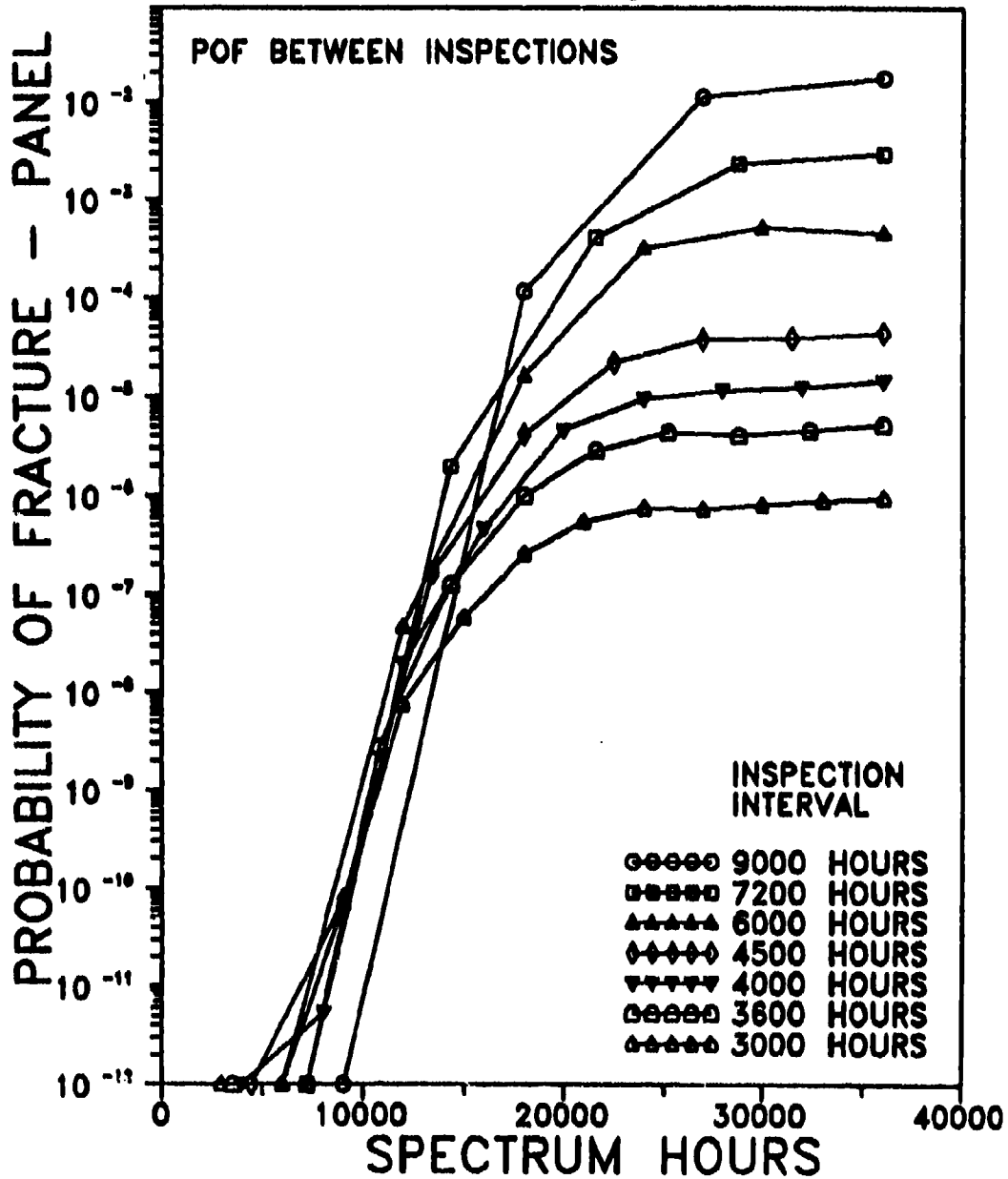


Figure 58. Probability of Panel Fracture in an Airframe between Inspections for Selected Inspection Intervals.

probabilities display somewhat similar behavior in the early period during which the upper tail of the initial crack size distribution grows to potentially significant sizes. Following this initial period, the interval fracture probabilities tend to stabilize at distinct levels - the shorter the inspection interval the lower the equilibrium fracture probability.

Because of the equilibrium POF levels, the expected costs associated with the possibility of panel fractures at the longer inspection intervals will be greater than those of the shorter intervals. On the other hand, the costs associated with the more frequent inspections may be greater than the expected costs of panel fracture. To evaluate the trade-off, the total expected maintenance and fracture cost for each of the inspection intervals was calculated. These expected costs are presented as a function of inspection interval in Figure 59. As noted earlier, the costs are normalized by the total expected cost for the baseline inspection interval of 7200 hours. (Inspection intervals of 9000 and 12,000 hours were also analyzed but the expected total costs were, respectively, 4.1 and 25.0 times greater than those of the 7200 hour increment. These intervals were not included in Figure 59 to provide more resolution for the shorter intervals.)

The expected total costs decrease with inspection interval down to about a 4000 hour interval and then tend to increase slightly. The decrease is the result of the reduced chances of panel fracture at the shorter inspection intervals. The equilibrium fracture probability for inspection intervals of 4500 hours and less produce only minor additions to the total expected costs. The costs due to the inspections and repairs increase for the shorter intervals but at a very slow rate. From a practical viewpoint, any interval less than about 4500 hours would have essentially equivalent expected total costs.

To investigate the potential for reducing total costs by extending the timing of the first inspection, various combinations of initial inspection interval and equal repeat

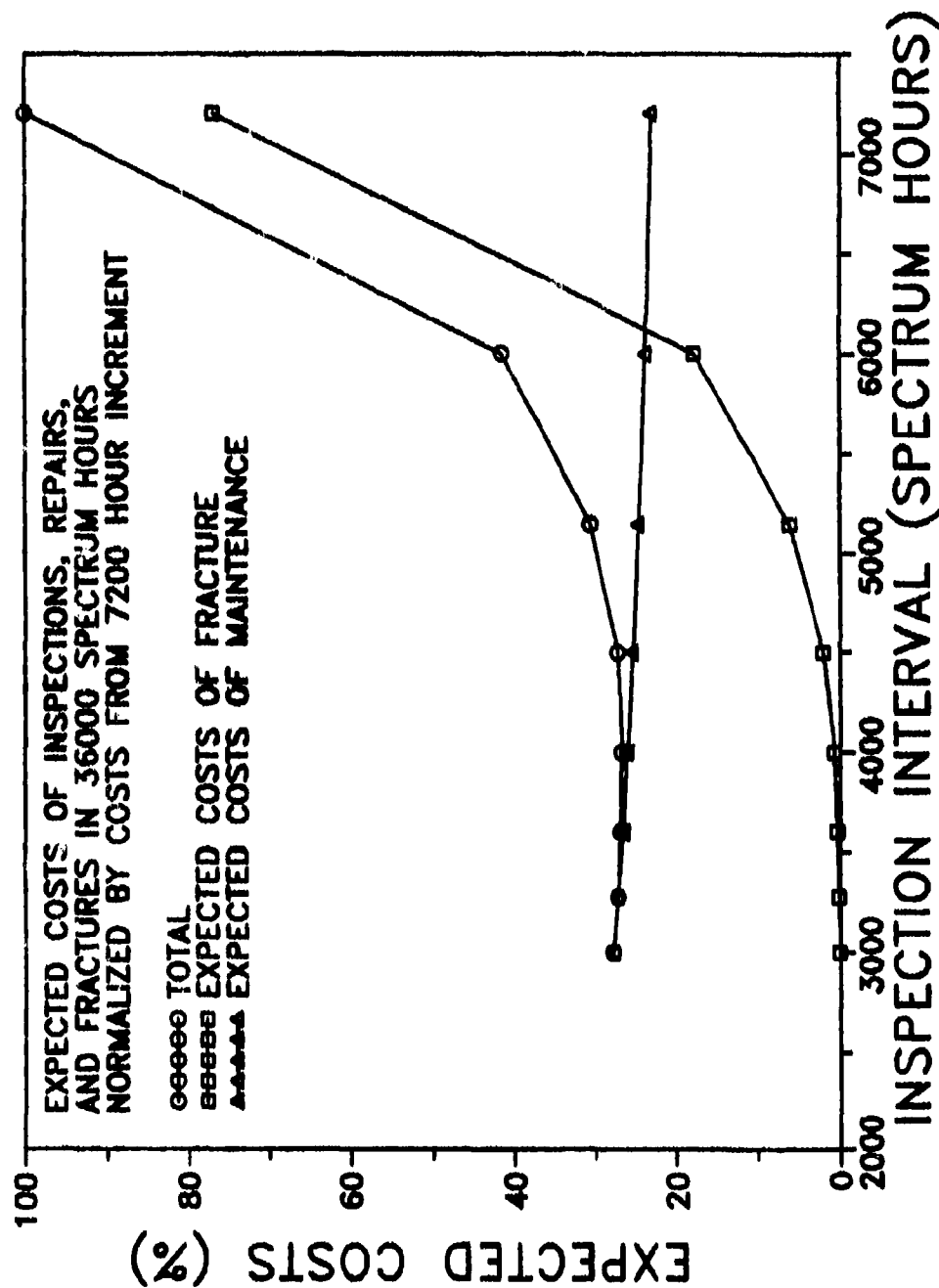


Figure 59. Normalized Expected Maintenance Costs as a Function of Inspection Interval.

inspections thereafter were analyzed. Table 12 presents a summary of the expected normalized costs due to fracture, maintenance, and the total. As noted earlier, the expected maintenance costs were approximately equal for all scenarios considered. The expected costs due to panel fracture varied somewhat depending on the particular combination. It is interesting to note that the minimum expected total cost was achieved at a 16,000 hour first inspection followed by 4000 hour intervals thereafter. The expected cost for this combination was slightly less than that of inspecting every 4000 hours.

For the assumed conditions, the above analyses imply that an inspection schedule with shorter intervals would provide significant savings in expected fracture and maintenance costs over those determined by the damage tolerance "rule." Although a minimum was achieved under the equal interval analysis, once the inspection interval was sufficiently short, the expected costs did not change significantly. This was true regardless of the timing of the first inspection. This latitude in setting inspection intervals could be important as the actual schedule should be determined by considering the many different populations of structural details on an airframe, each of which may have different optimum schedules.

5.3 INSPECTION CAPABILITY ANALYSIS

The inspection assumed for the baseline analysis was a close visual inspection that is inexpensive. The question might arise as to whether it would be cost effective to perform a more expensive inspection with an attendant increase in capability. Toward this end, it was assumed that an eddy current (EC) inspection could be used to inspect for cracks in the region and that the cost of the EC inspection is 10 times that of the visual. However, the reliably detected crack size is reduced to 0.150 in. Because the eddy current probe can detect cracks under the fastener head, it was assumed that the minimum detectable crack size is 0.050 in. The 50 percent detectable crack size

TABLE 12

**EXPECTED TOTAL FRACTURE AND MAINTENANCE COSTS
AS A PERCENTAGE OF TOTAL COSTS FOR 7200 HOUR
INSPECTION INTERVALS**

First Inspection (Hours)	Inspection Interval (Hours)	Fracture Cost %	Maintenance Cost %	Total Cost %
5143	5143	6.1	24.0	30.7
6000	5000	4.8	24.8	29.6
7200	4800	3.5	25.0	28.5
8400	4600	2.4	25.2	27.6
9000	5400	8.5	24.1	32.6
12000	4800	3.5	24.8	28.3
16000	4000	1.2	24.8	26.0
16000	5000	6.0	23.9	29.9
20000	4000	7.9	23.2	31.1

was assumed to be 0.075 in. The cumulative log normal POD(a) function that meets these requirements is shown in Figure 56 along with the POD(a) of the baseline analysis.

The usage interval fracture probabilities for the two inspection capabilities at 4000 and 7200 hour inspection intervals are presented in Figure 60. The eddy current inspection significantly reduces the chances of a panel fracture in the 36,000 hour period for both inspection intervals. However, when the total expected costs of inspections, repairs, and fractures are considered, the cost effectiveness of the eddy current inspection depends on the inspection interval. Figure 61 presents the normalized total expected costs in a 36,000 hour period for the two inspection systems and two inspection intervals.

At the 4000 hour inspection interval, the inspection and repair costs associated with the eddy current inspection are 2.2 times those of the visual inspection. At this 4000 hour inspection interval, the expected costs due to panel fracture are small (almost negligible) for both inspection methods. However, the better (EC) inspection system apparently requires more cracks to be repaired at each of the inspections, and these cracks are too small to be an imminent threat to the panel.

When the two inspection capabilities were analyzed at the 7200 hour inspection interval, the reverse conclusion was drawn. The chances of panel fracture at the longer usage interval was sufficiently great that the total expected costs over the 36,000 hour period were significantly reduced by repairing the smaller cracks. These results were tested for sensitivity to the assumed inspection and repair costs. The expected total maintenance costs were obtained for ranges of cost per inspection and cost per patch. The expected total costs were still significantly less when the EC inspection costs were 50 times greater than those of the visual and when the repair costs were 500 times greater than those of the baseline calculations.

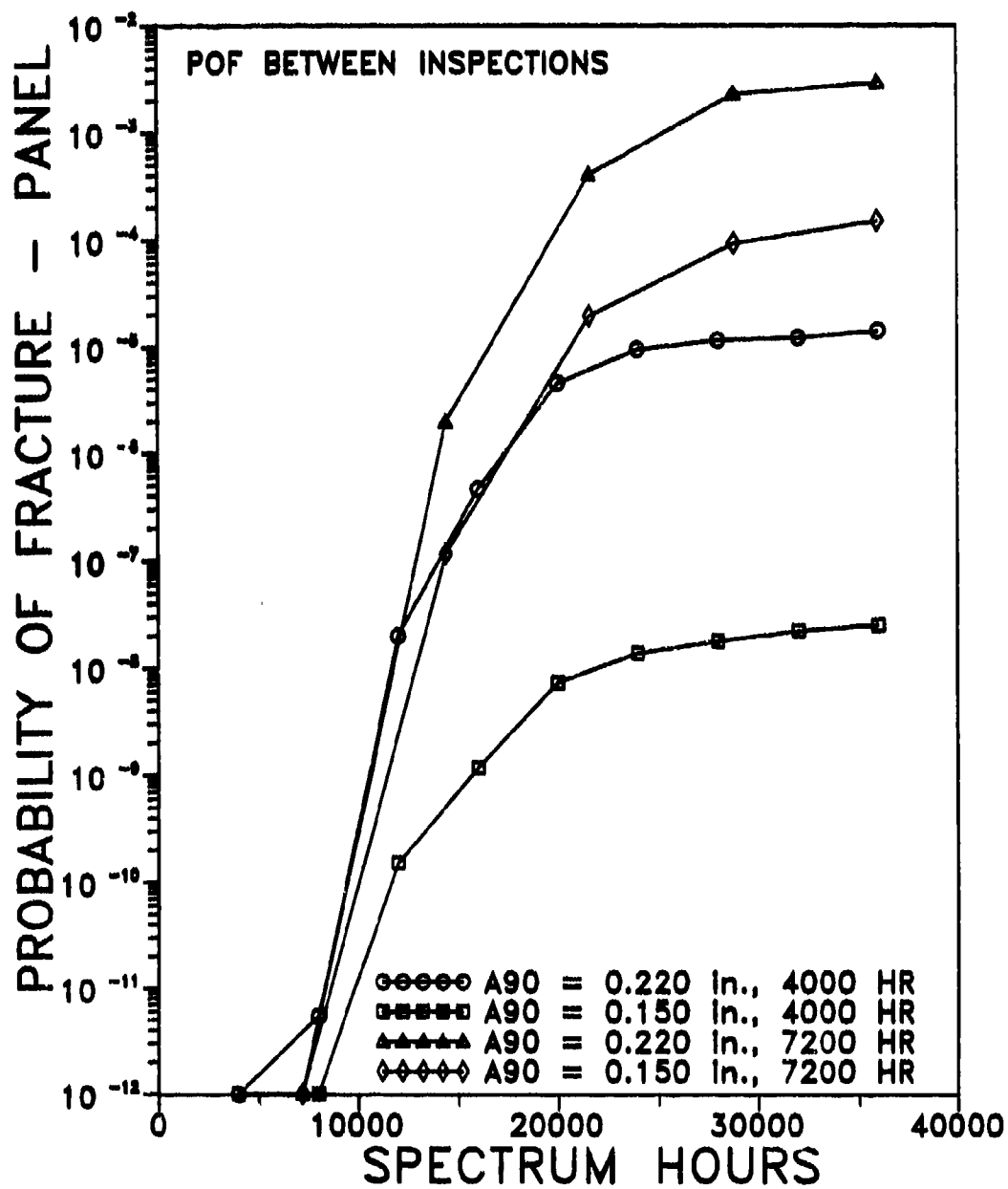


Figure 60. Probability of Panel Fracture in an Airframe between Inspections for Inspection Methods and Inspection Intervals.

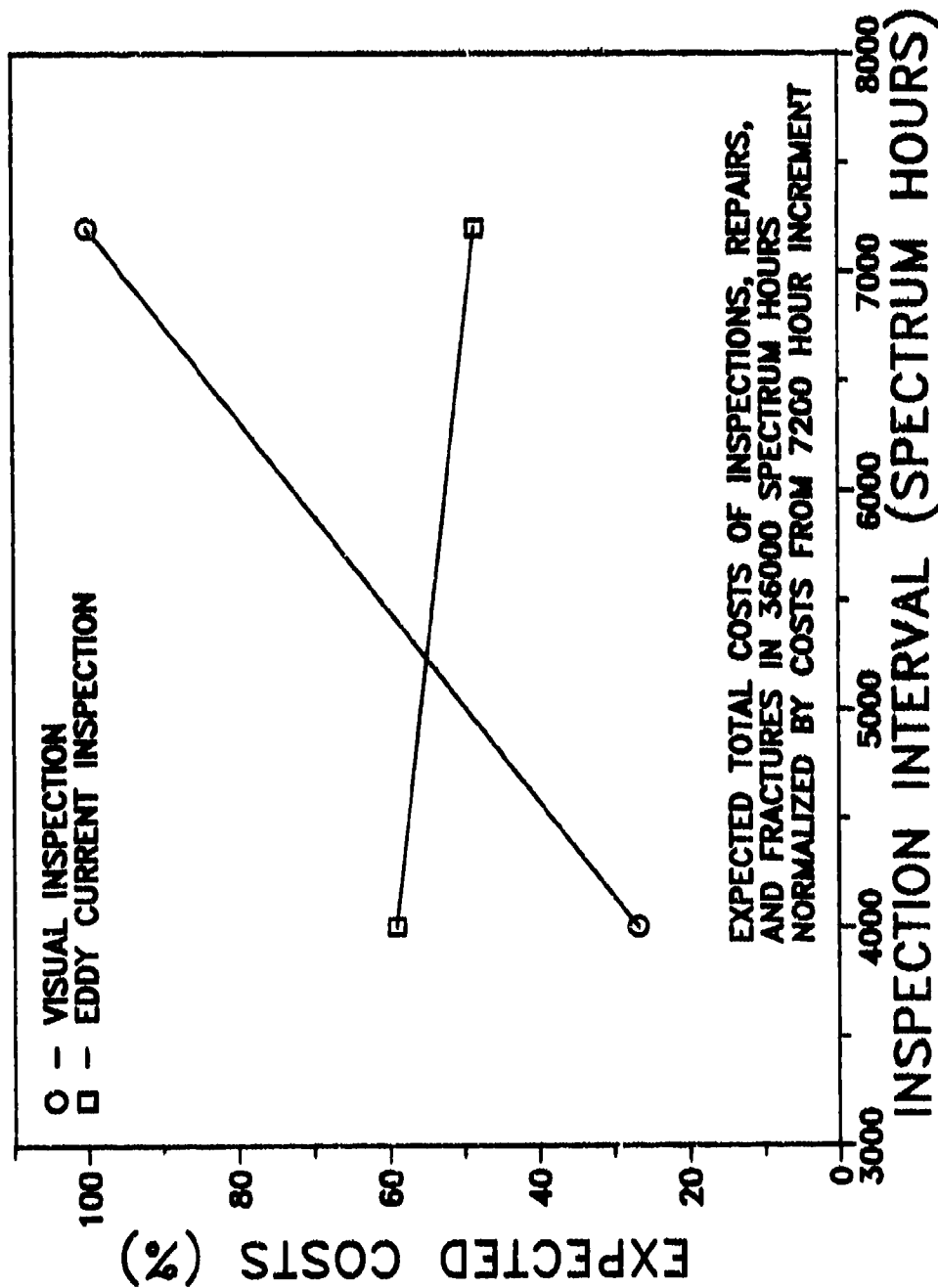


Figure 61. Normalized Total Expected Maintenance Cost for Two Inspection Methods as a Function of Inspection Interval.

No clear conclusion can be drawn on the cost effectiveness of the EC inspection system as compared to the visual. When the shorter and more cost effective intervals of this example are used, the visual inspection capability provides the more cost effective choice. If the longer damage tolerance defined inspection interval were to be used, the additional costs associated with the eddy current inspections would be justified.

5.4 EXAMPLE SUMMARY

The example application pertained to a fail-safe panel on a transport/bomber fuselage. In this application, a splice could be applied to repair a noncritical crack at a reasonably nominal cost. If a crack grew to unstable size, however, the panel would fracture and the repair (panel replacement) would be orders of magnitude greater than splicing. Applied stresses were not close to critical before the onset of unstable crack growth. Trade-offs in inspection intervals and inspection capabilities were evaluated in terms of total expected costs of inspections, splices, and fractures over a long usage period. For the data of this example application, the following conclusions could be drawn:

- a) The first inspection after the reference time can be delayed without a significant effect on expected maintenance costs. This interval is a function of the flight time required for a significant proportion of the initial crack size distribution to grow close to the unstable size.
- b) Expected costs using the damage tolerance "rule" for determining repeat inspection intervals were about five times greater than those of the optimum repeat inspection interval.
- c) For a reasonable range of repeat inspection intervals around the optimum, expected total maintenance costs were essentially equivalent. Once the repeat inspection

interval is sufficiently short, there is considerable freedom in acceptable choices.

- d) A more expensive and better inspection system produced significantly higher expected costs at the optimum inspection interval. At the optimum interval, the contribution to expected costs from the chances of panel fracture is minimal, while the better inspection system finds significantly more cracks to be repaired. Thus, the "better" inspection system leads to higher repair costs with no added fracture protection.
- e) The more expensive and better inspection system produced significantly lower expected maintenance costs at the longer repeat inspection intervals of the damage tolerance "rule." Postponing the inspections significantly increases the risk of fracture so that repairing the smaller cracks is cost effective for the longer inspection intervals.

These conclusions are highly dependent on the initial conditions assumed for the example application. PROF should be exercised to test their applicability for different conditions.

SECTION 6

SUMMARY AND CONCLUSIONS

The structural risk analysis computer program, PRObability Of Fracture (PROF), was written to provide an additional tool in the management of aging aircraft fleets. PROF evaluates structural safety and life in terms of fracture probabilities of equivalent details in any airframe in a fleet. The fracture probabilities are calculated for single flights as a function of spectrum hours and for entire intervals between maintenance actions. PROF evaluates durability by calculating the expected number of cracks to be detected at each inspection cycle. Expected costs of inspection, repair and fracture can then be calculated to estimate the cost effectiveness of planned maintenance scenarios.

The methodology implemented in PROF builds on data known to be available in the Air Force because of the requirements of MIL-STD-1530A. In essence, the growth of a population of cracks in like structural details is modelled using the crack size versus spectrum hour relationship derived to fulfill damage tolerance requirements. At maintenance actions, uncertainty in the inspection system is accounted for, and all detected cracks are assumed to be repaired. Fracture probability is calculated by combining the chances of the maximum stress in a flight exceeding the critical stress based on fracture mechanics calculations. The number and sizes of cracks to be detected are calculated from the probability distribution of crack sizes and the probability of crack detection as a function of crack size.

PROF quantifies structural risk of a population of details in terms of the probability of an in-service fracture and the number and sizes of fatigue cracks which are expected to be found at inspections. Fracture probability is synthesized from data which model the growth of a population of fatigue cracks in the details and which characterize the fracture resistance of the structural detail. The expected number of crack detections and

repairs is determined from the population of growing cracks and the capability of the inspection system. In realistic applications, fracture probabilities must be very small. The synthesis of these small probabilities from the many factors known to significantly influence the calculation is inherently subject to potentially large errors.

Seven of the nine types of input required by PROF are subject to error or uncertainty. Two of the seven are deterministic and are input in the same form as used in more traditional damage tolerance analyses. Four are stochastic and the tails of these distributions are critical in the calculation of fracture probability. The seventh is a stochastic characterization of the inspection process whose parameters are subject to sampling errors in the determination of the inspection capability.

Sensitivity analyses were performed to evaluate the influence of uncertainty in the characterization of these inputs on the output of PROF. Trade-off studies were also performed on the factors which are controllable through planned inspection scenarios. The following are general conclusions drawn from the sensitivity and trade-off analyses that were performed using the best available data.

- 1) Factors of two or more in fracture probability can result from commonly realized uncertainty in the characterization of any one of the PROF inputs. Much larger differences are possible. For example, order of magnitude differences can result from a ten percent error in maximum stress levels. Absolute interpretations of PROF generated fracture probabilities should be treated with caution. (The same is true of any other risk analysis results.)

- 2) Because of the consistency of the relative magnitudes of fracture probability when factors are varied, the PROF output can provide a basis for choices in the planning of maintenance actions. For example, it is reasonable to compare the relative

effects of shortening or lengthening the increment between inspections.

3) Although the best available data were used in the analyses, the number of predicted crack detections at inspections was unreasonably large. The model for describing the sizes of the cracks in the population of details was judged to be inadequate. The stochastic description of the large cracks which influence the fracture probabilities may have been adequate. However, the growth of the middle of the population of crack sizes resulted in too many detectable cracks at the inspection times. This may have been the result of an inadequate characterization of the size and growth of the equivalent initial flaw size distribution. A flaw size distribution derived from teardown inspection results also produced too many cracks in the mid ranges of the distribution. It is recommended that better methods for characterizing the sizes of the cracks in aging populations of details be developed. Combining a distribution of time to crack initiation with crack growth would be one approach to having a model for which real cracks are not present in all of the details.

4) In the attack/fighter/trainer aircraft application, shortening inspection intervals reduced both fracture probabilities and expected maintenance costs. The timing of the initial inspection did not have an apparently large effect on fracture probabilities until the upper tail of the crack size distribution was sufficiently large. However, the differences in fracture probability did show up as significant in the expected maintenance costs over an extended usage period. Shortening the increment between subsequent inspections after the first produced reductions in both fracture probabilities and expected maintenance costs. Determining inspection times can be based on a subjective interpretation of the magnitude of fracture probability differences until both a good characterization of the crack sizes and good cost data are available.

5) In the bomber/transport application to a fail-safe detail, shortening inspection intervals also reduced the fracture probabilities, but an optimum interval was achievable in terms of total expected costs due to inspection, repairs, and fractures of the detail. Although a minimum expected total cost was obtained, the expected costs were essentially equivalent for a broad range of inspection intervals.

6) In terms of its effect on fracture probability in the attack/fighter/trainer application, inspection capability was reasonably characterized by the crack size which is detected with a probability of 90 percent. Although two parameters are necessary to define the probability of detection function for an inspection system, the 90 percent detectable crack size occurs about the "knee" of the function. Higher detection probabilities above the knee were generally not as important in the calculation of the fracture probabilities as higher detection probabilities below the knee.

7) The effect of inspection capability in the bomber/transport aircraft interacted with the effect of inspection interval. Better inspection capability led to smaller fracture probabilities but not necessarily to lower expected total maintenance costs. Since the reliably detected crack size was much smaller than the critical crack sizes for the expected usage, the cost of detecting and repairing very small cracks was not necessarily offset by the reduced chances of a non-catastrophic fracture. For longer inspection intervals, the increased cost of a better inspection system was cost effective. For shorter inspection intervals, the increased cost of the better inspection system led to higher expected maintenance costs.

SECTION 7
REFERENCES

1. Military Standard, "Aircraft Structural Integrity Program, Airplane Requirements," MIL-STD-1530A (USAF), December 1975.
2. Military Specification, "General Specification for Aircraft Structures," MIL-A-87221, February 1985.
3. Gallagher, J.P., Giessler, F.J., Berens, A.P., and Engle, R.M., Jr., "USAF Damage Tolerant Design Handbook: Guidelines for the Analysis and Design of Damage Tolerant Structures," Air Force Wright Aeronautical Laboratories, AFWAL-TR-82-3073, May 1984.
4. Military Specification, "Airplane Strength, Rigidity, and Reliability Requirements, Repeated Loads, and Fatigue," MIL-A-8866B, August 1975.
5. Berens, A.P., et al., "Handbook of Force Management Methods," Air Force Wright Aeronautical Laboratories, AFWAL-TR-81-3079, April 1981.
6. Lincoln, J.W., "Risk Assessment of an Aging Military Aircraft," Journal of Aircraft, Vol. 22, No. 8, August 1985.
7. Manning S.D. and Yang, J.N., "USAF Durability Design Handbook: Guidelines for the Analysis and Design of Durable Aircraft Structures," Air Force Wright Aeronautical Laboratories, AFWAL-TR-83-3027, January 1984.
8. Swain, M.H., Everett, R.A., Newman, J.C., Jr., and Phillips, E.P., "The Growth of Short Cracks in 4340 Steels and Aluminum - Lithium 2090," AGARD Report No. 767, 1990.
9. Yang, J.N., "Statistical Estimation of Service Cracks and Maintenance Cost for Aircraft Structures," Journal of Aircraft, Vol. 13, No. 12, December 1976.
10. Stumpf, P.L., et al., "Damage Tolerant Design Data Handbook," Air Force Wright Aeronautical Laboratories, AFWAL-TR-83-4144, December 1983. (Also Damage Tolerant Design Handbook, MCIC-HB-01R, Metals and Ceramics Information Center, Battelle Columbus Laboratories, December 1983.)
11. Berens, A.P., "NDE Reliability Data Analysis," Metals Handbook, Volume 17, 9th Edition: Nondestructive Evaluation and Quality Control, 1988.
12. Tada, H., Paris, P.C., and Irwin, G.R., the Stress Analysis Of Cracks Handbook, Del Research Corporation, Hellertown, PA, 1973.

13. Sih, G.C., Handbook of Stress Intensity Factors, Institute of Fracture and Solid Mechanics, Lehigh University, Bethlehem, PA, 1973.
14. Chan, S.K., Tuba, I.S., and Wilson, W.K., "On the Finite-Element Method in Linear Fracture Mechanics," Eng. Frac. Mech., Vol. 2, 1970.
15. Byskov, E., "The Calculation of Stress-Intensity Factors Using the Finite Element Method with Cracked Elements," Int. J. Frac. Mech., Vol. 6, 1970.
16. Tracey, D.M., "Finite-Elements for Determination of Crack-Tip elastic Stress-Intensity Factors," Eng. Frac. Mech., Vol. 3, 1971.
17. Neville, D.J., "The Non-Conservatism of the Weibull Function when Applied to the Statistics of Fracture Toughness," Int. J. Fracture, Vol. 34, 1987.
18. Edwards, P.R. and Newman, J.C., Jr., An AGARD Supplemental Test Programme on the Behavior of Short Cracks under Constant Amplitude and Aircraft Spectrum Loading, AGARD Report NO. 767, Short-Crack Growth in Various Aircraft Materials, 1990.
19. Gumbel, E.J., Statistics of Extremes, Columbia University Press, New York, 1958.
20. Rudd, J.L. and Gray, T.D., "Quantification of Fastener-Hole Quality," Journal of Aircraft, Vol. 15, No. 3, March 1978.
21. Berens, A.P. and Hovey, P.W., "Evaluation of NDE Reliability Characterization," AFWAL-TR-81-4160, Air Force Wright Aeronautical Laboratories, Wright-Patterson Air Force Base, Ohio, 45433, December, 1981.
22. Berens, A.P., "Analysis of the RFC/NDE System Performance Evaluation Experiments," Review of Progress in Quantitative Nondestructive Evaluation 6A, Edited by Donald O. Thompson and Dale E Chimenti, Plenum Press, New York, 1987.
23. Lewis, W.H. Sproat, W.H., Dodd, B.D., and Hamilton, J.M., "Reliability of Nondestructive Inspections - Final Report," SA-ALC/MME 76-6-38-1, San Antonio Air Logistics Center, Kelly Air Force Base, Texas, December, 1978.
24. Wilhem, D.P., et al., "T-38, -29 Wing Damage Tolerance Assessment," NOR 83-107, Northrop Corporation, Hawthorne, CA 90250, August 1983.

APPENDIX A

CALCULATION DETAILS

A.1 INTRODUCTION

This appendix provides the mathematical details and justification for the risk calculations performed in PROF. The assumptions and approximation methods that affect the probability of fracture calculations are covered in detail. Procedures nonessential to the calculation of the probability of fracture, such as data handling and determining reporting intervals, are described in the Software Manual.

A functional flow chart of the basic steps used by PROF is given in Figure A1. The main steps are a) perform probability of fracture (POF) integrations, b) increment or grow the crack size distribution function, and, c) calculate effects of maintenance (repair of detected cracks) on the crack size distribution function. The POF integrations include both single flight POF, which is calculated at ten intermediate times in each usage interval, and usage interval POF, which is calculated only at the end of each usage interval. The crack size distribution is updated for each single flight POF calculation and is changed to reflect the effect of crack repairs at each maintenance cycle. The methods for modelling the crack size distribution will be presented first. These will be followed by the methods used to calculate the single flight and interval fracture probabilities.

A.2 CRACK GROWTH CALCULATIONS

The crack growth calculations involve determining the effect of aging (fatigue crack growth) and maintenance (inspection and repair) on the crack size distribution function. The basis of these operations is the cumulative probability distribution function for crack sizes. The first part of this section describes the methods used in PROF to interpolate and extrapolate the cumulative crack size distribution function at a fixed time. The second part provides a mathematical description

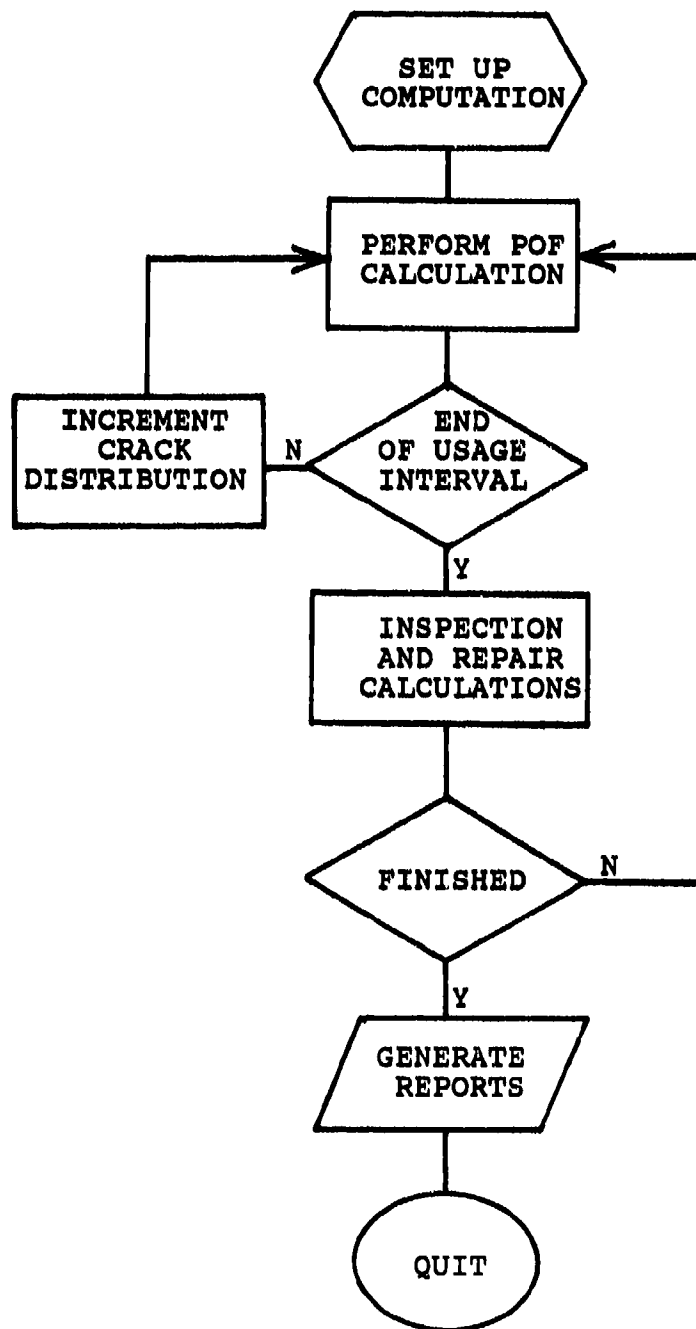


FIGURE A1. Flow Chart of PROF Calculations.

of the procedures for updating the crack size distribution to reflect fatigue crack growth. The third part describes the method for modifying the crack size distribution to account for the changes that result from repairing detected cracks at maintenance actions.

A.2.1 Interpolation and Extrapolation Methods

The PROF system uses a tabular cumulative distribution function as the core of the crack growth calculations. Specialized interpolation and extrapolation routines are used to evaluate the cumulative crack size distribution and the probability density function at arbitrary crack sizes. The crack size distribution function is projected through time by incrementing each percentile in the cumulative distribution function table according to the master crack growth curve.

The initial crack size distribution function is defined by the user and is read from a file by the PROF system as a table of crack length versus cumulative probability. The tabular format was chosen as the most convenient form in which the crack size data would be available. The tabular format also maintains generality since this format avoids the necessity of fitting (or assuming) a specific model (equation) whenever the crack size distribution is used in calculations. However, to use a tabular format for the crack size distribution function required establishing appropriate interpolation and extrapolation methods.

The cumulative crack size distribution function is read in as two arrays. The crack sizes, a_i ($i=1,n$), are contained in the first array while the second array contains the cumulative probability, F_i , for crack length a_i . The relationship between a_i and F_i is expressed as:

$$P(a \leq a_i) = F_i, \quad (A1)$$

and is read as the probability that the crack length is less than or equal to a_i is F_i . The only restriction on the table is that there should be at least two points greater than or equal to the 99th percentile to implement the extrapolation algorithm.

Linear interpolation is not appropriate through the entire range of the crack size distribution table. The upper tail of most crack size distribution functions approaches one at an exponential rate and therefore systematic errors in probability of fracture calculations can result when linear interpolation is used. To achieve consistent probability of fracture calculations with reasonable speed, three regions of the crack size distribution function were defined and different interpolation (or extrapolation) schemes were implemented in each region.

A schematic illustration of the three interpolation zones is given in Figure A2. The points of a crack size distribution table are plotted as circles in the figure, and the solid lines connecting the points are the interpolation or extrapolation curves. Linear interpolation provides a good fit in the first zone, $F_i < 0.95$, where the rate of change of the cumulative distribution function is nearly constant between points in the table. In the second zone, $0.95 < F_i < 0.99$, the rate of change becomes exponential in character and the linear fit, shown by the dashed line, is no longer adequate. (The interpolation curve and the linear fit are magnified in the lower portion of Figure A2 to illustrate the need for log-linear interpolation.) In the second zone, an exponential function is fit to the two adjacent points to interpolate. The exponential fit is still used in the third zone, $F_i > 0.99$; however, in this zone all points for which $F_i > 0.99$ are grouped together to provide a trend that can be used to both interpolate inside the zone and extrapolate outside the maximum crack size in the table.

The first zone consists of cracks up to the 95th percentile and uses simple linear interpolation. The cumulative distribution is relatively linear in the first zone and the cracks in this range do not contribute significantly to the

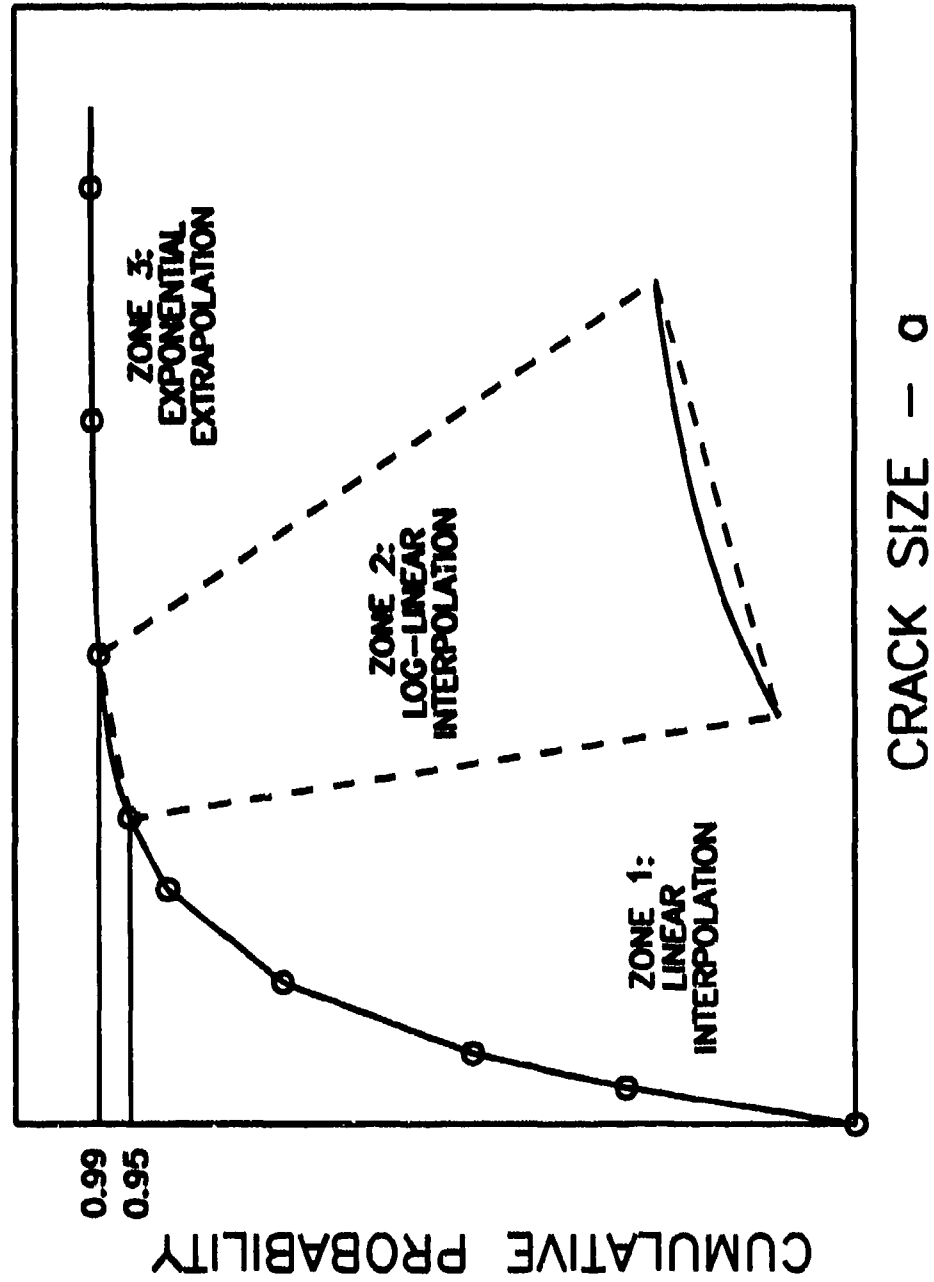


Figure A2. Illustration of the Three Interpolation Zones.

overall probability of fracture. The probability density function is calculated as the slope of the cumulative distribution in the crack length interval. The symbol f_i is used for the probability density between a_{i-1} and a_i and the formula is:

$$f_i = (F_i - F_{i-1}) / (a_i - a_{i-1}), \quad (A2)$$

where $F_0 = a_0 = 0$. The resultant probability density function is a step function.

A two-parameter cumulative exponential distribution function is fit to the data as the basis for interpolation and extrapolation in the second and third zones. The form of a two-parameter exponential cumulative distribution function is

$$F(a) = 1 - \exp(-\lambda(a-\gamma)), \quad (A3)$$

and the probability density is given by

$$f(a) = \lambda \exp(-\lambda(a-\gamma)). \quad (A4)$$

In the second zone, interpolation is accomplished by estimating the exponential parameters from the two adjacent points in the cumulative distribution table. The interpolation parameters, λ' and γ' , are determined from the two bounding points by:

$$\lambda' = -(\ln(1-F_i) - \ln(1-F_{i-1})) / (a_i - a_{i-1}) \quad (A5)$$

and

$$\gamma' = a_i + \ln(1-F_i) / \lambda'. \quad (A6)$$

The interpolation parameters, as determined by equations (A5) and (A6) are used in equations (A3) and (A4) to determine the cumulative probability and probability density at an arbitrary point between a_{i-1} and a_i .

The third zone is the extreme upper tail of the crack size distribution function. The whole tail cannot be covered by a finite table, so that extrapolation of the table is necessary for the third zone. The extrapolation is accomplished by fitting a two parameter exponential distribution function (equation (A3)) to the points in the table with cumulative probability greater than or equal to 0.99. The exponential distribution function was chosen because it provides a reasonable fit to the tails of many common crack size distribution functions.

The parameters for the exponential distribution function used in the extrapolation zone are given by:

$$\lambda'' = (\sum a_i \ln(1-F_i)) / (\sum a_i^2) \quad (A7)$$

$$\gamma'' = a_e - \ln(1-F_e) / \lambda'', \quad (A8)$$

where the summation extends over all points greater than or equal to the 99th percentile, F_e is the smallest percentile in the table that is greater than or equal to 0.99 and a_e is the corresponding crack length. The subscript e notation is used to cover crack size distribution tables that do not contain the 99th percentile. Equations (A3) and (A4) are used with the parameters determined by equations (A7) and (A8) to calculate the cumulative probability and probability density in Zone 3.

The inverse CDF is used in the inspection and repair calculations to reestablish the percentiles for the crack size distribution table. Simple linear interpolation is used in Zone 1, while the inverse CDF is given by:

$$a(F) = \gamma + \ln(1-F) / \lambda \quad (A9)$$

in Zones 2 and 3.

A.2.2 Crack Growth Calculations

The basic PROF probabilistic model of crack growth requires that percentiles of the crack size distribution grow through time in accordance with a master crack growth curve. The concept of constant percentile crack growth is shown in Figure A3, where the crack size distribution at T_1 is derived from the crack size distribution at T_{ref} by projecting each percentile at T_{ref} to time T_1 . The master crack growth curve is determined during the damage tolerance analysis and is specific to the structural geometry and the applied stress history. The PROF system requires a tabular input of crack length (a) versus time (T) for the master crack growth curve.

The data for the crack growth curve table are read from a file containing the two dimensional array of (a, T) values. After the table is read, the largest crack length in the table is compared to a_{last} ; which is the maximum crack length in the ($a, K/\sigma$) table of geometry corrections for the detail being analyzed. Cracks larger than a_{last} are assumed to exhibit unstable growth under typical (non-extreme) usage and are considered to lead to immediate fracture. If the crack growth curve does not extend to a_{last} , a point is added to include it in the table. The new point is given by:

$$a_{n+1} = a_{last} \quad (A10)$$

$$T_{n+1} = T_n + \frac{2}{3} (a_c - a_n) (T_n - T_{n-1}) / (a_n - a_{n-1}) \quad (A11)$$

where n is the number of points in the original crack growth table. Equation (A11) is basically a linear extrapolation with a 50 percent greater slope than the last interval in the original crack growth table.

Crack growth calculations are performed at nine or ten approximately equally spaced times in a usage interval. The length of the usage interval is supplied by the user and the exact number and spacing of subintervals depends on the length of

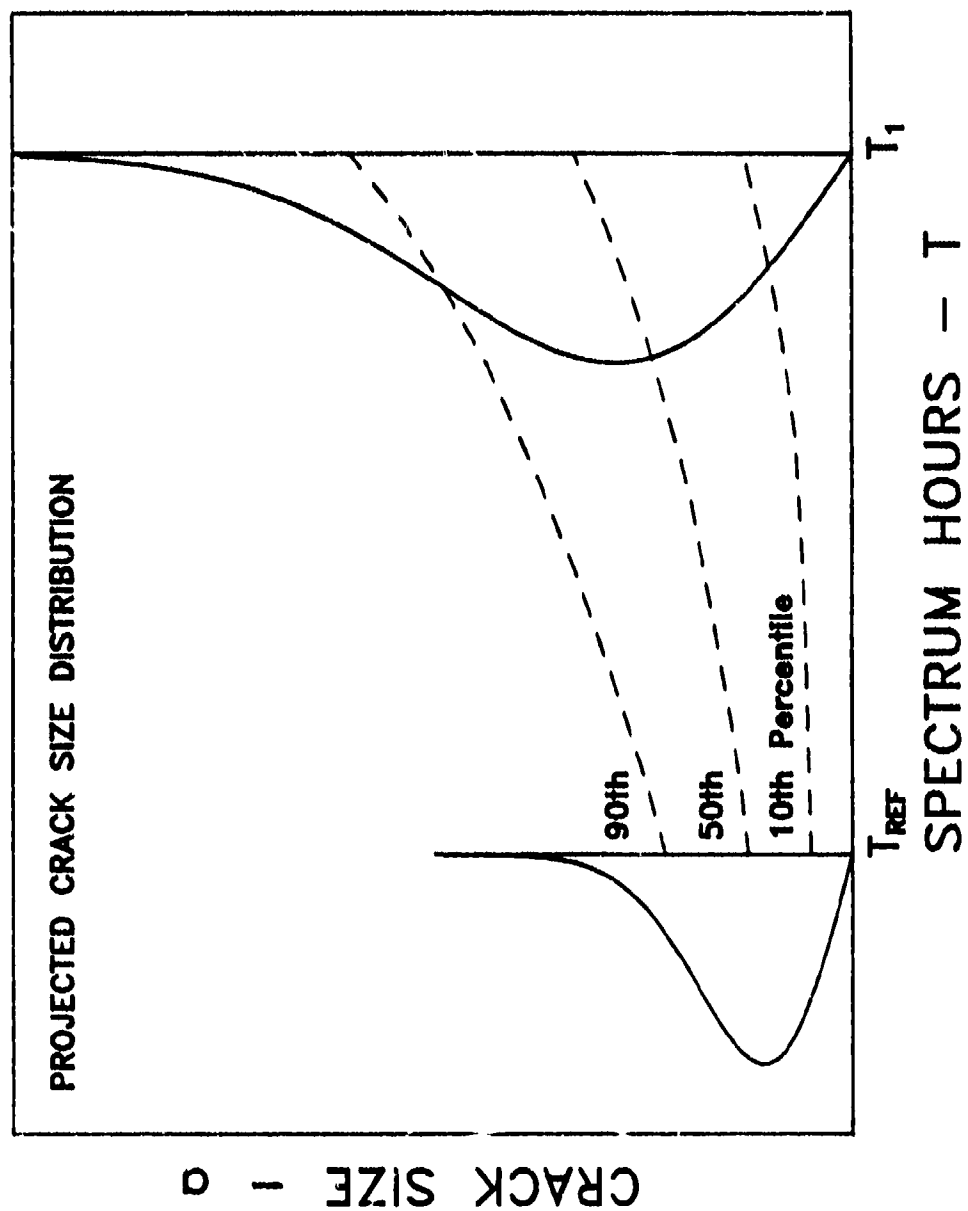


Figure A3. Growth of a Distribution of Flaws.

the usage interval. At the end of a usage interval, the effect of inspections and repairs on the crack size distribution is determined and the adjusted crack size distribution is calculated and reset for the start of the next usage interval.

The exact number and spacing of the points is a function of the length of the usage interval. An attempt is made to ensure that the interval between single flight calculations is a multiple of 10. The last interval might be shorter or longer than the rest to accommodate the multiple of ten requirement.

Crack sizes are increased incrementally through a usage period. At the end of a subinterval, the amount of incremental crack growth for each percentile in the crack size distribution table is determined and each percentile is increased accordingly. The extrapolation parameters are recalculated and the single flight probability of fracture is calculated. The process is continued until the end of the usage interval is reached.

Incremental crack growth is determined through log-linear interpolation of the crack growth curve. Crack growth curves typically increase at about the same rate as an exponential function. That is, although an exponential function may not fit the crack growth curve exactly, over a short interval the rate of increase of the crack growth curve is nearly exponential. Crack growth calculation errors can occur using linear interpolation even when a large number of points are included in the crack growth table.

Incremental crack growth is determined in three steps. First, the crack size cumulative distribution is truncated, if necessary, to the maximum crack size that will grow to a_{last} in the next time increment. Truncation is required because the crack growth curve does not typically extend beyond a_{last} so that crack growth calculations for percentiles that exceed the maximum crack length are unnecessary.

In the second step, the equivalent time on the crack growth curve is determined for each point in the current crack length distribution table. The equivalent current time is given by:

$$T_e = T_{i-1} + (\ln(a_{cur}) - \ln(a_{i-1})) \cdot (T_i - T_{i-1}) / (\ln(a_i) - \ln(a_{i-1})) \quad (A12)$$

where T_e is the equivalent current time, a_{cur} is the current crack length, $a_{i-1} \leq a_{cur} \leq a_i$, and T_i and T_{i-1} are the times corresponding to the crack lengths a_i and a_{i-1} . The time increment is added to the equivalent current time. In the third step, the new crack length is determined using linear-log interpolation. The formula for the natural log of the new crack length is

$$\ln(a_N) = \ln(a_{j-1}) + (T_e + \Delta T - T_{j-1}) \cdot (\ln(a_j) - \ln(a_{j-1})) / (T_j - T_{j-1}) \quad (A13)$$

where a_N is the new crack length, ΔT is the time increment and $T_{j-1} \leq T_e + \Delta T \leq T_j$.

A.2.3 Inspection and Repair Calculations

At the end of a usage interval, the crack size distribution is modified to reflect maintenance actions. The crack size distribution changes during maintenance because detected cracks are repaired. Repaired details are modelled by a distribution of equivalent initial crack sizes that reflect the quality of the repairs.

The cumulative distribution function of the crack size distribution after inspection and repair is given by:

$$F_{after}(a) = P \cdot F_R(a) + \int_0^a (1 - \text{POD}(x)) f_{before}(x) dx \quad (A14)$$

where P is the proportion of cracks that are found,

$$P = \int_0^{\infty} \text{POD}(a) f_{\text{before}}(a) da,$$

F_R is the equivalent crack size distribution for repaired structure, $\text{POD}(a)$ is the probability of detecting a crack of size " a ", and $f_{\text{before}}(a)$ is the crack size density function just prior to maintenance. For computational purposes the integral in equation (A14) is separated to give:

$$F_{\text{after}}(a) = P \cdot F_R(a) + F_{\text{before}}(a) - P(a), \quad (\text{A15})$$

where

$$P(a) = \int_0^a \text{POD}(x) f_{\text{before}}(x) dx \quad (\text{A16})$$

and $F_{\text{before}}(a)$ is the cumulative crack size distribution function just prior to maintenance. The form of equation (A14) facilitates computations because P is equal to the limit of $P(a)$, as " a " tends to infinity.

$F_{\text{after}}(a)$ is computed in three stages. In the first stage a table is constructed that contains all the crack sizes in both the current crack size distribution table and the repair crack size distribution table. The table includes the values of F_{before} , F_R , and f_{before} for each crack length in the table.

The second stage accumulates

$$F^*(a_i) = F_{\text{before}}(a_i) - P(a_i) \quad (\text{A17})$$

through an iterative scheme. The incremental integral part of $P(a_i)$ from a_{i-1} to a_i is calculated numerically using Simpson's rule [A1] and added to the value of $P(a_{i-1})$. Then, $P(a_i)$ is subtracted from $F_{\text{before}}(a_i)$ to get $F^*(a_i)$. After $F^*(a)$ has been determined for all crack lengths in the table, the tail integral part of P is computed using a 15-point Gauss-Laguerre quadrature

[A1] and added to the current value of $P(a)$ to get the final value of P . Gauss-Laguerre quadrature is an optimal approximation for an integral when the exponential density function is a factor in the integrand.

In the final stage of calculating $F_{\text{after}}(a)$, P times F_R is added to $F^*(a)$ to yield $F_{\text{after}}(a)$. At this point, the cumulative probabilities in the table of $F_{\text{after}}(a)$ do not correspond to the original percentiles of the crack size distribution. The inverse cumulative distribution function is used to restore the original percentiles to the current crack size distribution table for the start of the next usage interval.

The process of growing the crack size percentiles and resetting the crack size distribution to reflect inspection and repair is repeated for each subsequent usage interval.

A.3 PROBABILITY OF FRACTURE CALCULATIONS

Probability of fracture calculations are performed at various times within each usage interval. The single flight probability of fracture is calculated at the start and end of the usage interval and at approximately nine equally spaced points during the usage interval. The usage interval probability of fracture is calculated once for each usage interval. This section describes how the single flight and interval fracture probabilities are calculated.

In the PROF calculation, fracture is considered to result from either of two mutually exclusive events. First, fracture is assumed to have occurred at all crack sites which will have a crack size larger than a_{last} in an interval. Second, fracture can occur if an applied stress at a site exceeds the critical stress as determined by the crack size (less than a_{last}) and fracture toughness of the detail. It was necessary to introduce two fracture events to have a well defined upper bound in the integration calculations. The method of incorporating these two

factors depends on whether the calculations are for a single flight or the entire usage interval.

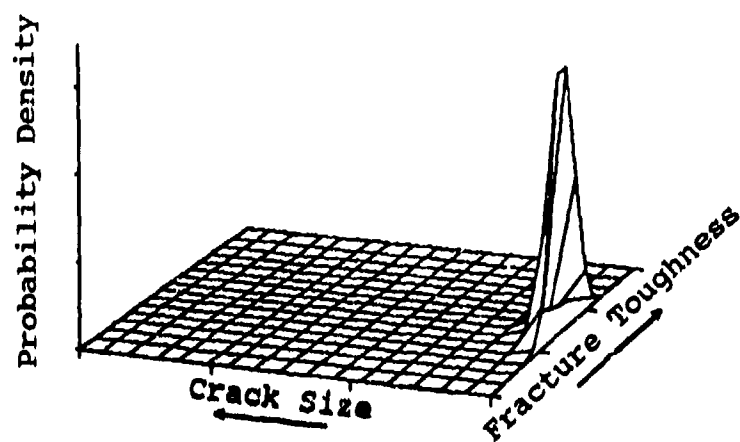
The crack size distribution that the crack growth module maintains is an integral part of the probability of fracture calculations. The POF calculation is performed through a double integral across crack size and across fracture toughness as given by:

$$POF = \int_0^{\infty} \int_0^{\infty} f(a) g(K_c) POF(a, K_c) dK_c da \quad (A18)$$

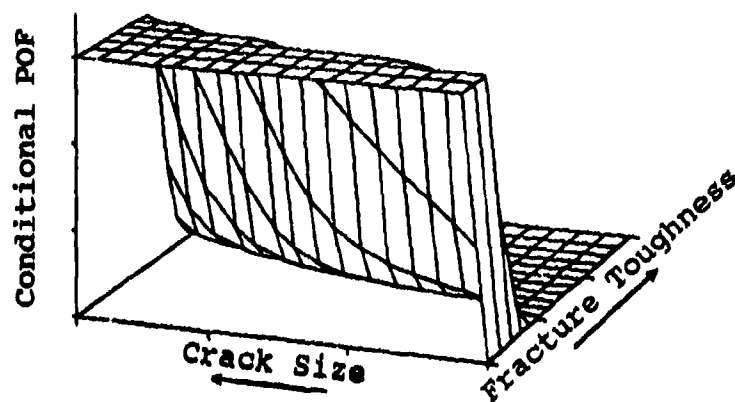
The integrand is the product of the crack size density function, the fracture toughness density function and the conditional probability of fracture (POF) given the crack size and toughness.

An illustration of the integration surface for a POF calculation is shown in Figure A4. Figure A4-a shows the joint density of crack length and fracture toughness and Figure A4-b shows the conditional POF given the crack length and the fracture toughness. The integrand for the unconditional POF integral is shown in Figure A4-c and is the product of the surfaces in Figures A4-a and A4-b.

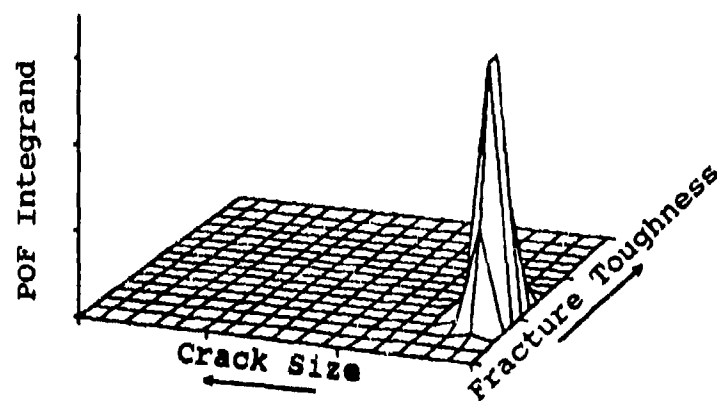
The basic difference in the calculations for the single flight POF and the interval POF is the form of the conditional POF function. The conditional POF for the single flight calculation is simply the probability that the peak stress in the flight is larger than the critical stress for the given crack length and toughness. The conditional POF for the usage interval is complicated by the fact that the cracks grow during the time period so that the critical stress is not a constant in the interval. An iterated calculation across time is required for the conditional POF for the usage interval.



a) Joint density of a and K_C



b) POF given a, K_C



c) $f(a) \cdot g(K_C) \cdot \text{POF}(a, K_C)$

Figure A4. Integration Surfaces for POF Calculations.

A.3.1 Single Flight Probability of Fracture

It is assumed that cracks do not grow during a single flight so that the single flight probability of fracture does not include a component due to cracks growing larger than the critical crack length. Some (very small) proportion of the cracks present at the start of the usage interval will, however, grow beyond a_{last} prior to the time at which a single flight probability of fracture is made. Since the population of cracks present at the start of a single flight is different from that present at the start of the usage interval, PROF calculates the conditional probability of fracture for a single flight given that the crack has not grown to a_{last} prior to the flight.

The equation for the single flight probability of fracture is:

$$SFPOF(T) = \left[\int_0^{a_{last}} f_T(a) \int_{-\infty}^{\infty} g(K_C) \bar{H}(\sigma_C(a, K_C)) dK_C da \right] / F_T(a_C) \quad (A19)$$

where T is the time of the flight, $f_T(a)$ and $F_T(a)$ are the current crack size probability density and cumulative probability functions respectively, a_{last} is the maximum crack length in the K/σ table, $g(K_C)$ is the fracture toughness probability density function, $\bar{H}(\sigma) = 1 - H(\sigma)$ is the exceedance probability distribution function for the peak stress in a single flight and $\sigma_{cr}(a, K_C)$ is the critical stress for the given crack length and fracture toughness. The double integral calculates the probability that a fracture will occur during the flight due to a stress cycle exceeding the critical stress for the current crack length and fracture toughness. Dividing the integral by the probability that the crack length is less than the critical crack length normalizes the probability to the subpopulation of cracks that would not grow to the critical length prior to the flight.

The integral with respect to a is approximated using CADRE [A2] which is an adaptive Rhomberg quadrature scheme. The

algorithm used by CADRE is an iterative procedure that stops when the desired accuracy is achieved. PROF requires a relative error of 0.001 which corresponds to three significant digits of accuracy.

The integrand for the integral across crack length includes an integral across fracture toughness, which is approximated with a 16-point Gauss-Hermite summation. Gauss-Hermite quadrature [A1] was specifically formulated for integrals involving the normal probability density function which is used for the distribution of K_c . Gauss-Hermite quadrature approximates the expected value of a function of a normal random variable and utilizes a weighted sum of the target function evaluated at strategically selected points.

The integral across K_c is the expected value of the conditional probability that the maximum stress on a given flight exceeds the critical stress for the fracture toughness and the current crack length. The critical stress is determined from the K/σ versus crack length table that is supplied by the user. K/σ values for the numerical integration are linearly interpolated from the " K/σ versus a " table. The fracture toughness is divided by K/σ to get the critical stress.

The Gumbel type 1 distribution is used to model the distribution of the maximum stress per flight and is given by:

$$P(\sigma > s) = \bar{H}(s) = 1 - \exp(-\exp((s-\beta)/\alpha)) \quad (A20)$$

where β and α are parameters that are supplied by the user and should be descriptive of the stress history used to generate the crack growth curve. The results of the double integral approximation are then divided by the probability that the crack length is less than a_{last} ; which is determined using the interpolation procedures described in the crack growth calculations section.

A.3.2 Usage Interval Probability of Fracture

The probability of fracture at any time during a usage interval is calculated from both the proportion of cracks that will grow to a size greater than a_{last} during the interval and the probability of encountering a critical stress for crack sizes less than a_{last} . Because the crack growth curve monotonically increases, a unique crack length, call it a_F , exists that is the boundary between cracks that will grow to a_{last} within the usage interval and those that will not. Crack lengths larger than a_F will automatically result in a fracture within the usage interval while a sufficiently large stress is required to cause fracture within the usage interval for cracks shorter than a_F . The probability of fracture for the usage interval includes both the probability that the crack length is greater than a_F and the probability that the crack length is smaller than a_F , but a stress greater than the critical stress is encountered during the usage interval.

The schematic of Figure A5 illustrates how a_F is determined from the length of the usage interval and the crack growth curve. The start of a usage interval is labeled as T_0 and the end of the usage interval as T_M . The master crack growth curve is shifted left or right so that it intersects the point (T_M, a_{last}) . The crack length at T_0 on the adjusted master crack growth curve is a_F . The effect of this process is to 'grow' the crack backwards from size a_{last} at the end of the usage interval to determine a_F at the start of the usage interval.

The formula for the probability of fracture in the usage interval is:

$$UIPOF = 1 - F(a_F) + \int_0^{a_F} f(a) \int_0^{\infty} g(K_C) PF(a, K_C) dK_C da \quad (A21)$$

where $F(a)$ and $f(a)$ are the crack size cumulative distribution and probability density functions at the start of the usage

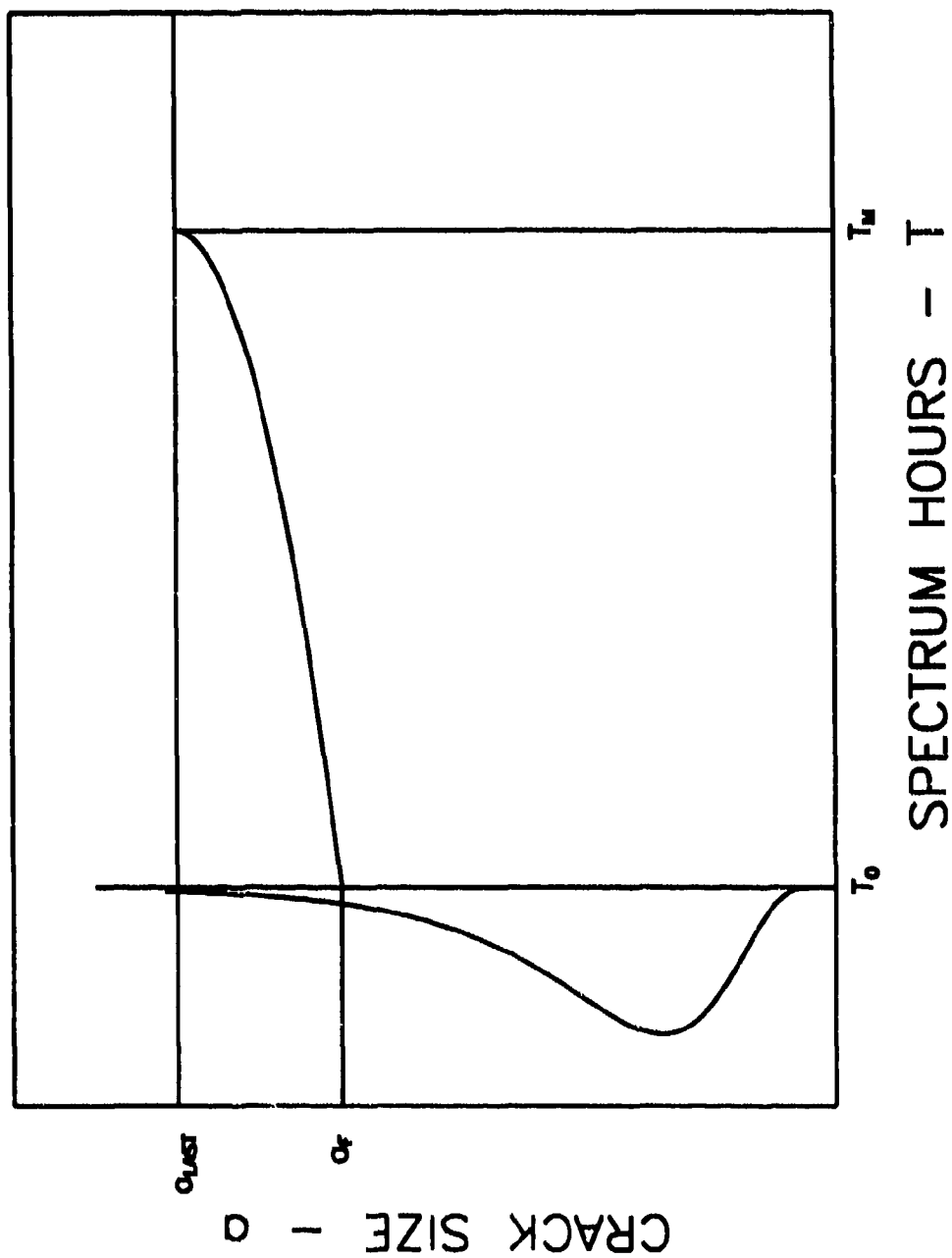


Figure A5. Determination of a_F , the crack size that will grow to a_{last} in a Usage Interval.

interval and $PF(a, K_C)$ is the probability that a large stress will cause a fracture within the usage interval given crack length, "a", and fracture toughness, K_C . The term $1-F(a_F)$ is the proportion of cracks that will fracture by growing to a_{last} within the usage interval and the double integral term is the probability that a crack will not exceed a_{last} but will experience a critical stress within the usage interval.

The conditional probability of fracture, given the starting crack length and the fracture toughness, is calculated by dividing the usage interval into a large number of subintervals. The endpoints of the subintervals are designated $T_0, T_1, T_2, \dots, T_M$ (the end of the usage interval) with $T_i - T_{i-1} = \Delta T$ for $i=1$ through $M-1$. ($T_M - T_{M-1}$ will not equal ΔT if the usage interval is not a multiple of ΔT .)

The subinterval mesh spacing (ΔT) used in PROF is 10 flights for usage intervals up to 1000 flights and 20 flights for usage intervals greater than 1000 flights and less than 2000 flights. For larger usage intervals, the subinterval size increases by 10 flights for each increase of 1000 flights in the usage interval length. The critical stress remains reasonably constant within the small subintervals of time defined by the spacing so that the probability of fracture within a subinterval is the probability that the peak stress exceeds the critical stress.

The principle of complementary events is used to simplify the calculation of the probability of fracture in the usage interval by subtracting the probability of no fracture from one. The peak stress distribution is independent for disjoint intervals so that the probability of no fracture in the usage interval is the product of the probabilities of no fracture in the subintervals. The function $PF(a, K_C)$ is given by:

$$PF(a, K_C) = 1 - \prod_{i=1}^M H_{\Delta T}(\sigma_{cr}(a_i, K_C)) \quad (A22)$$

where a_i is the crack length at time T_i given that the crack was length "a" at T_0 and σ_{cr} is determined as in the single flight POF calculation. $H_{\Delta T}$, the Gumbel type 1 distribution function adjusted for the subinterval of length ΔT , is derived from the peak stress per flight distribution and is given by:

$$H_{\Delta T}(\sigma) = \exp[-\Delta T \cdot \exp[-(\sigma-\beta)/\alpha]] \quad (A23)$$

where β and α are the single flight peak stress parameters and ΔT is the length of the subinterval measured in flights.

The same numerical procedures that were used in the single flight POF calculation are used to evaluate the double integral in equation A21. The cumulative probability of the crack length distribution at a_F is determined using the interpolation or extrapolation methods described in the crack growth calculation section. The above procedure is performed for each usage interval in the analysis request.

In addition to the probability of fracture for each usage interval, PROF reports the probability of fracture since the beginning of the analysis. The probability of fracture for the total interval since time zero is determined with a strategy similar to the calculation of the PF function. The form for the total interval probability of fracture at the end of the n 'th usage interval is:

$$TIPOF(T_n) = 1 - \prod_{i=1}^n (1 - UIPOF_i) \quad (A24)$$

where $UIPOF_i$ is the probability of fracture in the i th usage interval.

A.4 APPLICATION TO MULTIPLE DETAILS AND THE FLEET

The probability of fracture calculations described above apply to a single detail. PROF also reports the POF for a single aircraft, POF_A , and the POF for a fleet of aircraft, POF_F . The

single aircraft and fleet calculations are derived from the single detail results. Given that there are k equivalent details on a single airframe and N aircraft in the fleet, the single aircraft and fleet POF's are given by:

$$POF_A = 1 - [1 - POF_E]^k \quad (A25)$$

and

$$POF_F = 1 - [1 - POF_A]^N \quad (A26)$$

The single aircraft and fleetwide probabilities of fracture are calculated for the single flight, usage interval and total interval probabilities of fracture using equations (A25) and (A26).

A.5 REFERENCES

- A1. Carnahan, B., H. A. Luther, J. O. Wilkes, Applied Numerical Methods, John Wiley & Sons, Inc., New York, 1969.
- A2. de Boor, Carl, "CADRE: An Algorithm for Numerical Quadrature," Mathematical Software, (John R. Rice, Ed.), Academic Press, New York, Chapter 7, 1971.

APPENDIX B

STOCHASTIC CRACK GROWTH

PROF models the growing distribution of crack sizes for the population of structural elements by deterministically projecting the percentiles of the crack size distribution. This method of modeling crack growth ignores the stochastic nature of the growth of cracks of fixed size when subjected to identical stress sequences. Since an entire population of crack sizes is being projected, it can be anticipated that at least some of the stochastic effect will "average out" and the percentiles will remain relatively constant under the average crack growth model. This appendix presents a plausibility argument that ignoring the effect of stochastic crack growth has a second order effect on the projected crack size distribution and the analysis.

Most of the published literature on stochastic analyses have been directed at quantifying the variability in the growth of cracks of the same initial size. This concept is illustrated in the schematic of Figure B1. The dashed line represents the average growth of a crack of size "x" between T_1 and T_2 flight hours. The "small" probability density function, $g_{T_2}(a|x)$, represents the distribution of crack sizes that would be obtained if a large number of cracks of size x were subjected to the same stress sequence between T_1 and T_2 . In actuality, a population of cracks with density function, $f_{T_1}(a)$, is present at T_1 . The distribution of crack sizes at T_2 is a mixture of the different initial sizes at T_1 and the stochastic effect of the growth of cracks of any fixed size. In particular, the distribution of crack sizes at T_2 is given by

$$f_{T_2}(a) = \int_0^{\infty} f_{T_1}(x) \cdot g_{T_2}(a|x) dx \quad (B1)$$

(i.e. the probability of having a crack in the interval "a" to $a+da$ at time T_2 is the sum of the probabilities of having a crack

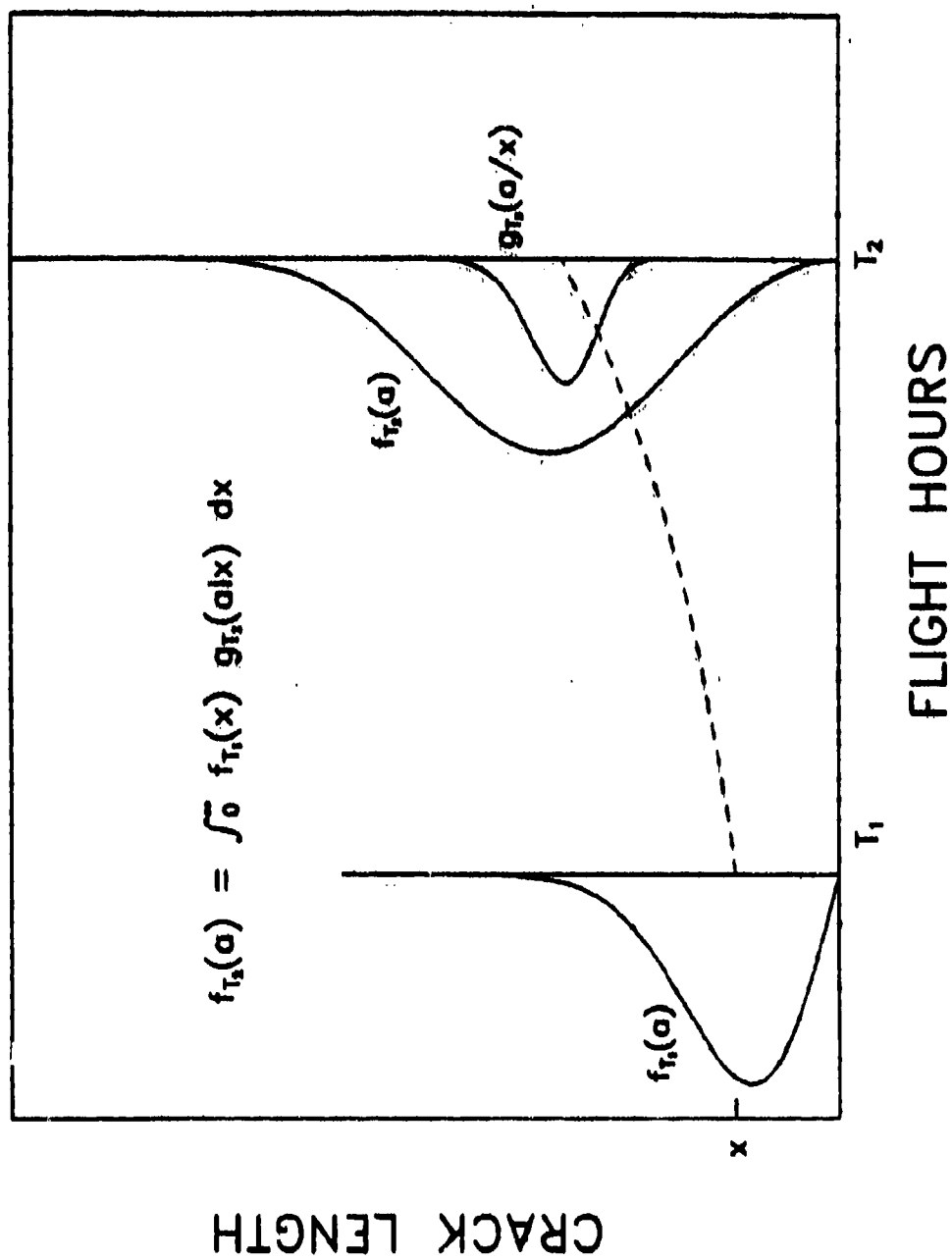


Figure B1. Schematic Illustrating Stochastic Crack Growth for a Population of Crack Sizes.

in the interval x to $x+dx$ at T_1 that will grow to size between " a " and $a+da$ at T_2).

To obtain an indication of the effect of the stochastic contribution to the crack size distribution at T_2 , an analysis was performed under the following assumptions:

- a) The crack size distribution at T_1 is either log normal ($\mu_1 = 0.010$ in. and $\sigma_1 = 1.0$) or Weibull ($\alpha_1 = 1.0$ and $\beta_1 = 0.012$). These distributions are representative of the sizes of cracks detected in a teardown inspection of A/F/T aircraft. [6]
- b) Crack growth is reasonably modeled by the equation

$$a(T) = a_0 \cdot \exp(Q \cdot T) \quad (B2)$$

The parameter Q was estimated from the moderate spectrum " a versus T " curve of Figure 7.

- c) The effect of stochastic crack growth on cracks of the same size produces either a log normal or a Weibull distribution. For the log normal assumption for $g_{T_2}(a|x)$, the median is given by $x \cdot \exp(Q \cdot T)$ and $\sigma = 0.05, 0.10, \text{ or } 0.20$. (For the lognormal distribution, σ approximates the coefficient of variation when σ is small.) For the Weibull assumption for $g_{T_2}(a|x)$, the scale parameter is given by $x \cdot \exp(Q \cdot T)$ and the shape parameter, α , is 12.5 (i.e., coefficient of variation of 0.10).
- d) $T_2 - T_1 = 3000$ hours. A relatively long interval was selected to exacerbate the differences that may result.

The percentiles of the initial distribution at T_1 were projected to T_2 using the crack growth of Equation B2. Equation B1 was used to obtain the "true" distribution of the crack sizes at T_2 for selected combinations of the assumptions. The

cumulative distributions of the resulting distributions were plotted to evaluate any differences. The results are presented in Figures B2 and B3.

Figure B2 presents a comparison of the estimated cumulative distributions at T_2 assuming a log normal initial crack size distribution and a log normal stochastic effect. Three degrees of scatter, σ , were considered for the stochastic crack growth effect. Under the conditions of this analysis, there is no significant difference between the projections of the initial distribution percentiles and the distributions which account for stochastic crack growth.

Figure B3 presents the cumulative distributions at T_2 assuming a Weibull initial crack size distribution and both Weibull and log normal stochastic effects. The coefficient of variation of the stochastic effects was approximately 0.10 for both models. Again the differences between the projected percentiles and the "true" distributions were not significant.

While recognizing that the assumptions of this analysis are not entirely realistic, the calculations do support the intuitive concept that the stochastic effect tends to "average out" when an entire population of initial crack sizes are under consideration.

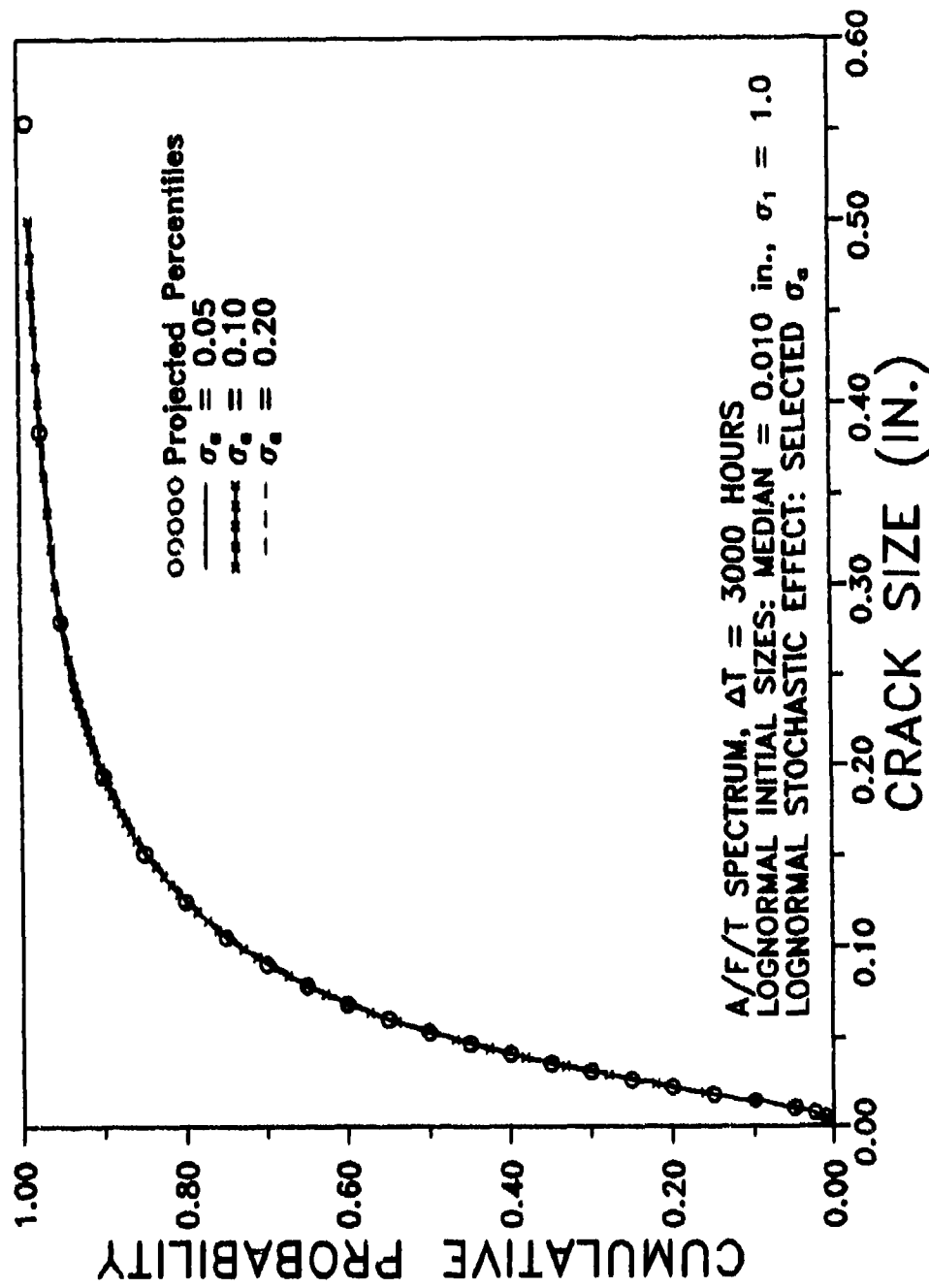


Figure B2. Comparison of Projected Percentiles of Log Normal Crack Sizes to Log Normal Stochastic Growth.

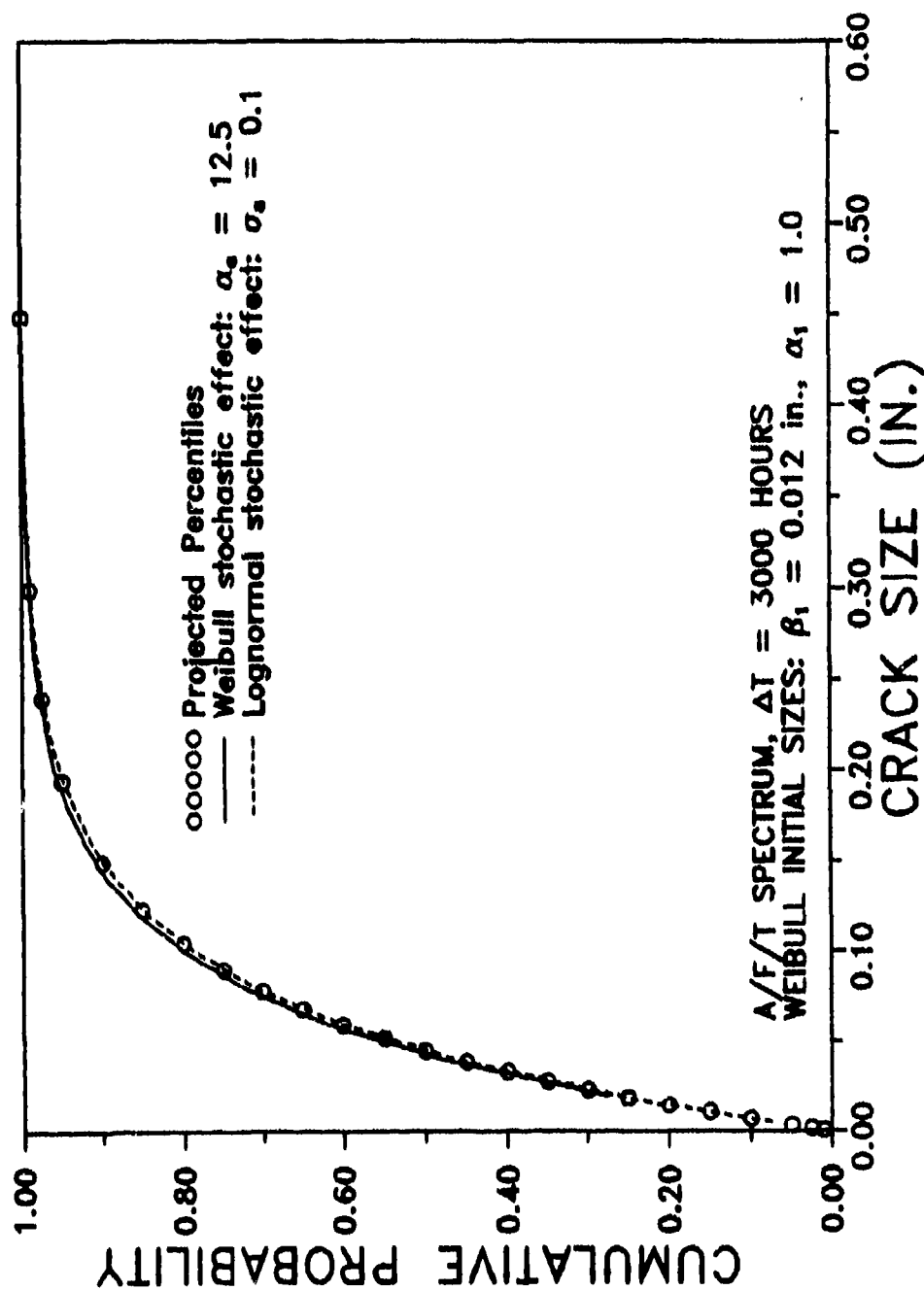


Figure B3. Comparison of Projected Percentiles of Weibull Crack Sizes to Weibull and Log Normal Stochastic Growth.

APPENDIX C

CRACK SIZE DISTRIBUTIONS

PROF requires that a cumulative distribution of crack sizes be identified at the beginning of the analysis. There are several potential sources for obtaining the crack size distribution depending on available data and the frame of reference of the calculations. If cracking problems have been observed during special teardown inspections to evaluate aging structures or during routine inspections, then real data would be available for estimating the crack size distribution. If PROF is being exercised to evaluate inspection scenarios in the absence of known cracks, then the crack size distribution will have to be estimated from analyses, laboratory test results, experience, or combinations of all three. Combinations of these data sources are also possible with inspection results being used to update any previous estimates of the crack size distribution. Approaches to estimating the crack size distribution are discussed in this appendix.

C.1 MODELS

The required PROF input for the population of crack sizes (initial or equivalent repair) is a file containing $(a, F(a))$ data pairs of the crack size cumulative distribution function at the start of the analysis. Any valid cumulative distribution can be used, provided there are at least two points with $F(a) > 0.99$. This general format provides considerable flexibility in describing the crack sizes. Although any standard distribution can easily be used, it is not necessary to fit a model to the available data. A table of the observed distribution function (with or without smoothing) could be used as input. Further, the format readily accommodates the use of mixtures for describing the crack size distribution. Examples of these concepts follow.

C.1.1 Theoretical Models

If a theoretical model for the initial crack size distribution is desired (for example, from the log normal or Weibull families), a table of cumulative distribution values will have to be generated. Computer programs for generating PROF input files of the log normal and Weibull families have been included as part of the PROF system. The programs request the median crack size and coefficient of variation (σ) for the log normal distribution and the shape (α) and scale (β) parameters for the Weibull distribution. Since the crack size data file must be available to PROF, the program for generating the crack size distribution file must be run before the start of a PROF analysis. Any other family can also be used. As a rough guide, it is suggested that the table of cumulative distribution values should contain approximately 20 or more percentiles (with at least two greater than or equal to 0.99).

C.1.2 Mixtures

If a mixture of distributions is selected as the best method for describing the crack size distribution, the mixture will have to be constructed before the PROF analysis. Mixtures of crack sizes can result from two or more modes of crack initiation for the same population of details. A mixture of crack sizes also results from the repair of detected cracks but PROF calculates this mixture.

If the population of cracks is believed to be comprised (a mixture) of two (or more) subpopulations, the cumulative distribution of the total population can be constructed as follows. Let p_i , with $\sum p_i = 1$, represent the proportion of cracks from population i and let $F_i(a)$ represent the cumulative distribution of the sizes of the cracks in population i . The cumulative distribution of the total population at each value of "a" in the $(a, F(a))$ array is then given by

$$F(a) = \sum p_i \cdot F_i(a) \quad (C1)$$

Equation C1 was used to generate the initial crack size distribution of the example, Figure 10. The example assumed that 99.9 percent ($p_1 = 0.999$) of the details were represented by an equivalent initial flaw size quality described by the log normal distribution with median size of 0.0008 in. and standard deviation of log size of 0.63. The remaining 0.1 percent ($p_2 = 0.001$) of the details were assumed to contain "rogue" flaws whose sizes were uniformly distributed between 0 and 0.050 in. The PROF input table for this mixture was generated using a spreadsheet program on a personal computer.

C.2 CRACK SIZE DATA AVAILABLE

If PROF analyses are to be run on an aircraft for which cracks have been detected in routine or teardown inspections of the population of details, these data provide the basis for estimating or updating the crack size distribution. The cumulative distribution of the observed crack sizes is obtained as follows:

- a) Adjust the crack sizes. To account for different airframe ages at the flight hours for which the cracks were detected, the crack size versus spectrum hours relation (Subsection 3.1.2.2) is used to translate the crack sizes to a common number of spectrum hours. To minimize errors associated with the translation, the common reference age should be at the approximate median of the ages of the inspected airframes.
- b) Determine the total number of inspected crack sites. The sample cumulative distribution function must be based on the total number of details that were inspected, not just the number of cracks that were detected.
- c) Estimate the number and sizes of the cracks that were missed at the inspections. In a complete teardown inspection, it is reasonable to assume that most (if not all) cracks were detected and that reasonable estimates

of the crack sizes were obtained. In routine inspections, the number of cracks that are not detected depend on the $POD(a)$ function and the sizes of detected cracks which may not have been recorded. Each data set will have to be evaluated individually to determine any adjustments that need to be made to account for missed cracks. At present, the adjustment will be made on the basis of the assumed $POD(a)$ function and experience. Note that the proportion of cracks less than crack size a that are missed at an inspection, $Q(a)$, is given by

$$Q(a) = \int_0^a [1 - POD(x)] \cdot f_{\text{before}}(x) \cdot dx \quad (C2)$$

where $f_{\text{before}}(x)$ is the probability density function of the crack sizes at the time of the inspection. The proportion of inspection sites at which cracks are detected that are less than " a " is given by $1 - Q(a)$. Since $f_{\text{before}}(x)$ is unknown, $Q(a)$ cannot be calculated. However, a range of $f_{\text{before}}(x)$ can be integrated (with the assumed $POD(x)$ function) to determine the pre-inspection crack size density function that gives results that are consistent with observed values of $1 - Q(a)$, the proportion of inspection sites in which cracks were detected. This analysis provides a basis for the adjustment of the observed distribution of crack sizes.

- d) Smooth the observed cumulative distribution of crack sizes. Smoothing can be accomplished either by fitting a family of distributions or faring a curve through a plot of the observed cumulative distribution function.
- e) Generate the input table of $(a, F(a))$ pairs.

As an example of the process, Figure C1 presents the results of a teardown inspection of a lower wing location on an aging A/F/T aircraft. These results are from 19 wings with 6 equivalent sites in each wing. Cracks were detected in 50 percent (57) of the locations, and it was believed that all

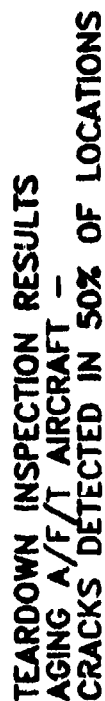


Figure C1. Sizes of cracks as a function of flight hours.

cracks were detected. After transforming the crack sizes to a common number of spectrum hours (10,000), the cumulative distribution of the crack sizes was obtained, Figure C2. Since Figure C2 is plotted on Weibull probability paper, a straight line fit indicates that the data are from a Weibull population. The data of this example appear to be a mixture of Weibull distributions since there are distinct slopes for the larger and the smaller crack sizes. The $(a, F(a))$ data pairs could be read directly from a fit (analytical or fared) of the straight lines to the data or calculated analytically from the parameters of the mixed Weibull distributions.

C.3 CRACK SIZE DATA NOT AVAILABLE

In the absence of inspection results, the crack size distribution to start a PROF analysis would be determined through analyses or experience. There are two viable analytical approaches to estimating the initiation and growth of a crack size distribution. These are the equivalent initial flaw size distribution and the distribution of time to initiate a crack of a specified size. Note that in either of these approaches, cracks less than some defined size (say 0.005 or 0.010 in.) may not be considered to be real cracks. If desired, such "cracks" can be eliminated as detectable cracks by starting the $POD(a)$ function at the defined size, e.g., $a_{min} = 0.005$ or 0.010 in.

C.3.1 Equivalent Initial Flaw Size Distribution

The Equivalent Initial Flaw Size Distribution (EIFSD) is the basis of the recently developed stochastic approach to the characterization of structural durability [7]. The EIFSD is a description of the initial quality of the structure. It quantifies quality in terms of a distribution of "equivalent flaw" sizes which are assumed to be present at every critical location and are correlatable with real flaws that will occur in the later life of the structure. The EIFSD is obtained by conducting tests of representative structure subjected to a specified loading history and determining the distribution of

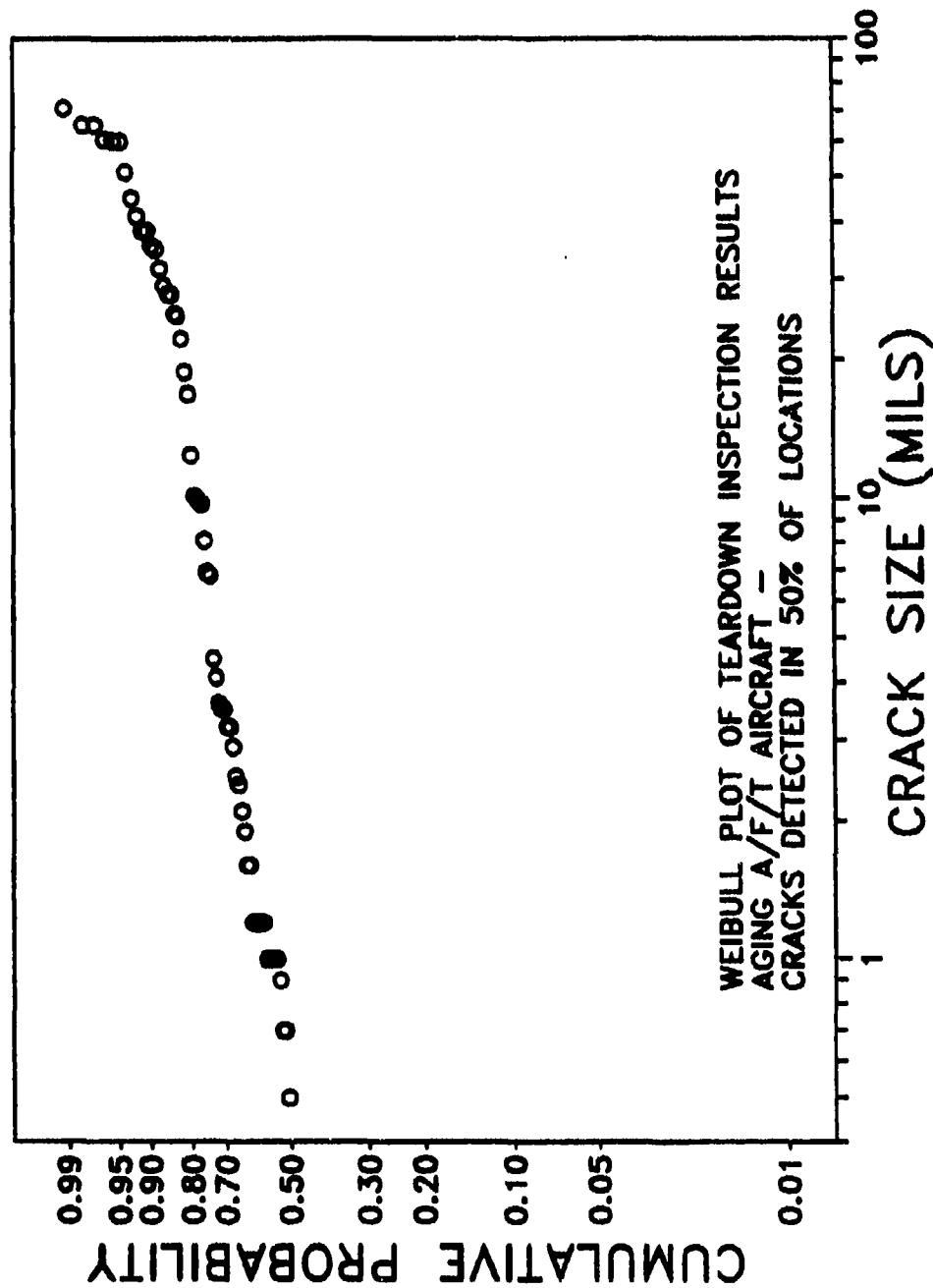


Figure C2. Weibull Plot of Crack Sizes Translated to a Common Number of Flight Hours.

times for the cracks to initiate and propagate to a given reference size. The Time To Crack Initiation (TTCI) distribution is then stochastically "grown" backwards in time to obtain the flaw size distribution at time zero (EIFSD). The EIFSD is then grown forward in time (using the same stochastic model but with parameters determined from the spectrum of interest) to determine the flaw size distribution at any service time. A schematic of this approach is shown in Figure C3.

Although the growth of the distribution of crack sizes is modeled differently in PROF, the equivalent initial flaw size distribution can be used as the initiating distribution. The "a versus T" relation of PROF can be defined by the stochastic model up to the minimum crack size for fracture mechanics analyses and by standard crack growth models thereafter. This essentially is the process that was used in the example of Sections 3.1.2.2.2 and 3.1.2.4.2. In the example, an equivalent initial crack size distribution was assumed that was representative of the initial quality of an A/F/T airframe. A modified Willenborg model was used to predict the growth of the percentiles of the crack size distribution which were greater than the threshold size for the A/F/T spectrum. An exponential model was used to extrapolate to crack sizes below the threshold.

C.3.2 Time to Crack Initiation

A method for modeling the growth of a distribution of crack sizes has also been proposed by Walker [C1]. In this model, it is assumed that a) time to initiate a crack of any fixed size has a log normal distribution, b) the standard deviation of log times to crack initiation is constant for all initiating crack sizes, i.e., a constant coefficient of variation, and, c) the median time to crack initiation is the "a versus T" relation modeled by standard fracture mechanics. There is a historical data base which supports these general assumptions. Further, for aluminum alloys $\sigma \approx 0.15$ [C2]. Under these assumptions and an estimate of the median time to initiate a fracture mechanics crack size, the

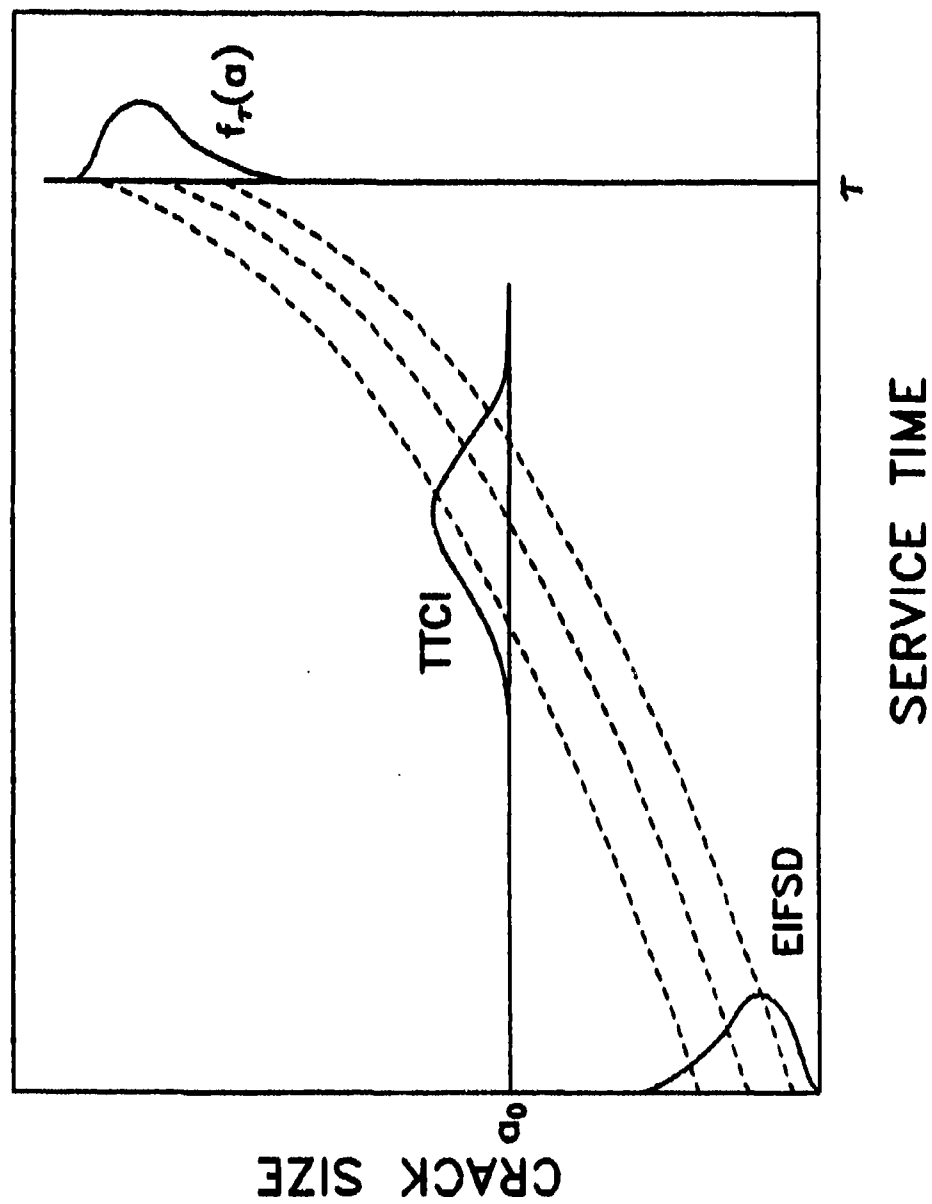


Figure C3. Schematic of Stochastic Structural Durability Analysis.

distribution of crack sizes at a fixed time can be calculated as illustrated in Figure C4.

This model can also be used to obtain a crack size distribution to initiate a PROF analysis. Given an estimate of the median time, T_0 , to initiate a crack of fixed size, e.g. 0.010 in., a reasonable estimate of the crack size distribution at T_0 can be calculated from

$$F_{T_0}(a) = 1 - \Phi\{[(\ln T_0 - \ln \phi^{-1}(a))/\sigma]\} \quad (C3)$$

where $\Phi(z)$ is the standard normal cumulative distribution function. Since the "a versus T" relation may only be defined in tabular form, the implementation of Equation C3 may require a separate computer program. The (a,F(a)) table could also be manually calculated.

It might be noted that the above approach could also be based on the Weibull distribution of time to initiate cracks of a defined size.

$$F_{T_0}(a) = \exp[-(T_0/\phi^{-1}(a))^\alpha] \quad (C4)$$

Under the Weibull assumption, it would be assumed that the shape parameter of the Weibull distribution is constant ($\alpha = 4$) and the characteristic life, β , is modeled by the "a versus T" curve. These Weibull assumptions have also been shown to be reasonable [C2].

C.4 CRACK SIZE DISTRIBUTION UPDATE

Regardless of the source of the crack size distribution originally used in an analysis, the availability of new data should be incorporated in a reevaluation of the crack size distribution. New PROF runs would then be performed with the new initiating crack size distribution.

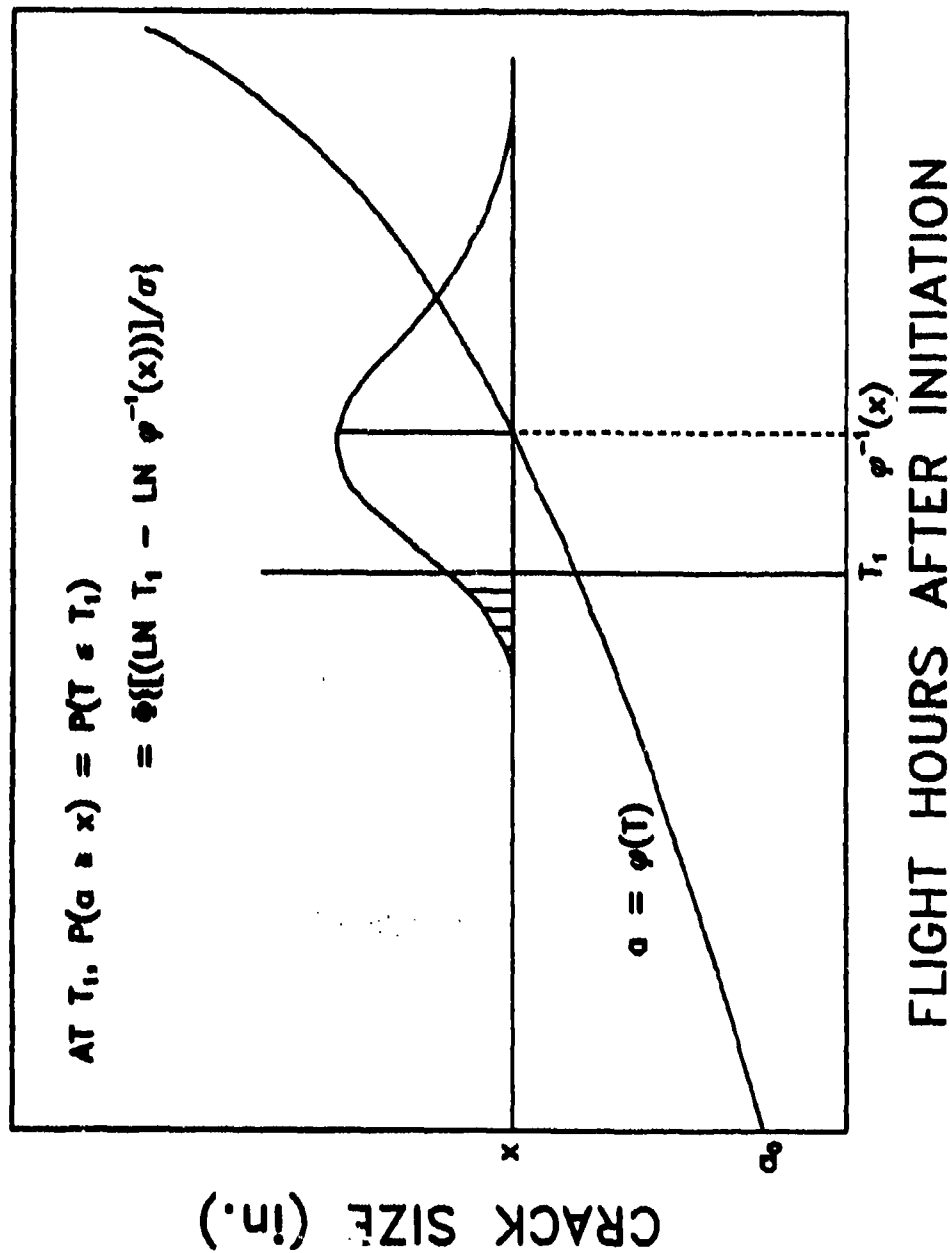


Figure C4. Schematic of the Calculation of Crack Size Distribution from Time to Crack Initiation Distribution.

Given crack sizes and spectrum hours obtained from routine or teardown inspections, the crack size distribution can be adjusted on the basis of either translation to a common number of spectrum hours or to a common crack size. Translating the sizes to a common number of spectrum hours would be performed as described above. The new distribution of crack sizes would be compared with the old. Any adjustments judged necessary could then be made. Translating to a common crack size would allow a reevaluation of the average time to crack initiation for the Walker approach to estimating the crack size distribution. The latter approach may be more robust in that the coefficient of variation is fixed. Adjustments would be made on the basis of changes in averages which tend to be less sensitive to sample size. Again, some consideration must be given to the cracks which were not detected due to the limitations of the inspection process.

C.5 REFERENCES

- C1. Walker, E.K., "Exploratory Study of Crack-Growth-Based Inspection Rationale," Probabilistic Fracture Mechanics and Fatigue Methods: Applications for Structural Design and Maintenance, ASTM STP 798, J.M. Bloom and J.C. Ekvall, Eds., American Society for Testing and Materials, 1983, pp. 116-130.
- C2. Whittaker, I.C. and Basuner, P.M., "A Reliability Analysis Approach to Fatigue Life Variability of Aircraft Structures," AFML-TR-69-65, Air Force Wright Aeronautical Laboratories, Wright-Patterson Air Force Base, OH, 45433, April, 1969.